



UNIVERSITY OF LIÈGE
Faculty of Medicine

Laboratory of Medicinal Chemistry
Pr. Bernard Pirotte
Center for Interdisciplinary
Research on Medicines (CIRM)

Laboratory of Molecular Pharmacology
Dr. Julien Hanson
GIGA - Molecular Biology of Diseases

**DEVELOPMENT OF PHARMACOLOGICAL
TOOLS FOR THE IDENTIFICATION OF G
PROTEIN-COUPLED RECEPTORS LIGANDS**

Julie Gilissen

Promoter : Dr. Julien Hanson & Co-promoter : Pr. Bernard Pirotte

**Thesis submitted to fulfill the requirements for the degree of
PhD in Biomedical and Pharmaceutical sciences**

2015 - 2016

Au terme de la rédaction de ce manuscrit, il m'est agréable de remercier les nombreuses personnes qui ont participé à ces travaux de recherches et sans qui la réalisation de ceux-ci n'aurait pas été possible. Ce projet pluridisciplinaire est le fruit de nombreux échanges et collaborations.

Je souhaite tout d'abord remercier mon promoteur, le Docteur Julien Hanson, pour m'avoir transmis l'envie de me spécialiser dans la pharmacologie des récepteurs couplés aux protéines G, de m'avoir initiée aux techniques de la biologie cellulaire et moléculaire ainsi que les techniques associées au criblage de librairies. Je le remercie chaleureusement pour son soutien, sa disponibilité, son implication, son enthousiasme, ses précieux conseils et ses grandes qualités scientifiques. Je lui suis reconnaissante de la confiance dont il a fait preuve à mon égard en me laissant mener à bien ce projet au sein du laboratoire de pharmacologie moléculaire.

J'exprime ma gratitude envers mon co-promoteur, le Professeur Bernard Pirotte qui m'a permis de mener à bien cette thèse de doctorat. Je le remercie de m'avoir accueillie au sein du laboratoire de chimie pharmaceutique, d'avoir suivi ce projet et d'avoir pris le temps de relire mes écrits. Je le remercie chaleureusement pour sa confiance, sa gentillesse, son aide et ses nombreux conseils.

J'exprime toute ma reconnaissance à l'ensemble de mon jury de thèse, le Professeur André Luxen, président de mon comité, ainsi qu'au Professeur Vincent Seutin et au Docteur Jacques Piette pour leurs conseils avisés et le temps qu'ils ont consacré à l'évaluation de mon travail. Je voudrais également remercier le Docteur Laurent Provins de chez UCB Biopharma et le Professeur Graeme Milligan de l'université de Glasgow, membres extérieurs du jury, pour leur aimable participation.

Merci à tous les scientifiques travaillant aux laboratoires de chimie pharmaceutique et de pharmacologie moléculaire avec qui j'ai eu plaisir à travailler. Je remercie particulièrement Pierre Geubelle pour son aide précieuse et sa rigueur scientifique. Pierre, ce travail n'aurait pas été aussi fructueux sans ta collaboration sur le projet SUCNR1, merci pour tout. Je remercie vivement Céline Piron, notre technicienne pour son enthousiasme, son implication et ses compétences scientifiques. Ton aide en culture cellulaire et biologie moléculaire m'a permis d'avancer plus rapidement et de générer de nombreux résultats. Je remercie Nadine Dupuis pour nos nombreuses conversations enrichissantes ainsi que pour le développement du test utilisé pour la mesure du recrutement des arrestines. Enfin, je remercie vivement Monsieur Anouar Derj et mademoiselle Céline Laschet pour m'avoir fait bénéficier de leur expérience sur les techniques de western blot. Je vous remercie également pour votre temps et nos nombreux échanges.

Je souhaite remercier le Docteur Sébastien Dilly pour sa collaboration et son aide indispensable pour la partie concernant la modélisation moléculaire de ce projet.

Je tiens à exprimer ma reconnaissance au Docteur François Jouret pour ses nombreux conseils pour la partie in vivo de ce projet ainsi que d'avoir pris le temps de relire mes écrits. Je remercie également Madame Laurence Poma pour avoir réalisé les expériences sur les rats au sein du laboratoire de chirurgie expérimentale (GIGA-Cardiovascular Sciences).

Je tiens à exprimer ma profonde gratitude envers la Fondation Léon Fredericq (FLF), le Fonds National de la Recherche Scientifique (F.N.R.S) ainsi que l'Université de Liège pour m'avoir accordé les moyens financiers indispensables à la réalisation de ces travaux.

Un grand merci à tous mes collègues et amis pour leur soutien et les moments que nous avons partagés : Nadine, Anouar, Céline L, Céline P, Pierre, Catherine, Monique, Céline D, Gaël, Aurélie et Philippe.

Je terminerai ces remerciements en ayant une pensée particulière pour mes proches, ma famille et mes amis pour leurs encouragements, leur patience et leur écoute. Je tiens également à remercier Daniel pour sa présence, son soutien et son aide tout au long de la réalisation de ce travail.

Abstract

G protein-coupled receptors (GPCRs) represent the protein family most successfully targeted for treating human diseases. They couple to G proteins to mobilize second messenger pathways that lead to cellular responses and ultimately to physiological changes. However many are poorly characterized with few ligands reported or remain completely orphans. Therefore, there is a growing need for screening-compatible and sensitive assays in order to identify new ligands.

The present project aims at developing pharmacological tools to characterize the pharmacology and physiology of GPCRs. Our approach rely on i) development of receptor models and assays for the identification of ligands, ii) screening of chemical and virtual small molecules libraries and iii) analysis of structure-activity relationships study of active molecules. The project has been divided in two parts.

To set-up assays for the evaluation of GPCRs activation, we selected the understudied succinate receptor 1 (SUCNR1) that is proposed to affect cellular metabolism and pathophysiology of diseases in multiple organs. Nevertheless the receptor has never been validated as a drug target because very few ligands have been described. So, developing pharmacological tools for SUCNR1 remains of great interest in therapeutic drug discovery.

First, we have started by examining SUCNR1 signaling pathways in HEK293 cells. Our investigations have highlighted the efficient coupling to G_{α_i} and thus the negative modulation of intracellular cAMP levels. Consequently we have implemented an assay sensitive to cAMP variations to identify ligands able to induce SUCNR1 activation. However, an important drawback to track agonists for G_{α_i} -coupled receptors is the mandatory stimulation of cAMP levels. Inducers such as forskolin must be used and are sources of variations and errors. In order to avoid these artifacts we have set-up and validated a cAMP-inducer free method based on the GloSensor biosensor. This real time assay was amenable to high-throughput screening for the detection of G_{α_i} -coupled receptors agonists. The strategy monitoring basal cAMP levels compared to the stimulated cAMP levels allowed to decrease recording time and artifacts from forskolin use, leading to the identification of fewer false positives and unidentified false negatives.

Although both methods found agonists in the chemical library screened, no active new scaffolds on SUCNR1 were discovered.

We infer that this method could facilitate the study and screening of $G_{\alpha i}$ -coupled receptors for active ligands.

Secondly, given the interesting potential of SUCNR1 for promising therapeutic advances, we have carried out the study of the receptor interaction with its natural ligand, succinate. We have optimized the previous three-dimensional model for SUCNR1 binding pocket by means of more detailed structure-activity relationships study of succinate related molecules. The study of structure-activity relationships performed by Pierre Geubelle, in parallel to this work, allowed the deduction of the structural elements required to be active on SUCNR1. Thus we have defined a pharmacophore for activity on the receptor and subsequently evaluated various cycloalkanes. With our cAMP assay, Pierre Geubelle has highlighted the (1*R*, 2*S*)-1,2-cyclopropanedicarboxylate to be able to activate SUCNR1. We confirmed the activity of this compound on SUCNR1 capacity to recruit arrestin 3 and determined the pharmacological properties of this new ligand as SUCNR1 agonist, *in vitro* and *in vivo*. To confirm our *in vitro* results, we have also assessed the hypertensive properties of this cyclic analogue. Intravenous addition at the dose of 0.1 mg.kg⁻¹ in rats has been demonstrated to increase blood pressure in the same range as succinate.

Consequently we have demonstrated that (1*R*, 2*S*)-1,2-cyclopropanedicarboxylate could be regarded as an original synthetic full agonist for SUCNR1. In addition, the pharmacophore for SUCNR1 should help to generate synthetic compounds characterized by an increased potency and/or efficacy compared to succinate.

Résumé

Les récepteurs couplés aux protéines G (RCPGs) constituent la plus grande famille de récepteurs membranaires intervenant dans la transduction des signaux extracellulaires. Via la régulation de messagers intracellulaires, ils sont responsables du contrôle de nombreuses fonctions physiologiques et sont la cible de nombreux médicaments commercialisés. Cependant, de nombreux RCPGs sont encore peu caractérisés avec peu de ligands décrits ou encore même orphelins. De ce fait, ils font l'objet de nombreuses études ayant pour but de déterminer leur(s) rôle(s) physiologique(s), mais également d'identifier leurs ligands afin de déterminer leur intérêt en tant que cibles pour la découverte de nouveaux médicaments. C'est pourquoi il y a un besoin croissant de disposer de tests pharmacologiques sensibles et compatibles avec le criblage de bibliothèques afin d'identifier de nouveaux ligands.

Ce projet a pour but de développer des outils pharmacologiques pour caractériser la pharmacologie et la physiologie de tels récepteurs. Notre approche est basée sur i) le développement de modèles cellulaires et de tests pharmacologiques pour identifier des ligands, ii) le criblage de bibliothèques chimiques et virtuelles, et iii) l'analyse des relations structure-activité des molécules actives. Le projet peut être divisé en deux parties.

Afin de développer des tests pharmacologiques et ainsi évaluer l'activation de RCPGs, nous avons sélectionné le récepteur au succinate, SUCNR1. Ce récepteur a été décrit comme affectant le métabolisme cellulaire ainsi que de nombreuses pathologies dans plusieurs organes. Il n'a toutefois jamais été validé comme cible thérapeutique. Ceci est dû au fait que peu de ligands ont été décrits. Le développement d'outils pharmacologiques pour SUCNR1 constitue donc un intérêt majeur en recherche thérapeutique.

D'abord, l'investigation des voies de signalisation de SUCNR1 surexprimé dans des cellules HEK293, nous a permis d'identifier le récepteur comme étant efficacement couplé à la protéine $G_{\alpha i}$ et donc capable de moduler négativement les taux d'AMPc intracellulaire. Par conséquent, nous avons mis au point un test pharmacologique capable de mesurer les variations d'AMPc pour identifier des ligands qui induisent l'activation de

SUCNR1. Toutefois, l'identification d'agonistes de récepteurs couplés à $G_{\alpha i}$ nécessite la stimulation préalable des taux d'AMPc par un activateur tel que la forskoline. Leur utilisation est un grand inconvénient puisqu'ils génèrent de nombreuses variations et erreurs. Dans le but de s'affranchir de cette source d'erreurs, nous avons mis au point et validé une méthode qui rend possible la mesure des taux d'AMPc de base sans nécessiter l'utilisation d'un activateur. Le test pharmacologique est basé sur un biosenseur appelé GloSensor qui permet une mesure en temps réel des taux d'AMPc et est facilement adaptable au criblage à haut débit pour détecter des agonistes pour les récepteurs couplés à $G_{\alpha i}$. Cette stratégie a dès lors permis de diminuer le temps de lecture ainsi que le nombre d'artéfacts liés à l'utilisation de la forskoline. En effet, la méthode sans activateur des taux d'AMPc a conduit à l'identification de moins de faux positifs mais a aussi permis de révéler des faux négatifs. Bien que les deux méthodes aient mené à l'identification d'agonistes, aucunes nouvelles structures actives sur SUCNR1 n'ont pu être découvertes.

L'intérêt de cette méthode reside dans le fait qu'elle facilitera l'étude et le criblage de récepteurs couplés à $G_{\alpha i}$ pour l'identification de ligands.

Ensuite, nous avons étudié l'interaction du récepteur avec son ligand naturel, le succinate. Nous avons optimisé le modèle tridimensionnel de la poche de liaison de SUCNR1 existant grâce à des informations obtenues lors de l'étude des relations structure-activité d'analogues du succinate menée par Pierre Geubelle. Son travail a permis de déduire les éléments structuraux importants pour l'activité sur SUCNR1. Dès lors nous avons pu en déduire un pharmacophore et nous avons investigué l'activité de cycloalcanes. Avec le système GloSensor, Pierre Geubelle a identifié un nouvel agoniste de SUCNR1, le (1*R*, 2*S*)-1,2-cyclopropanedicarboxylate. Son activité a été confirmée sur une deuxième voie de signalisation. En effet, il induit le recrutement de l'arrestine 3 via l'activation de SUCNR1. Nous avons ensuite investigué son activité *in vivo* et mesuré son effet hypertenseur. Le composé injecté par intraveineuse à la dose de 0.1 mg.kg⁻¹ augmente la pression artérielle chez le rat dans le même ordre de grandeur que le succinate.

Par conséquent, nous avons identifié un agoniste plein synthétique et original pour SUCNR1. De plus, le pharmacophore devrait aider à générer de nouveaux ligands pour SUCNR1, plus puissants et/ ou efficaces par rapport au succinate.

Publications

Forskolin-free cAMP assay for G_i-coupled receptors. Julie Gilissen, Pierre Geubelle, Nadine Dupuis, Bernard Pirotte, and Julien Hanson. *Biochemical Pharmacology*, 2015.

Insight into SUCNR1 (GPR91) structure and function. Julie, Gilissen; François, Jouret; Bernard Pirotte and Julien Hanson. *Pharmacology & Therapeutics*, 2016.

Manuscript in preparation

Discovery of the first synthetic agonist for SUCNR1. Pierre Geubelle, Julie Gilissen, Sébastien Dilly, Nadine Dupuis, Laurence Poma, Eric Goffin, François Jouret, Bernard Pirotte and Julien Hanson.

Abbreviations list

[Ca ²⁺] _i	intracellular free calcium	CHO cells	chinese hamster ovary cells
3D	three-dimensional	CNG	cyclic nucleotide-gated channel
7TM	seven transmembrane domains	CRE	cAMP-response element
AA	amino acid	CREB	cAMP response element-binding protein
AB	antibody	DAG	diacylglycerol
AC	adenylate cyclase	DMSO	dimethylsulphoxide
ALPHA	amplified luminescent proximity homogeneous assay	DOS	diversity-oriented synthesis
AMP	adenosine monophosphate	EC ₅₀	effective concentration
ATP	adenosine triphosphate	ECL	extracellular loop
BP	blood pressure	EFC	enzyme fragment complementation
BRET	bioluminescence resonance energy transfer	E _{max}	maximum efficacy
CAM	constitutively active mutant	ERKs	extracellular signal-regulated kinases
cAMP	cyclic adenosine 3',5'-monophosphate	FACS	fluorescence-activated cell sorting
CCD	charge-coupled device	FBS	fragment-based screening
CDS	cellular dielectric spectroscopy	FLIPR	fluorimetric imaging plate reader
CFP	cyan fluorescent protein	FLuc	firefly luciferase

FP	fluorescence polarization	IP ₃	inositol-1,4,5-triphosphate
FRET	fluorescence resonance energy transfer	JNKs	c-Jun N-terminal kinases
FSK	forskolin	KO	knockout
GDI	guanine nucleotide dissociation inhibitors	LTB ₄	leukotriene B ₄
GEFs	guanine nucleotide exchange factors	LOPAC	library of pharmacologically active compounds
GFP	green fluorescent protein	MAPKs	mitogen-activated protein kinases
GPCRs	G protein-coupled receptors	MDCK	madin darby canine kidney
GRKs	G protein-coupled receptor kinases	NMR	nuclear magnetic resonance
HCS	high-content screening	PCR	polymerase chain reaction
HEK293 cells	human embryonic kidney cells	PDE	phosphodiesterase
HRP	horseradish peroxidase	p-ERK1/2	phosphorylated ERK1/2
HTRF	homogeneous time-resolved fluorescence	PI3Ks	phosphatidylinositol 3-kinases
HTS	high-throughput screening	PIP ₂	phosphatidylinositol-4,5-bisphosphate
IBMX	1-methyl-3-(2-methylpropyl)-7H-purine-2,6-dione	PKA	protein kinase A
ICL	intracellular loop	PKC	protein kinases C
IP	inositol phosphate	PLC-β	phospholipase C-β
		PTX	pertussis toxin
		RNA	Ribonucleic acid

RGS	regulators of G protein signaling	SPA	scintillation proximity assays
RhoGAPs	GTPase-activating proteins	SREB	Super conserved receptor expressed in brain
SA	succinic acid	TR-FRET	time-resolved fluorescence resonance energy transfer
SAR	structure-activity relationships	VPR	Volume pressure recording
SDH	succinate dehydrogenase	WT	wild type
siRNA	small interfering RNA	YFP	yellow fluorescent protein
SOSA	selective optimization of side activities		

Table of contents

I. INTRODUCTION.....	23
I.1. PHARMACOLOGY OF G PROTEIN-COUPLED RECEPTORS	25
<i>I.1.1. GPCRs general description</i>	<i>25</i>
<i>I.1.2 Classification of GPCRs.....</i>	<i>26</i>
<i>I.1.3. Structure of GPCRs.....</i>	<i>27</i>
<i>I.1.4. Signal transduction and regulation</i>	<i>30</i>
<i>I.1.4.1. Heterotrimeric G proteins.....</i>	<i>30</i>
<i>I.1.4.2. G protein-coupled receptor kinases (GRKs).....</i>	<i>34</i>
<i>I.1.4.3. Arrestins</i>	<i>35</i>
<i>I.1.4.3.1. G protein-dependent mechanism.....</i>	<i>35</i>
<i>I.1.4.3.2. G protein-independent mechanism</i>	<i>39</i>
<i>I.1.4.4. Other mechanisms for the modulation of GPCRs signaling.....</i>	<i>41</i>
<i>I.1.5. GPCRs Ligands.....</i>	<i>43</i>
<i>I.1.5.1. Nature of ligands.....</i>	<i>43</i>
<i>I.1.5.2. Affinity and efficacy of ligands.....</i>	<i>43</i>
<i>I.1.5.3. Classification of ligands</i>	<i>45</i>
<i>I.1.5.4. Constitutive activity.....</i>	<i>47</i>
<i>I.1.5.5. Biased ligands.....</i>	<i>48</i>
I.2. SUCNR1	51
<i>I.2.1. "Deorphanization" and characterization of SUCNR1.....</i>	<i>51</i>
<i>I.2.2. Implications in (patho)physiology.....</i>	<i>55</i>
<i>I.2.3. Ligands and binding pocket</i>	<i>56</i>
<i>I.2.4. Signaling pathways.....</i>	<i>58</i>

I.3. METHODS FOR THE IDENTIFICATION OF LIGANDS FOR GPCRS	61
<i>I.3.1. Interest of ligands</i>	61
<i>I.3.2. Computational approach</i>	63
<i>I.3.3. Pharmacological approach</i>	64
<i>I.3.3.1. Pharmacological screenings</i>	65
<i>I.3.3.1.1. Biological extract preparations</i>	65
<i>I.3.3.1.2. Libraries</i>	65
<i>I.3.3.1.3. Cell-based assays</i>	68
<i>I.3.3.1.3.1. General receptor activity measurement</i>	68
<i>I.3.3.1.3.2. G protein activity measurement</i>	70
<i>I.3.3.1.3.2.1. Ca²⁺ measurement</i>	71
<i>I.3.3.1.3.2.2. cAMP measurement</i>	73
<i>I.3.3.1.3.2.2.1. Competition assays for cAMP detection</i>	74
<i>I.3.3.1.3.2.2.2. Biosensors</i>	79
<i>I.3.3.1.3.3. Challenges of the quantification of G_{αi} activation</i>	87
<i>I.3.3.1.4. Critical parameters for screening</i>	89
<i>I.3.3.2. Medicinal chemistry</i>	94
II. AIM OF THE WORK	97
III. RESULTS AND DISCUSSION	103
III.1. CHARACTERIZATION OF SUCNR1 SIGNALING PATHWAYS AND DEVELOPMENT OF CELL-BASED ASSAYS	105
<i>III.1.1. G_{αi} signaling pathway</i>	105
<i>III.1.1.1. The biosensor</i>	105
<i>III.1.1.2. G_{αi} signaling pathway activation measure</i>	106
<i>III.1.2. G_{αq} signaling pathway</i>	110
<i>III.1.2.1. The biosensor</i>	110

III.1.2.2. <i>G_{αq}</i> signaling pathway assessment.....	112
III.1.3. Arrestins recruitment.....	113
III.1.3.1. The biosensor.....	113
III.1.3.2. Ability of SUCNR1 to recruit arrestins.....	114
III.1.4. Determination of ERK phosphorylation	116
III.1.5. <i>G_{α12/13}</i> signaling pathway.....	118
III.2. SCREENING OF SUCNR1 WITH A FSK-FREE CAMP ASSAY	121
III.2.1. Real time analysis of cAMP levels modulation mediated by.....	122
SUCNR1 activation.....	122
III.2.2. Optimization of a screening protocol.....	127
III.2.3. Screening of the Sigma LOPAC1280™ library.....	129
III.2.3.1. Primary screening.....	129
III.2.3.2. Secondary screening of the selected hits.....	135
III.3. CHARACTERIZATION OF SUCCINATE BINDING SITE	141
III.3.1. In silico screening of a virtual library.....	141
III.3.1.1. Three-dimensional model of SUCNR1	141
III.3.1.2. Virtual screening of ZINC database	143
III.3.2. Optimization of the existing receptor model.....	145
III.3.2.1. Structural elements	145
III.3.2.1.1. Screening of analogues	145
III.3.2.1.2. Pharmacophore	147
III.3.2.2. Binding pocket	149
III.3.3. Characterization of cycloalkanes activity on SUCNR1.....	150
III.3.3.1. In vitro assays	150
III.3.3.2. In vivo assays	151

III.3.4. Other ligands.....	153
IV. CONCLUSIONS AND PERSPECTIVES.....	157
V. MATERIAL AND METHODS.....	167
V.1. CHARACTERIZATION OF SUCNR1 SIGNALING PATHWAYS AND DEVELOPMENT OF CELL-BASED ASSAYS	171
V.1.1. Protocols for transfections.....	171
V.1.1.1. Transfection using lipofectamine.....	171
V.1.1.2. Transfection using calcium phosphate.....	171
V.1.1.3. Transfection using Xtreme gene.....	171
V.1.2. Generation of stable cell lines.....	172
V.1.2.1. cAMP assay.....	172
V.1.2.2. Intracellular calcium mobilization assay.....	173
V.1.2.3. Arrestin complementation assay.....	173
V.1.2.4. Flow cytometry analysis.....	174
V.1.2.4.1. Non-permeabilized cells.....	174
V.1.2.4.2. Permeabilized cells.....	174
V.1.3. Immunofluorescence staining and confocal microscopy.....	175
V.1.4. Cell-based assays and second messengers measurement.....	175
V.1.4.1. cAMP Assay.....	175
V.1.4.2. Intracellular calcium mobilization assay.....	176
V.1.4.3. Arrestin complementation assay.....	176
V.1.4.4. Determination of ERK phosphorylation.....	176
V.1.4.5. Determination of Rho activation.....	177
V.2. SCREENING OF SUCNR1 WITH A FSK-FREE cAMP ASSAY	179
V.2.1. Calculation of Z' factor.....	179
V.2.2. Hit selection and activity cut-off criteria.....	179

<i>V.2.3. Data analysis and statistical procedure</i>	179
V.3. CHARACTERIZATION OF SUCCINATE BINDING SITE	181
<i>V.3.1. In silico models</i>	181
<i>V.3.1.1. Receptor model</i>	181
<i>V.3.1.2. Docking of the ZINC database</i>	181
<i>V.3.1.3. Pharmacophore model</i>	181
<i>V.3.2. SUCNR1 mutants</i>	182
<i>V.3.2.1. Site-Directed Mutagenesis</i>	182
<i>V.3.2.2. Transient transfection of mutants</i>	182
<i>V.3.3. In vivo experiments</i>	183
VI. BIBLIOGRAPHY	185
VII. APPENDIX	211
VII.1. SCREENING RESULTS	213
<i>VII.1.1 Primary screening</i>	213
<i>VII.1.2. Cherry pick for secondary screening</i>	238
VII.2. PUBLICATIONS RELATED TO THE DISSERTATION	239

I. INTRODUCTION

I.1. Pharmacology of G protein-coupled receptors

I.1.1. GPCRs general description

G protein-coupled receptors (GPCRs) belong to the largest known membrane receptors family in mammals (Fredriksson et al., 2003; Civelli et al., 2013), exhibiting seven transmembrane domains (7TM) as their characteristic feature (Strader et al., 1995). They couple to G proteins to mobilize second messenger pathways that lead to cellular responses and ultimately to physiological changes.

Since the pioneering works of Langley and Ehrlich at the beginning of the twentieth century, GPCRs became one of the most important pharmaceutical research areas (Langley, 1901; Limbird, 1996). They play an essential role in regulating various physiological functions (pain, neurotransmission, muscle contraction, insulin secretion, ...) and many are implicated in human diseases, making them the most druggable gene family (Overington et al., 2006). Approximately 82 GPCRs are the direct or indirect target of 30-50% of drugs currently on the market or in clinical trials for cancer, neurodegeneration, diabetes, pain, allergy, viral infection, ... (Wilson et al., 1998; Wittenberger et al., 2001; Civelli et al., 2013). In addition, some of them are expressed in therapeutically relevant tissues and may represent a source of therapeutic targets with similar potential for drug discovery as seen with known GPCRs (Wilson et al., 1998).

The completion of human genome sequence allowed the identification of 800 genes encoding GPCRs (Alexander et al., 2015). Most of these genes encode for chemosensory receptors that mediate the perception of sensory stimuli such as odors, light, sweet and bitter taste substances via specialized heterotrimeric G proteins modulating the activity of primary sensory cells (Wettschureck and Offermanns, 2005). 356 are coding for "nonsensory" GPCRs in which most are under-interrogated or poorly characterized with few physiologically relevant ligands reported, 61 are awaiting further input to be considered as orphanized and still 60 remain completely uncharacterized (Alexander et al., 2015). Although their DNA sequences look like known GPCRs, they are initially unmatched to their activating ligands and their signaling mechanisms are unknown. They

are designated as "orphan" GPCRs and are of considerable interest in enriched understanding of physiological responses. GPCRs represent an useful and important target class for therapeutic drug discovery and biochemical study (Davenport and Harmar, 2013).

The study of GPCRs is currently an intensive and exciting field of research, the 2012 Nobel Prize in chemistry was awarded jointly to Robert J. Lefkowitz and Brian K. Kobilka for studies of G-protein-coupled receptors" (NobelPrize.org, 2012). Their finding is of high interest as structure and mechanism characterization of GPCRs may help for the design of ligands and thus new drugs (Wilson et al., 1998; Jacoby et al., 2006).

I.1.2 Classification of GPCRs

GPCRs are classified into different families sharing characteristic highly conserved residues according to phylogenetic analyses and sequence homology (Fredriksson et al., 2003) as well as the various types of ligands they bind to (Foord et al., 2005).

The most recent sequence analysis proposes the clustering of human GPCRs into five groups named "GRAFS", on the basis of its five main classes : Glutamate, Rhodopsin, Adhesion, Frizzled, and Secretin (Fredriksson et al., 2003). The Rhodopsin family has the largest number of GPCRs with 719 members (284 "nonsensory" including 87 orphans (however endogenous ligand has been proposed in at least one publication for 54 of them) and 435 olfactory mostly orphans) and is divided into four α (amines, lipids, ...), β (peptides), γ (opioids, chemokines,...) and δ (glycoproteins, purines) groups.

However some orphan receptors, such as Super Conserved Receptor Expressed in Brain (SREB) show closer homology to each other than to known class A GPCRs, suggesting that they may represent new sub-families of receptors with distinct ligands. These sub-families are distributed throughout the GPCRs superfamily tree, suggesting that they will have a diverse range of functions (Wilson et al., 1998; Alexander et al., 2015).

Glutamate, frizzled and secretin families contain 12, 11 and 15 "deorphanized" GPCRs, respectively. Although the 26 adhesion members are orphans, endogenous ligand has been described in at least one publication for 6 of them (Alexander et al., 2015).

I.1.3. Structure of GPCRs

GPCRs share a common molecular architecture of 7TM helices connected by three extracellular loops (ECL1-3) and three intracellular loops (ICL1-3) which are involved in heterotrimeric G protein-coupling (*Figure I-1*) (Strader et al., 1995; Wettschureck and Offermanns, 2005).

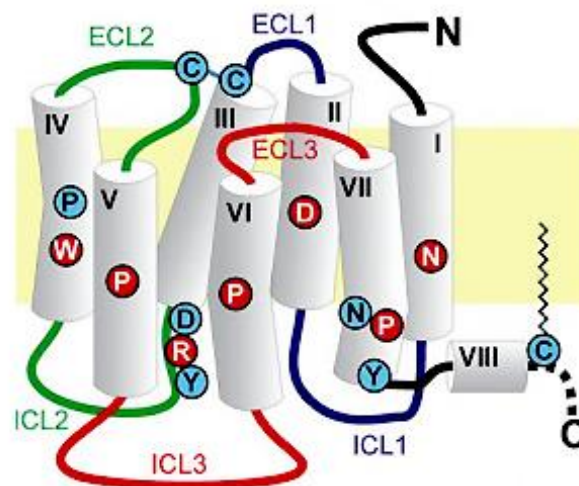


Figure I-1 : 3D general structure of GPCRs. Blue : Amino acids (AAs) conserved between GPCRs; Red : AAs conserved between GPCRs of the Rhodopsin family (Kenakin et al., 2010).

The characteristic 7TM structure was for the first time identified for rhodopsin, in 1975. However the sequence homology between β_2 -adrenoceptor and bovine rhodopsin was only revealed in the 1980s with the cloning of the adrenergic receptor. A structure-function relationship was established between the two receptors and the β_2 -adrenoceptor advances are considered as a historic breakthrough that catalyzed the molecular GPCRs research (Jacoby et al., 2006). Besides, the study of the rhodopsin

signaling mechanism highlighted its linkage to the G proteins. These significant information made rhodopsin the ideal model for other GPCRs investigations. However the speculation of a large family of such receptors with the 7TM arrangement as a fold characteristic was only confirmed in the following years by the successful cloning of other GPCRs (Jacoby et al., 2006).

Although GPCRs have been studied for almost a century, the first high-resolution structure (2.8 Å) of the rhodopsin was only available in 2000 (Palczewski, 2000). It allowed pharmacologists to understand GPCRs mechanisms and predict the overall folding of the 7TM (Audet and Bouvier, 2012). Methodological difficulties associated with the crystallization of transmembrane proteins resulted in a delay of many years in generating crystal structures of other GPCRs. But recent technological advances in engineering including the production and purification of membrane proteins, crystal formation and development of microfocus X-ray synchrotron technologies that deliver a microscale beam to a crystal, greatly contribute to the explosion of elucidated GPCRs structures. Notably in 2007, Brian K. Kobilka and co-workers published the first crystallographic structure of the active conformation of the β_2 -adrenoceptor (*Figure I-2*) (Rasmussen et al., 2011).

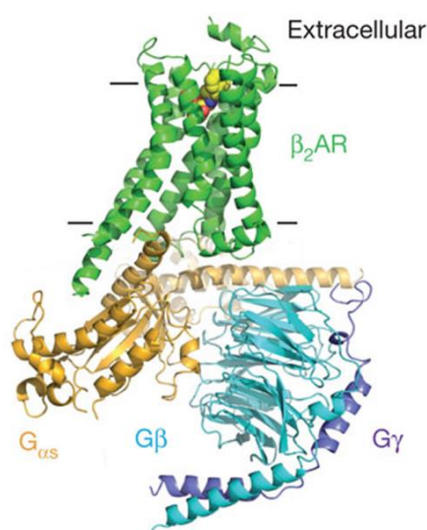


Figure I-2 : High resolution (3.2 Å) crystal structure of β_2 -adrenoceptor (green) bound to an agonist (BI-167107), interacting with the three sub-units of a G_{α_s} protein (Rasmussen et al., 2011).

Between 2007 and 2015, 47 high-resolution structures representing 13 distinct GPCRs have been solved. 20 were cocrystallized with antagonists, 16 with inverse agonists whereas 11 were cocrystallized with agonists (Audet and Bouvier, 2012; Zhang et al., 2015b). The structural and functional models that arise from them have changed our view of the way ligands bind to GPCRs and helped to understand conformational dynamics of GPCRs. In addition, GPCRs cocrystallization with G protein or G protein-mimetics provided insights into the activation processes and conformational rearrangement of the G protein (Audet and Bouvier, 2012). These studies resulted in the current paradigm that conformational changes leading to receptor activation require ligand binding and concomitant stabilization by G protein. Agonist binding promotes the folding of an active conformation and lock the receptor in a more stable state. As a consequence the receptor interacts with a G protein and triggers reliable signaling pathways (*Figure 1-2*) (Audet and Bouvier, 2012; Zhang et al., 2015b).

However GPCRs are highly dynamic proteins that adopt different conformational states and go through various transitions in their interactions with ligands and intracellular signaling. Although these crystal structures provide valuable information, they represent static frozen conformations of a single GPCR state (Millar and Newton, 2010). Therefore new biophysical techniques to monitor GPCR dynamic structural changes in relation to ligand activation are emerging (Millar and Newton, 2010). These ones include site-directed spin labelling of rhodopsin, substitution of putative interacting AA of a receptor with a labeled cysteine and tryptophan or even combination of two-dimensional nuclear magnetic resonance (NMR) spectroscopy and labelling lysine or methionine residues with ^{13}C (Millar and Newton, 2010). Recent structural dynamics study of the β_2 -adrenoceptor cytoplasmic domain revealed that unliganded or inverse-agonist-bound receptors exist predominantly in two inactive conformations that exchange within hundreds of microseconds. Stimulation with an agonist increases conformational heterogeneity (inactive, intermediate, and active states) and requires interaction with a G protein or an intracellular G protein mimetic to favor the active conformation (Manglik et al., 2015).

I.1.4. Signal transduction and regulation

Each component of the transmembrane signaling system, the receptor, the G proteins as well as the effectors can be regulated independently by additional proteins, soluble mediators, or even at transcriptional level. Upon agonist stimulation, the receptors undergo conformational changes that promote their binding to intracellular partners. Currently, three main families of proteins interacting with GPCRs have been extensively studied : heterotrimeric G proteins, G protein-coupled receptor kinases (GRKs), and arrestins. The complex organization of GPCRs provides a huge variety of signaling pathways that allow distinct cell types to respond adequately to extracellular signals (Wettschureck and Offermanns, 2005).

I.1.4.1. Heterotrimeric G proteins

GPCRs respond to a wide range of extracellular stimuli by activating intracellular signal transduction pathways that lead to second messengers changes and/or entry of ions at the plasma membrane. These elements of the signaling cascade including cyclic adenosine 3',5'-monophosphate (cAMP), adenylate cyclase (AC), intracellular free calcium ($[Ca^{2+}]_i$), inositol phosphate (IP), phospholipases, kinases and ion channels, emerged as important effector systems during 1960s and 1970s, even before knowing the molecular nature of the receptors (Jacoby et al., 2006).

A ligand activating GPCR is able to recruit one or more heterotrimeric G proteins that undergo an activation-inactivation cycle to dynamically couple activated receptors to effectors.

In the basal state, the heterotrimer composed of associated $\beta\gamma$ -complex and the GDP-bound α -subunit can be recognized by an appropriate activated receptor which couple to. This coupling promotes the exchange of GDP for GTP on the α -subunit. The GTP-bound α -subunit dissociates from the activated receptor as well as from the $\beta\gamma$ -complex. Consequently these free subunits are able to modulate the activity of effectors and thus mediate cellular responses. Signaling is ended by the intrinsic GTPase activity of the G protein α -subunit which hydrolysis the bound GTP to GDP, resulting in the re-association

of the GDP-bound α -subunit and the $\beta\gamma$ -complex (Figure I-3). The heterotrimeric G protein re-formed can then enter a new cycle if activated receptors are present.

Thirty regulators of G protein signaling (RGS proteins) are known to contribute to the deactivation of G protein-mediated signaling by increasing GTPase activity of G protein α -subunit (Wettschureck and Offermanns, 2005; Jacoby et al., 2006). Additionally to their role in the modulation of G protein-mediated signaling kinetics, they also influence the regulation of protein localization, the intracellular trafficking as well as the receptor selectivity (Magalhaes et al., 2012).

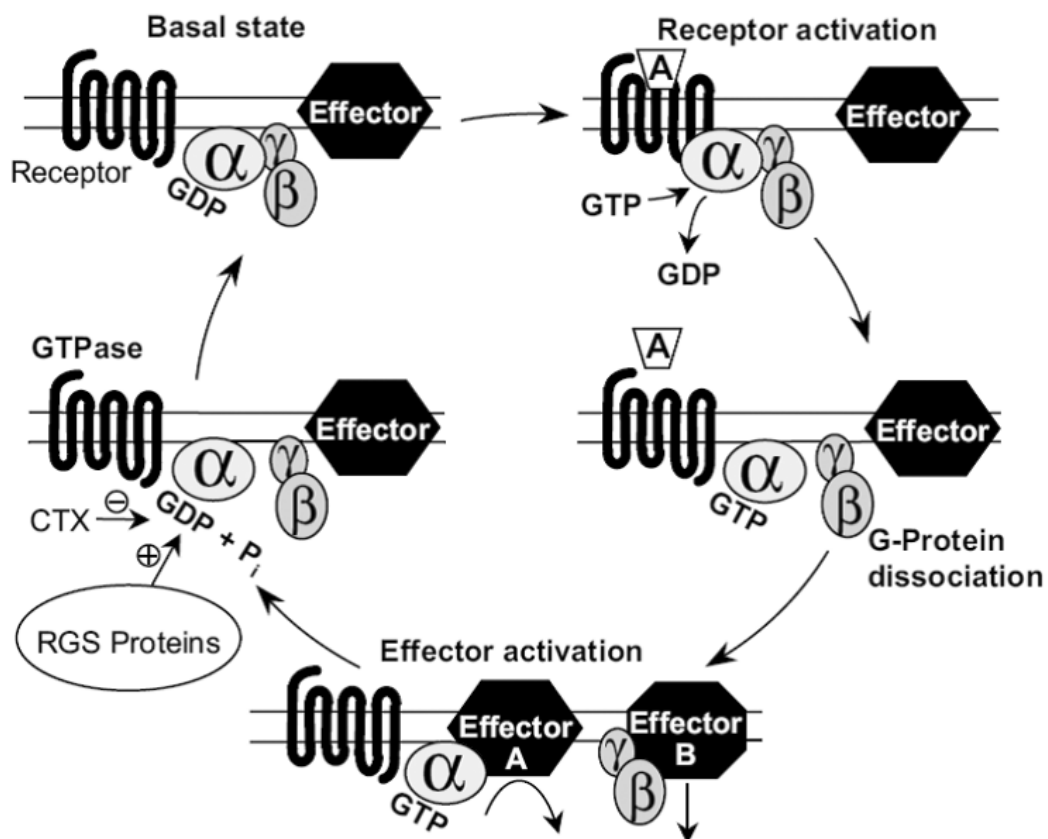


Figure I-3 : G protein activation cycle for a GPCR interacting with an agonist (Offermanns, 2003).

A GPCR can activate four main families of G_α proteins which differ in the signaling pathways they couple to (*Figure 1-4*) (Wettschureck and Offermanns, 2005) :

- G_{α_s} : this G protein subunit regulates positively cAMP through AC modulation. The AC enzyme catalyzes the conversion of adenosine triphosphate (ATP) to cAMP and inorganic pyrophosphate. In addition, AC can also be regulated by $\beta\gamma$ complex, $[Ca^{2+}]_i$, and protein kinase C (PKC).

- $G_{\alpha_i/o}$: G_{α_o} is mainly present in the nervous system and modulates the opening of voltage-gated Ca^{2+} channels. G_{α_i} family ($G_{\alpha_{i1,2,3}}$) activation induces AC shut down that leads to a downregulation of cAMP levels. G_{α_i} are also able to activate a variety of phospholipases and phosphodiesterases (PDE), and promote the opening of several ion channels.

- G_{α_q} : This family comprises five members, G_{α_q} , $G_{\alpha_{11}}$, $G_{\alpha_{14}}$, $G_{\alpha_{15}}$ and $G_{\alpha_{16}}$ that regulate the activity of phospholipase C- β (PLC- β) isoforms, resulting in the intramembrane hydrolysis of phosphatidylinositol-4,5-bisphosphate (PIP_2) to inositol-1,4,5-triphosphate (IP_3) and diacylglycerol (DAG) production. Subsequently, DAG increases the activity of protein kinases including PKC which regulate several processes inside the cell, and IP_3 triggers the release of $[Ca^{2+}]_i$ from endoplasmic reticulum to cytoplasm.

In addition, $G_{\alpha_{15}}$ and $G_{\alpha_{16}}$ are well-known to be able to link numerous G_{α_s} -, G_{α_i} - and G_{α_q} -GPCRs to PLC- β activation.

- $G_{\alpha_{12/13}}$: This last family triggers the activity of Rho GTPase (RhoA, RhoB and RhoC) mediated by GTPase-activating proteins (RhoGAPs), guanine nucleotide exchange factors (GEFs) and guanine nucleotide dissociation inhibitors (GDIs). Active Rho subsequently activates downstream effectors such as ROCK, which phosphorylates multiple cellular substrates (i.e. Rhotekin).

These $G_{\alpha_{12/13}}$ proteins are known to be involved in the formation of actomyosin-based structures and the modulation of their contractility. They also interact with numerous proteins such as cadherins, causing the release of β -catenin and induce many signaling pathways leading to various effectors. Therefore these proteins are related to cell proliferation, migration, growth and cell division (Siehler, 2007).

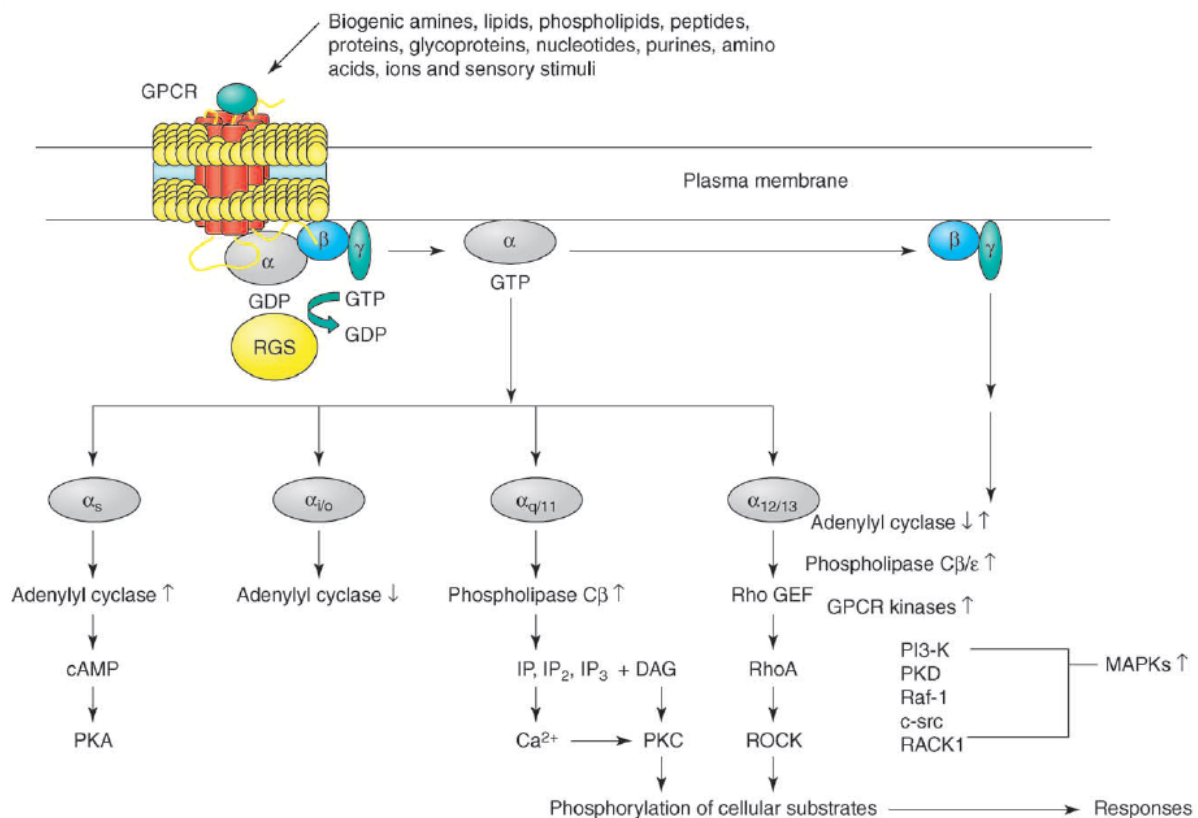


Figure I-4 : Signaling pathways of G proteins (Thomsen et al., 2005).

The second messengers modulated by G proteins, in turn, trigger activation of various signaling cascades, for instance phosphorylation events that regulate enzymes and transcription factors. A well-described example of kinases activated by an important number of GPCRs are the mitogen-activated protein kinase (MAPK) superfamily. This large group of enzymes comprises extracellular signal-regulated kinases (ERKs), c-Jun N-terminal kinases (JNKs), ERK3/4, ERK5, and p38 MAPKs. They are key components of intracellular signaling pathways that control cell proliferation, inflammation, apoptosis, ... Activation of MAPKs frequently results in their rapid translocation to the nucleus, where they phosphorylate and regulate the functional activity of various transcription factors by acting on their promoter (Gutkind, 2000; Qi and Elion, 2005). Other examples of GPCR-mediated signaling events also include phosphorylation of cytosolic factors through protein kinases A (PKA) and PKC, and also nuclear transcription factors (Brivanlou and Darnell, 2002). PKA and PKC are phosphotransferases, activated in some cell types by response to GPCR-stimulated increases in intracellular second messengers (cAMP, Ca²⁺ and DAG). The kinases can mediate the phosphorylation of downstream target proteins as well as the receptor itself (Ferguson, 2001).

$\beta\gamma$ dimers, for their part, are combinations of five known isoforms of the β subunit and thirteen known isoforms of the γ subunit. Although specific function of individual $\beta\gamma$ dimers is not fully explored, each individual isoform can associate with a set of effectors and regulators. Therefore, $\beta\gamma$ dimers themselves regulate the activity of many signaling molecules including ion channels, phospholipases, phosphoinositide kinases like phosphatidylinositol 3-kinases (PI3Ks), particular isoforms of AC and ERKs pathways (Wettschureck and Offermanns, 2005; Jacoby et al., 2006).

I.1.4.2. G protein-coupled receptor kinases (GRKs)

Seven GRKs (GRK1 - GRK7) exist and are divided into three subfamilies : GRK 1 and 7 localized to the retina; GRK 2 and 3 which interact with the $\beta\gamma$ complex via their pleckstrin homology domain; and membrane-associated GRK 4, 5, and 6. GRKs 2, 3, 5, and 6 are widely distributed in mammalian tissues (Pitcher et al., 1998). They are composed of three functional domains, an amino-terminal RGS homology domain, a central catalytic domain and a carboxyl-terminal membrane targeting domain (Ferguson, 2001).

Agonist-activated receptor (or activated conformation in case of constitutive activity) is able to recruit GRKs that translocate to the receptor and thus catalyze the phosphorylation of serine and threonine residues within either the third intracellular loop (such as M_2 receptor and A_{2A} receptor) (Nakata et al., 1994) or carboxyl-terminal tail domains (such as rhodopsin and β_2 -adrenoceptor) (Bouvier et al., 1988). They play a central role in the regulation of GPCRs, G protein signaling uncoupling (desensitization) and the endocytosis of GPCRs to endosomes to allow GPCR dephosphorylation and resensitization (Magalhaes et al., 2012). However receptor phosphorylation alone is insufficient to mediate the desensitization of many GPCRs which often requires arrestins binding (Magalhaes et al., 2012).

Besides their role as regulators of GPCR signaling at the level of the receptor, GRKs also regulate the activity of the G protein activity through their RGS domain (Ferguson, 2001). In addition, they are able to influence GPCR signaling via G protein-independent mechanisms. But still so, there are numerous factors, including the expression, activation-

deactivation, kinases and phosphatases that can regulate the phosphorylation of receptors. Indeed a receptor can be phosphorylated by different kinases at distinct sites and it is proposed that characteristic fingerprints of receptor phosphorylation exist for different cell types. This may translate to a "bar code" that directs the signaling outcome of the receptor and a different phenotype in cells (Millar and Newton, 2010).

I.1.4.3. Arrestins

I.1.4.3.1. G protein-dependent mechanism

The arrestin family consists of four isoforms (arrestin 1- arrestin 4), arrestin 1 and arrestin 4 (previously known as visual arrestin or v-arrestin and cone arrestin, respectively) are specifically localized to the visual system whereas arrestin 2 (initially termed β -adrenoceptor arrestin-1 or β -arrestin 1) and arrestin 3 (β -arrestin 2) are ubiquitously expressed (Pitcher et al., 1998). Arrestins have been widely investigated and are of important interest in physiology. For example, arrestin 2 knockout (KO) mice have altered cardiac responsiveness to β_2 -adrenoceptor stimulation (Conner et al., 1997) and arrestin 3 KO mice show enhanced morphine analgesia (Bohn et al., 1999) whereas both arrestins KO caused neonatal lethality in mice because of respiratory distress (Zhang et al., 2010).

Crystal structures of arrestins 1 and 2 in the "basal state" indicate an intact polar core at the junction of N and C domains, which are essentially composed of antiparallel β sheets, with the C tail in close proximity to the junction (*Figure I-5, inactive arrestin*) (Granzin et al., 1998; Han et al., 2001). Interaction with the phosphorylated tail of activated receptor promotes the disruption of the polar core. This leads to the activation of conformational changes in arrestin through the release of the C tail that results in the increase of the accessibility of both clathrin and AP2-binding domains (*Figure I-5, active arrestin*) (Gurevich and Gurevich, 2003; Xiao et al., 2004).

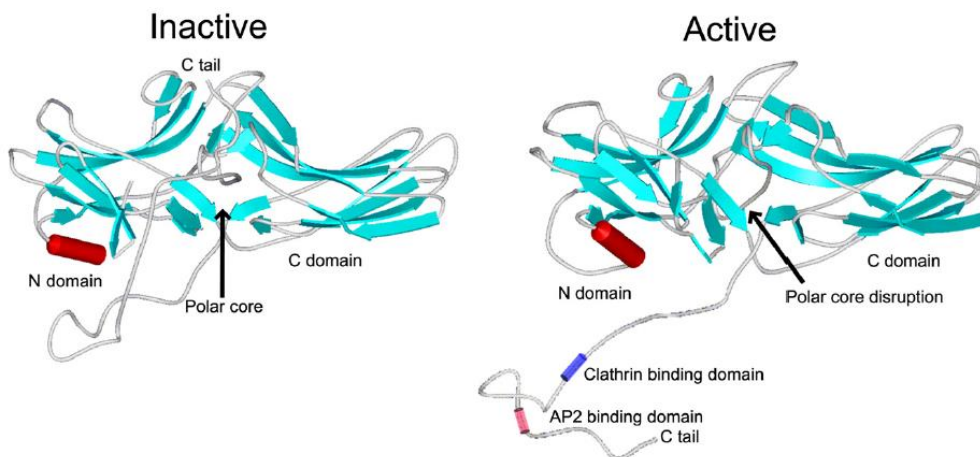


Figure 1-5 : Model of inactive and active conformations of arrestin 3 (Lefkowitz et al., 2006).

Originally arrestins were discovered as molecules that bind to activated rhodopsin or β_2 -adrenoceptor (Benovic et al., 1987; Lohse et al., 1990) contributing to desensitization by physically impairing further G protein binding or even inactivation by promoting internalization of the receptors. Next, many other GPCRs were reported to recruit arrestins and multiple endocytic mechanisms characterized by different kinetics emerged.

The activation of the receptor and its phosphorylation stabilizes a conformation state (higher arrestin binding affinity) that promotes the recruitment of arrestin. Thus the receptor-arrestin interaction competes with G protein interaction that results in the waning of G protein-dependent signal. Preventing primary signaling leads to a universal desensitization mechanism of GPCRs that may vary from attenuation of agonist potency (Von Zastrow and Kobilka, 1994) to termination of signaling (Magalhaes et al., 2012). This desensitization allows the protection against both acute and chronic receptor overstimulation (Ferguson, 2001; Kohout and Lefkowitz, 2003). Additionally PKA and PKC may also contribute to desensitization as they are able to phosphorylate both agonist-activated receptors and inactive receptors (Hausdorff et al., 1989).

Arrestins are also able to act as endocytic adaptors that link receptors to the clathrin-coated pits (Von Zastrow and Kobilka, 1994) and mediate further signaling (Kohout and

Lefkowitz, 2003; Shenoy and Lefkowitz, 2003). Arrestin can associate transiently with phosphorylated receptors, bring them to clathrin-coated pits, and then dissociate as the receptors internalize. These receptors including β_2 -adrenoceptor, belong to class A (Oakley et al., 2000; Magalhaes et al., 2012) and are generally resensitized by dephosphorylation in acidic endosomal compartment (Krueger et al., 1997) to rapidly recycle back to the membrane (*Figure I-6*) (Oakley et al., 2000; Magalhaes et al., 2012). By contrast, arrestin dissociates very slowly from class B receptors and the complex may reside for extended periods in endosomal vesicles before being degraded by lysosomes (i.e. ET_B and NTS receptors, PAR1 (Hermans et al., 1997; Trejo and Coughlin, 1999; Bremnes et al., 2000)) or slowly recycled (i.e. NK1 receptor (Grady et al., 1995)) back to the cell surface (*Figure I-6*) (Oakley et al., 2000; Magalhaes et al., 2012).

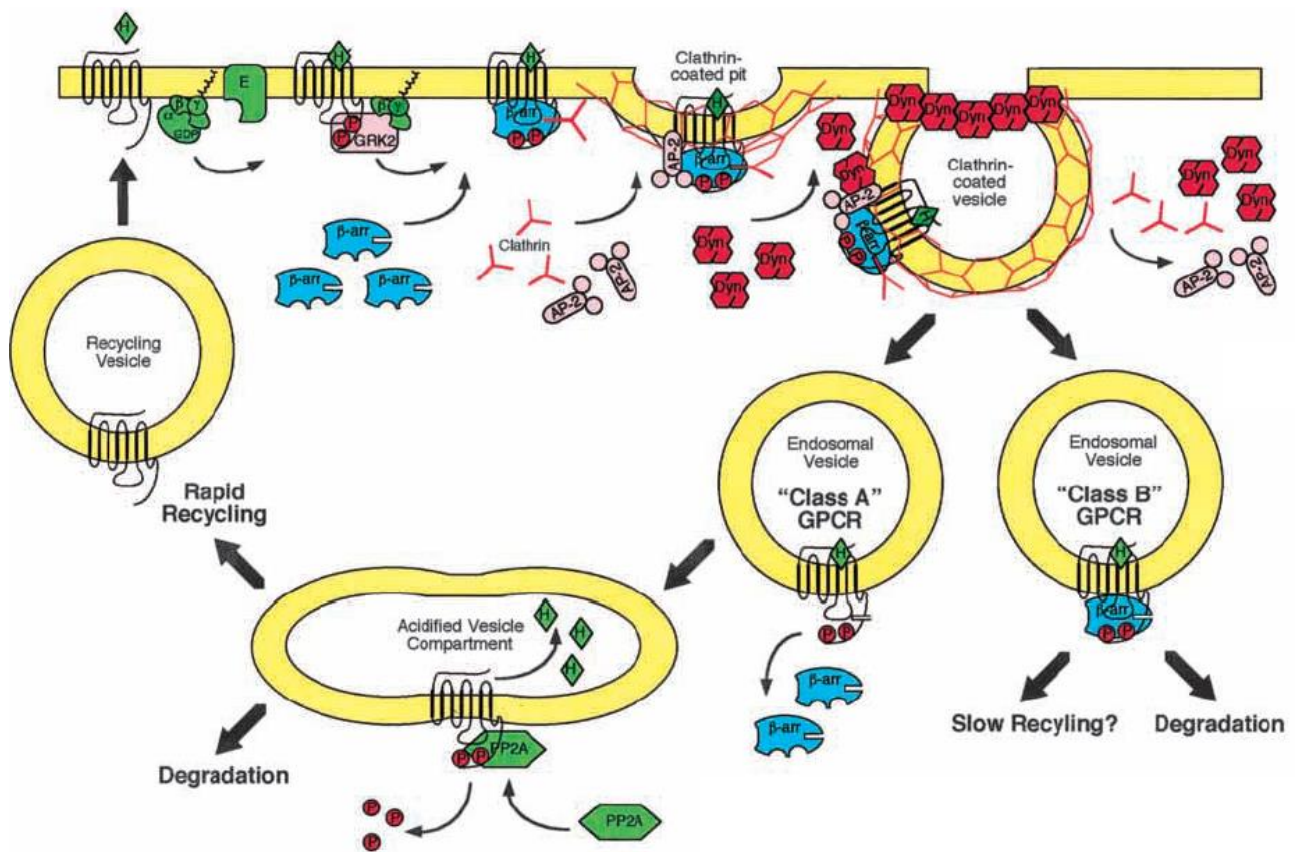


Figure I-6 : Arrestins-mediated internalization of GPCRs (Luttrell and Lefkowitz, 2002).

As a consequence GPCRs are involved in regulating receptor resensitization as well as desensitization. However kinetics of receptors endocytosis, which depend on GPCR subtype and cell line where it is expressed, are very different. Indeed receptor desensitization takes seconds to minutes whereas receptor recycling and resensitization is less efficient with a lower rate at a minimum of several minutes (Ferguson, 2001). In addition, arrestins are important for the regulation of the endocytic machinery, as they interact with protein complexes implicated in the regulation of clathrin-mediated endocytosis (Magalhaes et al., 2012).

Although arrestins represent the major mechanism of receptor internalization, several GPCRs do not require arrestins to internalize such as the secretin receptor (Walker et al., 1999), 5-HT_{2A} (Gray et al., 2001, 2003), PAR1 (Paing et al., 2002), IP (Smyth et al., 2000) or M₂ (Vögler et al., 1998) receptors. As an alternative, they can remain at the cell surface or internalize through a dynamin- and clathrin-dependent pathway, independent of arrestins (Zhang et al., 1996). But also, ligand-induced internalization can be dependent on GRK expression levels. For instance, BLT₁ internalization has been shown after leukotriene B₄ (LTB₄) stimulation in cell type that express high levels of endogenous GRK 2 or when it is overexpressed. This arrestins-independent internalization has been demonstrated to be blocked by coexpressing dominant-negative GRK 2 K220R (Chen et al., 2004). In addition, the agonist activation and the cell line in which the receptor is expressed are two important factors that regulate internalization. For example, etorphine, but not morphine, stimulates μ receptor phosphorylation and internalization in HEK293 cells whereas morphine requires GRK2 overexpression to induce phosphorylation (Zhang et al., 1998).

I.1.4.3.2. G protein-independent mechanism

In addition to their central role in GPCRs desensitization and internalization, a new paradigm shows GRKs and arrestins as being signal transducers themselves. Indeed, GPCRs are able to signal in a G protein-independent manner through arrestins that serve as adaptor and scaffold proteins, bringing molecules involved in signal transduction within spatial and thus functional proximity of each other (Lefkowitz and Shenoy, 2005). These proteins are described to dynamically assemble a wide range of multiprotein complexes that mediate receptor signaling, trafficking and degradation by modulating novel effectors through nonclassical pathways (Lefkowitz and Shenoy, 2005).

Arrestins scaffolding of intracellular signaling molecules was first demonstrated for the nonreceptor tyrosine kinase Src, facilitating activation of MAPK including ERK1/2 (Luttrell et al., 1999). Later, arrestins were identified to be involved in the recruitment of other nonreceptor tyrosine kinases (Lefkowitz and Shenoy, 2005) that results in the phosphorylation of various transcription factors (Morrison and Davis, 2003) and cytosolic substrates (Ge et al., 2003) through the activation of MAPK pathway signaling (Raf/MEK/ERK) (Azzi et al., 2003). Arrestin 3 for example, is described as a scaffold protein that aligns individual components of MAPK pathways in appropriate orientation that activates ERK1/2 as well as JNK3 (Ahn et al., 2004; Rajagopal et al., 2005).

In addition, GRKs play an important role in regulating ERK1/2 arrestin-mediated-signaling (Kim et al., 2005; Shenoy et al., 2006). More precisely GRK 5 and 6 isoforms favor ERK1/2 whereas GRK 2 and 3 behave as signaling inhibitors for AT₁ receptor (Kim et al., 2005).

In vitro the contribution of arrestins-mediated signaling pathways can be assessed with small interfering RNA (siRNA), specific inhibitors of PKC (Ahn et al., 2004) or negative mutants of arrestins (Azzi et al., 2003).

Although arrestins- and GRKs-dependent signaling pathways are largely demonstrated *in vitro*, it remains essential to establish the physiologic and pathophysiologic roles of such mechanisms *in vivo*. For instance, AT₁ receptor in the cardiovascular system was studied by Zhai et al. by using transgenic mice unable to couple to G protein signaling, they highlighted physiologic consequences (ventricular dilatation, hypertrophy and

myocardial apoptosis) that can be correlated with arrestin-mediated ERK activation (arrestin-Src-ERK signaling) (Rajagopal et al., 2005). GRKs and arrestins KO mice are also valuable tools to explore cellular responses mediated by G protein-independent signaling pathways *in vivo*. For example these models allow understanding the diversity of the effectiveness of β -blockers such as metoprolol. In addition to β -blocking action, metoprolol has been reported to signal through GRK 5 and arrestin 2-dependent pathway. This results in an expression of fibrotic genes increase that is responsible for cardiac fibrosis in cardiomyocytes and lead to cardiac dysfunction (Nakaya et al., 2012).

It seems likely that these G protein-independent mechanisms will lead to distinct physiological consequences due to their kinetics features. For example the initial phase of $G_{\alpha q}$ signaling is rapid and transient (inferior to 5 minutes) whereas arrestins signal in a slower and persistent manner (superior to 20 minutes) (Ahn et al., 2004; Kim et al., 2005; Lefkowitz et al., 2006). Another difference is the G protein-dependent distribution of the activated MAPK including ERK1/2, which accumulates in the nucleus where it phosphorylates and activates various transcription factors. In contrast ERK1/2 arrestin-mediated is confined to a cytoplasmic compartment where it presumably phosphorylates a distinct set of effectors (Kim et al., 2005).

As a consequence of arrestins acting as scaffolds and signal transducers, the diversity of signaling possibilities for a single receptor are significantly increased. In addition, it suggests that arrestins are involved in many physiological and pathophysiological cellular processes including chemotaxis, metastasis, apoptosis and behavior (Lefkowitz et al., 2006).

I.1.4.4. Other mechanisms for the modulation of GPCRs signaling

The preponderance of GPCRs and intracellular molecules is dynamically regulated at many levels from their biosynthesis including gene transcription, translation, and post-translation through their trafficking to the cell membrane. Many intracellular proteins including chaperones facilitate GPCRs translocation to the plasma membrane and thus their cell-surface expression (Millar and Newton, 2010). Once at the cell surface, GPCRs may interact with a wide variety of accessory proteins that modulate ligand affinity and selectivity, G protein-coupling and signaling, cytoskeletal and extracellular matrix interactions, as well as receptor desensitization and internalization (Millar and Newton, 2010; Magalhaes et al., 2012). These proteins may induce GPCRs phosphorylation, acetylation, palmitoylation, ubiquitination, and myristoylation that also modify receptor functional properties (Millar and Newton, 2010). Interactions with these proteins also allow the formation of novel signal transduction complexes that alter cellular functions.

In addition, GPCRs may undergo homo- or hetero-oligomerization to induce transactivation of other receptors or signal modification (Millar and Newton, 2010). They are designated as "homomeric/heteromeric receptors" when inactive monomers become active in binding or signaling as oligomers. For example GABA_{B1} when expressed alone is able to bind ligands but is non-functional. Co-expression of GABA_{B1} and GABA_{B2} leads to the formation of a heteromeric functional complex where GABA_{B2} mediates G protein-coupled signaling (Ahmad et al., 2015).

In contrast receptors that are intrinsically active as monomers but have new activities as oligomers are called "receptor homomers/heteromers" (Ferré et al., 2010). Oligomerization of GPCRs can affect receptor function either by influencing their signaling and diversifying the pharmacological responses or through "transactivation" in which oligomerization of two defective receptors is able to restore receptor functionality. For example, monomers D₁ and D₂ signal through G_{αs} and G_{αi}, respectively, whereas D₁/D₂ heteromers trigger G_{αq} signaling pathway, the more used in the brain, suggesting predominance of heteromers *in vivo* (Millar and Newton, 2010).

The discovery that some GPCRs appear to function in complexes with other signal transduction and scaffolding proteins highlighted numerous additional GPCR activities and offer many novel therapeutic possibilities (Jacoby et al., 2006). For example the understanding of side effects of a drug, rimonabant, a CB₁ receptor antagonist used as a medication to aid smoking cessation is associated with appetite suppression because of CB₁ receptor dimerization with appetite-stimulating OX₁ receptor, also antagonized by the drug (Millar and Newton, 2010).

I.1.5. GPCRs Ligands

I.1.5.1. Nature of ligands

The endogenous ligands for GPCRs have tremendous variations including ions, small molecules (organic odorants, amines, metabolites, ...), peptides, proteins, lipids, nucleotides, and photons. Analyses of physical properties of crystallized GPCR-ligand complexes revealed ligand properties important for crystallization propensity (an appropriate ligand improves receptor stability) such as thermal stability upon ligand binding, molecular weight between 200 and 500 kDa, easy access to the binding pocket, high affinity, sufficient solubility to remain in solution at the concentrations required to provide complete occupancy of the ligand-binding site and hydrogen bond-forming capacity (Zhang et al., 2015b).

I.1.5.2. Affinity and efficacy of ligands

To characterize a ligand-receptor pair, two fundamental and distinct parameters need to be determined : its propensity to bind to the receptor and its ability to produce a response once bound.

The capacity of a ligand to bind a receptor through electrostatic, hydrogen or Van der Waals interactions determines its affinity for one state of the receptor, resulting in the increase of the population of receptors in that conformation (Wermuth, 2008).

Ligand affinity for a protein is characterized by a dissociation constant K_D (equivalent to the ratio of the rate that the ligand leaves the surface of the protein (k_{off}) and the rate it approaches the protein surface (k_{on})), usually determined with saturation experiment with a radioactively labeled ligand (Wermuth, 2008; Kenakin, 2014). Competition-binding assays are performed to determine IC_{50} (of unlabeled ligand), which represents the ligand concentration that decreases half the radioactivity (*Figure I-7*). Classically labeled ligands are used to saturate all the binding sites of the receptor and evaluate the ability of an unlabeled ligand to displace it (Wermuth, 2008; Kenakin, 2014).

K_i and IC_{50} are used to compare affinity for receptors, a lower IC_{50} means a higher affinity for the receptor (Wermuth, 2008). The relation between these parameters is based on Cheng-Prusoff equation : $K_i = IC_{50}/(1 + ([L]/K_D))$ (Cheng and Prusoff, 1973).

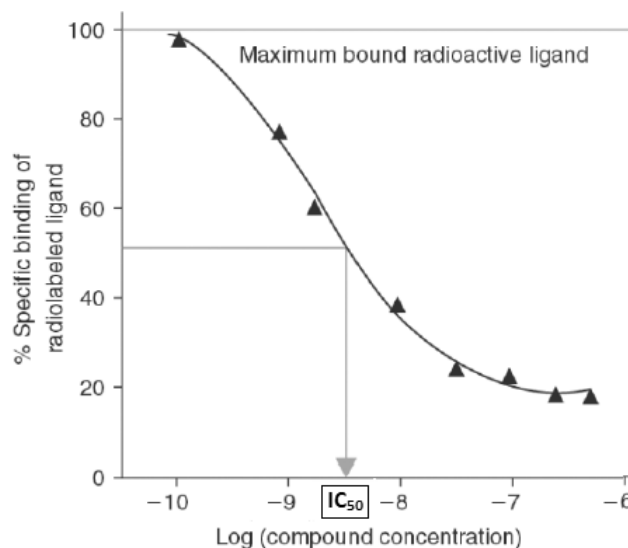


Figure I-7 : Theoretical curve of affinity of unlabeled ligand that displaces labeled bound ligand (Wermuth, 2008).

As a GPCR is a dynamic protein existing at equilibrium between numerous active and inactive states, classically the efficacy of a ligand represents its ability to displace this equilibrium. However the definition of the efficacy can be expanded to a wide variety of GPCRs behaviors (G proteins interaction, desensitization, internalization or oligomerization) as the property of a ligand to cause the receptor to change its behavior toward the host cell. The efficacy of a ligand is influenced by the coupling efficiency of the receptor pathway of interest and the receptor concentration (Kenakin, 2002; Wermuth, 2008). The comparison of efficacy of different ligands is based on their medium effective concentration, EC_{50} which corresponds to the ligand concentration required to get half the maximum efficacy (E_{max} ; maximal response capable of being produced in a given system) (Figure I-8). A lower EC_{50} means a better efficacy at lower concentrations (Wermuth, 2008).

IC_{50} is used to define the concentration of a blocker that reduces by 50% the maximum efficacy of the system (Wermuth, 2008).

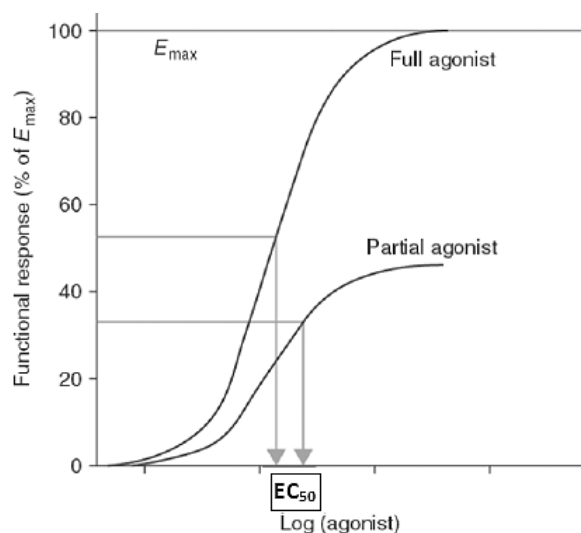


Figure 1-8 : Theoretical concentration-response curves of different ligands (Wermuth, 2008).

1.1.5.3. Classification of ligands

GPCRs are subject to constant local folding and unfolding reactions occurring in different regions that expose crucial regions. Therefore a receptor can adopt numerous micro-conformations, some of them are related to active states capable of producing a pharmacological effect. A ligand interacts with a GPCR binding site, which can promote receptor folding and stabilization (Kenakin, 2002; Congreve et al., 2011).

GPCR ligands are divided into two main categories, agonists and antagonists that promote and block receptor activation, respectively.

An agonist is a ligand that preferentially binds to and stabilizes active conformations of the GPCR that results in locking the receptor in a stable state and in a biological response increase. Full agonists stimulate the maximum capacity of the receptor (an endogenous ligand is classically considered as a full agonist) whereas a partial agonist does not reach

the maximum response capacity. The designation of full versus partial agonist is system-dependent, and a full agonist for one tissue or measurement might be a partial agonist in another (Jacoby et al., 2006; Congreve et al., 2011).

Antagonists can be subdivided into inverse agonists (See I.1.5.4.) and neutral antagonists, these ones block receptor activation by preventing the binding of agonists or inverse agonists to the receptor. In competitive antagonism, the binding of the agonist and antagonist is mutually exclusive, either because the agonist and antagonist compete for the same binding site or combine with spatially adjacent and overlapping binding sites (synoptic interaction) or occupy different binding sites in such way that simultaneous binding is impossible (Jacoby et al., 2006).

A non-endogenous agonist may combine either with the same site as the natural agonist (primary or orthosteric site) or with a topographically site distinct from the orthosteric one (allosteric or allotropic site), such that the receptor is able to accommodate two ligands simultaneously. An allosteric modulator is a ligand that enhances (PAM, positive allosteric modulator) or inhibits (NAM, negative allosteric modulator) the action of an orthosteric agonist or antagonist by simultaneously combining with an allosteric site on the receptor (Jacoby et al., 2006; Congreve et al., 2011). The effect of the allosteric modulator is dependent of the orthosteric ligand (Lazareno et al., 2000) but it is also able to directly activate the receptor in absence of orthosteric agonist (Langmead and Christopoulos, 2006).

I.1.5.4. Constitutive activity

Constitutive or intrinsic activity of a GPCR is defined by its ability to adopt constitutively or spontaneously an active conformation allowing the interaction with G proteins or regulatory proteins and subsequently triggering functional responses in the absence of ligand (Kenakin et al., 2010). This GPCR characteristic was introduced in 1989 with the description of antagonists able to inhibit basal GTPase activity with negative intrinsic activity at an endogenously expressed δ receptor (Costa and Herz, 1989). This kind of ligands that are able to specifically block constitutive activity, are nowadays commonly called inverse agonists. Further convincing data obtained with artificially generated constitutively active mutants (CAM) confirmed the concept of receptors constitutive activity (Smit et al., 2007). This GPCR ability is induced either by selective mutations in the sequence or by expression at high levels in the cell (Dunlop and Eglen, 2004). Many studies have shown that single point mutations of conserved motifs result in a loss of an intramolecular interaction that results in a constitutive activity (Parnot et al., 2002). For example, Hase et al. showed the importance of the DRY motif for G_{α_i} activation of the GPR20 receptor because the mutant R148A is not able to inhibit prostaglandin E₂-induced cAMP formation (Hase et al., 2008). In addition, N-terminus domain might maintain the constitutive activity by acting as a tethered intramolecular ligand in MC₄ receptor as well as deletion or specific mutations in the N-terminus impairs GPR61 constitutive activity (Toyooka et al., 2009).

However constitutive activity might reflect the presence of an endogenous ligand that either is difficult to remove or which is produced by the cell. For example the constitutive activity of FFA1 receptor is actually due to a permanent occupation of the receptor binding site by its endogenous FFA ligand (Ahmad et al., 2015). In addition, an inverse agonist might be responsible for the constitutive activity by stabilizing an inactive conformational state of the receptor, leading to a reduced signaling background (Toyooka et al., 2009). Finally an inverse agonist might improve GPCR expression at membrane by reducing internalization, enhancing membrane trafficking, and assisting in receptor folding (Zhang et al., 2015b).

I.1.5.5. Biased ligands

Although GPCRs have been described for a long time as being able to couple to multiple G proteins and activate various signaling pathways, some ligands were identified as possessing different efficacies toward separate pathways. In recent years such ligands have been called biased ligands.

A biased ligand favors one response over another (G protein, arrestin or another direct signaling partner of the GPCR) compared with the endogenous ligand, which is considered to be neutral (Rajagopal et al., 2010b). Indeed, an agonist toward a specific signaling pathway can act, through the same receptor, as an antagonist on a different pathway in the same cell (Galandrin et al., 2007). For example, ICI118551 and propranolol ligands for β_2 -adrenoceptor are inverse agonists of the G_{α_s} pathway whereas they have partial agonist efficacy on the arrestin-dependent MAPK pathway (Azzi et al., 2003).

The biased ligands concept is mechanistically explained by their capacity to selectively stabilize different receptor conformations that differ in their propensities to activate the various signaling pathways (Galandrin et al., 2007; Millar and Newton, 2010; Magalhaes et al., 2012).

This phenomenon might provide new insights in specific ligands that will restrict off-target effects of new developed drugs (Lefkowitz and Shenoy, 2005; Millar and Newton, 2010). In addition selectively blocking GPCR desensitization may improve a long-term agonist treatment or may even avoid the need to use receptor agonists (Ferguson, 2001). All currently known angiotensin receptor blockers and β -blockers act as antagonists for both signaling (McMurray and Pfeffer, 2005) but biased antagonists would provide great benefits in cardiovascular diseases by blocking the deleterious effects of chronic G protein signaling and simultaneously engage cytoprotective and anti-apoptotic arrestin signaling pathways (Lefkowitz et al., 2006).

However selective ligands might complicate the choice of an assay for a screening campaign which should measure the appropriate intracellular signal involved in desired phenotypic response of a cell for a disease state or pathophysiology (Millar and Newton, 2010). In addition, potential therapeutic compounds identified by high-throughput screening (HTS) based on a single signaling pathway will require deeper pharmacological investigations (Galandrin et al., 2007).

I.2. SUCNR1

I.2.1. "Deorphanization" and characterization of SUCNR1

Succinate receptor 1 or SUCNR1 (Figure I-9) (Davenport et al., 2013) was first spotted in a megacaryocytic cell line in 1995 and called "P2_{U2}", a name coined for its homology with the purinergic receptor P2Y₂, known as P2_U at that time (Gonzalez et al., 2004). SUCNR1 gene was later re-discovered as *GPR91* in 2001 on human chromosome 3q24-3q25 using an expressed sequence tag data mining strategy (Wittenberger et al., 2001).

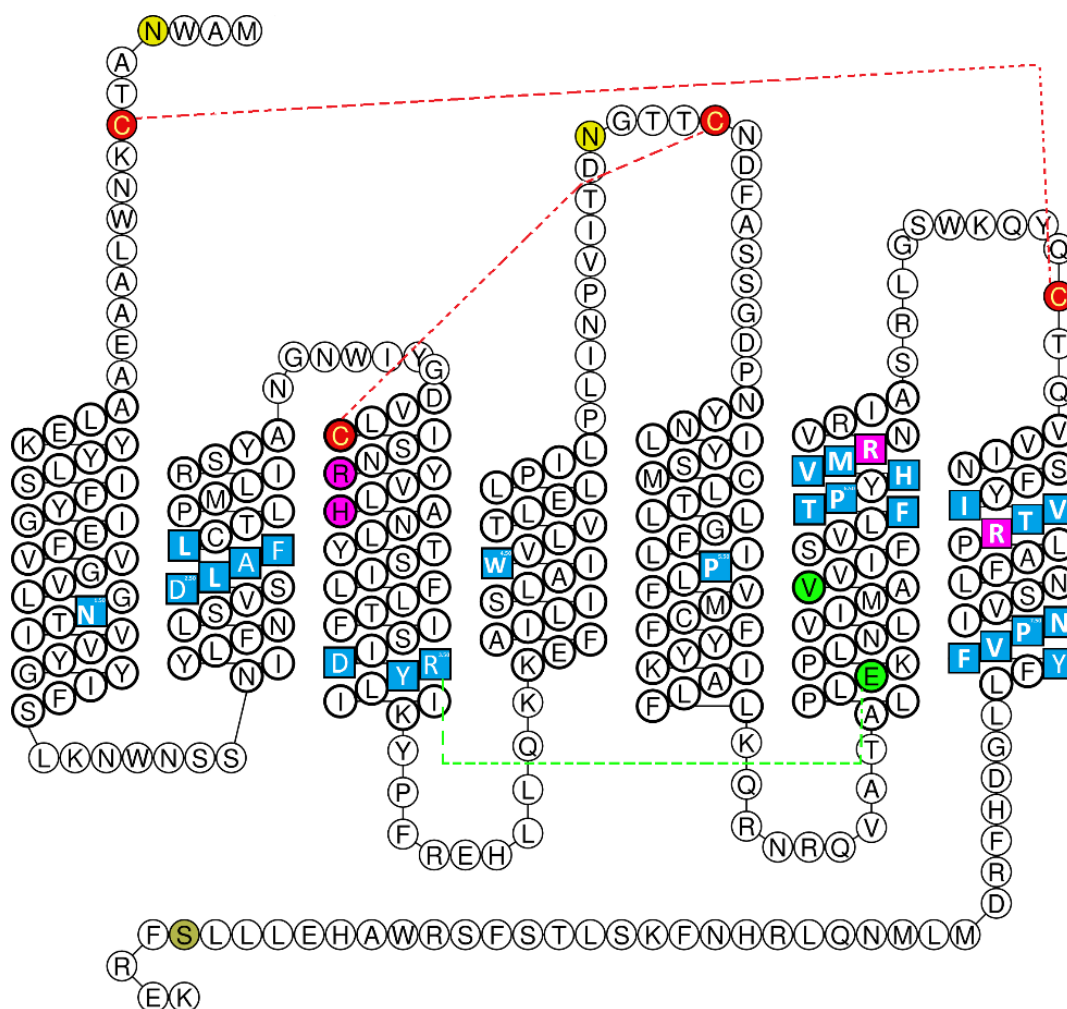


Figure I-9 : Snake plot of SUCNR1. Blue : AAs conserved within rhodopsin family; Red : disulphide bridges; Green : V^{6.42} may exclude the formation of an ionic lock between E^{6.32} and the DRY motif; Yellow : glycosylation sites; Brown : phosphorylation site; Purple : AAs involved in the interaction SUCNR1-succinate (Gilissen et al., 2016).

It encodes a protein of 330 AAs which shares a high degree of homology between human and mouse (68%) with exception of the C-terminus, which is 12 AAs shorter in rodents (Wittenberger et al., 2001; Ariza et al., 2012).

SUCNR1 belongs to the δ group of rhodopsin-like GPCRs family (Fredriksson et al., 2003) and was initially viewed as a purinergic receptor due to its high sequence homology with P2Y receptors (29% with P2Y₁ (Wittenberger et al., 2001)). P2Y family was described as a local gene amplification and genes encoding for these receptors were classified according to their chromosomal localization in two subgroups, "a" constituted of genes present on chromosome 3q24 and "b" are genes clustered on one hand to chromosome 11q13.5 and on the other hand on chromosome 3q24-25.1. These two subgroups are composed of nucleotide-receptors whereas "n" represent the related non-nucleotide receptors (*Figure I-10*) (Wittenberger et al., 2002).

Although it was predicted to bind purinergic ligands (Joost and Methner, 2002; Wittenberger et al., 2002; Fredriksson et al., 2003), SUCNR1 has been paired by He et al. with a molecule not even remotely similar to purines, i.e. succinate (He et al., 2004). Interestingly GPR99 (homology of 33%), the closest homologue of SUCNR1 (Wittenberger et al., 2002) also has a citric acid cycle intermediate as a natural ligand, α -ketoglutarate (Wittenberger et al., 2002; He et al., 2004).

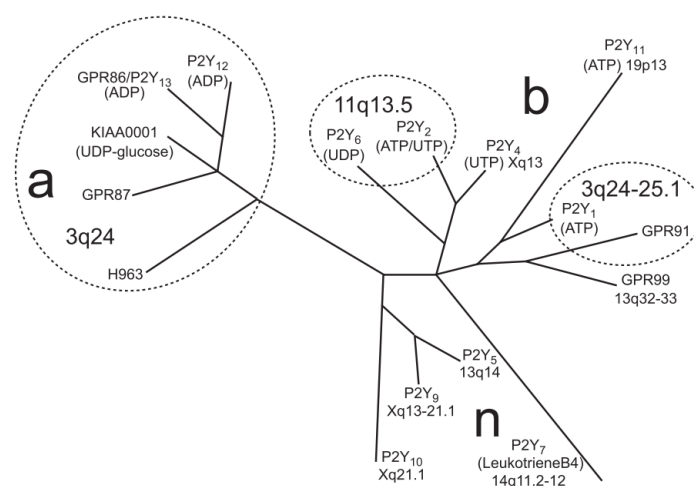


Figure I-10 : Phylogenetic analysis of P2Y human family (Wittenberger et al., 2002).

Succinate is a citric acid cycle intermediate (*Figure I-11*), which is generated in mitochondria from succinyl-CoA by succinyl-CoA synthetase and subsequently oxidized to fumarate by succinate dehydrogenase (SDH).

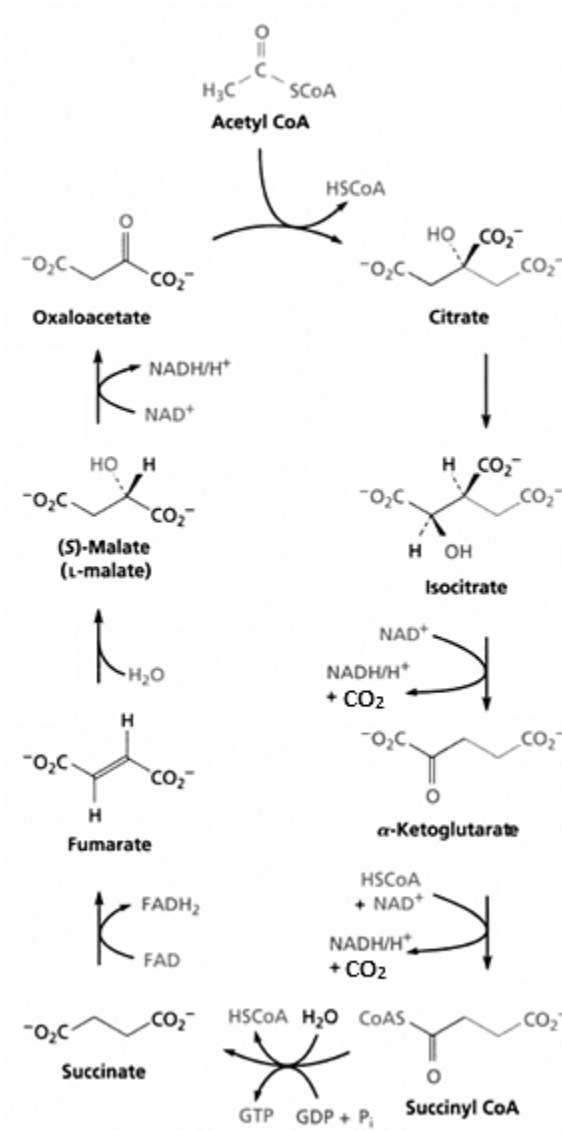


Figure I-11 : Citric acid cycle (McMurry, J.B., 2005).

SDH also called complex II takes part in the electron transport chain and indirectly depends on the availability of oxygen (*Figure I-12*) (Deen and Robben, 2011). Although succinate is produced in mitochondria, it has been reported in the systemic circulation with mean plasma levels around 1-20 μM (Kushnir et al., 2002; He et al., 2004; Toma et al., 2008).

Indeed succinate can also accumulate in cytosol and outside the cell in case of oxygen deprivation due to the mismatch of energy supply and demand (Feldkamp et al., 2004; Hebert, 2004; Toma et al., 2008; Peti-Peterdi et al., 2012). Chouchani et al. have demonstrated that succinate increase during ischemia is related to SDH reverse activity, reducing fumarate which is generated from malate/aspartate shuttle and the purine nucleotide cycle (Chouchani et al., 2014).

But also in conditions of mitochondrial stress, non-oxidized flavine, nicotinamide nucleotide and reactive oxygen species inhibit SDH resulting in a shunt of citric acid cycle followed by a succinate accumulation (Fedotcheva et al., 2006; Sapielha et al., 2009; Peti-Peterdi et al., 2012).

In addition, altered metabolism including chronic hyperglycaemia, may lead to intracellular accumulation and release of succinate into the blood stream (Deen and Robben, 2011; Ariza et al., 2012). This pathology characterized by changes in energy balance affects the concentration of succinate by increasing the activity of the citric acid cycle and the H^+ gradient across the mitochondrial membrane (Figure I-12) leading to inhibition of enzymatic steps mediated by complexes within the electron transport chain (i.e. SDH).

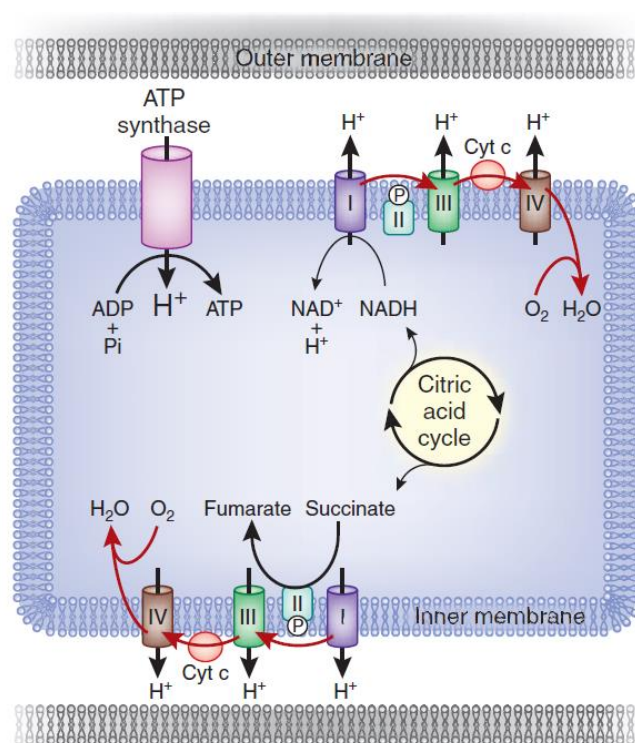


Figure I-12 : Generation of succinate in mitochondria (Deen and Robben, 2011).

Since negatively charged succinate is unable to efficiently diffuse through membranes, it requires specific dicarboxylate transporters, such as SLC25A10, to facilitate its transport from within the mitochondria to the cytosol. Subsequently, the transport of succinate across the outer mitochondrial membrane occurs through porins, which are large channels permeable to most molecules under 1.5 kDa. Dicarboxylate carriers and organic anion transporters are expressed in high amounts in the kidney, where they might be involved in extracellular succinate accumulation (Vargas et al., 2009).

Although succinate has been extensively studied for many years in the context of energy production, the receptor ligand pair is now described as a metabolism sensor (Hems and Brosnan, 1970; He et al., 2004) that may constitute an important regulator of basic physiology. According to the current paradigm, succinate activates SUCNR1 signaling pathways for the detection of local stress, including ischemia, hypoxia, toxicity, and hyperglycaemia, that affects cellular metabolism and pathophysiology of diseases in multiple organs (Gilissen et al., 2016).

1.2.2. Implications in (patho)physiology

For the past ten years, a lot of studies have investigated the roles of SUCNR1 in several *in vivo* and *in vitro* systems and identified its expression at the mRNA or protein level in almost all organs and many tissues, including the liver, spleen, breast (He et al., 2004), heart (Aguiar et al., 2010), brain (Hamel et al., 2014), retina (Sapieha et al., 2008; Hu et al., 2013; Li et al., 2014), blood vessels and immune cells (Macaulay et al., 2007; Rubic et al., 2008; Hakak et al., 2009). Nevertheless SUCNR1 is expressed most abundantly in the kidney, adipocytes and adipose tissues (Wittenberger et al., 2001; He et al., 2004; Regard et al., 2008) as well as platelets (Macaulay et al., 2007; Högberg et al., 2011).

Although SUCNR1-deficient mice are viable and have no obvious phenotype (He et al., 2004), several *in vivo* studies highlighted a link between succinate physiology and signaling function through SUCNR1 activation. Indeed its implication has been well-documented in renin-induced hypertension (He et al., 2004; Sadagopan et al., 2007; Toma et al., 2008; Robben et al., 2009; Pluznick and Caplan, 2015), ischemia/reperfusion injury,

inflammation and immune response, platelet aggregation (Macaulay et al., 2007; Högberg et al., 2011; Spath et al., 2012) and retinal angiogenesis (Hu et al., 2013, 2015; Li et al., 2014). In addition, the SUCNR1-induced increase of blood pressure may contribute to diabetic nephropathy (Toma et al., 2008; Robben et al., 2009) or cardiac hypertrophy (Aguilar et al., 2010, 2014). In a recent review, we discussed the link between SUCNR1 signaling pathways and its pathophysiological roles in multiple organs (Gilissen et al., 2016).

1.2.3. Ligands and binding pocket

During a GPCRs deorphanization campaign in 2004, fractions from pig kidney extracts specifically increased $[Ca^{2+}]_i$ on Chinese hamster ovary (CHO cells) cells heterologously transfected with SUCNR1. After the purification of the ligand by ion-exchange, size-exclusion and reversed-phase fast performance liquid chromatography/high-performance liquid chromatography, its chemical structure was revealed by mass spectrometry and NMR analyses (1H and ^{13}C NMR) to be succinic acid (SA). The succinate-induced increase in $[Ca^{2+}]_i$ was further confirmed with a fluorimetric imaging plate reader (FLIPR) system in the human embryonic kidney cell line (HEK293 cells) stably expressing human SUCNR1 and EC_{50} was determined as $28 \pm 5 \mu M$ (He et al., 2004). In mouse, succinate intravenous infusion induces an increase in blood pressure contrary to SUCNR1-deficient animals. In both mouse lines angiotensin II-induced hypertension was similar (He et al., 2004).

In their seminal article, He et al. assayed on the receptor 800 pharmacologically active compounds as well as 200 carboxylic acids and structurally related analogues, including other citric acid cycle intermediates. None of them was able to fully activate the receptor. Thus, the authors proposed that succinate response was highly specific, although the structures and identity of the compounds were not disclosed. Only maleate and methylmalonate were able to induce a response with 5- to 10-fold lower potency compared to succinate (He et al., 2004).

In addition, He et al. proposed a partial three-dimensional (3D) model of SUCNR1 generated from bovine rhodopsin. They demonstrated, through site-directed mutagenesis experiments, the importance of four positively charged AAs for activation, R99^{3.29}, R281^{7.39}, R252^{6.55} and H101^{3.33} (superscript indicates residue numbering using

Ballesteros-Weinstein nomenclature (Ballesteros, J., & Weinstein, 1995)) that may provide an electrostatic environment for succinate binding (He et al., 2004).

Up to now no synthetic agonists and very few ligands have been described as antagonists for SUCNR1 (Bhuniya et al., 2011).

In 2011, Bhuniya et al. reported a screening hit with antagonist profile following HTS. This hit compound was the first one reported as able to inhibit succinate mediated $[Ca^{2+}]_i$ mobilization ($IC_{50} = 0.8 \mu M$) in CHO-K1 cells overexpressing human SUCNR1. A structure-activity relationships (SAR) study provided potent and selective (with respect to GPR99) antagonists with IC_{50} in the nanomolar range. 2c and 4c antagonists (*Figure I-13*) were demonstrated to inhibit succinate-induced blood pressure in rat (Bhuniya et al., 2011). Recently, this family of compounds was used to generate ^{99m}Tc and ^{18}F radiotracers that may be useful for competition or labeling studies (Klenc et al., 2015).

However the pharmacological profile of these compounds was not investigated in other cell lines and still needs to be confirmed independently. In addition, the binding site for these compounds remains elusive because no competitive binding with succinate was performed. Interestingly, these antagonists showed no obvious structural relationship to succinate and no negative charges at physiological pH. Therefore it is tempting to speculate that the compounds might actually bind to a remote site compared to succinate and act as allosteric antagonists. These modulators represent interesting tools for the validation of the receptor as drug target, but require deeper pharmacological characterization.

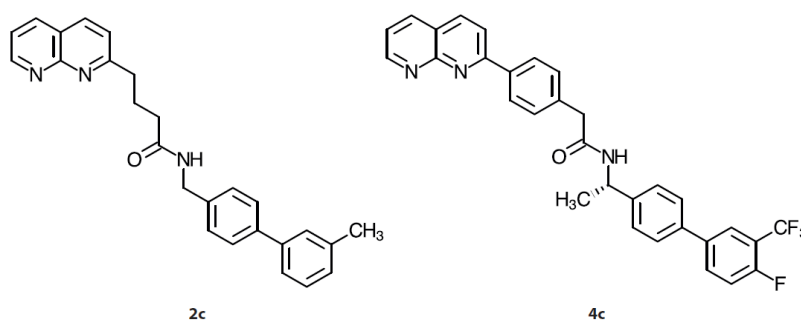


Figure I-13 : Antagonists 2c and 4c described by Bhuniya et al. (Bhuniya et al., 2011).

I.2.4. Signaling pathways

SUCNR1 was originally described as being coupled to both $G_{\alpha i}$ and $G_{\alpha q}$ proteins in HEK293 cells (He et al., 2004). The initial results were later confirmed by Robben et al., in polarized Madin Darby Canine Kidney (MDCK) cells (Robben et al., 2009). Several authors repeatedly confirmed $G_{\alpha i}$ activation by demonstrating a decrease of cAMP levels upon succinate binding to SUCNR1, in both heterologous and native systems (Hakak et al., 2009; Gnana-Prakasam et al., 2011; Högberg et al., 2011; Sundström et al., 2013). However, the view of SUCNR1 being coupled to $G_{\alpha q}$ has been challenged and Sundström et al. proposed that the observed $[Ca^{2+}]_i$ mobilization was a consequence of PLC- β activation by the $\beta\gamma$ dimer (Sundström et al., 2013).

In initial and further studies, authors also showed that succinate binding to SUCNR1 triggers the MAPKs pathway, especially ERK1/2 in HEK293 cells (He, et al., 2004), MDCK (Robben, et al., 2009), immature dendritic cells (Rubic et al., 2008), retinal ganglion neuronal cell line (Hu et al., 2013), TF-1 (human erythroleukaemia cell line) and cardiomyocytes (Aguiar et al., 2010). More precisely Robben et al. measured a transient ERK1/2 increase (inferior to 10 minutes), which reached its maximum at 2 minutes after addition of ligand in MDCK cells. This transient increase is usually associated with migration of p-ERK1/2 to the nucleus and cell proliferation (Robben, et al., 2009). Some results indicated that ERK activation is $G_{\alpha i}$ -dependent and would probably be mediated through the dimer $\beta\gamma$ (Hakak, et al., 2009).

Regarding internalization of the receptor and implication of arrestins in such mechanism, there are some discrepancies in literature that require more investigations. Although SUCNR1 is internalized into vesicular structures upon succinate exposure in HEK293 cells (He, et al., 2004), Robben et al., demonstrated that SUCNR1 is rapidly desensitized and resensitized but not internalized in polarized MDCK cells (Robben, et al., 2009). Högberg et al. also showed desensitization of SUCNR1 in platelets (Högberg, et al., 2011). In addition, SUCNR1 has been described as weakly coupled to arrestin 3 (Southern, et al., 2013).

I.3. Methods for the identification of ligands for GPCRs

I.3.1. Interest of ligands

Although the majority of orphan receptors remain without any known function, some of them have been partially characterized with genetic approaches. Indeed KO technologies (siRNA or KO animals for instance) which produce highly specific deletion of individual proteins, are commonly used to characterize GPCRs biological roles and their involvement in different pathophysiological conditions such as cancer, neurodegenerative disorders and metabolic diseases (Lazo et al., 2007). However comparison between KO and wild type (WT) populations might not highlight a particular phenotype in absence of an agonist (Jacoby et al., 2006). In addition, gene deficiency approach is not adapted to study splice variants or the functions of multiple independent domains within an individual protein. Finally, transgenic animals are restricted to few species, mostly mice for mammals, in which the gene removed from birth, as opposed to when it is eliminated in adult life by a drug, might bring into effect compensating mechanisms (Lazo et al., 2007; Kenakin, 2014).

Besides, the analysis of tissue distribution of the receptors can be helpful to postulate or identify their functions. Indeed biological expression and localization of GPCRs would be related to the potential physiological function and therapeutic indication of these proteins (Sчена et al., 1995). For example, although GPR22 was identified to be expressed in brain and heart (O'Dowd et al., 1997), murine GPR22 KO model did not lead to evidence any differences in heart morphology or function compared to WT population. However, in a model of cardiac hypertrophy, GPR22^{-/-} animals were shown to be slightly more prone to heart failure, resulting in a mild cardioprotective phenotype (Adams et al., 2008).

Therefore, ligands are an absolute prerequisite to dissect mechanisms and confirm the involvement of the target in pathological conditions or disease models. They are indispensable tools to establish the link between a given target and (patho)physiology (Sweis, 2015). In addition, they have the advantage to reversibly inhibit or potentiate

protein function as opposed to KO technologies that definitively eliminate or mutate the protein. They also can be used to probe the function of individual subunits in a multimeric protein complex or even different domains of the same protein subunit. Therefore they are considered as superior pharmacological tools with regard to valuable spatiotemporal information on a protein function while not modifying its expression (Lazo et al., 2007).

During the nineties some striking "deorphanization" occurred (Civelli et al., 2013) but the rate of discovery of natural ligands faces a constant decrease (Davenport et al., 2013). Indeed GPCRs "deorphanization" may be a daunting task as no ligands, signaling pathways or physiologic response are known. The "deorphanization" consists in receptor-ligand pairing by at least two independent groups and having a potency consistent with a physiological function (Davenport and Harmar, 2013).

Apart from orphan GPCRs, other receptors can be described as understudied or under-interrogated with few ligands and/or function reported or even completely uncharacterized. In all cases, the ligands proposed only in one publication must be confirmed by reproducing and validating, ideally using a different assay, the previous obtained results by other groups in the field. Despite endogenous ligand-receptor pairings, most of GPCRs remain uncharacterized or understudied in terms of structure, function or physiology. Therefore "deorphanized" receptors require further input such as the identification of surrogate or synthetic ligands to better characterize their pharmacology and physiology. Indeed, surrogate agonists help to investigate for instance biased signaling pathways (See I.1.5.5.). As some metabolites such as succinate or α -ketoglutarate (He et al., 2004) have been reported to activate GPCRs, it might be interesting to identify agonists that, for example, don't affect cell metabolism and mitochondrial function. To develop therapeutic drugs, antagonists or inverse agonists would help to shut down the undesired effect of a permanently activated GPCR. In addition, allosteric modulators can be used to potentiate or decrease the receptor activity in presence of the natural ligand (See I.1.5.3.).

Although some receptors have been associated with surrogate ligands, they are classically not considered as being "deorphanized". However these synthetic

pharmacological tools are valuable probes to explore the signaling pathways, function and therapeutic potential of receptors (Wilson et al., 1998; Civelli et al., 2013).

Besides, it has been postulated that the remaining receptors may have functions in the absence of an endogenous transmitter by being constitutively active or by modulating the activity of other GPCRs, for example, through heterodimerization (Davenport et al., 2013).

Obtaining active small-molecules modulators at GPCRs (or any receptor) requires a multidisciplinary approach including computational methods (bioinformatics and cheminformatics), molecular and cellular biology (cloning and expression of proteins, recombinant expression systems) and pharmacology (bioassays and screenings). The two most prominent approaches currently rely on *in silico* modelisation and biological screenings (Jacoby et al., 2006). Derivation of endogenous ligands was once the most efficient way to obtain new ligands for a receptor, but it is now less widely used because of the complexity of identifying, purifying and chemically optimizing the active components (Frearson and Collie, 2009) and also probably due to intellectual properties considerations.

1.3.2. Computational approach

Bioinformatics and cheminformatics are both low cost virtual approaches to GPCR characterization. Bioinformatics is used to classify genes or proteins, and establish sequence relationships (Dunlop and Eglen, 2004). An approach called phylogenetic analyses consists in analyzing the similarities in AAs sequence with other GPCRs to classify sequentially related GPCRs in clusters. Members of a cluster are postulated to be activated by similar ligands (Civelli et al., 2013). Nevertheless this approach frequently failed to match orphan receptors with cognate ligands and dissimilar ligands are usually found within a cluster. For example, SUCNR1 was first classified in P2Y receptors and predicted to be activated by purinergic ligands (Joost and Methner, 2002; Wittenberger et al., 2002) but it has later been paired with succinate (He et al., 2004).

Besides, cheminformatics are used to predict chemical and pharmacological properties of compounds. These computational approaches are relevant in drug discovery for *in*

silico screenings, to identify new putative ligands. GPCRs molecular models can be built by homology modelling from available crystal structures of closely related receptors. This approach consists in replacing the AAs sequence of a known structure by the homologous sequence of a receptor of interest (Cavasotto and Palomba, 2015). This "homology" model is then screened virtually by docking of libraries such as the ZINC database (Irwin and Shoichet, 2005). The hits with the best docking scores are likely to possess activity against the target and are assayed on cells expressing the receptor. However, to define a ligand-binding site (binding pocket), the AAs involved in the ligand interaction have to be confirmed by site-directed mutagenesis. Computational techniques are also helpful to propose a 3D pharmacophore (Cavasotto and Palomba, 2015). Recently, a pharmacophore model based on known surrogate ligands was defined for GPR139, a potential target involved in metabolism and Parkinson's disease (Isberg et al., 2014).

1.3.3. Pharmacological approach

Pharmacology is a field that studies the discovery and characterization of molecules interacting with receptors, often confirmed or putative therapeutic targets (uses, effects and modes of action of drugs). Molecular pharmacology of GPCRs focuses more particularly on mechanistic insight of GPCR activation and function. This field is relevant to the molecular study of diseases and development of pharmacologically active molecules, which would be used to address them.

Reverse pharmacology, a widely used strategy for ligands identification, consists in performing a screening to explore the effects of compounds on a biological system. This two-step method relies on the cloning and overexpressing of a GPCR of interest in a specific recombinant expression system such as immortalized mammalian cells (Wilson et al., 1998; Jacoby et al., 2006). These main tools of target based approach facilitate the detection of activated intracellular responses by ensuring the generation of high amounts of a selected receptor (Thomas and Smart, 2005). Nevertheless they might induce unexpected biochemical reactions. A molecule might trigger a non-canonical signaling pathway of the receptor, leading to the identification of a ligand, which would be inactive in cells where the protein is naturally expressed. Furthermore machinery of the

recombinant cell system might differ from those of the therapeutically relevant cells, including control of receptor levels, splice variants or interacting proteins (RAMPs, other receptors, ...) (Kenakin, 2003; Jacoby et al., 2006).

The second step includes a screening of these cells for a functional response to ligands present in biological extract preparations or libraries (Wilson et al., 1998). However a distinction must be made between two strategies commonly used in drug discovery, the reverse pharmacology, directed from a receptor to its natural ligand and HTS, promoting active synthetic compounds discovery (Civelli et al., 2013; Davenport and Harmar, 2013).

I.3.3.1. Pharmacological screenings

I.3.3.1.1. Biological extract preparations

A tissue-extract based approach tests various animal tissues on cells overexpressing an orphan receptor. Positive extracts that induce receptor activation are fractionated until the active compound is extracted and characterized (Gordon, 2007; Kenakin et al., 2010). However this method requires stable and sufficiently concentrated ligand to be detected. Additionally the active compound might be undetected because it is synthesized in another part of the body or only during specific conditions (inflammation, necrosis, ischemia, ...), its expression might be regulated by environmental factors or need additional accessory proteins (Civelli et al., 2013).

I.3.3.1.2. Libraries

To find an active compound, numerous collections of small molecules are commercially available and already formatted for screening. The libraries try to cover as many known active chemical classes as possible. They are essentially composed of natural products (peptides, proteins, lipids, ...), U.S. Food and Drug Administration-approved drugs, bioactive compounds and chemicals from synthesis.

- Combinatorial libraries

Combinatorial libraries are composed of large numbers of structurally simple and similar compounds generated by automated synthesis using a "one-synthesis/one-skeleton" approach. The molecules synthesized are not drug-like and possess a low diversity, which is inadequate for lead-discovery campaigns. However by combining many of these libraries, a certain degree of chemical diversity can be achieved (Galloway and Spring, 2009).

In addition, many laboratories collect the well-characterized molecules they have already synthesized to design their in-house libraries.

- Libraries based on diversity-oriented synthesis (DOS) and fragment-based screening (FBS) design

DOS libraries are a collection of structurally and functionally diverse molecules (building-block diversity - functional group diversity - stereochemical diversity - skeletal/scaffold diversity) produced by modular syntheses (*Figure 1-14*) (Morton et al., 2009). They are efficiently generated, in few steps and in a random manner, with molecular masses close to those of drug-like molecules. This diversity conducts to the interrogation of large known and "un-tapped" regions of chemical space simultaneously. In addition, DOS libraries are constituted of 3D molecular scaffolds, which are likely to be more selective for their targets as they too are 3D structures (Schreiber, 2009; Galloway et al., 2010).

By contrast, FBS design consists in screening small molecules (intrinsically not drug-like) that might become subunits/fragments of drug-like compounds (*Figure 1-14*). This approach is characterized by a more diverse library of compounds synthesized more efficiently as it avoids the wasteful production of compounds that have unknown biological activities (Hajduk, 2011). However these small molecules might not bind to drug targets with sufficient affinity and specificity to be identified in a screening (Galloway and Spring, 2011).

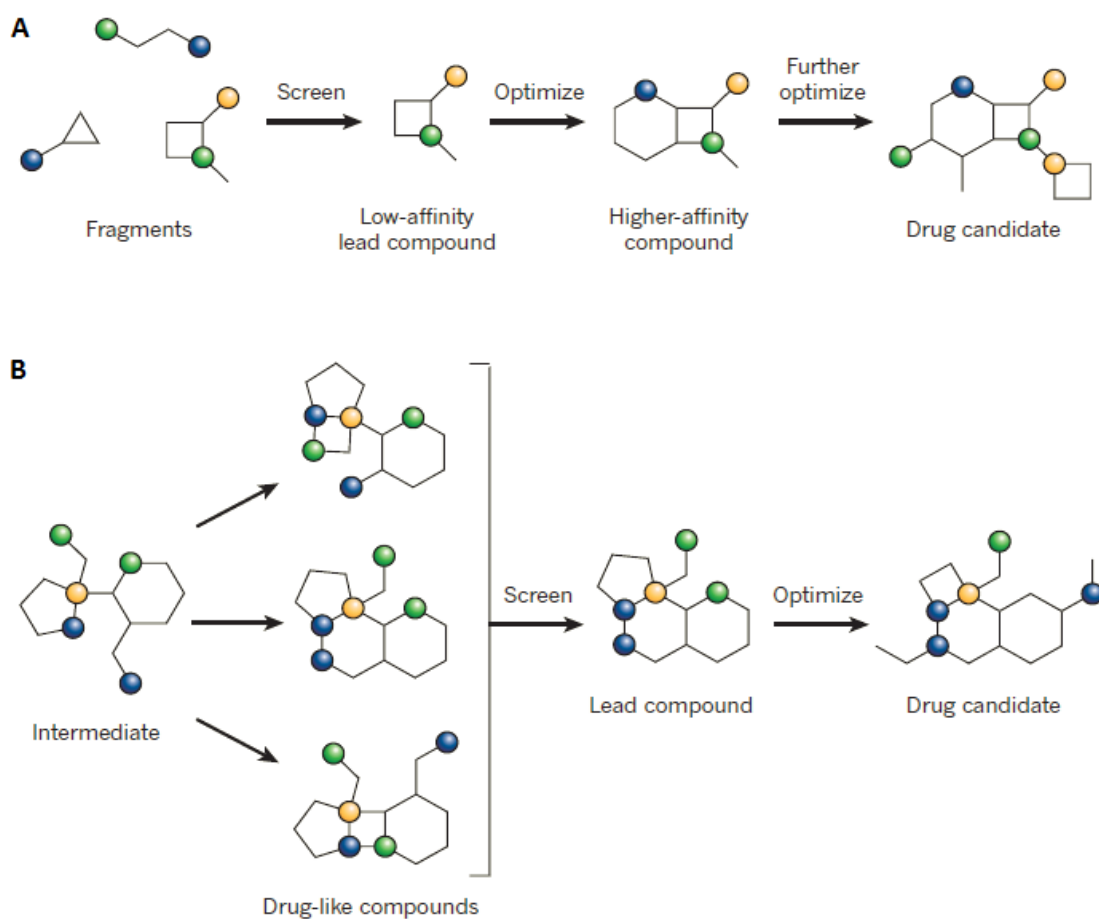


Figure I-14 : Generating drug candidates from (A) FBS, (B) DOS. Circles represent different functional groups (Galloway and Spring, 2011).

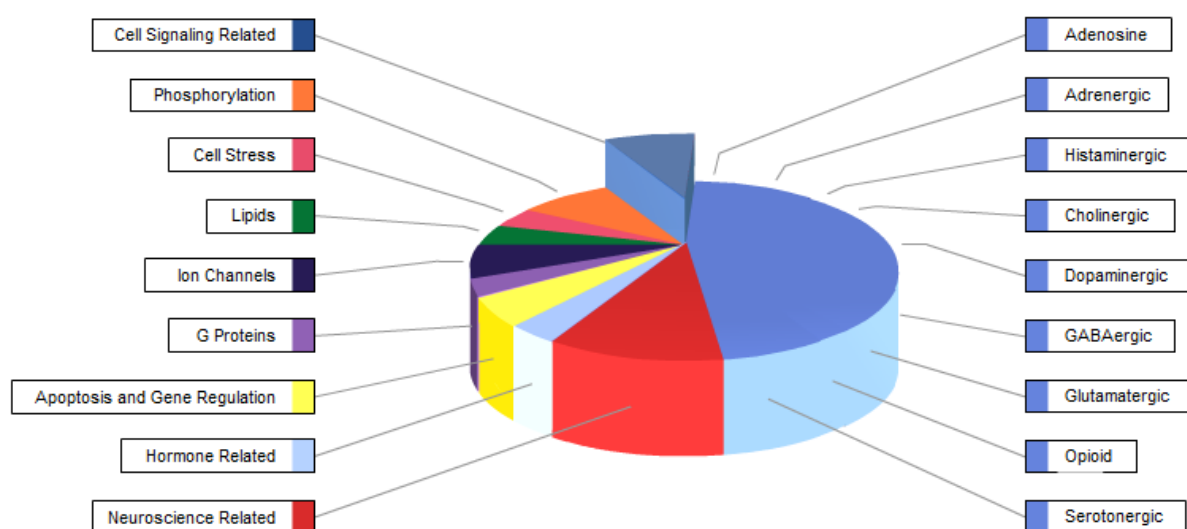


Figure I-15 : Composition of the LOPAC library sold by Sigma-Aldrich.

- Library of pharmacologically active compounds (LOPAC)

Knowledge-based libraries are composed of structurally and therapeutically diverse molecules with known bioactivity (*Figure 1-15*). These libraries are based on a selective optimization of side activities (SOSA) approach according to the famous statement of Sir James Black : "the most fruitful basis for the discovery of a new drug is to start with an old drug". The strategy employed consists in testing old drugs on new targets by taking advantage of molecules side activities (Wermuth, 2004). An advantage of the SOSA approach lies on the safety and bioavailability of compounds already given to humans. As a consequence, a hit could rapidly be tested in patients after optimization of the desired side activity and strongly reduced or abolished initial activity.

1.3.3.1.3. Cell-based assays

1.3.3.1.3.1. General receptor activity measurement

Functional cell-based assays constitute the best option to identify active ligands during a "deorphanization" screening campaign. As signaling pathways of orphan GPCRs are typically not known, a heterologous or engineered system that reports general receptor activity can be helpful. Two main strategies are commonly used, co-expression of the receptor with a promiscuous murine $G_{\alpha 15}$ or human $G_{\alpha 16}$ protein but also arrestin recruitment and translocation studies.

Using promiscuous proteins enables receptor to activate $PLC\beta$ to induce $[Ca^{2+}]_i$ transient mobilization, thus allowing the detection in a screening setting, via for instance a luminescence-based FLIPR™ technology (molecular devices) (Kostenis, 2001). However some GPCRs already paired with ligand do not, or only poorly, couple to $G_{\alpha 16}$ (review of these receptors in (Kostenis, 2001)), therefore more efficient promiscuous G proteins have been generated. These chimeric proteins possess for example a C-terminal of five or six AAs of $G_{\alpha q}$ exchanged with those of $G_{\alpha s}$ or $G_{\alpha i}$, which confers the ability of a receptor coupled to $G_{\alpha s}$ or $G_{\alpha i}$ to activate $PLC\beta$ (Kostenis et al., 1997, 2005; Heydorn et al., 2004). Therefore several optimized promiscuous G_{α} -subunits might collectively be

used as a universal tool for general receptor activity detection. The main drawback of using artificial G protein system is the unintentional identification of ligands with nonphysiological and pharmacologically irrelevant efficacies (Kostenis, 2001). Although FLIPR represents an efficient platform for assessing GPCR induced calcium release and dynamics (Emkey and Rankl, 2009), it is a very expensive technology out of reach for most academic laboratories or small sized companies.

Besides, other strategies to measure general receptor activity is based on arrestin either by studying arrestin recruitment to the activated receptor or arrestin-GPCR complex translocation. Based on arrestin recruitment many assays were developed among different technologies including bioluminescence resonance energy transfer (BRET), complementation assays (for example enzymatic activity of a re-formed β -galactosidase, PathHunter™), protease-mediated transcriptional reporter gene (Tango™) (Chen et al., 2012), pH sensitive probes, enzyme fragment complementation (EFC) or fluorescence (Kenakin et al., 2010). Other methods allow to visualize GPCR trafficking by high-resolution fluorescence microscopy including the Norak Biosciences Transfluor® technology. This cell-based assay in which arrestin-Green fluorescent protein (GFP) conjugate enables to monitor the location and redistribution of the receptor-arrestin complex upon GPCR activation (Oakley et al., 2002).

However a general paradigm in terms of signaling is difficult to apply to all GPCRs. Indeed some receptors have been described as being not, or not well, coupled to arrestins including the β_3 -adrenoceptor (Liggett et al., 1993; Cao et al., 2000), the relaxin family peptide receptor 1 (RXFP1) and 2 (RXFP2) (Callander et al., 2009), or the glucose-dependent insulinotropic polypeptide (GIP) receptor (Al-Sabah et al., 2014). Moreover some GPCRs such as LGR5 (de Lau et al., 2011) and the atypical chemokine receptor ACKR3 are described to lack G protein-coupling (Rajagopal et al., 2010a).

In addition, it is well established that some ligands selectively activate discrete signaling pathways when binding to a receptor (See I.1.5.5.). Consequently the choice of an assay for a screening campaign is complicated by signaling capabilities of the receptor and therefore there is a renewed interest in screening-compatible and sensitive assays directed selectively toward a pathway of interest (Millar and Newton, 2010).

More general assays called "label free" have been also described. They use various types of technology to measure subtle changes in cell phenotype. For instance, the cellKey™ system employs an electrical impedance-based sensor that allows recording impedance changes according to the changes in cell adherence, shape and volume, cell-to-cell interactions, and other cellular alterations. This real time and cell-based assay approach is able to distinguish between signals through the different GPCR partners with different kinetics. Although this technique appears to be very helpful, it requires more investment to determine how impedance changes are correlated to particular cell signaling (Miyano et al., 2014).

I.3.3.1.3.2. G protein activity measurement

GPCRs signaling cascade offers many possibilities in monitoring ligand activity through G protein interaction and second messengers modulation, which can mediate gene expression. Receptors can also trigger changes in cellular metabolism leading to end organ response. However the farther down the stimulus-response pathway monitored, the more the signal will be amplified as a function of the distance from the initial receptor event. This amplification phenomenon can lead to a greatly increased sensitivity to ligands. Although taking advantage of signal amplification for weakly efficacious agonists detection, it also can result in the misidentification of a ligand with an improved coupling efficiency that might not be reproduced in a more physiologically relevant system (Kenakin, 2014).

The majority of current GPCR assays were developed to specifically report effectors modulation caused by the activation of a selected G protein subfamily. These assays amenable to functional screenings rely on the quantitative evaluation of second messengers. In this manuscript we will extensively describe principal methods to measure cAMP and Ca²⁺ effectors.

Obviously the signaling pathways of understudied GPCRs that have already been associated with their ligands can be rapidly characterized and thus facilitate the choice of a cell-based assay for a screening campaign. Concerning orphan receptors, if more

information about their signaling pathway is first obtained, it may facilitate ligands identification through HTS (choice of the best assay with a highly amplified pathway). In this context, study of GPCRs constitutive activity can be a good starting point as such receptors are defined to spontaneously adopt a conformation able to activate G proteins in absence of ligand. Prior to ligand identification, taking advantage of GPCRs constitutive activity can help to determine their likely signaling mechanism (Parnot et al., 2002). In practice, the measure of the increase in a second messenger production such as cAMP, is directly correlated with the transient expression of a GPCR, which is transfected with increasing amounts of DNA, demonstrating the constitutive activity of the receptor coupled to $G_{\alpha s}$ for example (Parnot et al., 2002).

I.3.3.1.3.2.1. Ca^{2+} measurement

As $G_{\alpha q}$ activation triggers the stimulation of $PLC\beta$ which leads to Ca^{2+} release from internal stores (See I.1.4.1.). Several assays monitoring transient changes in $[Ca^{2+}]_i$ are commonly used to characterize receptors coupled to this signaling pathway.

By contrast with radioactive assays based on IP accumulation or IP-One ELISA assays (IP_1^{TM} assay; Cisbio), fluorescent probes are of a great interest to follow $[Ca^{2+}]_i$ dynamic in cells (Thomsen et al., 2005). They are easy to set-up and require basic laboratory instruments (Cobbold and Rink, 1987). Tsien team in 1980s developed the first fluorescent dyes able to report variations in $[Ca^{2+}]_i$ (Grynkiewicz et al., 1985). All these fluorescence indicators of Ca^{2+} are based on a common characteristic, a covalent combination of a Ca^{2+} chelating group (tetracarboxylic acid core) and a fluorophore group. They are classified into two groups based on the quantification method used :

The first group contains the non-ratiometric fluorescent dyes including fluo-3 or 4-(2,7-Dichloro-6-hydroxy-3-oxo-9-xanthenyl)-4'-methyl-2,2'-(ethylenedioxy)dianiline- N,N,N',N' -tetraacetic acid characterized by a fluorescence intensity increase on Ca^{2+} binding without shift in the fluorescent spectra.

The second group is composed of ratiometric fluorescent dyes including fura-2 or 2-{6-[Bis(carboxymethyl)amino]-5-(2-{2-[bis(carboxymethyl)amino]-5-methylphenoxy}ethoxy)-1-benzofuran-2-yl]-1,3-oxazole-5-carboxylic acid characterized by a shift in their

emission or excitation spectra when they bind to Ca^{2+} , allowing ratio between two fluorescence intensities. The ratiometric method (based on the use of a ratio between two fluorescence intensities) allows the correction of artifacts due to bleaching, changes in focus, variations in laser intensity...

This simple procedure to measure Ca^{2+} transients has improved with the development of new dyes (i.e. Fluo-4 and Calcium 3) and automated real time charge-coupled device (CCD)-based fluorescence plate readers, such as FLIPR™ (Molecular Devices), which enables the simultaneous measurement of an entire microplate (96-, 384- and, 1536-well formats) in the time normally taken to complete one measurement using previous techniques (Monteith and Bird, 2005; Thomsen et al., 2005).

Breakthrough in genetic tools provided additional Ca^{2+} sensors. The first category uses the principle of intramolecular fluorescence resonance energy transfer (FRET) between two variants of the GFP (cloned in 1992 (Prasher et al., 1992)) in response to Ca^{2+} variations. The second category is composed of bioluminescent proteins such as aequorin, which was first isolated from jellyfish *Aequorea victoria* (Shimomura et al., 1962) and cloned in 1985 (Prasher et al., 1985). Aequorin is nontoxic, binds specifically with Ca^{2+} , and does not interfere with calcium ions contained in the buffer.

The bioluminescent process provides many advantages over fluorescent probes, which display non-selective localization and are also more sensitive to changes in their environment than aequorin (Eglen and Reisine, 2008). Additionally it doesn't require light excitation that allows increasing signal-to-noise ratio and avoiding autofluorescence, photobleaching as well as any biological degradation problems. The high sensitivity using photoprotein leads to lower number of cells required and enables detection of even small ligands activity (Eglen and Reisine, 2008).

I.3.3.1.3.2.2. cAMP measurement

Many assays enable the detection of G_{α_s} - and G_{α_i} -coupled receptors by directly or indirectly monitoring intracellular fluctuations of the second messenger cAMP (See I.1.4.1.) (Williams, 2004).

For the indirect measure, some methods are available, including BD™ ACTOne technology that allows to indirectly measure cAMP changes through the detection of $[Ca^{2+}]_i$ mobilization, reporter gene assay. Actually BD™ ACTOne cAMP assay uses a modified cyclic nucleotide-gated (CNG) Ca^{2+} channel which is opened by intracellular cAMP increase. Thus, changes in cAMP levels are translated into Ca^{2+} flux measured by conventional fluorescent Ca^{2+} or membrane-potential dyes (Reinscheid et al., 2003; Visegrády et al., 2007). This assay amenable to HTS without a cell lysis step allows end point and real time measurements in living cells with standard instrumentation. However up to now only one BD™ ACTOne-based HTS was reported and show a detection limit around 100 fmol/well (Visegrády et al., 2007).

cAMP response element-based reporter gene assays that rely on cAMP sensitive transcription factor activation constitute another method for cAMP indirect measurement. Reporter gene assays have been developed by monitoring the expression levels of a particular reporter, the transcription of which is tightly controlled by the cAMP response element-binding protein (CREB) that binds to upstream cAMP response elements (CRE) (Hill et al., 2001). These assays have been optimized by using reporter proteins such as β -galactosidase, GFP mutant, luciferase or β -lactamase, which are easily distinguished from other cell products. Different protocols are available and differ in the choice of reporter gene and the method for measuring its activity *in vitro* (lysate or whole cells) and *in vivo*. Reporter gene assays have been successfully amenable to HTS with 1536-well format with simpler protocols and less reactants need than cAMP accumulations ones (Goetz et al., 2000; Kunapuli et al., 2003). Although reporter assays have been extensively applied to G_{α_s} - and G_{α_i} -coupled receptors investigation, they might yield numerous false positives due to the detection of an amplified signal far downstream of the signaling cascade. In addition, the signal detected might be generated by another signalling pathway (Baker et al., 2003). A major advantage of these assays is that they

allow the real time measurement of cAMP levels. Such studies have shown that the detection of a change in reporter gene activity requires a stimulation time of 30 minutes with an agonist (Baker et al., 2004). However, it is likely that the number of identified false positives increased when cells are longer exposed to ligands (Hill et al., 2001; Baker et al., 2004; Kenakin, 2014).

However, the direct measurement of endogenous cAMP has the advantage of inducing less artifacts. These ones might be generated by compounds that might nonspecifically interfere at many points of the complex pathway. In the section below we will extensively discuss main available assays and techniques of detection for cAMP changes.

1.3.3.1.3.2.2.1. Competition assays for cAMP detection

Most of the classical cAMP assays consist in immunoassays based on competition between endogenously produced cAMP and exogenously added labeled cAMP for interaction with anti-cAMP antibodies using a variety of detection technologies. These assays range from radiometric to enzymatic, with some variations in protocol and sensitivity (Williams, 2004). Mostly were amenable to HTS in different formats whit Z' (See 1.3.3.1.4.) described to be superior to 0.5. The assays depend on the antibody quality, they are homogeneous (no physical separation step) compared to heterogeneous traditional radiometric assay but still require a many steps protocol. In general, they are performed on whole lysed cells as end point assays (the response is a history of the temporal process of response production from the initiation of the experiment to the time of measurement). A major problem with end point assays is to ensure that the recording signal is within the dynamic range of the assay. In addition, an important drawback to detect cAMP accumulated across a population of cells during the time course of the assay, is that kinetics and temporal nature of the cAMP changes are lost (Williams, 2004; Hill et al., 2010). However if no spatial or temporal resolution is required and a cAMP single point measure reflecting the total cAMP levels present in cellular populations is sufficient, these biochemical cAMP assays constitute the easiest, ready-to-use and highly reliable choice.

- Radioactive assays

Traditional radiometric method consist in prelabeling adenine nucleotide with [³H]-adenine and then separating it from other [³H]-adenine derivatives by using column chromatography to monitor [³H]-cAMP generation. This method is time-consuming (long time of incubation, numerous wash steps) and require a separation step (heterogeneous assay) increasing errors rate. In addition, the single point measure of radioactivity requires specific equipment such as liquid scintillation counting on a dual label program ([¹⁴C]-cAMP serves as a ratio control) (Donaldson et al., 1988; Hill et al., 2010).

Further advances in cAMP assays led to the development of homogeneous and radiometric proximity methods such as the most common scintillation proximity assays (SPA, Amersham Biosciences) and automated cAMP FlashPlate technology (PerkinElmer). These methods are based on immunoassays enabling the detection of light produced by [¹²⁵I]-labeled cAMP in close proximity with scintillant plates coated with anti-cAMP antibody (AB). When endogenous cAMP is present, it competes with [¹²⁵I]-labelled cAMP that results in a signal decrease. FlashPlate technology enables the stimulation and radioactivity detection in a same well without the need for separation and wash steps, leading to a lower experiment time and errors rate (Williams, 2004; Chen et al., 2012). These features facilitated its successfully use in HTS but further miniaturization beyond the 384-well plate format and the need of large quantities of radiolabeled tracer limit its application in HTS (Kenakin et al., 2010).

However non-radiometric read-outs readily miniaturized emerged and supplanted these technologies due to safety, cost and throughput considerations (Williams, 2004; Chen et al., 2012).

- Fluorescence-based assays

Fluorescence polarization (FP) cAMP assays (Perkin Elmer and Amersham Biosciences) monitor the light emitted from a fluorescently labeled cAMP molecule following excitation with a polarized light source. This technology is based on the principle that rotation of a molecule induces a depolarization of the emission light. A higher polarization value (lower depolarization) is observed when rotation is reduced by the binding of labeled cAMP to antibody. By contrast a lower polarization value is observed in the presence of free-labeled cAMP, unable to bind antibody, when the labeled cAMP is free in solution. Although this technology is simple to implement as it doesn't require a specialized equipment, one major disadvantage is the artifacts induced by the commonly employed fluorescein-labeled cAMP. However they have been successfully eliminated by using an alternative dye (i.e. Bodipy-TMR, MR121, Alexa, Cy3 and Cy5 compounds) displaying percentage activities outside the expected range (Williams, 2004; Hill et al., 2010). A major advantage of this assay is the possibility to use cell membranes. Use of membranes in a membrane-based ligand binding screening avoids the need for continuous cell supply (i.e. quantity of cells and technical considerations such as time for cells preparation) required for a cell-based functional screening and allows high-efficiency bulk supply of membranes that are stable frozen (Allen et al., 2002).

A strategy based on time-resolved fluorescence resonance energy transfer (TR-FRET, LANCE[®] Ultra cAMP assay) offers significant advantages over the FP technology including reduced compound interferences, higher sensitivity and detection limits inferior to 10 fmol cAMP per well. However it requires specific equipment compatible with time-resolved fluorescence read-out. The first-generation homogeneous time-resolved fluorescence (HTRF) assay employs a cAMP antibody labeled with europium cryptate and a modified allophycocyanin labeled-cAMP. The close proximity of the two fluorophores allows FRET and results in the emission of fluorescence at two different wavelengths. By contrast only the emission from the europium is detected when the fluorophores are separated by competition with endogenous cAMP (Williams, 2004; Chen et al., 2012). A major advantage of using FRET technologies is the ratiometric read-out that enables to correct well to well variation, minimizes short-lived background fluorescence, limits quenching and autofluorescence effects (Hill et al., 2010). A second-generation donor,

Terbium cryptate enhancing screening performance due to an increased quantum yield compared to europium, has been developed and commercialized in 2008. Although HTRF is the most frequently used generic assay technology and represents an ideal platform for drug target studies in HTS, this technology requires specialized equipment that is not affordable for every lab (Degorce et al., 2009). Some limitations also exist, for example, quenching generated by external interactions with the intramolecular excitation process (electron transfer, FRET, and bleaching) and fluorescence of evaluated compounds. By contrast, techniques monitoring luminescence enable to avoid these interferences (See 1.3.3.1.3.2.) (Eglen and Reisine, 2008).

- Luminescence-based assays

Several technologies have been designed with the aim of providing high-sensitivity assays for the evaluation of cAMP levels. The following technologies using luminescence allow the detection of cAMP levels inferior to 10 fmol cAMP per well, compared to FlashPlate and FP technologies, which have limits in the order of 50-100 fmol cAMP per well (Williams, 2004).

Amplified luminescent proximity homogeneous assay (ALPHA Screen[®] cAMP assay, Packard Bioscience/Perkin Elmer) is based on sensitive bead-based proximity chemiluminescent technology. The assay uses a donor bead coated with streptavidin and an acceptor bead coated with an anti-cAMP antibody. The excitation of a photosensitizer at 680 nm in the donor bead converts O₂ to its free-radical form, which reacts with thioxene derivatives in an acceptor bead when biotinylated cAMP binds to streptavidin, keeping beads in close proximity (Eglen et al., 2008; Hill et al., 2010). The resulting chemiluminescent upon interaction with acceptor beads initiates an amplification cascade by activating fluorophores, contained within the acceptor bead which lead to a highly amplified emission signal at 520-620 nm (Ullman et al., 1994). Novel generation of beads have been modified to contain europium that allows higher intensity at 615 nm (AlphaLISA technology). In presence of cellular cAMP the two beads are not held in close proximity and no signal is generated (Eglen et al., 2008; Hill et al., 2010).

ALPHAScreen is a high-sensitive luminescence technology amenable to HTS with a simplified protocol (no-wash step). In addition, this assay can be employed with cell lysate, serum and plasma and various cellular/body fluid matrices that don't easily affect the assay read-out. Interestingly it doesn't require insertion of large fluorescent label that may sterically hinder interactions. However this technology is more limited than other luminescence technologies because the equipment is limited to reader with an excitation source. A major disadvantage of AlphaScreen technology is its sensitivity to intense light or long exposure to ambient light but this problem can be easily overcome by simple assay adjustments.

Multi-Array™ technology (Meso Scale Discovery) combines electrochemiluminescence and arrays. In the absence of endogenous cAMP, cAMP labeled with a ruthenium derivative binds anti-cAMP antibodies attached to multi-array plates. Addition of a chemical substrate and electrical stimulation trigger electrochemical reactions leading to the production of light (Williams, 2004; Chen et al., 2012). This technology is simple but require a specific reader. Multi-Array™ technology has a high sensitivity due to the possibility to amplify signals through multiple excitation cycles and is less sensitive to compound interference (Williams, 2004). This technology has been described by provider to be amenable to HTS with 384-well plates.

By contrast with all these technologies that measure a signal decrease when cAMP is produced, HitHunter® cAMP assay (DiscoverRx) enables to measure a positive signal when endogenous cAMP levels increase leading to decrease the number of false positives (Golla and Seethala, 2002; Hill et al., 2010). This assay employs the EFC technology principle based on the restoring enzymatic activity of a two fragments β -galactosidase. β -galactosidase donor fragment-cAMP (ED-cAMP) conjugate complements with the β -galactosidase enzyme acceptor (EA) fragment to re-form an active β -galactosidase enzyme. Binding of ED-cAMP conjugate to the anti-cAMP antibody prevents its complementation with the EA fragment. When endogenous cAMP is present, it competes with ED-cAMP to bind to the anti-cAMP antibody, leading to an increase of free ED-cAMP that can complement with the EA fragment to form an active enzyme (Golla and Seethala, 2002). Enzymatic activity of the β -galactosidase formed is detected using substrates that are converted to either fluorescent or luminescent products (Williams,

2004; Chen et al., 2012). This assay is compatible with a variety of readers and readily compatible with automated HTS (Williams, 2004). Despite of its high sensitivity due to the addition of a wash step, other methods such as HTRF are preferred against HitHunter because of a higher number of steps (Gabriel et al., 2003).

I.3.3.1.3.2.2.2. Biosensors

Recent advances in fluorescence- and bioluminescence-based sensors development have provided sensitive indicators for cAMP levels in living cells. They represent an innovative alternative strategy for cAMP detection compared to competitive assays using labeled cAMP and cAMP-driven gene transcription measurements. Biosensors can be considered superior compared to previous techniques on several aspects because they are sensitive probes allowing direct real time/kinetic measurements of cAMP levels in living cells (Paramonov et al., 2015). Another key advantage of genetically encoding sensors is that transgenic animals expressing the sensors can be employed for monitoring intracellular cAMP fluctuations in different cells or tissues including pancreatic islets or in heart for example (Kim et al., 2008; Nikolaev et al., 2010). However a problem inherent to any genetically encoding sensors is the buffering phenomenon of cAMP sensors (high concentrations within subcellular compartments) that might affect cAMP synthesis, transport or breakdown and consequently limit the actual information on cAMP changes in living cells (Willoughby and Cooper, 2008).

Besides being all genetically-encoded proteins used for studies in living cells, biosensors are heterogeneously based on distinct biological phenomena and detection techniques.

- FRET-based biosensors

Many FRET-based sensors are available and represent the most popular and widely used tools for cAMP studies in living cells (Lefkimmiatis and Zaccolo, 2014). They are regarded as valuable tools for monitoring cAMP real time dynamics in defined subcellular regions with outstanding spatial resolution, unattainable with other biosensors. They are also characterized by a quick response and reversible nature of conformational changes induced upon cAMP binding (Paramonov et al., 2015). Additionally to their use in cell

culture, they provide insights into cAMP life-cycle in non-perturbed microenvironment in laboratory animals (Nikolaev et al., 2006). By contrast with bioluminescence-based methods, they don't require additional expensive substrates and ratiometric measurement allows to limit variations due to different expression levels of sensors. Although it is possible to use FRET assays in multiwell plate format on a fluorescence reader, other sensors are used preferentially to perform HTS (Paramonov et al., 2015).

FRET is a mechanism describing a non-radiative energy transfer between a pair of light-sensitive molecules (donor and acceptor fluorophores) with partially overlapping spectra. The efficiency of this energy transfer is inversely proportional to the sixth power of the distance between donor and acceptor, making FRET exceptionally sensitive to small changes in distance.

In general, all FRET biosensors are designed to operate in the similar fashion and are composed of three principle domains : a sensor domain and two fluorophore domains making a FRET pair. A target binding triggers conformational changes in the biosensor tertiary structure that lead to a change of distance between donor and acceptor fluorophores and result in alteration of FRET efficiency. They are divided into two families, multimolecular sensors having at least two different molecular units carrying separate domains and unimolecular sensors composed of a sensor and a FRET pair within a single molecule (Paramonov et al., 2015).

The *multimolecular sensors* for cAMP represent different genetically engineered modifications of PKA, a heterotetrameric enzyme composed of two catalytic subunits and two regulatory subunits. Upon cAMP binding to regulatory subunits, the two active catalytic subunits dissociate.

The first FRET sensor was reported in 1991 (Adams et al., 1991), a chemically modified PKA (catalytic subunits labeled with fluorescein and regulatory subunits labeled with rhodamine) named FICRhR. However this system use was limited because the sensor has to be microinjected in cytoplasm of single cells. The development of genetically-encoded FICRhR analogs, which are expressed in living cells by means of transfection or viral transduction allowed to improve dynamic range and resistance to photobleaching

(Lissandron et al., 2005). However these sensors are likely to be subject to interferences due to the activation of effectors downstream of PKA, the incorporation of endogenous non-fluorescent catalytic subunits when the enzyme is re-formed and the need of both co-transfected subunits high equal expression levels (Paramonov et al., 2015).

The *unimolecular sensors* for cAMP represent different genetically engineered modifications of Epac proteins-exchange factors, directly activated by cAMP. Binding of cAMP to the CNBD of Epac1/2 triggers a conformational change allowing the catalytic domain to bind and activate Rap1/2. This native or modified CNBD of Epac is labeled with two fluorophores involved in FRET. The change in conformation triggered by cAMP binding results in an alteration of FRET intensity. Unimolecular sensors provide several advantages over multimolecular ones, they have a higher temporal resolution because of a greater kinetic favored by all functional domains localized in a single molecule. In addition, only one vector is transfected in cells and an inactive catalytic domain-modified Epac ensures to eliminate interferences from downstream signaling. Furthermore, a lower sensitivity and a greater dynamic range allows for measurements of cAMP at higher physiologically relevant levels compared to multimolecular sensors that are subject to saturation (Paramonov et al., 2015). PKA multimolecular sensor limitations can be overpassed with PKA unimolecular sensor where regulatory II β -subunit is labeled with two fluorophores making a FRET pair (Nikolaev et al., 2004).

- BRET-based biosensors

BRET sensors are well-suited for real time measurement of cAMP in pools of living cells (Jiang et al., 2007). Although they are applicable to transgenic animals and can be targeted to desired subcellular compartments, the weaker intensity signal they induce is not appropriate for single cell measurements or for tracing cAMP fluctuations in subcellular domains (Willoughby and Cooper, 2008). However a major advantage of this technique is that cAMP assays based on BRET sensors are amenable to HTS (Boute et al., 2002; Couturier and Deprez, 2012).

In BRET a bioluminescent protein is used instead of a fluorophore as a donor of energy (FRET). The typical donor employed is the enzymatically active variants of *Renilla reniformis* luciferase (RLuc). The oxidation of its substrate results in the release of energy emitted in photons or transferred to an acceptor fluorophore.

BRET cAMP sensors are divided in two categories, the first one is based on the same principle as FRET principle, a multimolecular BRET sensor uses a PKA labeled with RLuc and GFP. Unimolecular sensors are characterized by a cAMP binding motif of either Epac or PKA regulatory subunit labeled with a luciferase and a fluorescent protein. A second category contains a sensor called Nano-lantern (cAMP1.6) that combines BRET and complementation of split luciferase principles and thus provides lower background signal and increased sensitivity for the assay (Paramonov et al., 2015).

- Conformation-sensitive fluorophores-based biosensors

These sensors are based on a fusion of a sensor and a fluorescent reporter, a permuted variant of enhanced GFP. However no conformation-sensitive sensors for direct probing of cAMP are yet available. Another strategy relies on two fluorescent protein, a red one fused to PKA subunits and a green one free cytoplasm. Upon cAMP binding, the red fluorophore dissociates from PKA that will subsequently bind the green fluorophore resulting in an increase green-to-red emission ratio. However these sensors required to be deeply characterized (Paramonov et al., 2015).

- Luminescent enzymes-based biosensors

In general, these sensors are genetically encoded proteins based on a variant of luciferase fused with functional domains responsible for sensing of cAMP. Interaction of a sensing domain with its substrate triggers conformational rearrangement of the luciferase, resulting in a change of enzymatic activity and output of light.

Few years ago, firefly luciferase (FLuc)-based cAMP biosensors have been developed, opening the possibility of investigating the kinetics of cAMP accumulation in living cells (Fan et al., 2008; Hill et al., 2010). FLuc is 61 kDa enzyme responsive of firefly bioluminescence. The concept of the biosensor is based on the FLuc capacity to emit light (550-570 nm) by oxidation of its substrate, luciferin in presence of oxygen, Mg^{2+} and ATP according to the following reaction (*Figure I-16*) (Koo et al., 1978; Shinde et al., 2006).

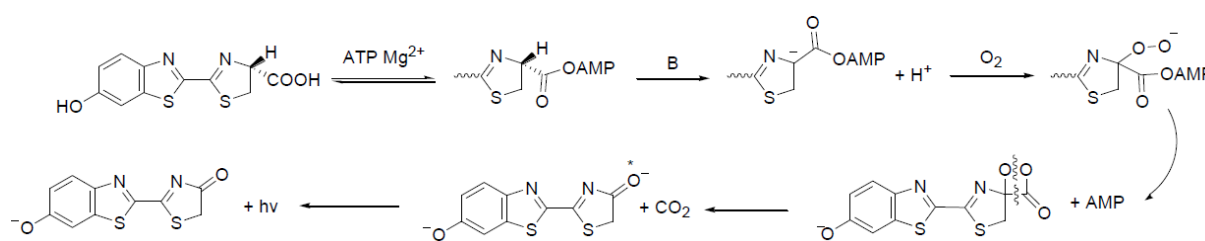


Figure I-16 : Oxidation of luciferin into oxoluciferin with emission of a photon ($h\nu$) (Shinde et al., 2006).

Unlike fluorescence, luminescence provides high sensitivity with a high signal-to-background ratio. In addition, elimination of an excitation light source prevents interferences by compound autofluorescence and fluorophore photobleaching. By contrast with fluorescent proteins, luciferases minimize effect on cellular physiology because they can be used at lower expression levels. In addition, these enzymes possess short half-lives compared to nonenzymatic fluorescent protein reporters (i.e. GFP) that minimize their basal accumulation and allow the measure of dynamic changes (Thorne et al., 2010; Paramonov et al., 2015).

One of the most sensitive cAMP sensors available with a detection limit in low nanomolar range and outstanding dynamic window (0.003-100 μM) is the pGloSensor-20F and its successor with improved characteristics pGloSensor-22F. These biosensors are based on a recombinant FLuc fused with a cAMP binding domain (Fan et al., 2008; Binkowski et al., 2009, 2011). Fast dynamics and reversibility of sensor conformational changes in response to alterations in cAMP levels (within several seconds) make GloSensor probes valuable tools for direct monitoring of real time cAMP dynamics in living cells.

This system should be also applicable in laboratory animals. In addition, this sensor encoded by a single plasmid eliminates difficulties related to non-equality of expression of sensor different domains (Paramonov et al., 2015).

The GloSensor™ cAMP assay has been developed and marketed in 2008 by Promega Corporation. It has been extensively reported in the literature for various uses, from ligand identifications for $G_{\alpha s}$ -coupled receptors (Pantel et al., 2011) to the dissection of subtle pharmacological aspects of cAMP regulation such as biased signaling or endosomal cAMP generation (Irannejad et al., 2013). In addition, Buccioni et al. proved that the GloSensor system constitute a reproducible and robust alternative to traditional methods for screening either $G_{\alpha s}$ - or $G_{\alpha i}$ -coupled receptors. Indeed they obtained similar results with known agonists of $G_{\alpha s}$ - and $G_{\alpha i}$ - coupled receptors, by using the GloSensor system or [35 S]GTP γ S binding assay (Buccioni et al., 2011). More recently, DiRaddo et al. confirmed the asset to employ this real time assay for investigating $G_{\alpha i}$ -coupled receptors (DiRaddo et al., 2014). This technology is cost-effective, any luminescence detector is sufficient and affordable substrate is required. In addition the assay is efficient with set-up and assay times particularly short and allows to compare kinetic differences between any $G_{\alpha i}$ -coupled receptors (DiRaddo et al., 2014).

<u>cAMP Assay</u>	<u>Type of assay</u>				<u>Type of measure</u>				
<i>Indirect measure</i>		Material	Steps	Reagents		Read-out	Equipment	Miniaturization	Detection limit (384-well)
<i>Direct measure</i>	ACTOne	Living cells	homogeneous	Reporter gene	End point Real time	Fluorescent	Fluorescence reader	384-well	1000 fmol
	Reporter gene	Cell lysate Living cells <i>In vivo</i>	homogeneous Long incubation time	Reporter gene	End point Real time	Luminescent /fluorescent	Fluorescence /luminescence reader	1536-well Z' = 0.6	High sensitivity but amplified signal
cAMP accumulation	[³ H]-cAMP	Cell lysate	heterogenous	[³ H]-adenosine	End point	Radioactive	Radioactive counting	No	
	SPA	Cell lysate	homogenous	[¹²⁵ I]-cAMP ABs	End point	Radioactive	Radioactive counting β counter	No	
	Flash plate	Cell lysate	homogeneous	[¹²⁵ I]-cAMP ABs	End point	Radioactive	Radioactive counting β counter	384-well Z' = 0.5-0.6	50-100 fmol
	FP	Cell lysate	homogeneous	Fluorescent cAMP AB	End point	Fluorescent	Fluorescence reader	1536 well compatible Z' = 0.5-0.7	50-100 fmol 500-1000 fmol for membranes

Biosensors	HTRF (Lance)	Cell lysate	homogeneous	Eu ³⁺ cryptate-cAMP ABs allophycocyanin-cAMP	End point	Fluorescent ratiometric	HTRF compatible reader	1536-well Z' = 0.7-0.8	Inferior to 10 fmol
	ALPHA Screen	Cell lysate cellular/body fluids	homogeneous	Biotin-cAMP Strep bead cAMP ABs bead	End point	Luminescent	Luminescence reader (excitation source)	1536-well Z' = 0.5-0.7	10 fmol
	Hit Hunter	Cell lysate	homogeneous	ED-cAMP EA substrate	End point	Luminescent /fluorescent	Luminescence /fluorescence reader	1536-well Z' = 0.7-0.8	1-1000 fmol
	Multi- array	Cell lysate	homogeneous	cAMP ABs cAMP Ru	End point	Luminescent	Luminescence reader (electrical stimulation)	384-well Z' = 0.7	10 fmol
	FRET	Living cells <i>In vivo</i> <i>Single cell</i>	homogeneous	Fluorophores	End point Real time	Fluorescent ratiometric	Fluorescence reader (excitation source)		
	BRET	Living cells <i>In vivo</i>	homogeneous	Fluorophore substrate	End point Real time	Luminescent	Luminescence reader		
	Luminescent enzyme	Living cells <i>In vivo</i>	homogeneous	Enzyme substrate	End point Real time	Luminescent	Luminescence reader	1536-well Z' = 0.5	Inferior to nmol

Table I-1 : Main available cAMP assays (See text for details).

I.3.3.1.3.3. Challenges of the quantification of G_{αi} activation

The G_{αs}-coupled receptors activation is relatively easy and straightforward to detect because they activate AC and consequently increase cAMP levels. Accordingly, many examples of successful screening campaigns on G_{αs}-coupled receptors have been published (Titus et al., 2008; Pantel et al., 2011; Chen et al., 2013). In contrast, agonist ligands for G_{αi}-coupled receptors are much more difficult to track with cAMP measurement. This is due to the fact that basal AC activity and cAMP levels in the cell are relatively low (Houslay and Milligan, 1997). Therefore inducers of AC must first be added to detect a signal inhibition when assessing a putative agonist (Wong, 1994).

A commonly used direct activator of AC is forskolin (FSK), isolated from the Indian plant *Coleus forskohlii* (Bhat et al., 1977) that causes a rapid and reversible cAMP increase in a wide variety of cell types (Seamon et al., 1981). Structural analyses of AC-FSK crystal show the catalytic site of the AC to be composed of two monomers, which interact in a "head-to-tail" fashion. At both central cavity endings are two hydrophobic pockets that provide the binding site for two molecules of FSK. FSK appears to activate AC by altering the conformation of its catalytic site by changing the interaction between the two monomeric units through the creation of a stabilizing hydrophobic bridge (Houslay and Milligan, 1997; Zhang et al., 1997).

There are severe drawbacks in the use of FSK as a pharmacological tool such as artifacts and non-specific effects. For example, one of the consequence of FSK structural similarities with hexoses (Joost et al., 1988) and steroids is the production of cAMP-independent effects by binding to glucose transporters (Shanahan et al., 1987; Wadzinski et al., 1987) and acting at different ion channels including nicotinic receptors, GABA_A receptors and voltage-dependent K⁺ channels (Laurenza et al., 1989). The cAMP-independent effects of FSK cannot be discriminated from dependent ones only with response-concentration curves as both effects fall in the same range of EC₅₀ (1-20 μM). Such differentiation requires deeper investigations with well-known analogues of FSK, for example 1,9-dideoxyforskolin, which is a derivative that doesn't activate AC. The noncompetitive effect of this analogue would reflect a cAMP-dependent effect of FSK (Laurenza et al., 1989).

The potency of FSK on the system depends of the cell type and assay format used, therefore its EC_{50} must be evaluated via a concentration-response curve prior to other experiments (Williams, 2004; Hill et al., 2010). Accordingly FSK might produce greater changes in cAMP than would be generated via receptor-mediated action, so careful evaluation of the concentration to use is required to ensure a correct assay window. A small window might lead to a failed assay sensitivity and consequently variable ligand activities (Williams, 2004; Wang et al., 2011).

Alternative stratagem to FSK as the direct stimulation of endogenous G_{α_s} -coupled receptors can be employed when assessing a putative G_{α_i} agonist (Wang et al., 2011). Wang et al. described a strategy to robustly increase the basal cAMP level in CHO cells by using endogenous activity of CT receptor. They demonstrated that agonists of well-known G_{α_i} -coupled receptors stably expressed in CHO cells attenuated calcitonin-induced cAMP production. They proposed this strategy, instead of FSK, to screen for agonists and antagonists/inverse agonists of G_{α_i} -coupled GPCRs. Although this method appears to be suitable for G_{α_i} ligands screening, it is limited by the use of an adequate concentration of calcitonin. In addition, the artificial manipulation of the signal and the important artifacts caused by cAMP inducers complicates the assay by increasing the sources of variation and errors (Hill et al., 2010). Therefore the development of a cAMP-inducer free method constitute a major challenge to avoid these limitations.

I.3.3.1.4. Critical parameters for screening

Small-molecule screenings are an invaluable method for the identification of biological tools if only properly planned and judiciously executed (Gordon, 2007). HTS consists in assaying large libraries with a robust biological assay to identify active compounds called hits. Use of robotic automation allows the evaluation of several thousand compounds in very small volumes (different plate formats available) (Kenakin, 2014).

An ideal GPCR screening should be nonradioactive, homogenous, simple, robust and amenable to a microtiter plate format to facilitate robotic automation (reduction of cost and gain of time). Important factors must be carefully considered to set-up a screening (Gordon, 2007; Begley, 2013) :

- Library

High number of compounds with different structures to test must be contained in the library (See I.3.3.1). These compounds must be validated and well-defined (i.e. purity (> 95%), stability, accuracy of compounds concentration and sufficient solubility). The solvent used is also important to consider, the assay should tolerate organic solvents such as dimethylsulphoxide (DMSO) (Gordon, 2007; Begley, 2013).

- Assay

The type of assay to choose has to be related to the information requested (phenotype, target based, microarray, ...). For example, HCS also called phenotypic screening, is based on automated imaging of cells treated with small molecules. This method is particularly useful when the relevant information concerns a change in cellular phenotype. Besides, the signaling cascade induced by GPCR activation gives access to versatile opportunities to develop screening assays based on proximal or distal signaling steps (G protein activation, determination of secondary messengers or nuclear activation) (Jacoby et al., 2006). Measurement of events proximal to GPCR activation tend to reduce the number of false positives whereas signal-to-noise ratio can be enhanced moving down the signal transduction cascade owing to signal amplification (Thomsen et al., 2005).

In addition, the assay and the detection technology employed must be appropriate for evaluating the target of interest (biochemical, cellular, ...). The availability of the infrastructure and instrumentation (fluorescence, luminescence, radioactivity, UV absorption, label free, ...) are important to consider but also material (living cells or lysates, ...) used as well as the availability and cost of reagents required (antibodies, proteins, enzyme substrates, detection reagents, ...) (Gordon, 2007). The assay also should be easily amenable to automation. Simple assays with less steps such as homogenous assays (no separation step) and assays with minimal reagent additions are often preferred. If an assay optimization (number of cells, reagents quantities, incubation time, ...) is required, it should be rapid.

The robustness of the assay is an important parameter as it directly affects screening results. The robustness of an assay describes its capacity to be unaffected by technical or instrumental variations, an assay is robust if results are reproducible. To avoid measurement variations, the protocol must be optimized and under controlled (temperature, humidity, amount of light, incubation and reading times). To ensure assay reproducibility, plate-to-plate and week-to-week stability should be evaluated by introducing positive and negative controls (Gordon, 2007; Begley, 2013).

- Screening

To be confident about the robustness of the screening or the reliability of the results, variations and source of errors must be minimize. Although automation allows to decrease human-related influences (liquid dispensing differences, reagent or sample preparation and handling, ...), potential sources of random error including biological (compound-related problems involving stability, solubility, autofluorescence, solvent evaporation, ...) and instrumental (measurement variations such as voltage, robotic failures, ...) influences might affect the measurement precision and thus results reproducibility. In addition, systematic factors such as across-plate and within-plate column or row biases (i.e. edge effects) are less amenable to procedural quality control. The random and systematic errors decrease the validity of results by unpredictably over- or underestimating true values, leading to false positives (falsely identified hits) and false negatives (true hits that are not identified). To repeat measurements under the same experimental conditions improve measurement precision and thus minimize variability. The generation of false negatives are an important drawback in HTS as there is no way

of knowing which compounds are active but not detected by the assay. Evaluating compounds, in parallel, on two different assays might highlight unidentified active compounds but HTS goal is to identify hits rapidly. Therefore, screening robustness and quality should be appreciated with statistical factors described below (data analyses). However, it is important to emphasize that replicates reduce the number of false negatives without increasing the number of false positives (Malo et al., 2006).

A screening is generally composed of three major steps :

- Primary screening

A screening is generally performed only once on a library compounds distributed in plates at a single concentration because of time and cost issues. In addition, a counter-screening on WT cells or another heterologously expressed receptor can be made to estimate compounds effect on the system in absence of the protein of interest (specificity for the protein). Nevertheless a concentration profiling can also be investigated as a primary screening approach (Malo et al., 2006; Frearson and Collie, 2009).

- Secondary screening

While primary screening data have been preprocessed with quality control checks and normalization procedures, active compounds are selected with defined criteria (See data analyses below) to be engaged in one or more secondary screenings. Replicate measurements that are repeated for the same compound under the same experimental conditions improve measurement precision, leading to the identification of less hits than those generated from the primary screening.

- Confirmation of hits activity

Confirmed hits are next validated by establishing classic concentration-response curves (Malo et al., 2006; Frearson and Collie, 2009). Precise mechanisms of action must be investigated by using databases that provide chemical and biological information (Gordon, 2007)). Important follow-up steps for drug development are discussed below (See I.3.3.2.).

- Data analyses

Since the majority of compounds are screened only once in the primary screening, two parameters of the assay are critical to detect the active ones : high sensitivity and accuracy. Intuitively, the lower measurement variability, which is reflected by standard deviation (SD or σ) is related to the higher confidence and quality of "real" active compounds identification. Historically, the quality of an assay was assessed with signal-to-noise and signal-to-background ratios. However neither of these factors take into account both the variability in the positive control (or sample) and background measurements and the dynamic range. Therefore a statistical factor Z' (calculated only with control data whereas Z factor takes into account signal of samples) has been described to characterize assay quality when a positive control is available in the plate. Z' is sensitive to the separation between the mean of the negative control (background signal, wells containing negative controls, μ_{c-}) and mean of the positive control (wells containing a ligand that gives a positive signal, μ_{c+}), also called the dynamic range of the screening or separation band ($\mu_{c+} - \mu_{c-}$). Z' also depends on the relative standard deviations of both of those means (or distribution of the values around the mean, σ_{c-} and σ_{c+}). Data variability is represented by the bandwidth of values 3σ either side of the mean. An optimal screening with a low frequency of false positives, is described by a maximum dynamic range which maximizes signal-to-background ratio and a minimum data variability band (*Figure I-16*) (Kenakin, 2014). Z' factor (See V.2.1.) is appropriate for evaluating assay quality, without intervention of test compounds (*Table I-2*).

<i>Z' value</i>	<i>Assay description</i>	<i>Interpretation</i>
1	Infinite band of separation	Ideal assay
$1 > Z' > 0.5$	Large dynamic range	Excellent assay
$0 < Z' < 0.5$	Small dynamic range	Adequate assay
0	No band of separation, σ_{c+} and σ_{c-} touch	Dubious quality

Table I-2 : Z' interpretation (Kenakin, 2014).

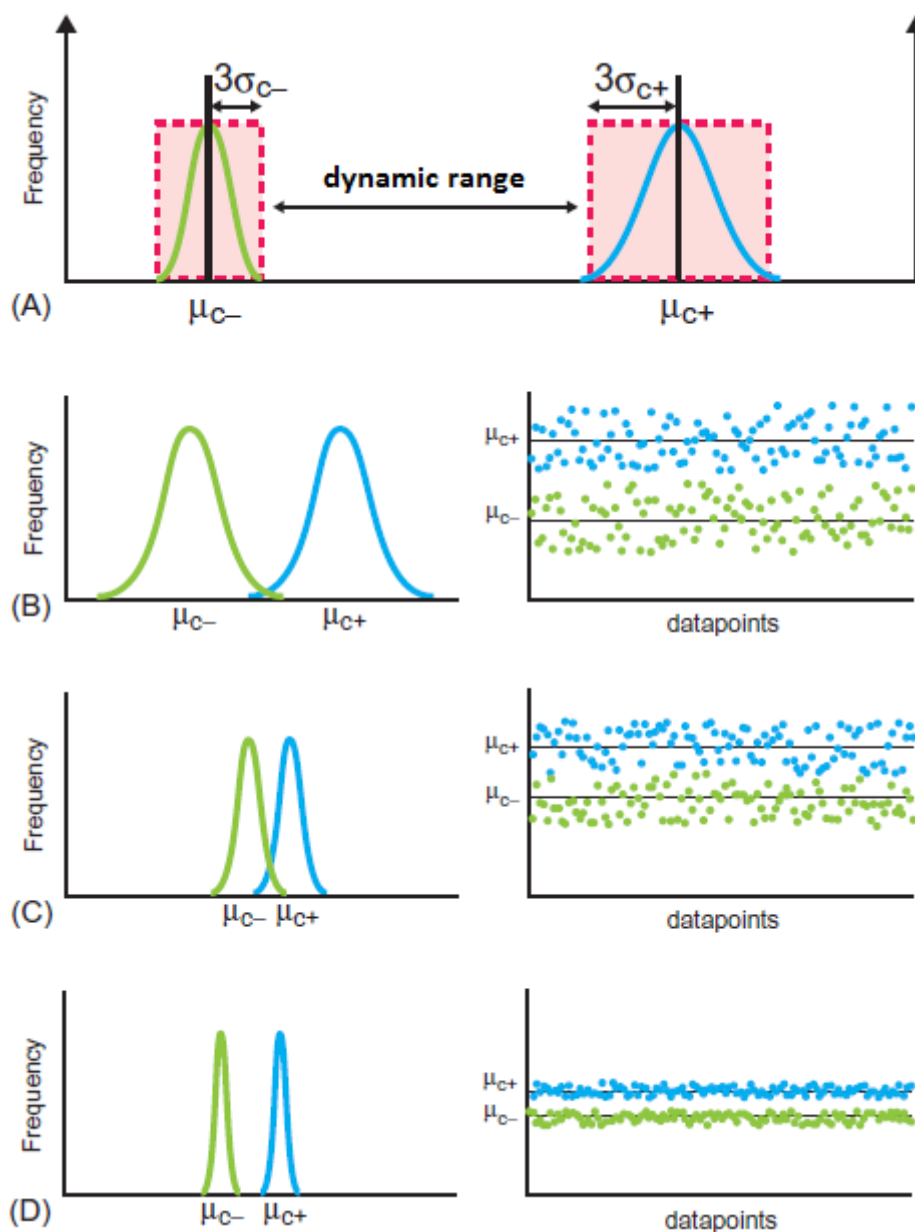


Figure I-16 : Representation of Z' values.

(A) Representation of the dynamic range and data variability (B) for a large intrinsic standard error of measurement (C) for a low dynamic range (D) for a correct dynamic range and low intrinsic standard error of measurement (good Z') (Kenakin, 2014).

It is assumed that 3σ represent a 99.73% confidence that a value outside this limit is different from the mean or a compound has a 99.73% chance of being confirmed upon secondary screening. Therefore compounds with a value superior to 3σ (typical threshold) are commonly retested in a secondary screening. However if the hit rate is so high that it is not possible to test all compounds showing an effect superior to 3σ from the mean,

a more stringent criterion or a small arbitrary percentage of active compounds will be selected to retest a lower number of them (Brideau, 2003; Kenakin, 2014). By contrast, if too few compounds are engaged in a secondary screening, an interesting hit might be missed (false negative rate increased).

Different statistical methods might be combined to represent an overall picture of the assay performance (Brideau, 2003) and further validation of hits will help to establish the robustness of the screening (Gordon, 2007).

1.3.3.2. Medicinal chemistry

Screening campaigns, the early stage in drug discovery aim finding an active molecule targeted to a disease-related protein, a hit compound that can serve as a starting point for therapeutic development. An identified hit compound is confirmed by performing concentration-response curves; it must show a relative activity and selectivity for the target that will be improved during hit to lead optimization. However, achieving sufficient *in vitro* target selectivity is often very difficult and requires numerous chemical modifications as well as testing on endogenous receptors expressed by the heterologous expression system. In addition further investigations with cell-based, tissue, or *in vivo* models are mandatory to confirm selective activity for the receptor targeted. Structure-activity relationship (SAR) studies allow the determination of a pharmacophore, structural elements required for biological activity. The verification of activity within a series of related structures and optimization of activity, efficacy and selectivity aim at generate lead compounds. Other features including favorable physicochemical properties, absence of toxophores and the capability for the rapid production of chemical analogs are also very important in the choice of lead molecules. Finally, ADMET (absorption, distribution, metabolism, excretion, and toxicity) properties and *in vivo* effects of the drug must be characterized and upgraded. A final step consists in the testing of candidates in humans (the ultimate model) in a clinical trial setting composed of three phases (Wermuth, 2008; Kenakin, 2014).

II. AIM OF THE WORK

Our strategy relies on a pharmacological approach to address the (patho)physiological roles of GPCRs. More precisely we attempt to characterize the pharmacology and physiology of GPCRs through pharmacological tools identification. Small-molecules modulators or "chemical probes" are an absolute prerequisite to confirm the involvement of a target in pathological conditions and disease models. As they reversibly inhibit or potentiate protein function, they give access to superior spatiotemporal information on a protein and its signaling mechanisms. In addition, their effects can often be controlled precisely in a dose-dependent manner, which is ideal for investigating biological mechanisms of GPCRs. Therefore, addressing a GPCR role with modulators is currently a recognized approach in drug discovery.

Our work can be divided in three major steps. The first one consists in the development of receptor models and assays for the characterization of signaling pathways as well as ligands identification. As the screening of libraries is a common approach to identify modulators for GPCRs, the second step of this work is to set-up an efficient assay for a GPCR screening campaign. The assay employed must be first optimized before the screening of a chemical small molecules library. The third step relies on another strategy that involves the characterization of the receptor binding pocket and the determination of a model which can be used to screen a virtual library. Subsequently, a structure-activity relationships study would help to design a pharmacophore for the GPCR under study.

To get active modulators of uncharacterized receptors, we first need sensitive assays to investigate receptor activation and signaling pathways. To set-up assays, **we selected** a receptor paired with its natural ligand, **succinate receptor 1 (SUCNR1)**. By contrast with orphan receptors, SUCNR1 can be used with its ligand as a positive control **to develop and validate our method.**

The understanding of SUCNR1 activation, signaling pathways and functions remains largely elusive, and calls for deeper investigations. SUCNR1 has high potential therapeutic application in a number of diseases area and is probably an important regulator of basic physiology.

However, the current paucity of specific pharmacological tools delays its validation as a drug target. In order to achieve the full characterization of this receptor, more specific pharmacological tools such as small-molecules modulators will represent an important asset. In addition, more widely available tools should rapidly prompt further investigations on the putative binding pocket to facilitate the design of new modulators. Such ligands might be used to address more deeply the role of the receptor, particularly in systems more relevant to human physiology.

Part 1 : Characterization of SUCNR1 signaling pathways and development of cell-based assays.

Firstly our intent is to improve the characterization of SUCNR1 signaling pathways described in the literature by developing assays to measure receptor capacity to couple to G proteins.

Part 2 : Chemical screening of SUCNR1

In order to identify new ligands for SUCNR1, we plan to perform a screening of a chemical library. As succinate has been well-described to induce $G_{\alpha i}$ signaling activation of SUCNR1, we are intent to develop an assay that allows to record cAMP levels variations via the measure of a signal stable over time that does not affect the system. However a well-known disadvantage of measuring cAMP decrease is the mandatory stimulation of cAMP levels. The inducers that must be employed generate various well-described artifacts and constitute a major challenge in the characterization of $G_{\alpha i}$ -coupled receptors. Therefore we attempt **to propose a cAMP-inducer free method for the detection of $G_{\alpha i}$ -coupled receptor agonists compatible with HTS**. To reach this goal we will investigate the improved GloSensor system (22F construct) already suggested to offer an assay sensitivity sufficient for recording cAMP inhibition of basal levels. Next we will apply our protocol on a test screening of a small chemical SOSA library, based on the principle that active compounds might have an activity on new targets at high concentration. Classically, we will perform a primary screening on SUCNR1 that will highlight potential active compounds. Then these ones will be retested in a secondary screening. Confirmed active compounds will be thoroughly investigated.

Part 3 : Virtual screening of SUCNR1

In order to discover new agonist scaffolds, we plan to conduct a virtual screening, which consists in modeling the receptor and dock several millions compounds *in silico*. This computer-based approach selects molecular patterns that have the best theoretical score to fit in the binding site of SUCNR1, previously described by He et al. The potential active compounds will subsequently be assayed.

The compounds identified to activate the receptor will be deeply characterized on other signaling pathways. All the information gathered from both chemical and virtual screenings will help to determine a pharmacophore for SUCNR1 that may serve as a template for the design and improvement of SUCNR1 modulators. Specific modulators (agonist/antagonist/allosteric modulators) would be invaluable tools to analyze carefully SUCNR1 signaling pathways and further dissect receptor functions in more relevant physiological models or animal models.

III. RESULTS AND DISCUSSION

III.1. Characterization of SUCNR1 signaling pathways and development of cell-based assays

III.1.1. G_{αi} signaling pathway

III.1.1.1. The biosensor

SUCNR1 was originally described to be coupled to G_{αi} in HEK293 cells (He et al., 2004). This result was later confirmed by Robben et al., in MDCK cells (Robben et al., 2009) and in several heterologous and native systems (Hakak et al., 2009; Gnana-Prakasam et al., 2011; Högberg et al., 2011; Sundström et al., 2013) (See I.2.4.). As SA induces G_{αi} activation which results in the decrease of cAMP levels (See I.1.4.1.), we critically assessed the available strategies to measure cAMP (See I.3.3.1.3.2.2.) and chose a biosensor-based strategy. For our project, the technique had to be sensitive, cost-effective, and permit real time kinetic analysis to monitor G_{αi}-coupled GPCR activity through cAMP levels changes. We selected the GloSensor™ cAMP assay (Promega) based on a recombinant FLuc fused with a cAMP binding domain (Fan et al., 2008).

Crystal structure of luciferase (Conti et al., 1996) reveals two domains linked by a flexible hinge region that rotate and close together upon luciferin binding (*Figure III-1*). The biosensor was constructed to modulate the motion of this hinge by generating a gene encoding a circular mutant luciferase fused with an allosteric domain closed to the hinge region. The consequence is that luciferase activity inducing luminescence is modulated by conformational changes within this domain. The fusion with cAMP-binding domain B from PKA regulatory subunit type IIβ (RIIβB) enables the detection of cAMP variations in living cells. Consequently cAMP levels are positively correlated with light output that allows evaluating ligands activity by using a luminometer (*Figure III-2*) (Binkowski et al., 2009). The optimized construct (*Figure III-1*) was reported to display a 70-fold increase in luminescence when selectively activated by cAMP at 100 μM (Fan et al., 2008).

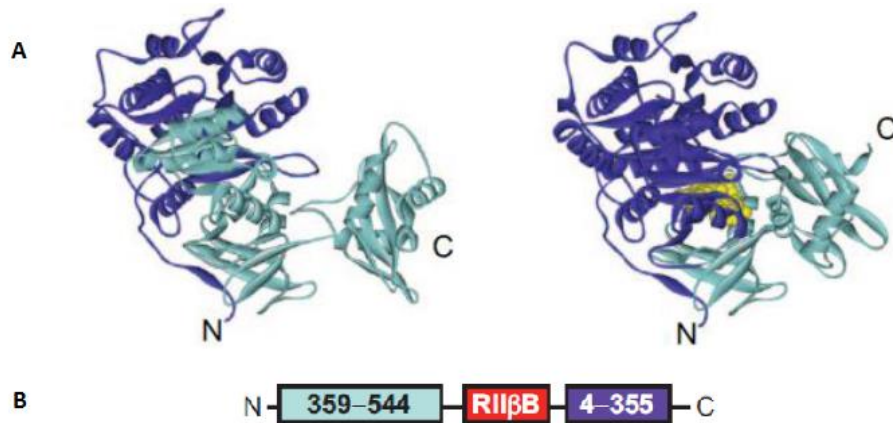


Figure III-1 : (A) Modelisation of FLuc in open conformation in absence of substrate (left) and closed conformation when a substrate analogue is present (yellow, right). (B) Optimized construct design of luciferase fused with the RIIβB domain (Fan et al., 2008).

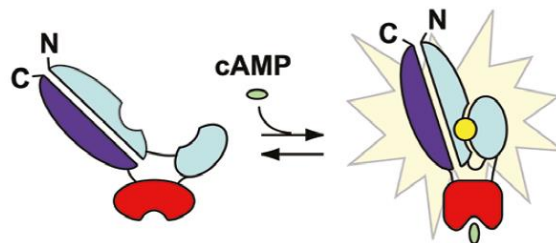


Figure III-2 : cAMP binding induces luminescence in presence of luciferin (Fan et al., 2008).

III.1.1.2. $G_{\alpha i}$ signaling pathway activation measure

We first generated HEK293 cell lines stably expressing N-terminus FLAG-tag SUCNR1 and verified its expression at the cell membrane by fluorescence-activated cell sorting (FACS) analysis (Figure III-3). Next we investigated the capacity of SA to activate SUCNR1 $G_{\alpha i}$ signaling pathway. To reach this goal we set-up a GloSensor cAMP assay by stably transfecting the plasmid pGloSensorTM-22F (pGlo) (Binkowski et al., 2011) into HEK293 cells.

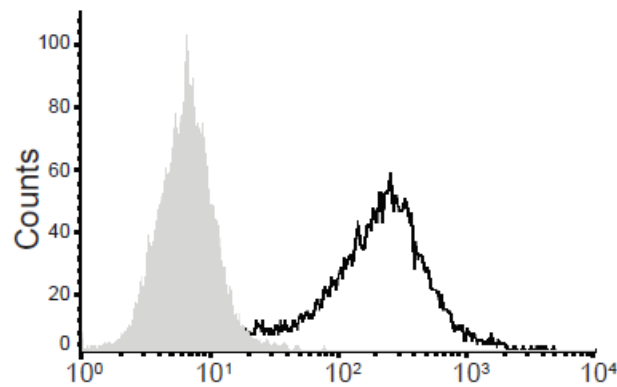


Figure III-3 : Cell-surface receptor expression analyzed by flow cytometry on HEK293.pGlo.SUCNR1 cells (not labeled in grey compared to Flag labeled in white).

We calculated the EC_{50} of different cAMP inducers in order to determine the concentrations that should be used in our system. We could detect a robust signal with increasing levels of FSK ($EC_{50} = 870.5 \pm 89.0$ nM) and isoproterenol ($EC_{50} = 153.6 \pm 4.1$ nM), a potent agonist for endogenous adrenoceptors coupled to G_{α_s} in HEK293 cells (Figure III-4).

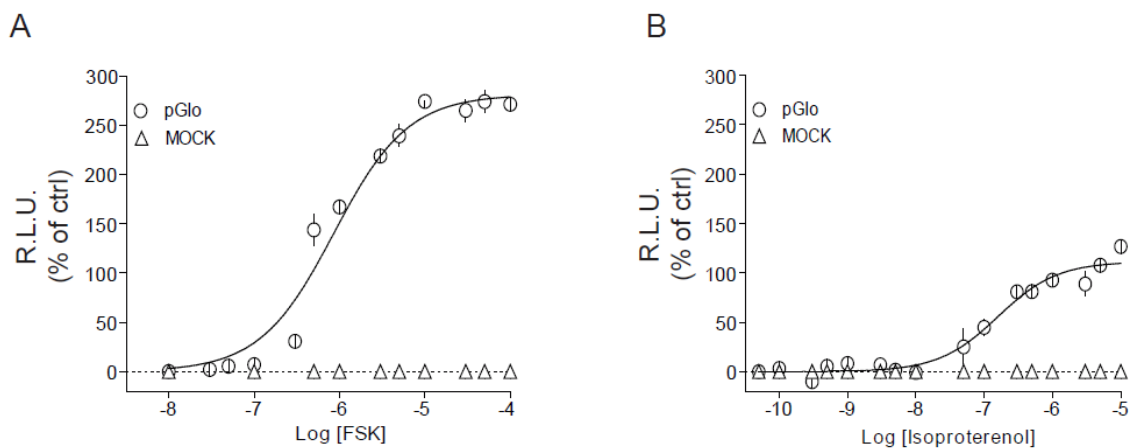


Figure III-4 : cAMP increase in a concentration-response manner in HEK293.pGlo cells when treated with (A) FSK and (B) isoproterenol. Data are expressed as mean \pm SEM of at least 3 experiments.

Thus, we stably transfected this HEK293.pGlo cell line with SUCNR1 subcloned in a bicistronic IRES vector allowing the simultaneous expression of two proteins from the same transcript. Double transfectants were selected for further experiments based on

FACS analysis of SUCNR1 expression at the cell membrane. The generated cell line HEK293.pGlo.SUCNR1 displayed a stable expression of the receptor over time, when the cells were grown in a selection medium.

We confirmed SUCNR1 as a G_{α_i} -coupled receptor by performing end-point assays in presence of its described ligand. Cells were incubated at RT for 1 h in a buffer supplemented with luciferin (the recommended GloSensor cAMP reagent is mainly composed of luciferin) and 1-methyl-3-(2-methylpropyl)-7H-purine-2,6-dione (IBMX), a non-selective PDE inhibitor to prevent cAMP degradation (Williams, 2004) (Figure III-5). The enzymes cAMP PDEs act as important negative-feedback system on the signaling cascade through cAMP degradation. cAMP PDEs activated by cAMP-dependent protein kinases phosphorylation catalyze the hydrolysis of the 3'5' ester bond of cAMP to form inactive 5' adenosine monophosphate (AMP) (Figure III-5).

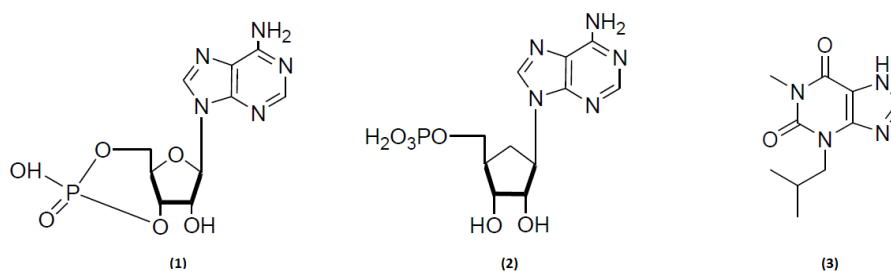


Figure III-5 : Structure of (1) cAMP, (2) AMP, (3) IBMX.

After incubation, cells were distributed in 96-well plates and basal levels were measured in each well. Next, cells were stimulated with FSK at 1 μM , the approximate EC_{50} in our system as determined by titration experiment (Figure III-4). Incubation of cells with SA at 500 μM at RT for 40 minutes in the presence of FSK resulted in a 28.3 ± 1.4 % decrease compared to control upon activation of SUCNR1 (Figure III-6 A). Complete concentration-response curves permitted the calculation of an EC_{50} of 79 ± 0.1 μM , consistent with published literature (Figure III-6 B) (He et al., 2004). Cells preincubated with pertussis toxin (PTX, 100 $\text{ng}\cdot\text{mL}^{-1}$) or devoid of receptor didn't respond to SA. PTX catalyzes the ADP-ribosylation of specific α -subunits of the G_{α_i} family that results in the uncoupling of the receptor and the protein (Figure III-7) (Fields and Casey, 1997; Kelley et al., 2006).

These results demonstrated that cAMP levels are specifically inhibited through SUCNR1 $G_{\alpha i}$ signaling pathway in presence of SA.

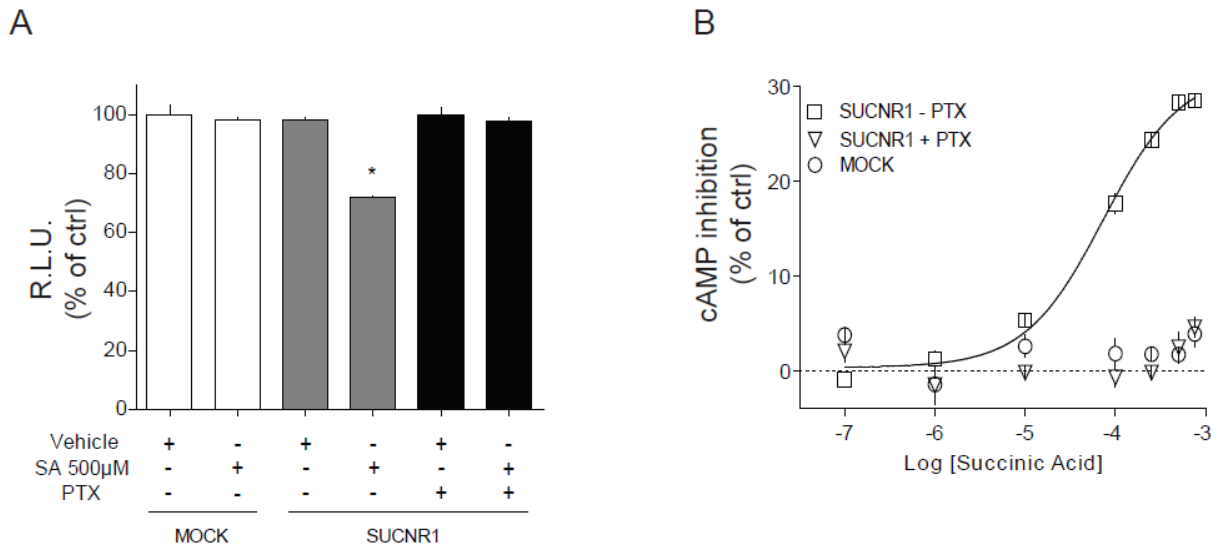


Figure III-6 : (A) End point measure of SA (500 μ M) effect on intracellular cAMP stimulated with 1 μ M FSK using HEK293.pGlo.SUCNR1 cells ($n = 3$; $p < 0.05$). (B) SA decreases cAMP levels stimulated with FSK 1 μ M in HEK293.pGlo.SUCNR1 cells in a PTX-sensitive and concentration dependent manner. Data are expressed as mean \pm SEM of at least 3 experiments.

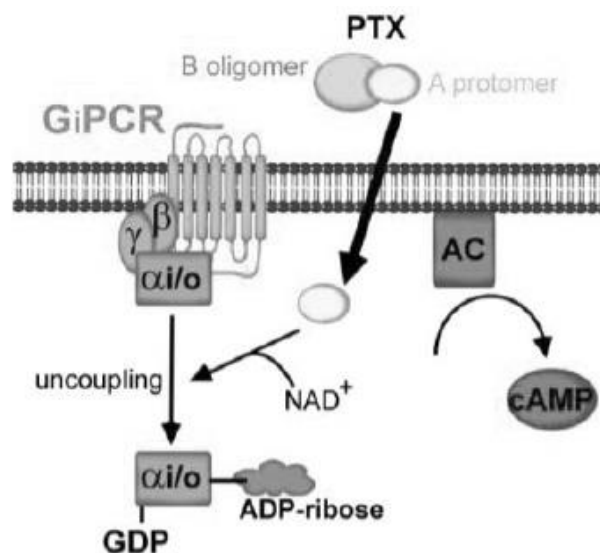


Figure III-7 : PTX mechanism that blocks $G_{\alpha i}$ -receptor interaction (Mangmool and Kurose, 2011).

III.1.2. $G_{\alpha q}$ signaling pathway

III.1.2.1. The biosensor

SUCNR1 was previously described to be coupled to $G_{\alpha q}$ (He et al., 2004; Robben et al., 2009) which ultimately leads to a release of $[Ca^{2+}]_i$ from intracellular stores upon action of IP_3 (See I.1.4.1.). Therefore we applied a calcium-sensitive bioluminescent assay by using an aequorin biosensor (*Figure III-8*) that allows real time measure of $[Ca^{2+}]_i$ by using a luminometer (See I.3.3.1.3.2.1.) (Ungrin et al., 1999; Le Poul et al., 2002).

The biosensor is composed of a fusion protein consisting of apoaequorin and GFP (*Figure III-8*) (Baubet et al., 2000).



Figure III-8 : Aequorin biosensor (plasmid G5A) containing the fusion protein construct. Linker has been added to optimize the energy transfer (Baubet et al., 2000).

The active protein aequorin (See I.3.3.1.3.2.1.) is formed in the presence of molecular oxygen from apoaequorin and its luciferin, coelenterazine (Shimomura and Johnson, 1969). Aequorin contains three EF-hand structures, described for the first time in the crystal structure of parvalbumin to comprise two nearly perpendicular α -helices (named after helices E and F in parvalbumin) (Kretsinger and Nockolds, 1973) separated by a 12-residue loop (Strynadka and James, 1989). The AAs of the loop provide the ligands for complexing Ca^{2+} ions. The binding of Ca^{2+} to aequorin induces a conformational change resulting in the oxidation of coelenterazine via an intramolecular reaction (Tsuji et al., 1986). The coelenteramide so produced is in an excited state and blue light (λ_{max} 470 nm) is emitted when it returns to its ground state (Shimomura and Johnson, 1978). However aequorin has a low light quantum yield (number of emitted photons per protein that bind Ca^{2+}) and consequently signals are difficult to detect. Therefore it is associated with GFP, which serves as an energy acceptor in the aequorin bioluminescent reaction (Inouye and Tsuji, 1994). Therefore, a green light (λ_{max} 509 nm) is emitted when the

excited GFP returns to its ground state (Figure III-9) (Cubitt et al., 1995). As a consequence, the reporter gene results in much more light being emitted (Baubet et al., 2000). The products of the reaction are coelenteramide and CO_2 , apoaequorin is finally recover.

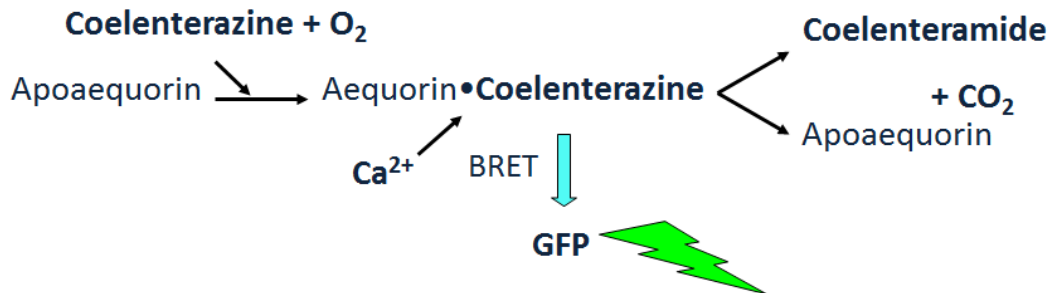


Figure III-9 : Aequorin assay principle (adapted from (Inouye and Tsuji, 1994)).

We first generated HEK293 cell lines expressing the aequorin biosensor together with SUCNR1 (HEK293.pG5A.SUCNR1 cells). As a next step for assay optimization, we determined concentration-response curves for SUCNR1 stimulated with SA at RT and confirmed the ability of the ligand to induce $[\text{Ca}^{2+}]_i$ mobilization with an $\text{EC}_{50} = 292.9 \pm 0.9 \mu\text{M}$ (Figure III-10).

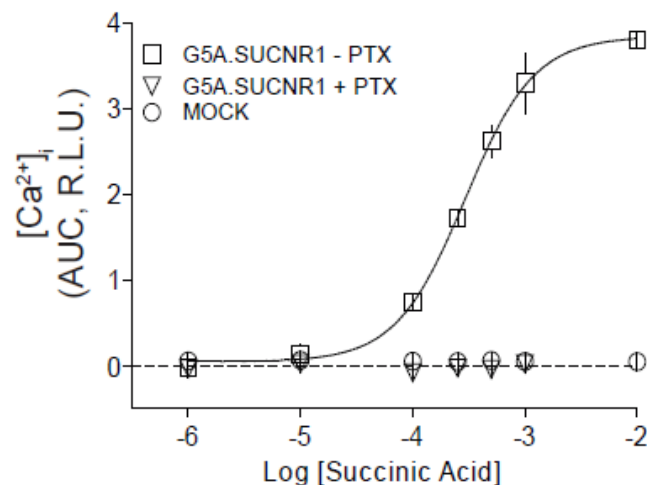


Figure III-10 : Calcium mobilization induced by SA in HEK293.pG5A.SUCNR1 cells. Pretreatment with PTX completely abolished the calcium mobilization induced by SA. Data are expressed as mean \pm SEM of at least 3 experiments.

III.1.2.2. G_{αq} signaling pathway assessment

Although SUCNR1 was well established as being coupled to G_{αi}, the view of SUCNR1 being coupled to G_{αq} has been challenged (Sundström et al., 2013). While Sundström et al. proposed that the observed [Ca²⁺]_i mobilization was a consequence of PLC-β activation by the βγ dimer in HEK293 cells, we investigated SUCNR1 signaling pathway involved in [Ca²⁺]_i mobilization using PTX described above. We observed that the signal was abolished when the cells were preincubated overnight with the toxin (100 ng.mL⁻¹). Therefore succinate triggers a concentration-dependent PTX-sensitive [Ca²⁺]_i mobilization (*Figure III-10*). Our results suggest, in accordance with Sundstrom et al., that SUCNR1 is not coupled to G_{αq}, at least when heterologously expressed in HEK293 cells.

The discrepancy with results obtained by Robben, He and co-workers, who suggest that [Ca²⁺]_i mobilization shut down requires the blockade of both G_{αi} and G_{αq} signaling, may reflect distinct G protein partners among different cell types or artifacts induced by overexpression of the receptor. The existence of G_{αq}-coupling with SUCNR1 requires additional investigations, especially in native and physiologically relevant systems.

III.1.3. Arrestins recruitment

III.1.3.1. The biosensor

To characterize the ability of GPCRs to recruit arrestins, Nadine Dupuis developed a split firefly luciferase complementation strategy based on the work of Takakura et al. (Takakura et al., 2012). The assay consists in the measurement of bioluminescence signal emitted in the presence of luciferin when the two parts of the luciferase reconstitute a functional enzyme. In order to measure arrestin translocation, one part is fixed at the C-terminal end of the GPCR of interest, the other on the N-terminal end of arrestin. Once the receptor gets activated, phosphorylation occurs and arrestin comes nearby, bringing each luciferase fragment into proximity. Thus the two parts are reunited and the reconstituted luciferase becomes active, resulting in the emission of bioluminescence measurable with a luminometer (*Figure III-11*). This strategy was validated with the β_2 -adrenoceptor by Nadine Dupuis.

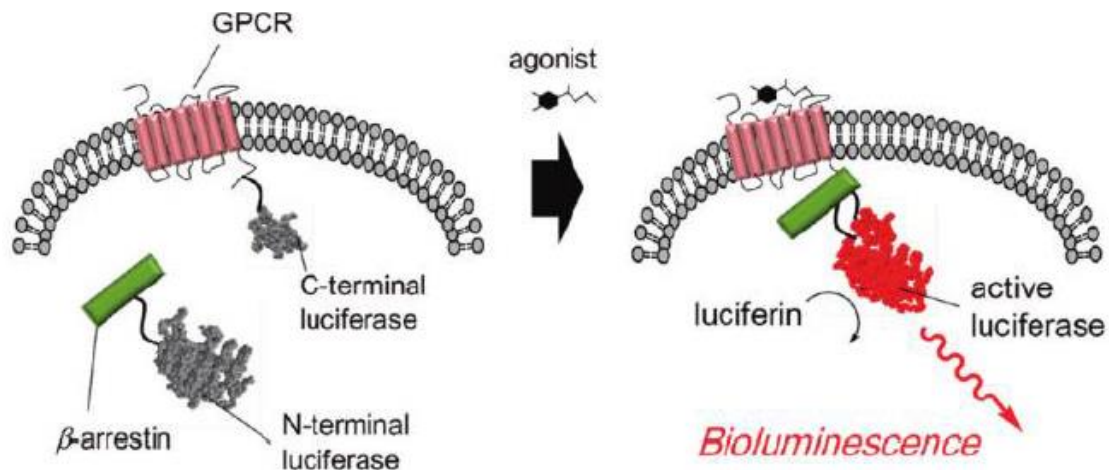


Figure III-11 : Complementation of a split luciferase induced by arrestin recruitment to the activated-receptor (Takakura et al., 2012).

III.1.3.2. Ability of SUCNR1 to recruit arrestins

He et al. described SUCNR1 to be internalized into vesicular structures upon succinate exposure in HEK293 cells (He, et al., 2004). Therefore, we first investigated its ability to internalize in a constitutive manner at 37°C. We showed SUCNR1 localization in an endosome-like structure within the cytosol by immunofluorescence staining and confocal microscopy (*Figure III-12*).

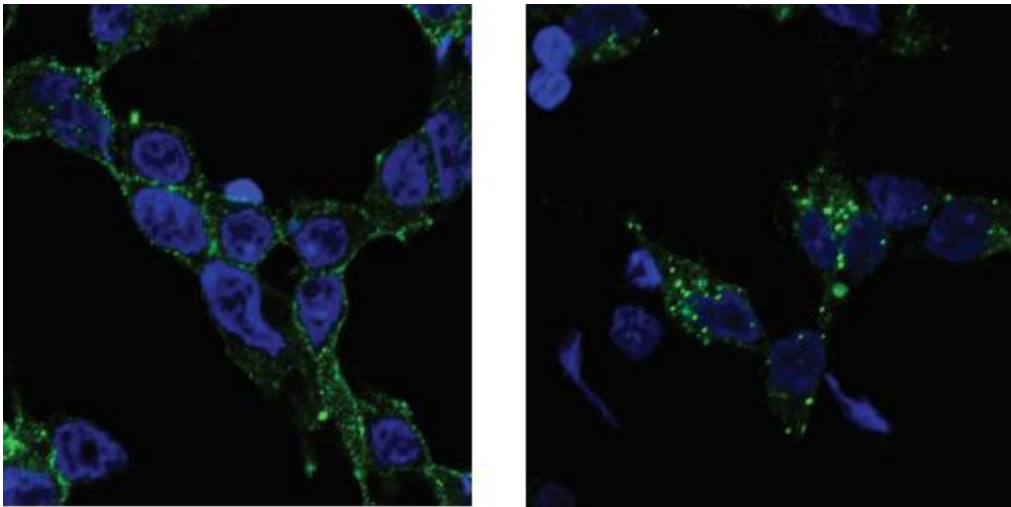


Figure III-12 : SUCNR1 is internalized in a constitutive manner in HEK293 cells expressing FLAG-tag SUCNR1 at 37°C (right) compare to 0°C (left).

Since arrestins are reported as being responsible for GPCRs internalization in many receptors (Gurevich and Gurevich, 2006), we analyzed the capacity of activated SUCNR1 to recruit arrestin 2 and 3. We first generated HEK293 cell lines stably expressing SUCNR1 and arrestin 2 or 3 connected with the firefly luciferase fragments (HEK293.pIRESHygroFnLARR2.pIRESpuroSUCNR1 (ARR2.SUCNR1) and HEK293.pIRESHygroFnLARR3.pIRESpuroSUCNR1 (ARR3.SUCNR1) cell lines) and verified both expression at the cell membrane by FACS analysis.

Following the optimization of the assay protocol to SUCNR1 (number of cells, buffer, time of stimulation), we determined concentration-response curves for SUCNR1 stimulated with SA at RT and we showed that the coupling of activated receptor to

arrestins 2 ($EC_{50} > 2 \text{ mM}$) and 3 ($EC_{50} > 1 \text{ mM}$) is very weak (Figure III-13). Nevertheless results for arrestin 3 were consistent with those reported by Southern et al. in CHO cells (Southern et al., 2013). As a consequence of this weak coupling, we were not able to classify SUCNR1 as a class A or B receptor when we followed time-dependent changes in the association and dissociation process of the receptor-arrestin complex (Hattori et al., 2013).

We also generated and characterized cell lines stably expressing the β_2 -adrenoceptor as a negative control of SA effect (Mock transfected cells).

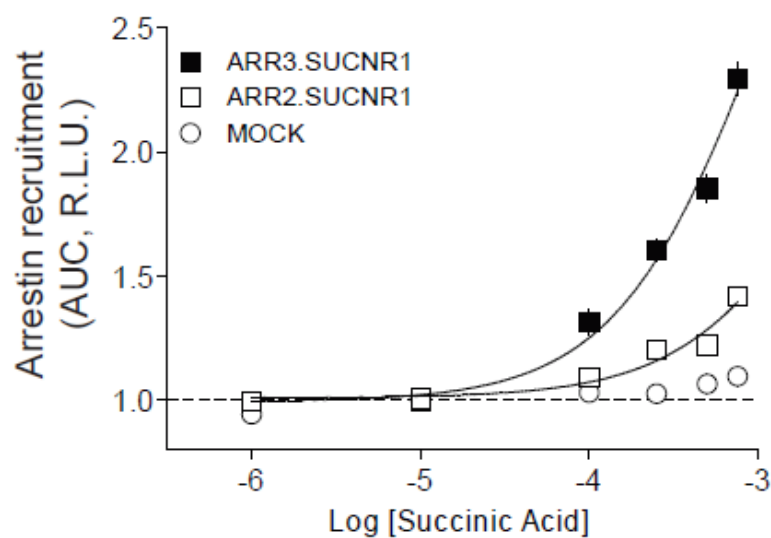


Figure III-13 : SUCNR1 is weakly coupled to arrestin 3 ($EC_{50} > 1 \text{ mM}$) and arrestin 2 ($EC_{50} > 2 \text{ mM}$) when stimulated with SA in ARR3.SUCNR1 and ARR2.SUCNR1 cells, respectively; SA has no effect on Mock transfected cells. Data are expressed as mean \pm SEM of at least 3 experiments.

Therefore, we postulated that arrestin doesn't play a significant physiological role in this receptor-ligand system since SA would have to reach important concentration (above 1 mM) to weakly activate this pathway.

In addition, it is likely that homologous desensitization and internalization occur by a mechanism, which doesn't involve arrestins (See I.1.4.3.1.). However, these questions have never been addressed directly.

III.1.4. Determination of ERK phosphorylation

Authors showed that SA binding to SUCNR1 triggers the phosphorylation of ERK in different cell types (See I.1.4.1.). Therefore we investigated SA capacity to increase phosphorylated ERK (p-ERK) in HEK293.SUCNR1 cells. In a previous work, Céline Laschet measured a p-ERK maximum increase at 3 minutes after addition of SA that was followed by a rapid decrease in HEK293.SUCNR1 cells (*Figure III-14*) (Laschet, 2014). These results suggested a rapid and transient p-ERK activation mediated by G protein, which is usually associated with migration of p-ERK to the nucleus and cell proliferation (See I.1.4.3.2.). This hypothesis is in accordance with the results of Hakak et al. who demonstrated that activation of ERK mediate cell proliferation (Hakak et al., 2009) and thus might be investigated in more cell types than TF-1 cells.

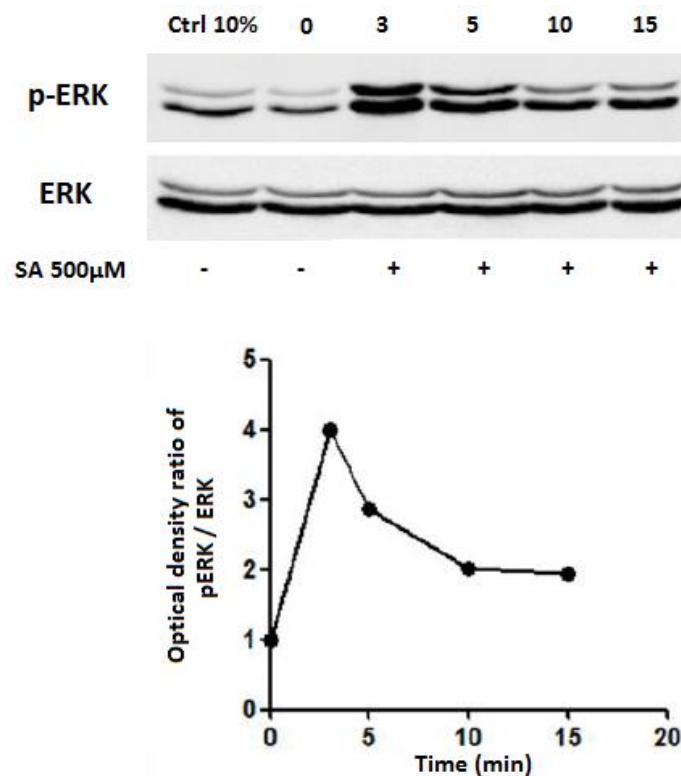


Figure III-14 : Time-dependent ERK phosphorylation in HEK293.SUCNR1 cells. Cells were grown to confluence, starved overnight (0.2 % FBS; except for Ctrl 10%) and subsequently incubated with 500 μM of SA for the indicated times. Adapted from (Laschet, 2014).

We showed that stimulation with SA (100 and 500 μM) for 3 minutes induces a p-ERK increase in a concentration-response manner in HEK293.pGlo.SUCNR1 cells (*Figure III-15*). In addition, as described earlier in TF-1 cells overnight treatment with PTX indicated that ERK activation is $G_{\alpha i}$ -dependent (*Figure III-15*). Many studies have contributed to identify mechanisms by which GPCRs mediate MAPK signaling. SUCNR1-induced p-ERK stimulation requires further investigations. It might be mediated through $G_{\alpha i}$ inhibition of AC or activation of an alternative Ras-dependent mechanism. In addition, Ras activation might also be involved through the dimer $\beta\gamma$ (Goldsmith and Dhanasekaran, 2007).

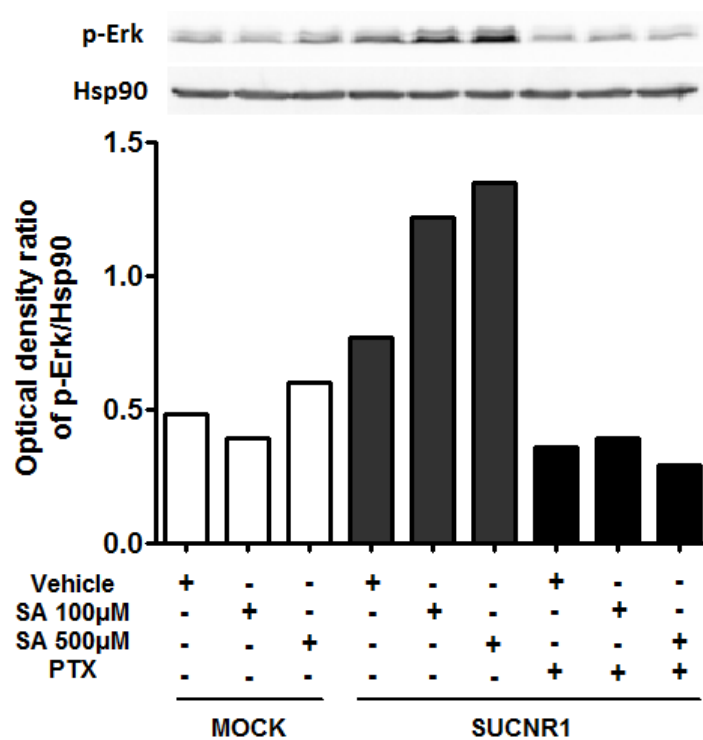


Figure III-15 : Activation of p-ERK by stimulation of untreated and PTX-treated HEK293.pGlo.SUCNR1 cells with SA (100 and 500 μM) during 3 minutes. Results shown are representative of at least 4 experiments performed by Céline Laschet.

III.1.5. $G_{\alpha 12/13}$ signaling pathway

HEK293 cells stably transfected with SUCNR1 display a particular phenotype in culture where they seem to be subject to a modification of their shape compared to WT cells. Particularly if cells are too much diluted ($> 1/3$), they grow up with a characteristic pseudopods-like structure (*Figure III-16*).

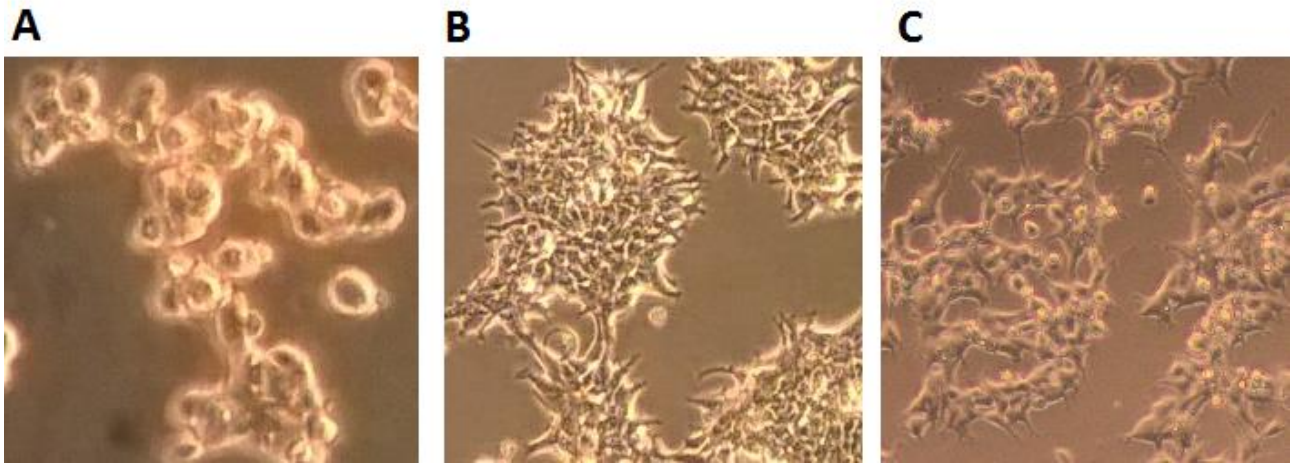


Figure III-16 : Evolution of cells growth. (A) HEK293.SUCNR1 cells one day after dilution ($> 1/3$). (B) third day and (C) HEK293.SUCNR1 cells one day after dilution ($1/3$).

We hypothesized that this modification might be due to $G_{\alpha 12/13}$ signaling pathway activation (See I.1.4.1.), known to mediate cell shape changes and migration during normal gastrulation (Lin et al., 2005). In addition, Rho GTPases were shown to bind to the actin-binding and -scaffolding protein filamin A which participates in the regulation of changes in cellular shape and motility (Scott et al., 2006).

Besides, SA induces (Högberg et al., 2011) or at least co-stimulates platelet aggregation (Spath et al., 2012) via SUCNR1, highly expressed in human platelets (Macaulay et al., 2007; Amisten et al., 2008; Högberg et al., 2011; Spath et al., 2012). Although SUCNR1 has never been identified as coupled to $G_{\alpha 12/13}$, the discrepancies concerning its effect on platelets might be explained by the activation of this signaling pathway. Indeed $G_{\alpha 13}$ genetic deletion in platelets results in mice with increased bleeding times and reduced sensitivity to aggregation-inducing stimuli (Moers et al., 2003).

To assess $G_{\alpha 12/13}$ signaling we chose to evaluate Rho activation in lysed cells with a Rhotekin Rho pull-down assay. This method uses a GST-Rhotekin-Rho binding domain

fusion protein to bind the activated GTP-bound Rho and a glutathione resin to immunoprecipitate the complex. Next, the sample is eluted and Rho activation levels are analyzed by western blot using a Rho rabbit antibody (Ren and Schwartz, 2000; Siehler, 2007). We applied this method to HEK293.SUCNR1 cells stimulated with SA at 500 μ M compared with WT cells (*Figure III-17*). However we were not able to measure an increase in activated Rho levels and thus cannot validate this hypothesis.

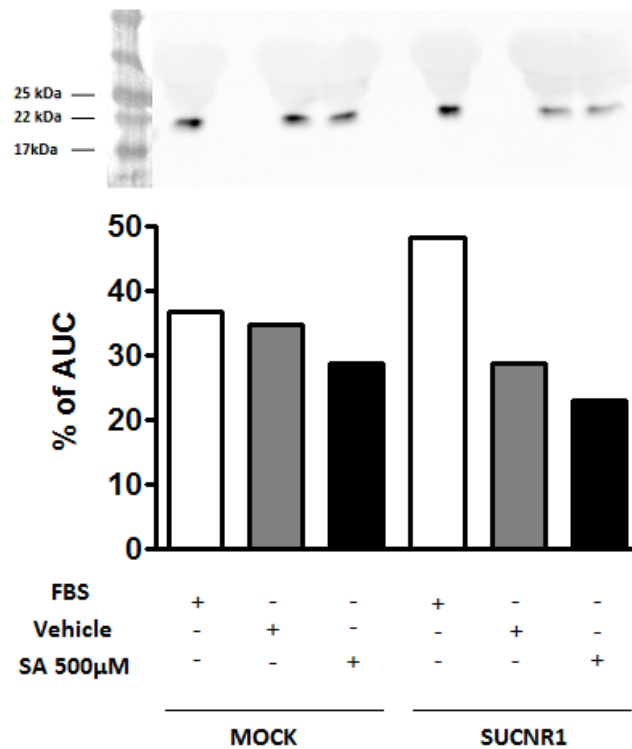


Figure III-17 : Rho activation levels induced by stimulation of HEK293.SUCNR1 cells with FBS 10% or SA (500 μ M) during 10 minutes. Results shown are representative of one experiment.

III.2. Screening of SUCNR1 with a FSK-free cAMP assay

Arrestins bind to an important number of GPCRs and their interactions with the receptor last for several hours. Therefore, arrestin assays allowing to monitor general receptor activity are often described as being a superior set-up. They are thus widely emphasized for the identification of GPCRs ligands (See I.3.3.1.3.1.) (Chen et al., 2012).

Investigation of SUCNR1 signaling pathways with its natural ligand SA, revealed that this receptor is weakly coupled to arrestins (See III.1.3.2.). For that reason a screening based on arrestin assay would not be a good option, ligands less effective than SA would probably never be detected. By contrast SUCNR1 appears to be more efficiently coupled to $G_{\alpha i}$ ($EC_{50} = 79 \pm 0.1 \mu M$). Therefore we chose an assay directly recording endogenous cAMP levels variations that allows the measure of a signal stable over time and doesn't affect the system.

As biosensors technology offers many advantages over other cAMP accumulation and reporter based methods, we selected the GloSensor system marketed in 2008 (See III.1.1.). The assay using GloSensor system has been reported as a reproducible and robust alternative to traditional methods for screening either $G_{\alpha s}$ - or $G_{\alpha i}$ -coupled receptors (Buccioni et al., 2011; Pantel et al., 2011; DiRaddo et al., 2014). However to detect a signal inhibition of $G_{\alpha i}$ -coupled receptors agonists, cAMP levels must be stimulated. But the cAMP-inducers used generate various artifacts and constitute a major challenge in the characterization of $G_{\alpha i}$ -coupled receptors (See I.3.3.1.3.3.).

In this study, we attempted to propose a cAMP-inducer free method for the detection of $G_{\alpha i}$ -coupled receptors agonists compatible with HTS. To reach this goal, firstly we characterized the GloSensor system (22F construct) for investigating $G_{\alpha i}$ -coupled receptors without cAMP-inducer. This biosensor was suggested to offer an assay sensitivity sufficient for recording cAMP inhibition of basal levels without FSK (Binkowski et al., 2011). In a second part we set-up this real time assay to HTS of $G_{\alpha i}$ -coupled receptors. Finally we applied our protocol on a test screening of a library and compared results obtained without FSK to those gained following cAMP stimulation.

III.2.1. Real time analysis of cAMP levels modulation mediated by

SUCNR1 activation

As the GloSensor system is described to be compatible with kinetic measurement (See I.3.3.1.3.2.2.3.), we were able to follow the stable over time effect (experiment of 40 minutes) of the addition of SA after the injection of FSK (*Figure III-18 A*). We observed that the levels of cAMP were already decreased in the presence of SA at the first measure compared to control. This effect was concentration-dependent and we reasoned that it could be the actual effect of SA on the system.

In order to validate this hypothesis, as the improved GloSensor system is reported to offer the best increased dynamic range, we investigated if the assay sensitivity could be sufficient for recording cAMP inhibition of basal levels without FSK. We followed the unstimulated levels of cAMP for 30 minutes and injected SA at the concentration of 500 μM (*Figure III-18 B*). Although the signal was stable before the addition of SA, it immediately dropped further below the baseline.

Then we reversed the experiment and classically analyzed the effect of the addition of the ligand following cAMP levels stimulation with FSK (*Figure III-18 C*). The signal induced by FSK was inhibited by SA although the level didn't go back to basal but reached a plateau (*Figure III-18 C*). The integration over time (Area under the curve or AUC) for 5 minutes on basal levels (*Figure III-18 D, white bars*) or for 40 minutes post-addition of FSK (*Figure III-18 D, black bars*), showed that the effect of SA reached significance in both conditions ($p < 0.01$).

Therefore we inferred that the biosensor in our set-up and receptor system possesses an unprecedented dynamic range that allows robust measure of basal cAMP levels inhibition without FSK. In addition, an FSK-free method enables an improved measurement time of only 5 minutes compared to longer times required for FSK protocol.

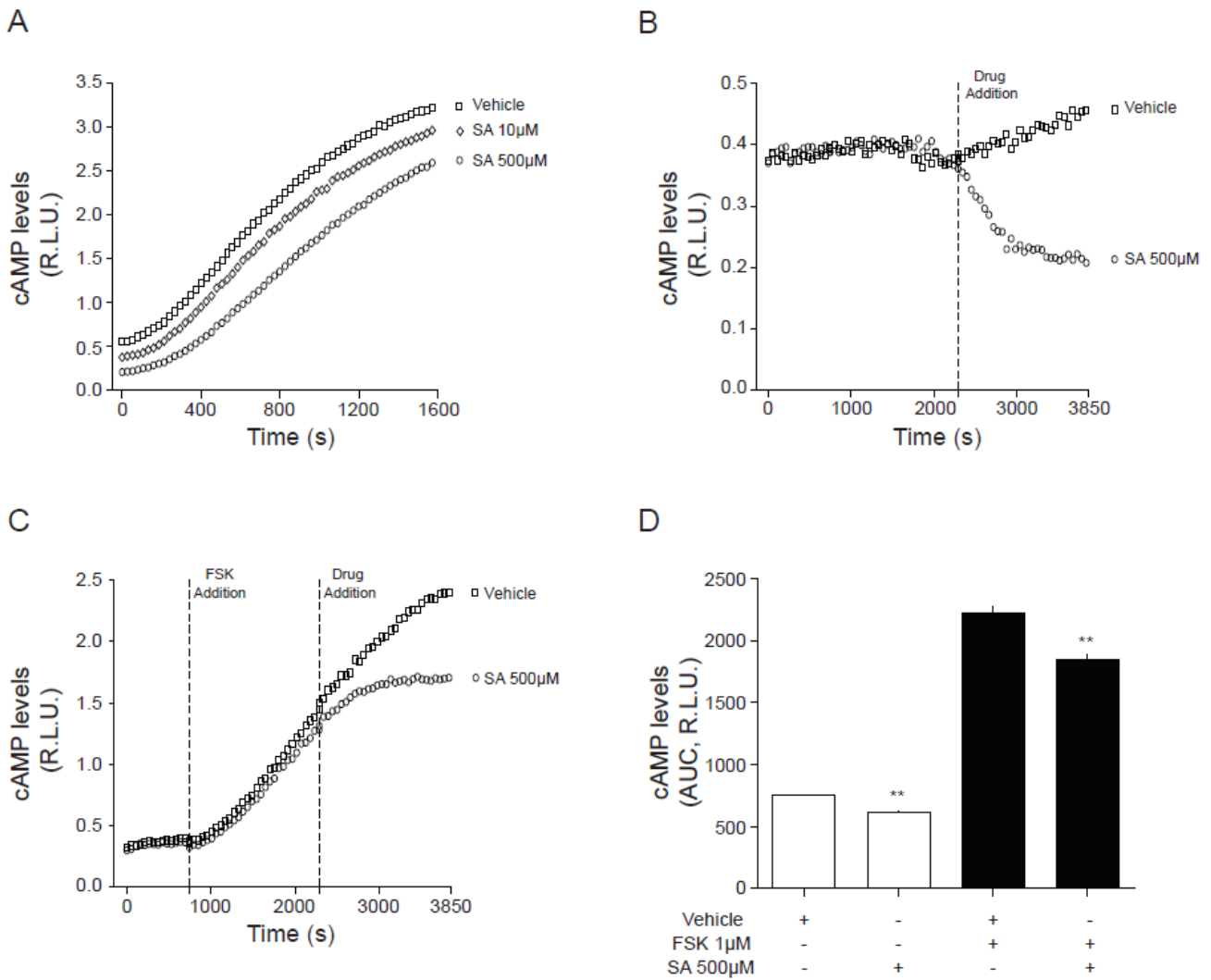
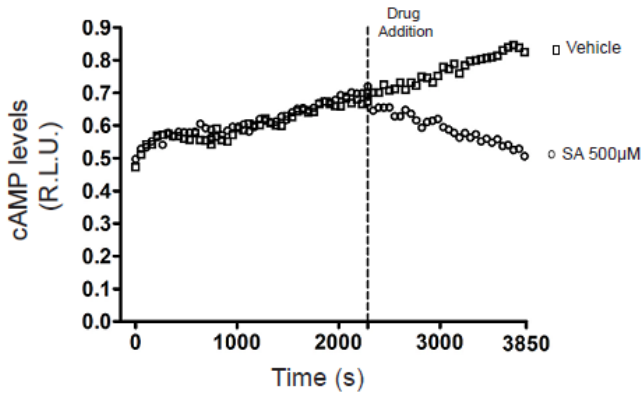


Figure III-18 : Real time analysis of cAMP levels modulation mediated by SUCNR1 activation. (A) SA effect is stable over the time of experiment (40 minutes). (B) Basal cAMP levels dropped below the baseline after injection of SA at 500 µM. (C) cAMP levels induced by 1 µM of FSK are inhibited by SA at 500 µM until to reach a plateau. (D) Comparison of AUC on basal levels (white bars) or for 40 minutes post-addition of FSK (black bars) in presence of SA at 500 µM ($p < 0.01$). Data are expressed as mean \pm SEM of at least 3 experiments.

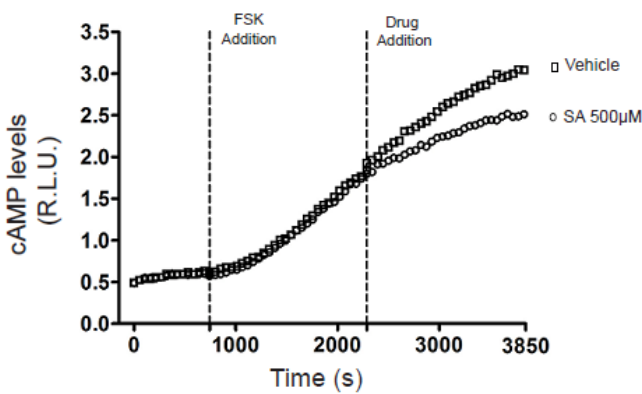
Although the system worked well without incubating cells with PDE inhibitors, we evaluated the impact of IBMX, which is reported as being able to modify the sensitivity of the system (Williams, 2004; Pantel et al., 2011). The integration over time was calculated as previously for results obtained without IBMX (Figure III-18). The effect of SA reached significance in both conditions, basal levels ($p < 0.001$) and post-addition of SA ($p < 0.01$) (Figure III-19 C). We confirmed that using IBMX in our assay improved the potency of FSK and also increase basal levels of cAMP (Figure III-19 A&B) compared to maximal values obtained without IBMX (Figure III-18 B&C). Therefore we decided to

incubate cells with IBMX in subsequent experiments to further potentiate basal cAMP levels.

A



B



C

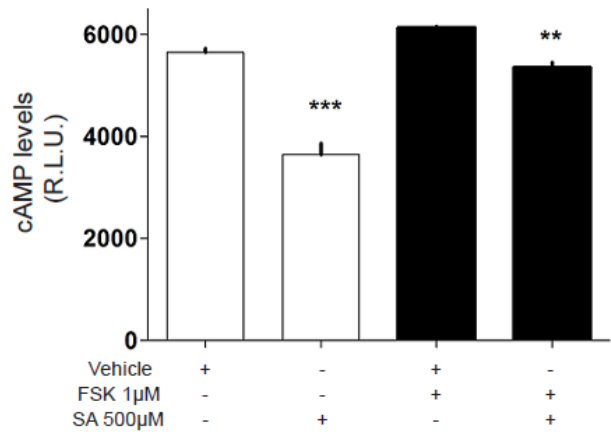


Figure III-19 : Real time analysis of cAMP levels modulation mediated by SUCNR1 activation in presence of IBMX. (A) Basal cAMP levels and (B) cAMP levels induced by FSK at 1 µM were increased in presence of IBMX compared to Figure III-18. (C) Comparison of AUC on basal levels (white bars ; $p < 0.001$) or for 40 minutes post-addition of FSK (black bars ; $p < 0.01$) in presence of SA at 500 µM. Data are expressed as mean \pm SEM of at least 3 experiments.

Next, we determined the activity of SA on basal cAMP levels through SUCNR1 activation by establishing a complete concentration-response curve (Figure III-20 A). We calculated an $EC_{50} = 22.83 \pm 0.03 \mu\text{M}$ for SA decrease of basal cAMP levels and an $EC_{50} = 45.79 \pm 0.08 \mu\text{M}$ for the inhibitory effect of SA on FSK induced cAMP (Figure III-20 A) that were significantly different ($p < 0.05$). Interestingly, the E_{max} ($E_{\text{max}} = 52.3 \pm 2.7 \%$ of control) obtained on cAMP basal levels was significantly ($p < 0.05$) greater than maximal inhibition in the presence of FSK ($E_{\text{max}} = 38.0 \pm 1.5 \%$ of control). In order to exclude that the effect on cAMP basal levels was limited to SUCNR1 or heterologously expressed receptors, we determined agonist potency of CXCL12 on endogenous CXCR4 (Wu et al., 2010; Atwood et al., 2011) with the same methodology (Figure III-20 B). We calculated an $EC_{50} = 16.01 \pm 1.07 \text{ nM}$ and $E_{\text{max}} = 62.9 \pm 0.2 \%$ (% of control) for CXCL12-induced decrease of basal cAMP levels and an $EC_{50} = 13.93 \pm 1.12 \text{ nM}$ and $E_{\text{max}} = 16.9 \pm 2.4 \%$ (% of control) for the inhibitory effect of CXCL12 on FSK-induced cAMP production. The differences between E_{max} were statistically significant ($p < 0.0001$).

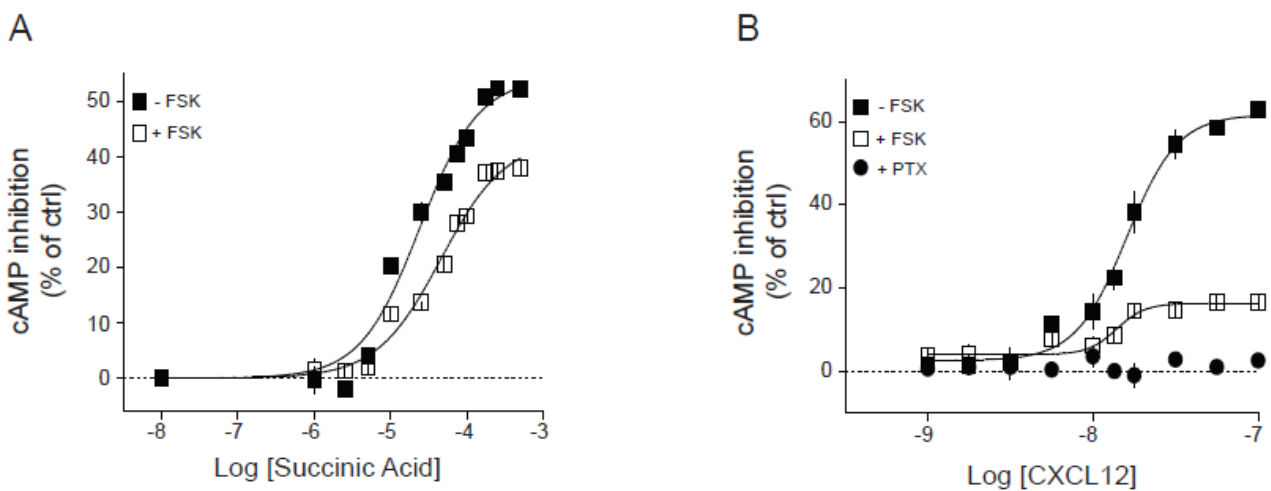


Figure III-20 : (A) Concentration-response curve for SA on HEK293.pGlo.SUCNR1 cells stimulated with FSK $1 \mu\text{M}$ (\square) or not stimulated (\blacksquare). (B) Concentration-response curve for CXCL12 on HEK293.pGlo cells stimulated with FSK $1 \mu\text{M}$ (\square) or not stimulated (\blacksquare). Pretreatment with PTX completely abolished the effect of CXCL12 on HEK293.pGlo cells. Data are expressed as mean \pm SEM of at least 3 experiments.

The use of FSK affected EC_{50} and E_{max} values, therefore we investigated a range of FSK concentrations (0.1-1 μ M) and observed that SA EC_{50} and E_{max} were dependent on FSK concentration (Figure III-21 A). Indeed EC_{50} increased following rising concentrations of FSK whereas E_{max} for SA decreased (EC_{50} = 18.86 ± 4.33 μ M; E_{max} = $74.1 \pm 1.7\%$ of control without FSK; EC_{50} = 26.96 ± 5.31 μ M; E_{max} = $72.3 \pm 2.3\%$ of control for 0.1 μ M FSK; EC_{50} = 41.73 ± 10.5 μ M; E_{max} = $58.28 \pm 5.9\%$ of control for 0.5 μ M FSK; EC_{50} = 26.96 ± 5.31 μ M; E_{max} = $54.87 \pm 9.1\%$ of control for 1 μ M FSK).

The observed differences in EC_{50} and E_{max} may also be partially explained by variations in luciferin concentration in assay buffer, before and after FSK injection. We tested several assay buffers with different luciferin content but didn't see any effect on SA response (Figure III-21 B).

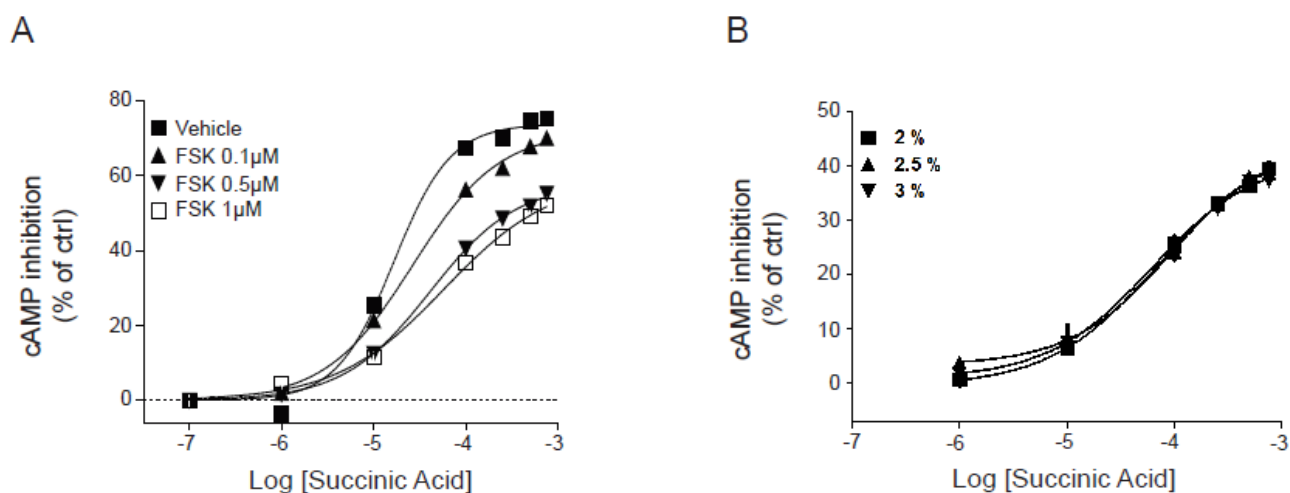


Figure III-21 : Evaluation of FSK and luciferin on the system (A) Concentration-response curve for SA on HEK293.pGlo.SUCNR1 cells stimulated with different concentrations of FSK. (B) Concentration-response curve of SA on HEK293.pGlo.SUCNR1 cells incubated with different concentrations of luciferin (2% correspond to 833.3 μ M according to manufacturer instructions; 2.5% correspond to 1041.7 μ M and 3% correspond to 1250 μ M).

In conclusion of this section, we set-up a cAMP assay method with a sufficient sensitivity to detect basal cAMP levels inhibition for $G_{\alpha i}$ -coupled receptors, heterologously expressed as well as endogenously present in HEK293 cells.

III.2.2. Optimization of a screening protocol

In order to assess if our FSK-free assay was compatible with the screening of chemical libraries, we designed a protocol to compare the effects of compounds on basal and FSK-induced cAMP levels. The first step of the protocol consisted in the distribution of 1 μ L of drug solutions from the library in 96- or 384-well plates. Next, a cell suspension previously incubated with luciferin and IBMX for 1 h at RT, was added and mixed thoroughly in the plate. The mixture between drugs and cells was incubated at RT for 10 minutes. The basal level of each well was measured for 5 minutes and the AUC was determined. These results constituted the "basal level screen", pictured in green in *Figure III-22 A*. FSK at 1 μ M final concentration was added to each well and a kinetic measurement was recorded for 40 minutes. The signal was integrated and expressed as AUC for each well. These results were called the "FSK-induced screen", pictured in red, in *Figure III-22 A*.

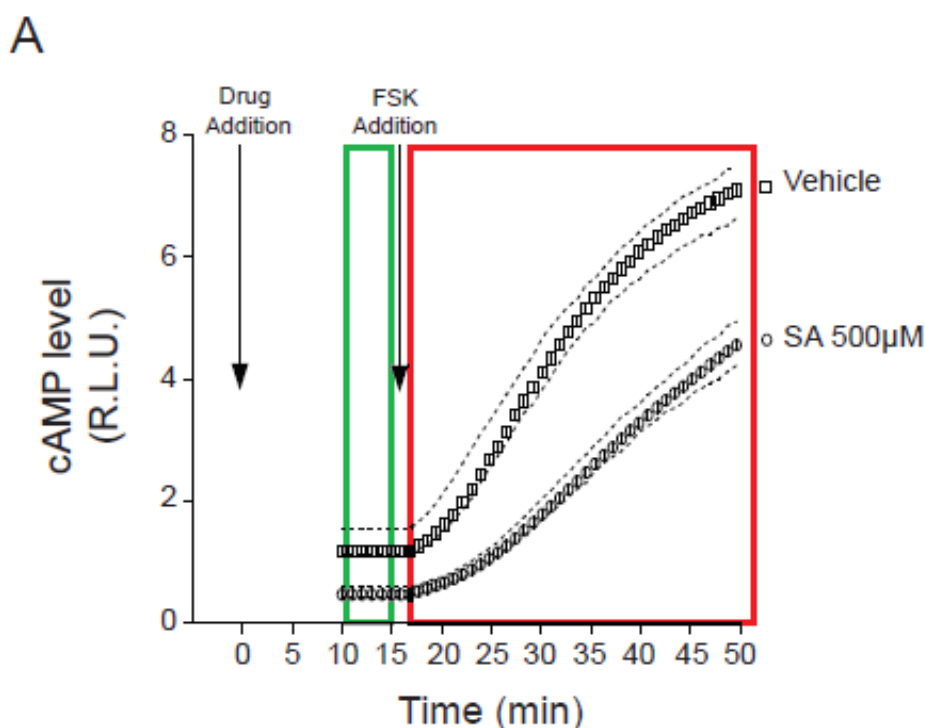


Figure III-22 : Optimization of a screening protocol and assay performance. (A) Design of a screening protocol for direct comparison between the effect of compounds on basal and FSK-induced cAMP levels.

The "basal level screen" (in green) corresponds to AUC of basal level of each well measured for 5 minutes whereas the "FSK-induced screen" (in red) is the 40 minutes kinetic measure of cAMP levels stimulated with FSK at 1 μ M.

We characterized the quality of the assay (Z') (See I.3.3.1.4.) for both conditions in 96- and 384-well plates with SA at 500 μ M and vehicle controls. In 96-well plates, we calculated the Z' factor for basal cAMP levels to be 0.81 (Figure III-22 B). The values obtained following FSK stimulation are shown in Figure III-22 C and the calculated Z' factor was 0.74. Next, we evaluated the assay quality on 384-wells plates and found a Z' factor of 0.75 for SA inhibition of basal cAMP levels (Figure III-22 D) and 0.61 for SA inhibition of FSK-induced cAMP production (Figure III-22 E).

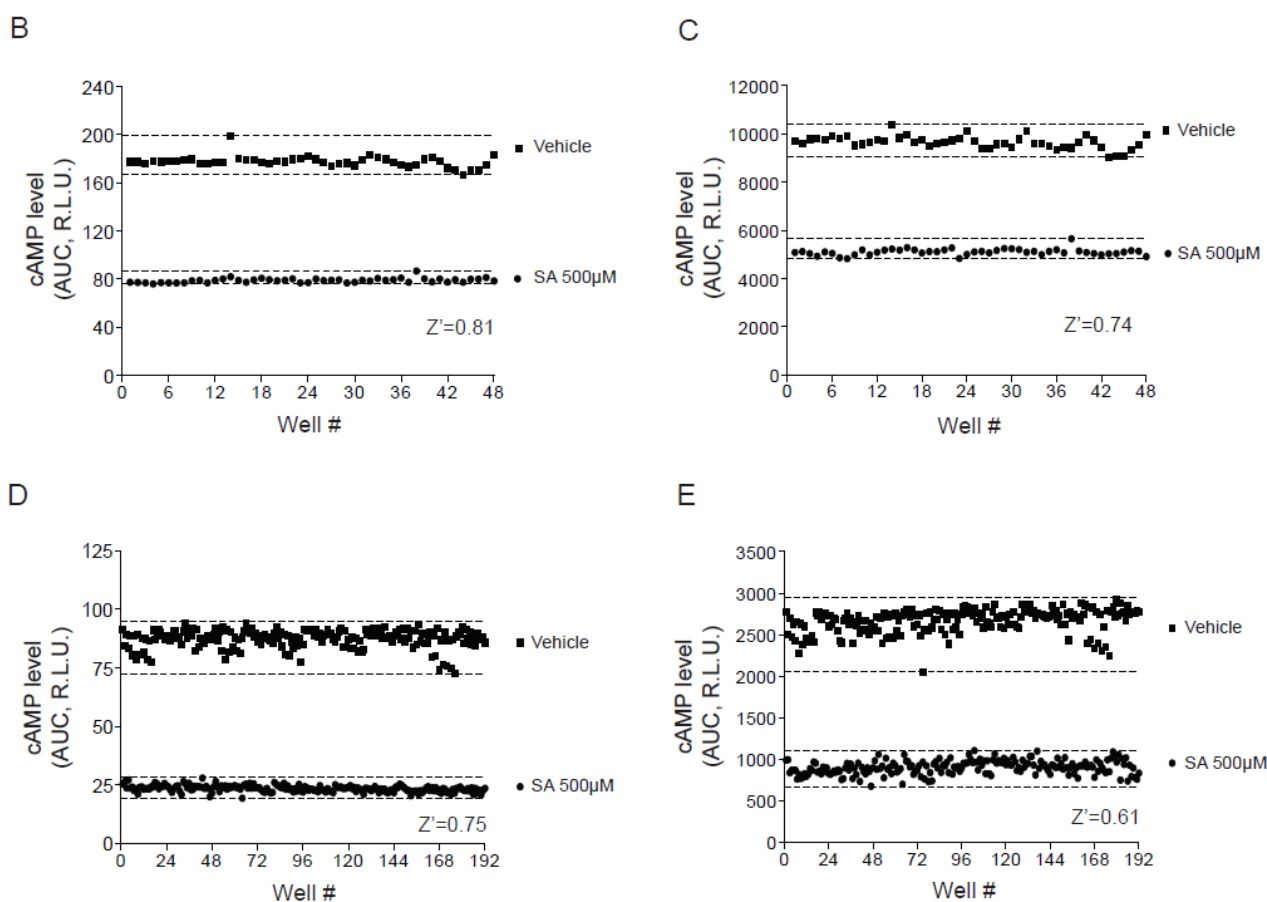


Figure III-22 : Optimization of a screening protocol and assay performance. (B) Assay performance for the two different measurements with 96-well plates: Z' factor calculated for basal level measurement is 0.81 (C) and after FSK stimulation is 0.74. (D) Z' factor for basal level measurement has been calculated for 384-wells plate to be $Z' = 0.75$ and (E) 0.61 after FSK stimulation.

According to the calculated Z' , the assay appears to be sensitive and compatible with screening of $G_{\alpha i}$ -coupled receptors. Therefore we applied this protocol to a test screening of a chemical library on SUCNR1.

III.2.3. Screening of the Sigma LOPAC1280™ library

III.2.3.1. Primary screening

We applied our protocol on a test screening of the Sigma LOPAC1280™ library, constituted by 1280 compounds of known activity (See I.3.3.1.2.) distributed in sixteen 96-well plates. The compounds were diluted to give a final concentration of 100 μ M, a concentration already used in previous different screenings (Wigdal et al., 2008; Drake and Gulick, 2011; Mukherjee et al., 2012). We chose to perform the screening on the HEK293.pGlo.SUCNR1 cells at this relatively high concentration to increase the probability of finding a weakly potent SUCNR1 agonist.

However we were cautious about the fact that higher concentrations mechanistically increase both true hits and false positives. With a second messenger assay, false positives can be for example molecules interacting with other endogenous $G_{\alpha i}$ -coupled receptors present in HEK293 cells. We reasoned that the increase of sensitivity obtained by artificially raising SUCNR1 receptor number (overexpression) would not be sufficient to overcome this problem. Therefore, we performed a counter-screening on the HEK293.pGlo cells to estimate their effect on cAMP levels in the absence of SUCNR1.

As screening results are affected by random and systematic errors (See I.3.3.1.4.), we minimized biological and instrumental variations. To keep intra- and inter-day assay variability to a minimum, we worked with cell lines stably expressing SUCNR1 and the modified luciferase grown in a selection medium. We verified regularly the expression of the protein of interest by FACS analysis. Moreover we also performed the screening of each plate rigorously in the same experimental conditions (cell number, cell starvation, temperature, reagents, incubation and reading times). To keep under control and prevent assay variability, we used SA at 500 μ M as a positive control in A1-D1 and E12-H12 wells of each plate (*Figure III-23*). Z' factors on the individual plates were determined and was estimated to be 0.72 and 0.59 over all plates for basal level screen and FSK-induced screen, respectively.

P1	1	2	3	4	5	6	7	8	9	10	11	12
A	+	P1A02	P1A03	P1A04	P1A05	P1A06	P1A07	P1A08	P1A09	P1A10	P1A11	-
B	+	P1B02	P1B03	P1B04	P1B05	P1B06	P1B07	P1B08	P1B09	P1B10	P1B11	-
C	+	P1C02	P1C03	P1C04	P1C05	P1C06	P1C07	P1C08	P1C09	P1C10	P1C11	-
D	+	P1D02	P1D03	P1D04	P1D05	P1D06	P1D07	P1D08	P1D09	P1D10	P1D11	-
E	-	P1E02	P1E03	P1E04	P1E05	P1E06	P1E07	P1E08	P1E09	P1E10	P1E11	+
F	-	P1F02	P1F03	P1F04	P1F05	P1F06	P1F07	P1F08	P1F09	P1F10	P1F11	+
G	-	P1G02	P1G03	P1G04	P1G05	P1G06	P1G07	P1G08	P1G09	P1G10	P1G11	+
H	-	P1H02	P1H03	P1H04	P1H05	P1H06	P1H07	P1H08	P1H09	P1H10	P1H11	+

Figure III-23 : Design of a 96-well plate. Only the first and the last columns are typically available for controls, since compounds are stored in the 80 middle wells. (+) represents wells containing SA at 500 μM (A1-D1 and E12-H12) whereas (-) is for wells containing DMSO vehicle (E1-H1 and A12-D12). Arrows show the reading direction : the reader starts to measure A1 well until H1 well, next it measures H2 well until A2 well and so on. At the end (well A12), it starts a new cycle at A1.

As expected, many compounds had an influence on both the basal and FSK-induced cAMP levels (See VII Appendix). Therefore, we distributed the results on 2 axes : y axis representing the effect of compounds on HEK293.pGlo.SUCNR1 cells and x axis representing the effect on HEK293.pGlo cells (*Figure III-24&25*). *Figure III-24* presents the plotted values of the basal measurements ("basal level screen") whereas *Figure III-25* corresponds to the measurements after FSK stimulation ("FSK-induced screen"). The positive values (above the red dotted line) of the plots represent the importance of cAMP levels decrease. The most promising compounds (as SUCNR1 agonists) are theoretically those distributed along the vertical green dotted line in the superior part of the plots. However, most of the compounds are not specific for SUCNR1, they also show an activity on HEK293.pGlo cells. Compounds on the blue dotted line show the same activity on both cell lines and probably interact with endogenously expressed G_{α_i} -coupled receptors or act directly on the system.

In addition, numerous compounds induced cAMP level increase (negative values; below the red line). These non-specific compounds might directly act on GPCRs endogenously expressed in HEK293 cells including G_{α_s} - and G_{α_i} -coupled receptors. They also might interfere with the production of ATP as well as cAMP such as PDE inhibitors, AC activators, ... Besides, the effect on HEK293.pGlo cells might also be due to firefly luciferase inhibitors including simple competitive inhibitors to substrate-like molecules, which are reported to increase cAMP levels (Thorne et al., 2010).

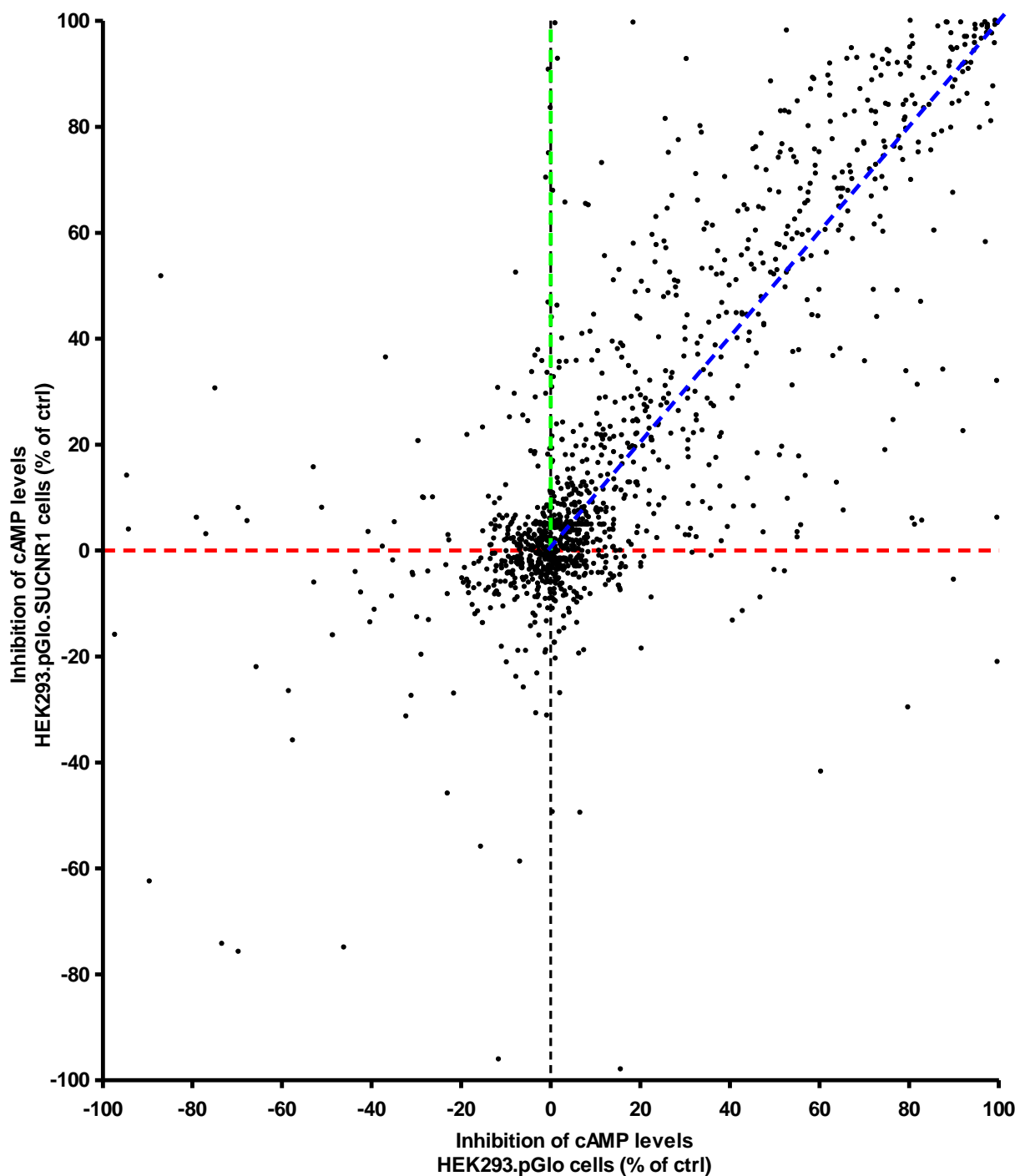


Figure III-24 : Results of the "basal level screen" of the Sigma LOPAC1280TM library on HEK293.pGlo.SUCNR1 cells and counter-screened on HEK293.pGlo cells. Green dotted line represents the most promising SUCNR1 agonists whereas blue dotted line indicates compounds with same activity on both cells.

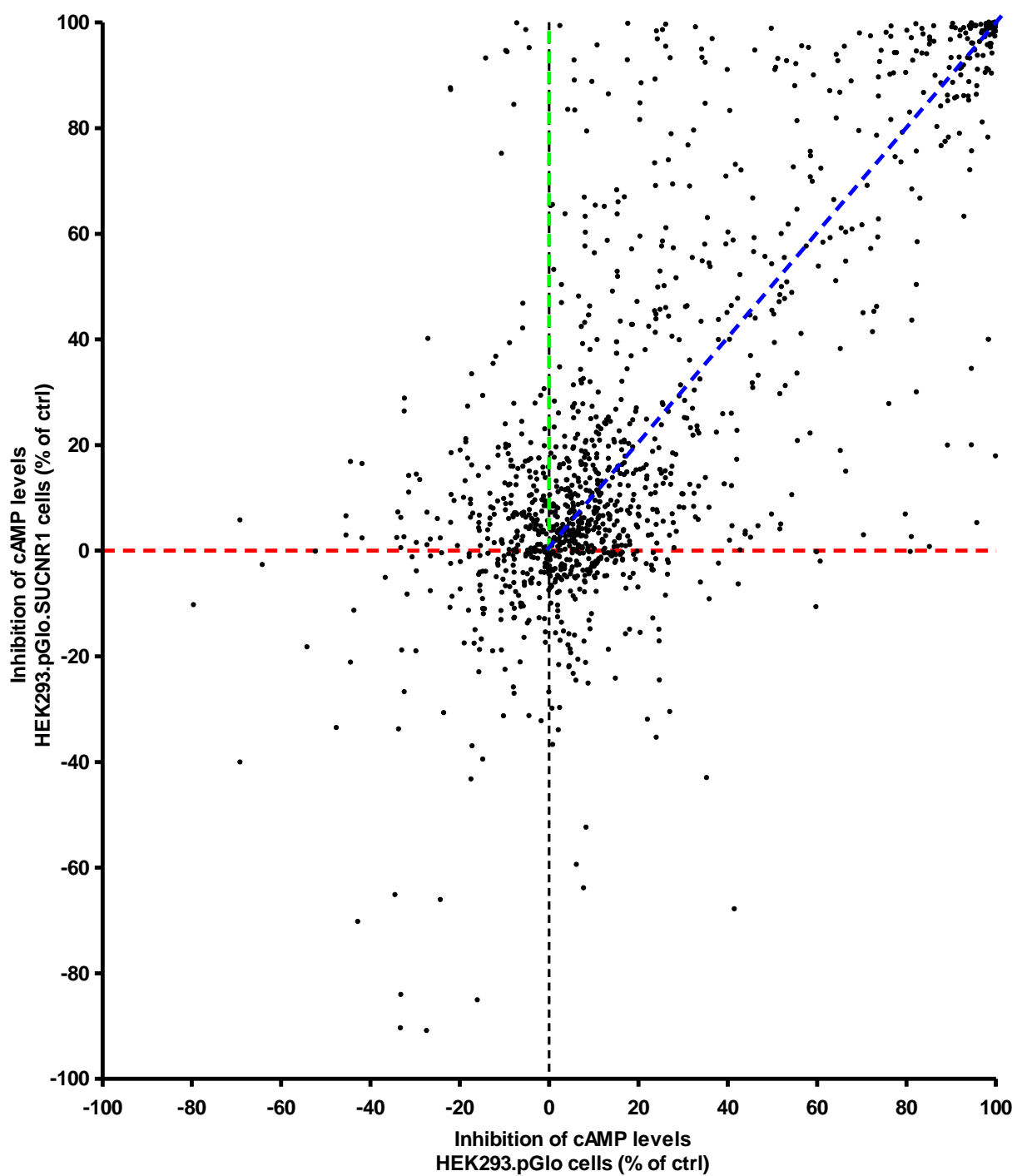


Figure III-25 : Results of the "FSK-induced screen" of the Sigma LOPAC1280TM library on HEK293.pGlo.SUCNR1 cells and counter-screened on HEK293.pGlo cells. Green dotted line represents the most promising SUCNR1 agonists whereas blue dotted line indicates compounds with same activity on both cells.

Although the compounds with a value superior to 3σ should typically be retested in a secondary screening (See I.3.3.1.4.), the hit rate was too high to test all compounds. This is probably due to the high concentration used, compounds might be insoluble for example. Therefore we chose a more stringent criterion to retest a lower number of compounds (hit rate = $\sim 0.15\%$) and set two complementary thresholds for the selection of hits : a signal above mean + 6σ intra-plate on HEK293.pGlo.SUCNR1 cells and an activity comprised within mean $\pm 3\sigma$ intra-plate on HEK293.pGlo cells.

For the "basal level screen", 30 compounds met the criteria whereas 48 compounds were selected in the "FSK-induced screen". 11 compounds were common to the two sets (*Figure III-26*).

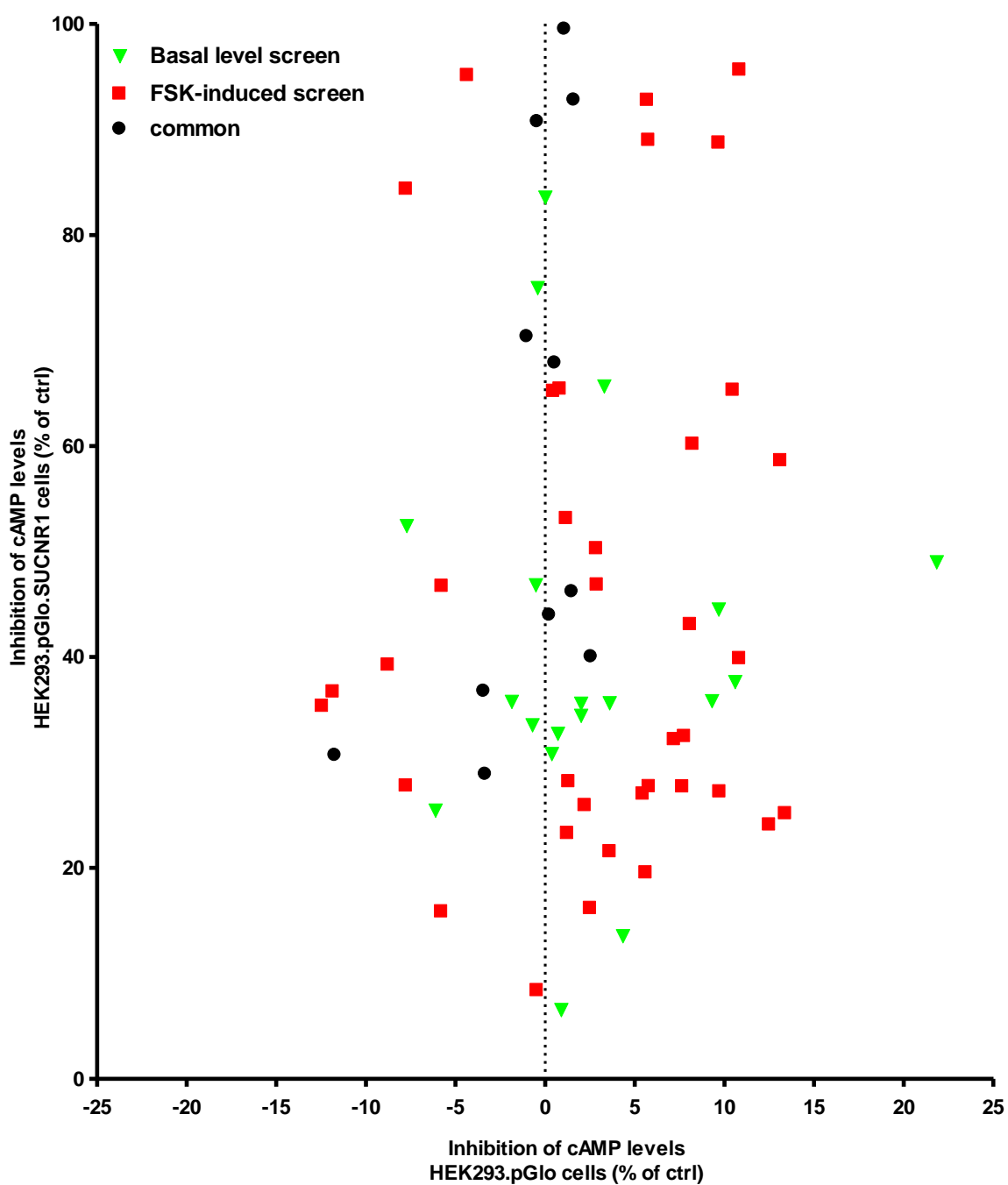


Figure III-26 : Comparison of the results obtained for the "basal level screen" (30 compounds identified as green inverted triangles) and the "FSK-induced screen" (48 compounds identified by red squares), 11 compounds common to the two sets are represented as black filled circles.

III.2.3.2. Secondary screening of the selected hits

We further performed a cherry pick of the compounds that met our criteria in both conditions (67 compounds; See VII Appendix) and tested them in triplicate on both cell lines. 13 compounds displayed a statistically significant difference between activity on HEK293.pGlo.SUCNR1 and HEK293.pGlo cells (*Figure III-27*), others were considered as false positives.

7 compounds in the set of 13 confirmed hits (3E2, 5D3, 11A4, 11C4, 11H3, 11H6 and 15G10) were identified in the "basal level screen" but remained unnoticed in the "FSK-induced screen". These results highlighted a major consideration in screening, the detection capability of false negatives (true hits that are not identified). Contrary to false positives, easily detected in a secondary screening, there is no way of knowing which compounds are active but not detected by the assay.

The response measured for the false positives was not due to the activity of interest, they are falsely identified hits. It was already shown that the false positive rate increased with the exposure time of the assay to the compounds. For example, it is lower for calcium transient studies compared to reporter assays where the time of exposure is around 24 h (Kenakin, 2014). Here, the "FSK-induced screen" identified 53 (48 compounds identified by red squares + 11 compounds represented as black filled circles - 6 identified hits) compounds that were not confirmed in the secondary screening whereas the "basal level screen", which was recorded only for 5 minutes without FSK identified 28 (30 compounds identified as green inverted triangles + 11 compounds represented as black filled circles - 13 identified hits).

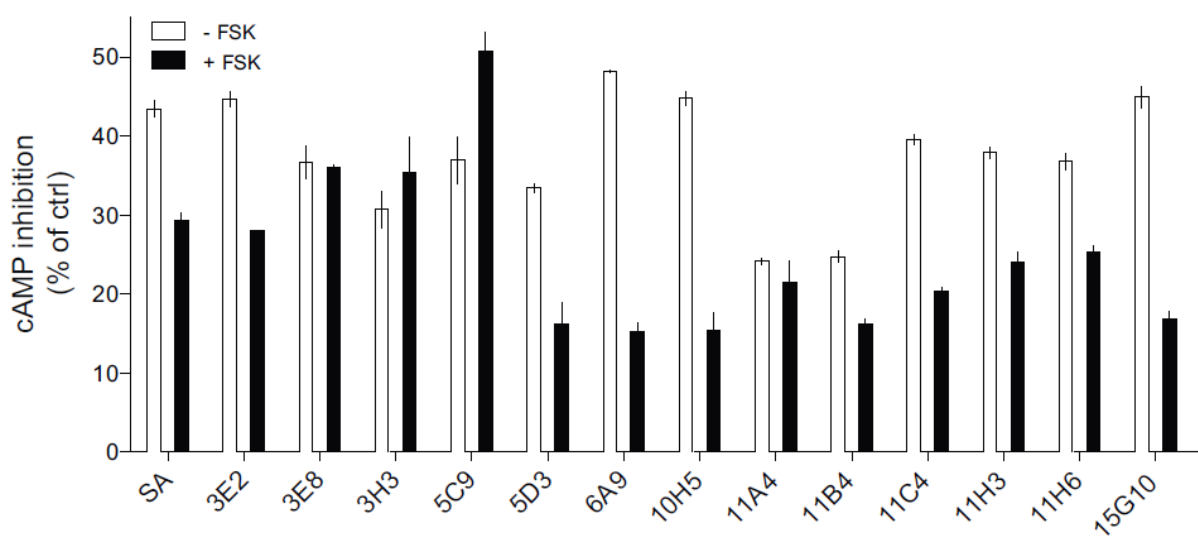


Figure III-27 : Results of the active compounds identified from secondary screening that showed a statistically significant difference between activity on HEK293.pGlo.SUCNR1 and HEK293.pGlo cells.

All the 13 confirmed active compounds had succinate or maleate (a weaker SUCNR1 agonist (He et al., 2004)) as a counter ion (*Table III-1*). We reasoned that we detected an agonist activity because of the presence of the counter ion. We bought some of the compounds in another chemical form to confirm this hypothesis. For instance, compound 3E8 in the library, BRL 54443, a 5-hydroxytryptamine receptor 5-HT_{1e} & 5-HT_{1F} agonist (Klein et al., 2011) showed no activity alone in our assay (*Figure III-28 A*) whereas maleic acid (*Figure III-28 B*) confirmed its activity and showed an EC₅₀ = 93.8 ± 1.3 μM and E_{max} = 32.6 ± 3 % when assayed in the presence of FSK. Its EC₅₀ on basal cAMP levels was 79.4 ± 1.1 μM and E_{max} = 49.4 ± 3.9 % compared to control.

3E2	(±)-Brompheniramine maleate
3E8	BRL 54443 maleate
3H3	(+)-Brompheniramine maleate
5C9	Doxylamine succinate
5D3	5-Carboxamidotryptamine maleate
6A9	N,N-Dipropyl-5- Carboxamidotryptamine maleate
10H5	Methylergonovine maleate
11A4	(-)-MK-801 hydrogen maleate
11B4	2-Methyl-5-hydroxytryptamine maleate
11C4	Alpha-methylserotonin maleate
11H3	Dizocilpine maleate
11H6	Nomifensine maleate
15G10	S-(-)-Timolol maleate

Table III-1 : Confirmed active compounds have succinate or maleate as counter ion.

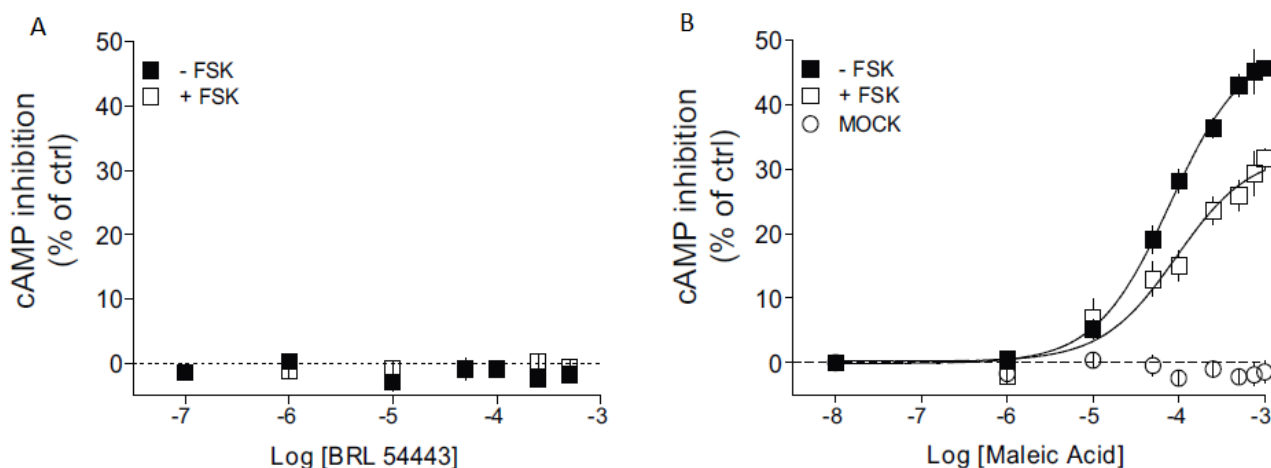


Figure III-28 : (A) BRL 54443 without maleate as a counter ion is inactive on HEK293.pGlo.SUCNR1 cells. (B) Concentration-response curve of maleic acid on HEK293.pGlo.SUCNR1 cells. Data are expressed as mean \pm SEM of at least 3 independent experiments.

Interestingly, we noticed that many compounds having the trans-isomer of maleic acid, fumaric acid as counter ion didn't specifically decrease cAMP levels in HEK293.pGlo.SUCNR1 cells (Table III-2). The different results generated by SA, the cis-isomer maleic acid and the trans-isomer fumaric acid will be deeply characterized in a follow-up study discussed below (See III.3.2.2.1.).

1F6	3-Aminopropionitrile fumarate
7H4	(-)-Eseroline fumarate
8B3	GR-89696 fumarate
9B10	VER-3323 hemifumarate
9G7	Ketotifen fumarate
12D5	Oxotremorine sesquifumarate
12H2	Bisoprolol hemifumarate
14G5	Rilmenidine hemifumarate

Table III-2 : Compounds having fumarate as counter ion are inactives on HEK293.pGlo.SUCNR1 cells.

Although any new scaffolds were discovered during SUCNR1 screening, this test screening enables the establishment of the GloSensor biosensor as a tool compatible with HTS of $G_{\alpha i}$ -coupled receptors. It is a significant improvement given the FSK-induced artifacts and the difficulty of screening $G_{\alpha i}$ -coupled receptors. In addition, it considerably reduces the time of experiment and the number of steps, an important source of assay variation, responsible of false positives/negatives generation.

The protocol is readily available, easy to set-up, fast and relatively cheap. Therefore, it should facilitate screening campaigns for $G_{\alpha i}$ -coupled receptors, especially for academic labs and small sized biotech companies that don't have access to the $[Ca^{2+}]_i$ -FLIPR assay. Facilitating screening of $G_{\alpha i}$ pathway brings also renewed opportunities to screen $G_{\alpha i}$ -exclusive receptors that are unable to efficiently couple to promiscuous G proteins and arrestins.

Because of the high concentration of compounds that were tested, 100 μ M, we got numerous non-specific active compounds and we might have missed potential SUCNR1 agonists. Therefore we also tested the same library at a lower concentration, 10 μ M. However no attractive ligands, apart from succinic acid and maleic acid, were identified. This might be explained by the fact that SOSA library is relatively small and represented only a small fraction of the pharmacological chemical space.

III.3. Characterization of succinate binding site

III.3.1. *In silico* screening of a virtual library

III.3.1.1. Three-dimensional model of SUCNR1

A 3D model of SUCNR1 generated by homology from RX structure of bovine rhodopsin was proposed during the initial study of the receptor (He et al., 2004). He et al. postulated that dicarboxylate groups of succinate were required for the activation of SUCNR1 and might interact with basic residues. This hypothesis was confirmed through site-directed mutagenesis experiments. Four positively charged AAs were demonstrated to be necessary for activation, R99^{3.29}, R281^{7.39}, R252^{6.55} and H103^{3.33} (He et al., 2004) (See I.2.3.).

These AAs may provide an electrostatic environment for succinate binding similarly to P2Y receptors and nucleotide ligands. R^{7.39} and R^{6.55} are topologically shared with crystallized P2Y receptors. Therefore it can be hypothesized that they might neutralize the carboxylate negative charges of succinate (Gonzalez et al., 2004; He et al., 2004) as phosphate negative charges do for nucleotides (Zhang et al., 2014, 2015a). In contradiction with a shared mechanism for activation, the mutation of the highly conserved H^{6.52} that contributes to ligand recognition in P2Y₁, P2Y₂ and P2Y₁₂ receptors doesn't abolish the interaction between SUCNR1 and succinate whereas a mutant of H^{3.33} does (He et al., 2004).

Little information is currently available concerning SUCNR1 tridimensional structure. Recently, the crystal structure of many GPCRs, and more specifically Rhodopsin-like GPCRs, have been determined and represented a major breakthrough in the field. Although SUCNR1 structure has not been determined yet, the publication of close receptors both in active (β_2 -adrenoceptor (Rasmussen et al., 2011)) and inactive (P₂Y₁₂ (Zhang et al., 2014), P₂Y₁ (Zhang et al., 2015a)) conformations may serve as more suitable models for the prediction of SUCNR1 structure by homology modelling.

In order to get new scaffolds for SUCNR1 agonists, we worked in collaboration with Dr. Sebastien Dilly, a molecular modeller from the laboratory of medicinal chemistry of ULg (now working at university of Bordeaux in France).

SUCNR1 molecular model was created by homology modelling with an available active-state crystal structure of the agonist-bound β_2 -adrenoceptor component of the receptor-nanobody complex (β_2 -adrenoceptor-T4L-Nb80 complex ; ProteinData Bank : accession code 3P0G) (Rasmussen et al., 2011). We selected this template for homology modelling because bovine rhodopsin crystal structure (previously used as a template for generating a partial SUCNR1 structure model (He et al., 2004)) usefulness is limited in many aspects. In addition to be more distant in sequence homology than the β_2 -adrenoceptor to other Rhodopsin-like GPCRs, rhodopsin binding site is blocked by the E2 loop, which folds into the receptor to help completely enclose retinal (Topiol and Sabio, 2009). The β_2 -adrenoceptor structure provides a more interesting template because the conformation of E2 loop facilitates ligand entry into the active site (Topiol and Sabio, 2009). Finally, as active structures are reported to generate better results for the prediction of agonist ligands, an active-state GPCR structure is more appropriate. By contrast with retinal, the agonist BI-167107 is not covalently bound to the receptor but interacts through polar and hydrophobic interactions (Rasmussen et al., 2011).

III.3.1.2. Virtual screening of ZINC database

The SUCNR1 molecular model was used to perform *in silico* screening of a virtual library. First, the docking protocol was validated by comparing the binding mode of succinate to RX data and a docking score for succinate was obtained. Next, a virtual screening by docking 2/3 of the ZINC database "lead-like" molecules was performed (Irwin and Shoichet, 2005) against the succinate binding site reported by He et al. Since the hits with the best docking scores are likely to possess activity against the receptor, the compounds with a score superior or equal to succinate were selected. We investigated the activity of fourteen putative ligands that fit this criterion (*Table III-3*) with our cAMP assay on both HEK293.pGlo.SUCNR1 and HEK293.pGlo cells. Unfortunately all the predicted compounds tested were inactive, as shown for the (3-amino-1H-pyrazol-5-yl) acetic acid (*Figure III-29*). It was unlikely that the structures predicted by the model didn't affect specifically SUCNR1. Therefore, we questioned the accuracy of the existing model as well as the described binding pocket through AAs confirmation and the succinate interaction with the receptor.

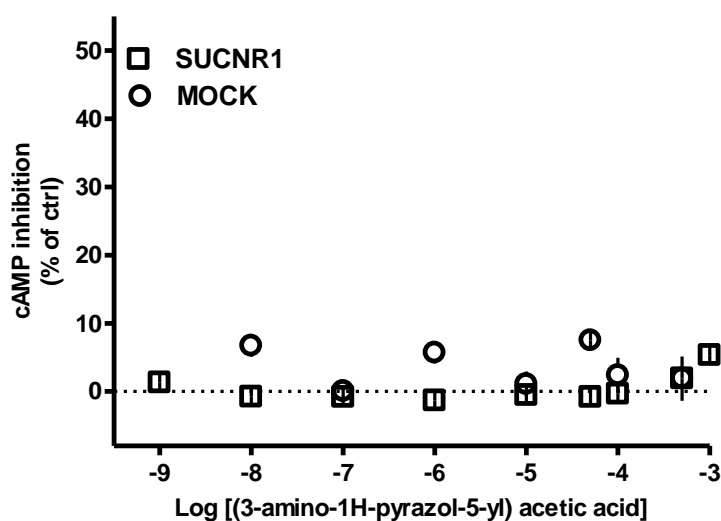


Figure III-29 : (3-amino-1H-pyrazol-5-yl) acetic acid is inactive on HEK293.pGlo.SUCNR1 cells. Data are expressed as mean \pm SEM of at least 3 independent experiments.

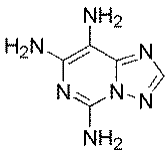
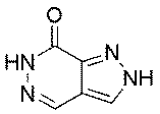
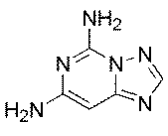
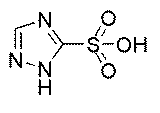
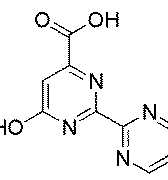
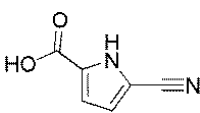
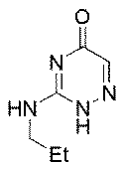
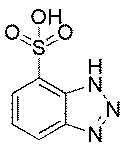
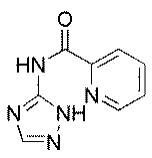
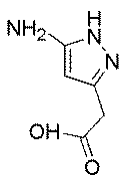
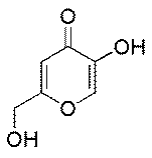
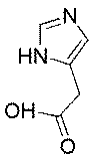
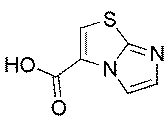
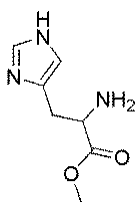
Name	Structure	Name	Structure
[1,2,4]triazolo[1,5-c]pyrimidine-5,7,8-triamine ZINC01418566		2,6-dihydro-7H-pyrazolo[3,4-d]pyridazin-7-one ZINC75109309	
[1,2,4]triazolo[1,5-c]pyrimidine-5,7-diamine ZINC01418565		1H-1,2,4-triazole-5-sulfonic acid ZINC19881725	
6-hydroxy-2-pyrimidin-2-yl-pyrimidine-4-carboxylic acid ZINC63110929		4-cyano-1H-pyrrole-2-carboxylic acid ZINC72338653	
3-(propylamino)-1,2,4-triazin-5(2H)-one ZINC05009506		1H-benzotriazole-1-sulfonic acid ZINC32603167	
N-(1H-1,2,4-triazol-3-yl)-2-pyridinecarboxamide ZINC40071197		(3-amino-1H-pyrazol-5-yl) acetic acid ZINC16696916	
5-hydroxy-2-(hydroxymethyl)-4H-pyran-4-one ZINC13831818		(1H-imidazol-4-yl) acetic acid hydrochloride ZINC197351384	
imidazo[5,1-b][1,3]thiazole-3-carboxylic acid ZINC68590010		methyl histidinate hydrochloride ZINC19418999	

Table III-3 : Predicted ligands tested with our cAMP assay were inactive on HEK293.pGlo.SUCNR1 cells.

III.3.2. Optimization of the existing receptor model

III.3.2.1. Structural elements

III.3.2.1.1. Screening of analogues

SA response was reported to be highly specific because 800 pharmacologically active compounds as well as other citric acid cycle intermediates were unable to activate SUCNR1 (He, et al., 2004). In addition, the binding pocket seems to be extremely constrained since it doesn't accommodate 200 carboxylic acids and structurally related analogues (He, et al., 2004). Only maleate and methylmalonate were able to induce a response with 5- to 10-fold lower potency compared to succinate (He, et al., 2004). We confirmed the partial agonist nature of maleate on SUCNR1, an active analogue identified in the screening of the SOSA library (*Figure III-28*).

In order to establish basic rules for activity at SUCNR1, a screening of a home-made library composed of thirty nucleotides and succinate related molecules was conducted in a parallel project led by Pierre Geubelle (Pierre Geubelle et al., unpublished data). Using our cAMP assay, he highlighted the importance of compounds to bear at least two negative charges (at physiological pH) as compounds bearing any or one negative charge are inactive. Additionally, he noticed that the binding pocket is constrained to interact with molecules that are three (malonate, a weak agonist) or four carbons (succinate) long. Interestingly, he deeply characterized the difference of activity between maleate and fumarate previously observed by He et al. For the first time this effect was precisely understood because he inferred that the spatial conformation of the two negatively charged carboxylates was a critical feature for activity on SUCNR1. Indeed, they must be positioned in a "cis" conformation as they do in maleate. In stark contrast, the trans-isomer fumarate (*Figure III-30*) is completely inactive.

Furthermore, he examined the capacity of substituents to affect the activity of succinate analogues. Simple substitution as well as disubstitutions of succinate revealed the constraints in steric hindrance. Since SUCNR1 has been classified as a purinergic receptor and initially predicted to bind purinergic ligands, he also investigated the activity of

nucleotides and nucleosides (di or triphosphate). But none of these compounds were able to activate SUCNR1 or displace succinate curve.

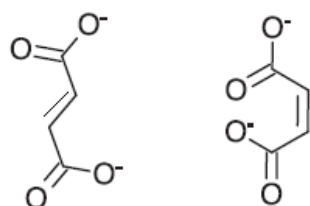


Figure III-30 : *trans*-isomer fumarate (left) compared to the *cis*-isomer maleate (right).

Compounds reported by Pierre Geubelle as partial agonists on $G_{\alpha i}$ signaling pathway were next evaluated for their ability to induce the recruitment of arrestins. (*S*)-(-)-2-bromobutanedioate (bromosuccinate), (*R*)-(+)-2-methylbutanedioate (methylsuccinate), (*S*)-(-)-2-hydroxybutanedioate (malate) and 2-oxobutanedioate (oxaloacetate) didn't induce a detectable arrestin recruitment to SUCNR1 in our complementation assay (See III.1.3.) (Figure III-31). Nevertheless, we were able to measure the ability of maleate to specifically induce the recruitment of arrestin 3 in ARR3.SUCNR1 cells compared to Mock transfected cells (data not shown). This analogue acting as a partial agonist is less potent than succinate. However, inactive ligands must be confirmed on another second signaling pathway or at least with another assay, for example intracellular calcium mobilization assay or cAMP assay on cells treated with PTX.

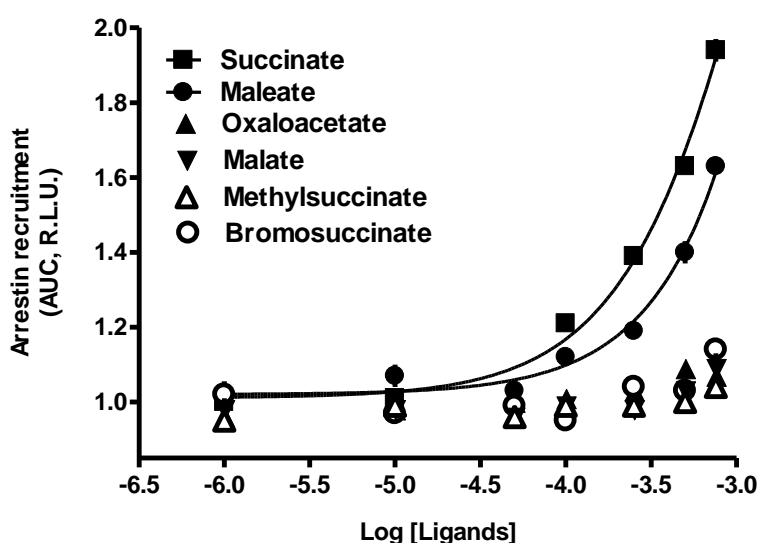


Figure III-31 : SUCNR1 is able to recruit arrestin 3 when stimulated with maleate in ARR3.SUCNR1 cells. Data are expressed as mean \pm SEM of at least 3 independent experiments.

III.3.2.1.2. Pharmacophore

SAR study of succinate related molecules performed by Pierre Geubelle allowed to infer essential structural elements that lead to the determination of a pharmacophore for SUCNR1 (Figure III-32). To be active, compounds must possess at least two negative charges, three or four carbon atoms away, positioned in a "cis" conformation (Pierre Geubelle et al., unpublished data).

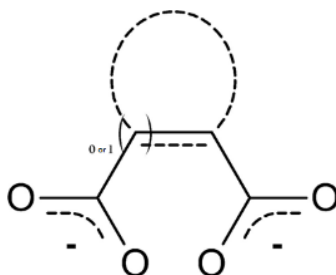


Figure III-32 : Pharmacophore for SUCNR1 (Pierre Geubelle et al., unpublished data).

The pharmacophore model established by using the pharmacophore program of Schrödinger Suite was based on both active and inactive ligands from the succinate related analogues library screening. Actually the model might continually be improved by new experimental data. Up to now, the pharmacophore model contains two hydrogen bond acceptor elements and two negative charges. Inactive compounds and the ones with lower activity due to substituents serve to add excluded volumes.

Subsequently the pharmacophore-based screening of small molecules (molecular mass and number of rotations similar to succinate) of the ZINC database (ZINCpharmer) with the developed pharmacophore model led us to propose cycloalkanes analogues ("cis" conformation) as potential ligands. In addition, the model suggested that carboxylic acid bioisosteres including sulphonic acids and tetrazoles could be active ligands. Furthermore the docking led to the identification of the oxaloacetic acid as a putative agonist for SUCNR1, which was already confirmed during the screening of home-made library.

According to these information, a potential explanation for the failure of the predicted ligands of our ZINC database screening can be postulated. Although they possessed hydrogen bond acceptor elements none of them bore two negative charges. In addition, it seems likely that compounds showing a high steric hindrance could not fit in the constrained binding pocket. These compounds were mistakenly identified as potential ligands for SUCNR1 because of a misunderstanding of succinate conformation. Indeed the succinate docked in the binding site of SUCNR1 was not positioned in a "cis" conformation but in a position similar to the one reported by He et al.

However these negative results can be used to improve our pharmacophore model.

III.3.2.2. Binding pocket

Since two negative charges are required for activity, agonists compounds probably interact with two positively charged AAs. Based on these observations, we constructed a compatible model where succinate in a "cis" conformation interacts primarily with R252 and R281. This model differs significantly from published literature that we previously used to perform a suboptimal docking of the ZINC database (See III.3.1). We may hypothesize that the initial model of He et al. depicted a slightly inaccurate binding site geometry based on an incorrect succinate conformation. Our postulated model could refine it with a more detailed SAR study. Although it was quite clear in the He et al. work that the four AAs proposed were necessary for SUCNR1 activation, the respective importance of each AA was not described because the mutants have been only tested at one concentration (200 μ M) (He et al., 2004). Consequently the actual binding pocket remains elusive. Therefore, the complete concentration-response curves on the different mutants should be performed to have a more precise information on succinate binding pocket.

Our model should be validated by extensive targeted mutagenesis (replacement of critical AAs by alanine, or positively/negatively charged AAs, displacement and exchange of adjacent AAs, ...). Therefore, we first generated mutants to study the putative ligand-binding site of SUCNR1. Each of the fourth AAs proposed to be involved in the interaction with succinate were replaced by alanine (A) and termed psG5.FLAG.SUCNR1 R99A, R281A, R252A and H103A. They were transiently transfected in HEK293.pGlo cells and the expression of SUCNR1 mutants was verified using immunofluorescence staining and confocal microscopy. Transfected cells were assayed by measuring cAMP levels.

Although the conditions of transfection were optimized (conditions of transfection, agent of transfection, number of cells), the expression of the mutated receptor was too low to measure a sufficient cAMP decrease to attest that the AAs are mandatory for the interaction or just facilitate it. Further characterizations will be achieved using stable cell lines expressing mutants. These cell lines must be generated and fully characterized. They will be used to precisely identify the binding pocket for succinate.

Furthermore, the redefined binding pocket will serve for a new virtual screening of the ZINC database as well as investigating the binding site of new ligands.

III.3.3. Characterization of cycloalkanes activity on SUCNR1

III.3.3.1. *In vitro* assays

As suggested by the pharmacophore model, succinate cycloalkanes analogues (cyclopropane, cyclobutane, cyclopentane and cyclohexane) were evaluated with our cAMP levels. Pierre Geubelle reported (1*R*, 2*S*)-1,2-cyclopentanedicarboxylate as a weak agonist and (1*R*, 2*S*)-1,2-cyclobutanedicarboxylate as a partial agonist while (1*R*, 2*S*)-1,2-cyclohexanedicarboxylate was inactive on HEK293.pGlo.SUCNR1 cells. More interestingly, (1*R*, 2*S*)-1,2-cyclopropanedicarboxylate (termed cis-CPDC) was demonstrated to act as a full agonist on SUCNR1 with a higher EC_{50} ($EC_{50} = 49.85 \pm 3.13 \mu\text{M}$) compared to succinate ($EC_{50} = 27.64 \pm 3.88 \mu\text{M}$) and an E_{max} ($E_{\text{max}} = 64.64 \pm 1.14 \%$) similar to succinate ($E_{\text{max}} = 62.78 \pm 2.63 \%$) (Figure III-33). By contrast, all the trans-isomer compounds were identified to be inactive on HEK293.pGlo.SUCNR1 cells (Pierre Geubelle et al., unpublished data).

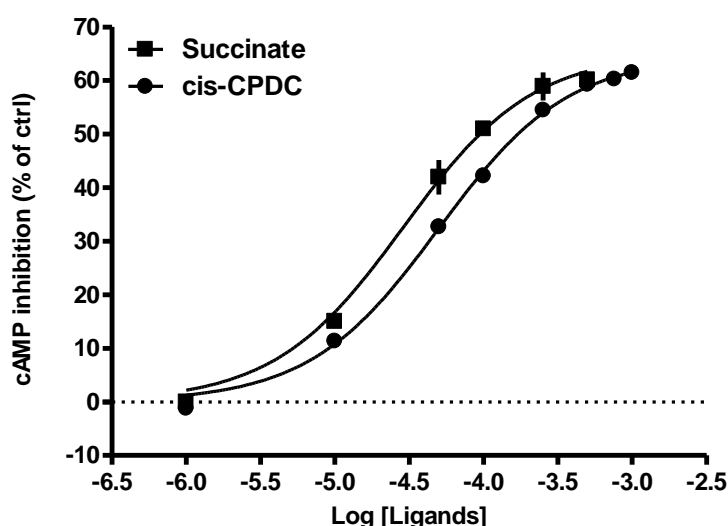


Figure III-33 : (1*R*, 2*S*)-1,2-cyclopropanedicarboxylate is active on HEK293.pGlo.SUCNR1 cells (Pierre Geubelle et al., unpublished data). Data are expressed as mean \pm SEM of at least 3 independent experiments.

Although these compounds were evaluated on HEK293.pGlo cells to ensure their specific activity on SUCNR1, it is essential to confirm the activity of a compound on a second signaling pathway to validate it as a ligand. Therefore we investigated the activity of the cis-isomer compounds on the arrestins recruitment. We confirmed (1*R*, 2*S*)-1,2-cyclobutanedicarboxylate (termed cis-CBDC) and (1*R*, 2*S*)-1,2-cyclopropanedicarboxylate (termed cis-CPDC) as ligands for SUCNR1 by measuring their capacity to trigger arrestin 3 recruitment compared to Mock transfected cells (data not shown) (Figure III-34).

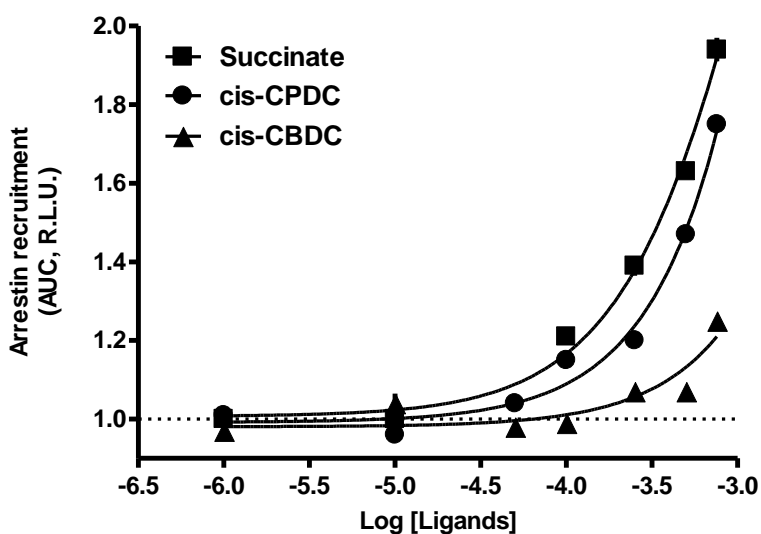


Figure III-34 : SUCNR1 is able to recruit arrestin 3 when stimulated with cis-CBPC or cis-CPDC in ARR3.SUCNR1 cells. Data are expressed as mean \pm SEM of at least 3 independent experiments.

III.3.3.2. *In vivo* assays

In mouse, succinate intravenous infusion induces a significant increase in blood pressure (BP) levels. This effect is abolished in SUCNR1-deficient animals, although angiotensin II-induced hypertension is similar in both genotypes (He et al., 2004). The dose-dependent increase of mean arterial BP induced by succinate was also shown in male Sprague-Dawley rats (He et al., 2004). Therefore we planned to assess the *in vivo* hypertensive properties of the (1*R*, 2*S*)-1,2-cyclopropanedicarboxylate (cis-CPDC) compared to the corresponding trans-isomer (trans-CPDC). In order to evaluate the *in vivo* effect of our new ligand, we collaborated with Dr. François Jouret's team (Laboratory of Experimental

Surgery, GIGA-Cardiovascular Sciences). Laurence Poma first set-up a tail-cuff method to measure BP induced by succinate. She used a CODA 8-Channel High Throughput Non-Invasive Blood Pressure system which allows measure BP in up to 4 rats simultaneously. The CODA tail-cuff system uses Volume Pressure Recording (VPR) to measure BP by determining the tail blood volume. A specially designed differential pressure transducer and an occlusion tail-cuff measure the total blood volume in the tail without the need to obtain the individual pulse signal (Daugherty et al., 2009). Next, the experiments measuring cis-CPDC and trans-CPDC effect on rats BP at 0.1 mg.kg^{-1} were performed. It was demonstrated that intravenous addition of cis-CPDC at 0.1 mg.kg^{-1} in rats increases BP in the same range as succinate. The increase BP levels is statistically significant compared to trans-CPDC (Figure III-35). All together, these data suggest that (1*R*, 2*S*)-1,2-cyclopropanedicarboxylate could be regarded as a new full agonist for SUCNR1. In contrast with succinate, this agonist is not a metabolite and thus could not interfere with the citric acid cycle. Further experimental investigations are required to validate this hypothesis, including measuring the activity of SDH in presence versus absence of the compound.

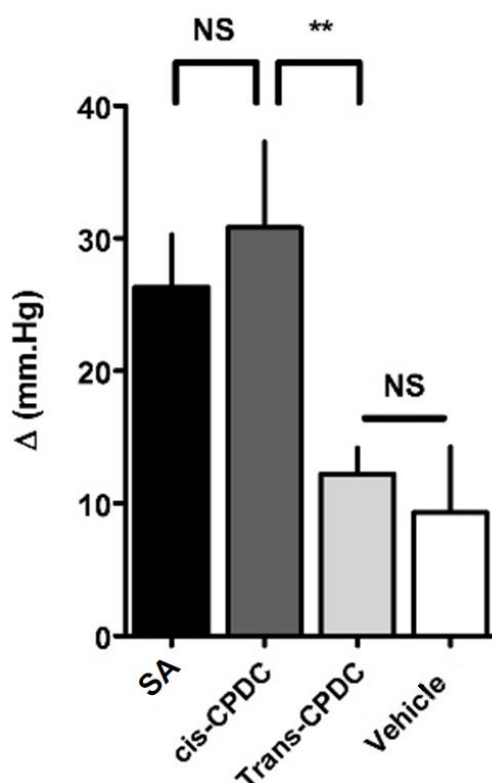


Figure III-35 : cis-CPDC at 0.1 mg.kg^{-1} in rats increases BP in the same range as succinate. Data are expressed as mean \pm SEM, $N=12$.

III.3.4. Other ligands

The pharmacophore model for SUCNR1 should help to generate synthetic compounds characterized by an increased potency and/or efficacy compared to SA. We could for instance propose diversely substituted cis-cycloalkane dicarboxylic acids or either bioisosteres of the carboxylic acid functions.

Although several series of antagonists have been reported in the literature (Bhuniya et al., 2011), the activity of these compounds has never been confirmed by competition experiments. These ligands would be helpful to investigate SUCNR1 pharmacology, to define its binding pocket and to set-up an antagonist screening. However these ligands are not available commercially and must be first synthesized. Next, their pharmacology (competitive antagonist, allosteric modulators, ...) must be precisely defined.

Additionally, our pharmacophore model might be helpful to generate antagonists or inverse agonists identification. A new chemical serie of antagonists might offer new scaffolds active at SUCNR1. In addition, these ligands might be an alternative to those described by Bhuniya et al., which could lead to inadequate bioavailability, toxicity, ... (Klenc et al., 2015).

IV. CONCLUSIONS AND PERSPECTIVES

Part 1

In the present work, we characterized SUCNR1, a GPCR that has been paired with its natural ligand succinate. SUCNR1 was originally described as coupled to both G_{α_i} and G_{α_q} and to be internalized upon succinate exposure in HEK293 cells but its signaling pathways remained somehow elusive with some discrepancies in the literature. Therefore we thoroughly characterized its signaling pathways in HEK293 cells and developed various cell-based assays.

As many other authors, we confirmed SUCNR1 to be efficiently coupled to G_{α_i} when stimulated by its ligand. However our observation that succinate elicits a concentration-dependent PTX-sensitive $[Ca^{2+}]_i$ mobilization is consistent with SUCNR1 being not coupled to G_{α_q} . During this work, similar results in HEK293 cells were obtained and $[Ca^{2+}]_i$ mobilization has been proposed by Sundström et al. as a consequence of PLC- β activation by the dimer $\beta\gamma$. We suggested that the discrepancy between results may reflect distinct G protein partners among different cell types or artifacts induced by overexpression of the receptor. Therefore SUCNR1 coupling with G_{α_q} should be investigated especially in native and physiologically relevant systems.

Besides, we measured a rapid and transient p-ERK activation mediated by G_{α_i} protein upon succinate exposure. These results tend to indicate that G_{α_i} -dependent ERK activation might probably be mediated through the dimer $\beta\gamma$.

We also showed that SUCNR1 is able to induce arrestins 2 and 3 recruitment even if the receptor seems to be weakly coupled to these proteins. Therefore we postulated that arrestins don't play a significant physiological role in this receptor-ligand system. As M_2 receptor (and many others (See I.1.4.3.1.)), SUCNR1 might be internalized through a dynamin- and clathrin-dependent pathway, or either internalization might be dependent of GRK expression in a similar fashion than BLT_1 receptor internalization. These mechanisms, independent of arrestins, should be investigated in further studies.

Part 2

According to the current paradigm, succinate triggers SUCNR1 signaling pathways to indicate local stress that may affect cellular metabolism and pathophysiology of diseases in multiple organs. SUCNR1 implication has been well documented in renin-induced hypertension, ischemia/reperfusion injury, inflammation and immune response, platelet aggregation and retinal angiogenesis. In addition, the SUCNR1-induced increase of blood pressure may contribute to diabetic nephropathy or cardiac hypertrophy. On the basis of these existing observations mostly acquired from *in vitro* and *in vivo* rodent models, SUCNR1 has high potential therapeutic application in a number of diseases area and is considered as an important regulator of basic physiology.

However, the current paucity of specific pharmacological tools delays its validation as a drug target. In order to achieve the full characterization of this receptor, we proposed to identify small-molecules modulators or "chemical probes" that might be used to address more deeply the role of the receptor, particularly in systems more relevant to human physiology.

Although arrestin assays are widely employed for the identification of GPCRs ligands, the weak coupling of SUCNR1 to these proteins indicates that a screening based on arrestin assay would not be a good option since ligands less potent than succinate would probably never be detected. Therefore we set-up an assay that allows to record cAMP levels variations via the measure of a signal stable over time that doesn't affect the system. However an important drawback in tracking agonists for $G_{\alpha i}$ -coupled receptors is the mandatory stimulation of cAMP levels. The inducers that must be employed generate various artifacts and constitute a major challenge in the characterization of $G_{\alpha i}$ -coupled receptors. To avoid these artifacts we set-up and validated a cAMP-inducer free method based on a biosensor, the GloSensor system (22F construct). We ensured that this assay offers a sensitivity and a dynamic range sufficient for recording cAMP inhibition of basal levels for $G_{\alpha i}$ -coupled receptors, heterologously expressed as well as endogenously present in HEK293 cells.

Next we examined the quality of high-throughput screenings (96- and 384-well plates) based on this assay. According to the calculated statistical factor Z' , the assay appeared to be sensitive and compatible with screening of G_{α_i} -coupled receptors. As this real time assay was easily amenable to high-throughput screening for the detection of G_{α_i} -coupled receptors agonists, we applied our protocol on a test screening of a small chemical SOSA library. The library contains 1280 structurally and therapeutically diverse molecules with known bioactivity. The principle of such library is that active compounds might have an activity on new targets at high concentration.

The strategy monitoring basal cAMP levels compared to the forskolin-stimulated cAMP levels allowed to decrease recording time and artifacts from forskolin use, leading to the identification of fewer false positives and previously unnoticed false negatives. Although both methods found succinate and maleate agonists in the chemical library screened, no new scaffolds active on SUCNR1 were discovered.

The establishment of the GloSensor (22F construct) biosensor as a tool compatible with high-throughput screening of G_{α_i} -coupled receptors represents a significant improvement given the forskolin-induced artifacts and the difficulty of screening G_{α_i} -coupled receptors. In addition, the assay based on the GloSensor system (22F construct) considerably reduces the time of experiment and the number of steps, an important source of assay variations, responsible of false positive/negative generation in chemical screening. The protocol is readily available, easy to set-up, fast and relatively cheap. Therefore, it should rapidly facilitate screening campaigns for G_{α_i} -coupled receptors. Facilitating screening of G_{α_i} pathway brings also renewed opportunities to screen G_{α_i} -exclusive receptors that are unable to efficiently couple to promiscuous G proteins and/or arrestins.

Part 3

In order to identify new agonist scaffolds for SUCNR1, we worked in collaboration with Dr. Sebastien Dilly (a molecular modeller from the laboratory of medicinal chemistry of ULg, now working at university of Bordeaux in France) to perform a virtual screening on SUCNR1.

A SUCNR1 molecular model, created by homology modelling with the crystal structure of the agonist-bound β_2 -adrenoceptor, was used to perform *in silico* screening of a virtual "lead-like" molecules library against the succinate binding site (previously reported by He et al.). The activity of compounds with a score superior or equal to succinate was investigated with our cAMP assay. However all the predicted compounds tested were inactive.

The investigation of succinate related molecules that was conducted in a parallel project led by Pierre Geubelle (Pierre Geubelle et al., unpublished data), provided basic rules for activity at SUCNR1. This structure-activity relationships study provides valuable information on the spatial conformation of the two negatively charged carboxylates that must be positioned in a "cis" conformation. This critical feature helped to understand why the potential active molecules identified with the virtual screening were inactive. Indeed the succinate docked in the binding site of SUCNR1 was not positioned in a "cis" conformation but in a position similar to the one reported by He et al.

In order to get new synthetic ligands for SUCNR1, we established a pharmacophore model that contains two hydrogen bond acceptor elements and two negative charges.

A pharmacophore-based screening of small molecules (molecular mass and number of rotations similar to succinate) of the ZINC database (ZINCpharmer) with the developed pharmacophore model led us to propose cycloalkanes analogues ("cis" conformation) as potential ligands. Interestingly, Pierre Geubelle identified (1*R*, 2*S*)-1,2-cyclobutanedicarboxylate as a weak agonist and (1*R*, 2*S*)-1,2-cyclopropanedicarboxylate as a full agonist on SUCNR1 with a higher EC₅₀ and a similar E_{max} to succinate (Pierre Geubelle et al., unpublished data). To validate these two compounds as agonists for SUCNR1, we investigated their activity on a second signaling pathway. We confirmed

(1*R*, 2*S*)-1,2-cyclobutanedicarboxylate and (1*R*, 2*S*)-1,2-cyclopropanedicarboxylate as ligands for SUCNR1 by measuring their capacity to trigger arrestin 3 recruitment.

As (1*R*, 2*S*)-1,2-cyclopropanedicarboxylate appeared as a promising agonist for SUCNR1, we collaborated with Dr. François Jouret's team (Laboratory of Experimental Surgery, GIGA-Cardiovascular Sciences) to assess *in vivo* hypertensive properties. We showed that intravenous addition of the (1*R*, 2*S*)-1,2-cyclopropanedicarboxylate at the dose of 0.1 mg.kg⁻¹ in rats increases blood pressure (tail-cuff method) in the same range as succinate. In addition, this increase in blood pressure is statistically significant compared to the trans-isomer.

Therefore (1*R*, 2*S*)-1,2-cyclopropanedicarboxylate could be regarded as an original synthetic full agonist for SUCNR1. This ligand might be very helpful to investigate the (pato)physiological roles of SUCNR1 without directly interfering with the citric acid cycle. However further experimental investigations are required to validate this hypothesis, including measuring the activity of succinate dehydrogenase in presence and absence of the compound. In addition, dose-response curves should be determined for (1*R*, 2*S*)-1,2-cyclopropanedicarboxylate and succinate in rats.

Identification of other ligands for SUCNR1

The pharmacophore model for SUCNR1 should help to generate synthetic ligands characterized by an increased potency and/or efficacy compared to succinate. We could for instance propose diversely substituted cis-cycloalkane dicarboxylic acids or either bioisosteres of the carboxylic functions including sulphonic acids and tetrazoles.

Additionally to the structure-activity relationships study, the optimization and validation of the ligand-binding site of SUCNR1 by extensive site-directed mutagenesis might be useful to conduct a new virtual screening of the ZINC database as well as investigating the binding site of new ligands.

Up to now several series of antagonists have been reported in the literature by Bhuniya et al. but required further investigations to precisely define their pharmacology. However these ligands are not available commercially and must be first synthesized. Additionally, our pharmacophore model might be helpful to generate antagonists or inverse agonists identification. A new chemical serie of antagonists might offer new scaffolds active at SUCNR1 and might be an alternative to those described by Bhuniya et al., which could lead to inadequate bioavailability, toxicity, ...

V. MATERIAL AND METHODS

Material

All chemicals used were from Sigma-Aldrich (St. Louis, Missouri, USA) unless otherwise stated. CXCL12 (300-28A; also termed SDF-1) was from PeproTech (Rocky Hill, New Jersey, USA). The following commercially available antibodies were used for several applications: monoclonal anti-FLAG clone M2 (F3165) from Sigma-Aldrich (St. Louis, Missouri, USA); anti-Mouse IgG (H+L), F(ab')₂ Fragment (#4408, Alexa Fluor® 488 Conjugate) from Cell Signaling Technology (Danvers, Massachusetts, USA); HA-tag rabbit antibody (C29F4) from Cell Signaling Technology (Danvers, Massachusetts, USA); anti-Rabbit IgG (H+L), F(ab')₂ Fragment (#4414, Alexa Fluor® 647 Conjugate) from Cell Signaling Technology (Danvers, Massachusetts, USA); rabbit monoclonal anti-phospho-p42/44 MAPK antibody (Y202/Y204, D13.14.4E) from Cell Signaling Technology (Danvers, Massachusetts, USA); rabbit polyclonal IgG anti-Hsp90 α/β antibody (H-114) from Santa Cruz Biotechnology (Dallas, Texas, USA); Rho rabbit antibody (#8789) from Cell Signaling Technology (Danvers, Massachusetts, USA) and anti-rabbit IgG, HRP-linked antibody (#7074) from Cell Signaling Technology (Danvers, Massachusetts, USA).

Cell culture

Human embryonic kidney 293 (HEK293) cells were from American Type Culture Collection (ATCC, USA) and grown in DMEM adjusted to contain 10% fetal bovine serum (FBS, Biochrom AG, Berlin, Germany), 1% penicillin and streptomycin (Lonza, Verviers, Belgium), 1% L-glutamine (Lonza, Verviers, Belgium) at 5% CO₂ and 37°C.

SUCNR1 coding sequence was previously amplified from human genomic DNA and cloned in pcDNA3.1 by Dr. Julien Hanson. Subsequently SUCNR1 was subcloned into the pIRESpuro expression vector (Clontech Laboratories, Mountain View, California, USA) with a FLAG-tag by inserting EcoRV and BamHI restriction sites. SUCNR1 DNA was amplified by polymerase chain reaction (PCR) (forward primer: GAGAGATATCGACCATGGATTATAAAGATGATGATGATAAACTGGGGATCATGGCATGG and

reverse primer: GAGAGGATCCTCACTTTTCTCTGAATGAAAGTAGGAGTTCATG). 34 cycles of the following conditions were executed : 30 s at 98°C, 30 s at $T_{\text{annealing}}$ of 65.4°C and extended for 100 s at 72°C. Next, PCR product and pRESpuro vector were digested by adequate restriction enzymes (EcoRV and BamHI). The plasmid obtained by ligation of both insert and vector was used to generate large amounts of proteins through *E. Coli* transformation. One of the pRESpuro.FLAG.SUCNR1 clone was selected after DNA sequencing performed at sequencing platform (GIGA).

The pGloSensor™-22F cAMP (cAMP GloSensor) plasmid was obtained from Promega Corporation (Madison, Wisconsin, USA).

Human arrestin 2 was amplified from cDNA prepared from HEK293 cells and cloned into the pRESHygro expression vector (Clontech Laboratories, Mountain View, California, USA) by Nadine Dupuis.

Arrestin 3 was amplified from β -arrestin 2 GFP WT (#35411, Addgene, Cambridge, Massachusetts, USA) and cloned into the pRESHygro expression vector by Nadine Dupuis. The pRES.hygro.FnLARR2, pRES.hygro.FnLARR3, pRESHygroFnLARR2.pRESpuroSUCNR1 and pRESHygroFnLARR3.pRESpuroSUCNR1 were developed by Nadine Dupuis based on Takakura et al. (Takakura et al., 2012). Briefly, the 1-415 first AAs of firefly luciferase were fused with N-Arrestin 2 or 3 (FN-Arr 2 or 3) and the 413-549 AAs were fused with C-SUCNR1 (SUCNR1-FC).

V.1. Characterization of SUCNR1 signaling pathways and development of cell-based assays

V.1.1. Protocols for transfections

V.1.1.1. Transfection using lipofectamine

30 μL of lipofectamine[®] 2000 (11668027 ; Thermo Fischer Scientific/Life Technologies, Waltham, Massachusetts, USA) were incubated with 50 μL of Opti-MEM (Reduced Serum Media, Invitrogen) for 5 min at RT. Next this solution was added to a solution of 50 μL Opti-MEM containing 12 μg of DNA and incubated for 20 min at RT. Medium of cells (at a confluence of 80 % in a 20 cm^2 dish) were stably transfected with plasmid containing cAMP GloSensor or pGlo using lipofectamine. Medium was removed and replaced by 5 mL of fresh medium. The transfection solution was dispensed dropwise on cells. After 6 h of incubation, medium containing the transfection solution was removed, cells were washed with PBS before adding fresh medium.

V.1.1.2. Transfection using calcium phosphate

A solution of CaCl_2 (83.3 μL ; 2.5 M) was added to 833 μL BBS (BES 50 mM, NaCl 280 mM, Na_2HPO_4 1.5 mM; pH=7.02 optimized for a best transfection rate) containing 20 μg of DNA. The mixture was completed with 73.4 μL of water and incubated 20 min at RT. The transfection solution was dispensed dropwise on cells (at a confluence of 60 %) in a 60 cm^2 dish with 9 mL of fresh medium. Medium was removed after 3h30 and cells are rinsed with PBS.

V.1.1.3. Transfection using Xtreme gene

A solution of DMEM without FBS containing 2.5 μg of DNA was added to another containing 7.5 μL of Xtreme gene 9 DNA transfection reagent (#, Roche, Basel,

Switzerland). The mixture was incubated at RT for 15 min before dispensed dropwise on cells (at a confluence of 60 %) in a 20 cm² dish containing 5 mL of fresh medium.

V.1.2. Generation of stable cell lines

V.1.2.1. cAMP assay

HEK293 cells were stably transfected with plasmid containing pGloSensorTM-22F or pGlo using lipofectamine protocol. The next day, cells were trypsinised and diluted in a 120 cm² dish where they grew and expressed the protein for hygromycin resistance under non-selective conditions for at least 24 h. For the selection of stably expressing cells, they were cultivated in medium supplemented with appropriate amount of antibiotic (pre-tested by titration), hygromycin 200 µg.mL⁻¹ (A.G. scientific, San Diego, California, USA). Medium supplemented with antibiotic was changed every 2 days to compensate for loss of selection pressure. Negative control cells (not transfected) should be inspected by light microscopy and should not contain any signs of cell growth.

When colonies formed, cells were picked up and placed in a 48-well plate. Following cells growth, they were trypsinised and placed subsequently in 24-well plate, 6-well plate and eventually 20 cm² dishes. Ten clones were evaluated with our cAMP assay when stimulated with isoproterenol. Three clones, HEK293.pGlo showing the best results were selected, amplified and frozen in liquid nitrogen.

To generate the stable cell line HEK293.pGlo.SUCNR1, one HEK293.pGlo clone was used to stably transfect SUCNR1 subcloned in a bicistronic IRES vector allowing the simultaneous expression of two proteins from the same transcript (SUCNR1 and a resistance for puromycin). The method used was similar to the one for HEK293.pGlo cell line except that cells were selected with puromycin 2 mg.mL⁻¹ (pre-tested by titration) in addition to hygromycin 200 µg.mL⁻¹.

Double transfectants were selected by using FACS analysis of SUCNR1 expression at the cell membrane with a monoclonal ANTI-FLAG M2. The generated cell lines HEK293.pGlo.SUCNR1 were characterized using our cAMP assay when stimulated with SA. Three clones showing the best results were selected, amplified and frozen in liquid

nitrogen. We also ensured that HEK293.pGlo.SUCNR1 cell lines displayed a stable expression of the receptor over time, when the cells were grown in a selection medium. In parallel, we generated HEK293.SUCNR1 cell lines from HEK293 cells. Cells were selected with puromycin 2 mg.mL⁻¹ and expression of the receptor was verified using FACS analysis.

V.1.2.2. Intracellular calcium mobilization assay

Briefly, HEK293 cells were stably transfected with plasmid containing the aequorin biosensor or pG5A using lipofectamine protocol. We generated HEK293.pG5A cell lines by selection with hygromycin 200 µg.mL⁻¹ (method described previously 1.2.1.). Clones were evaluated according to the best fluorescence as the aequorin sensor contains a sequence coding for GFP.

The double stable cell lines HEK293.pG5A.SUCNR1 were generated from three HEK293.pG5A clones stably transfected with SUCNR1 subcloned in a bicistronic IRES vector. Selection was performed with puromycin 2 mg.mL⁻¹ (pre-tested by titration) in addition to hygromycin 200 µg.mL⁻¹. The expression of SUCNR1 was evaluated by FACS analysis and the best clone was used to set-up calcium mobilization assay.

V.1.2.3. Arrestin complementation assay

HEK293 cells stably transfected with pIREShygroFnLARR3 in a previous work were used to generate the double stable cell lines HEK293.pIREShygroFnLARR3.pIRESpuroSUCNR1 (ARR3.SUCNR1) with pIRESpuro.FLAG.SUCNR1. Cells were selected with hygromycin 400 µg.mL⁻¹ and puromycin 1 µg.mL⁻¹. HEK293 cells were stably transfected with pIREShygroFnLARR2 and selected with hygromycin 200 µg.mL⁻¹. Three clones were chosen by FACS analysis and one of them was transfected with pIRESpuro.FLAG.SUCNR1 to generate double stable cell lines HEK293.pIREShygroFnLARR2.pIRESpuroSUCNR1 (ARR2.SUCNR1), selected with puromycin 1 µg.mL⁻¹.

Double transfectants ARR2.SUCNR1 and ARR3.SUCNR1 were selected by using FACS analysis of SUCNR1 expression at the cell membrane with a monoclonal ANTI-FLAG M2. pIREShygroFnLARR2 was selected by a HA-tag rabbit antibody (C29F4) from Cell Signaling Technology (Danvers, Massachusetts, USA) using permeabilized cells. Stable cell line HEK293.pIREShygroFnLARR3.pIRESpuro β_2 -adrenoceptor (ARR3. β_2 -adrenoceptor) was generated by Nadine Dupuis and used as a negative control or Mock cell line.

We also generated stable cell line HEK293.pIREShygroFnLARR2.pIRESpuro β_2 -adrenoceptor (ARR2. β_2 -adrenoceptor) from pIREShygroFnLARR2 and pIRESpuro β_2 -adrenoceptor with puromycin 1 $\mu\text{g}\cdot\text{mL}^{-1}$, which we used as Mock cell line.

V.1.2.4. Flow cytometry analysis

V.1.2.4.1. Non-permeabilized cells

Cells ($2\cdot 10^5$ cells per tube) were incubated with monoclonal ANTI-FLAG M2 (1:1000) for 45 min at 4°C. Following buffer wash, cells were incubated with anti-Mouse IgG (H+L), F(ab')₂ Fragment (Alexa Fluor® 488 Conjugate; 1:1000) for 45 min at 4°C in the dark. Data were acquired on BD FACSCalibur 2 lasers (Becton Dickinson, New Jersey, USA) and analyzed with Cellquest pro.

The gate on living cells was determined using the SSC/FSC dot plot.

V.1.2.4.2. Permeabilized cells

Cells ($2\cdot 10^5$ cells per tube) were fixed for 45 min at 4°C in PBS containing 1% paraformaldehyde. Cells were permeabilized at 4°C for 15 min with PBS containing 0.3% saponine. After wash, cells were incubated with HA-tag rabbit antibody (1:800) for 45 min at 4°C. Following buffer wash, cells were incubated with anti-Rabbit IgG (H+L), F(ab')₂ Fragment (#4414, Alexa Fluor® 647 Conjugate; 1:800) for 45 min at 4°C in the dark. Data were acquired on BD FACSCalibur 2 lasers (Becton Dickinson, New Jersey, USA) and analyzed with Cellquest pro.

The gate on living cells was determined using the SSC/FSC dot plot.

V.1.3. Immunofluorescence staining and confocal microscopy

HEK293 cells lines were grown on poly-(D-lysine)-treated glass coverslips (VWR, 20x20 mm) at 37°C in 5% CO₂ for 24 h. The cells were incubated on ice 1 h in HBSS (120 mM NaCl, 5.4 mM KCl, 0.8 mM MgSO₄, 10 mM HEPES; pH 7.4; 10 mM glucose) containing ANTI-FLAG M2 (1:1000). After several washing steps, cells were incubated 10 min in HBSS at 37°C, fixed for 5 min on ice and 15 min at RT in PBS containing 4% paraformaldehyde. Cells were blocked and permeabilized at RT for 30 min with PBS containing 2% BSA and 0.12% Triton X-100. After wash, cells were incubated with PBS containing 2% BSA, 0.12% Triton X-100 and for 1 h and 45 min at RT in the dark. Cells were washed and glass coverslips mounted on slides (Marienfeld, Germany) with Prolong Gold Antifade reagent containing dapi (Thermo Fischer Scientific/Life Technologies, Waltham, Massachusetts, USA). Images were acquired using confocal microscope (Nikon A1R).

V.1.4. Cell-based assays and second messengers measurement

V.1.4.1. cAMP Assay

Prior to the experiment, cells were starved for 5 h with 1% FBS. Cells from a confluent T175 flask were detached and incubated 1 h in the dark at RT in assay buffer HBSS (120 mM NaCl, 5.4 mM KCl, 0.8 mM MgSO₄, 10 mM HEPES; pH 7.4, 10 mM glucose) containing IBMX (300 µM) and luciferin in HEPES buffer (GloSensor reagent, Promega) according to manufacturer instructions. Cells were distributed into 96-well plates (150 000 cells per well or 37 000 cells per well in 384-well plates, white Lumitrac™, Greiner) containing the ligands at different concentrations. After 1 min agitation at 1200 rpm and 9 min incubation with compounds, basal luminescence level was recorded. Similarly, luminescence was recorded following injection of FSK (40 measures; 500 ms integration time).

The luminometer was a Fluoroskan Ascent FL plate reader (Thermo Electron Corp., ascent software version 2.6) equipped with 2 dispensers. In the experiment with PTX, cells were incubated overnight with 100 ng.mL⁻¹ of PTX (Calbiochem/Merck Millipore, USA) prior to assay.

V.1.4.2. Intracellular calcium mobilization assay

The assay has been conducted according to previous description (Hanson et al., 2013). Briefly, cells from a confluent T175 flask were detached and incubated in assay buffer (HBSS : 120 mM NaCl, 5.4 mM KCl, 0.8 mM MgSO₄, 10 mM HEPES; pH 7.4, 10 mM glucose) containing 5 μM coelenterazine h (regis technologies, USA) for 1 h in the dark at 37°C. Before stimulation with ligands, the coelenterazine-containing buffer was replaced by assay buffer supplemented with 1.8 mM CaCl₂. Luminescence was followed for 8 seconds (40 measures; 200ms integration) immediately upon ligand addition. Measurements were acquired with a Fluoroskan Ascent FL (Thermo Electron Corp., ascent software version 2.6, equipped with 2 dispensers).

V.1.4.3. Arrestin complementation assay

Cells in suspension (HBSS with 20 mM HEPES, pH 7.4, 10 mM glucose) were incubated into 96-well plates (100 000 cells per well) containing the ligands at different concentrations for 10 min at RT. Following injection of 50 μM luciferin (Synchem, Germany), luminescence was recorded for 30 min using a high sensitivity luminometer (Berthold technologies, Centro XS³ LB 960, MicroWin 2000 software, equipped with 2 dispensers).

V.1.4.4. Determination of ERK phosphorylation

HEK293 cells stably transfected with pIRESpuroSUCNR1 (selected with puromycin 1 μg.mL⁻¹) were plated in 6-well plates, starved with 1% FBS and pre-treated with 100 ng.mL⁻¹ PTX or vehicle overnight. Cells were incubated with SA for 3 min at 37°C. Cells were immediately put on ice, lysed with ice-cold RIPA Buffer (25 mM Tris HCl, 150 mM NaCl, 1% NP-40, 1% sodium deoxycholate, 0.1% SDS; pH 7.6) supplemented with protease inhibitors and phosphatase inhibitors (Roche, Basel, Switzerland). Cell lysate were separated by SDS page electrophoresis (10 % acrylamide gel) and proteins were transferred to a membrane of polyvinylidene fluoride (PVDF). Membranes were blocked in a blocking buffer (TBS + 0.1% Tween-20 (BP337-100, Fisher scientific, Waltham,

Massachusetts, USA) + 5% BSA) for 1 h at RT and next incubated with primary antibody overnight at 4°C. ERK phosphorylation was detected with a rabbit monoclonal anti-phospho-p42/44 MAPK antibody (Y202/Y204, D13.14.4E, Cell Signaling, 1:2000), and Hsp90 was detected with a rabbit polyclonal IgG anti-Hsp90 α/β antibody (Santa Cruz Biotechnology, 1:5000). Following wash, membranes were then incubated 1 h at RT with corresponding HRP-conjugated secondary antibody (Cell Signaling, 1:2000) diluted in blocking buffer containing 5 % of non-fat dry milk. Proteins were revealed using Pierce™ ECL western blotting substrate (32106, Thermo Fischer Scientific/Life Technologies, Waltham, Massachusetts, USA).

V.1.4.5. Determination of Rho activation

HEK293 cells stably transfected with pRESpuRO-SUCNR1 (selected with puromycin 1 $\mu\text{g}\cdot\text{mL}^{-1}$) were plated in 6-well plates, starved for 5 h with 0.1% FBS. Cells were incubated with SA (500 μM) for 10 min at RT. Cells were immediately put on ice, lysed with ice-cold RIPA Buffer (25 mM Tris HCl, 150 mM NaCl, 1% NP-40, 1% sodium deoxycholate, 0.1% SDS; pH 7.6) supplemented with protease inhibitors and phosphatase inhibitors (Roche, Basel, Switzerland). Lysate protein concentration was determined by using Pierce® BCA protein assay kit (23225, Thermo Fischer Scientific/Life Technologies, Waltham, Massachusetts, USA). The active Rho detection kit protocol was used according to the provider instructions (8820, Cell Signaling). Briefly, lysate is added to the glutathione resin containing GST-Rhotekin-RBD and incubated for 1 h at 4°C with agitation. Reaction mixture is centrifuged and washed with cell Lysis/Binding/Wash Buffer three times. Active Rho is eluted with SDS Sample Buffer supplemented with 200 mM dithiothreitol (R086, Thermo Fischer Scientific/Life Technologies, Waltham, Massachusetts, USA) and 2.5% β -mercaptoethanol (M6250) and then heated for 5 min at 100°C with agitation. Eluted samples were separated by SDS page electrophoresis (10 % acrylamide gel) and transferred to a membrane of PVDF. Membrane was blocked in a blocking buffer (TBS + 0.1% Tween-20 (BP337-100, Fisher scientific, Waltham,

Massachusetts, USA) + 5% BSA) for 1 h at RT and next incubated with a Rho rabbit antibody (Cell Signaling, 1:667) for 2 h at RT. Following washing, membranes were incubated with corresponding Anti-rabbit IgG, HRP-linked antibody (Cell Signaling, 1:2000) diluted in blocking buffer containing 5 % of non-fat dry milk. Rho activation was

revealed using Pierce™ ECL western blotting substrate (32106, Thermo Fischer Scientific/Life Technologies, Waltham, Massachusetts, USA).

V.2. Screening of SUCNR1 with a FSK-free cAMP assay

V.2.1. Calculation of Z' factor

Z' values were determined to monitor assay quality and were calculated according to the formula $Z' = 1 - ((3\sigma_{c+} + 3\sigma_{c-}) / |\mu_{c+} - \mu_{c-}|)$ (Zhang et al., 1999).

V.2.2. Hit selection and activity cut-off criteria

We set-up two criteria for hit selection: 1) a positive activity on SUCNR1 expressing cells > negative control (vehicle) mean + 6 σ and 2) activity on Mock cells (HEK293.pGlo) comprised within negative control (vehicle) mean \pm 3 σ . Compounds fulfilling these 2 criteria were selected for secondary screening. The number of compounds selected represented approximately 0.15% of the collection (Hit rate). Following cherry picking, compounds were assayed in triplicate at one concentration on SUCNR1 and mock cells. Compounds showing statistically significant activity on SUCNR1 were selected for complete concentration-response curves.

V.2.3. Data analysis and statistical procedure

All data analyses were performed using computer software (GraphPad Prism version 5.0 for Windows).

Statistical analyses of differences between 2 groups were performed by non-parametric, unpaired, 2-tailed Mann-Whitney test. P values less than 0.05 were considered as statistically significant.

V.3. Characterization of succinate binding site

V.3.1. *In silico* models

V.3.1.1. Receptor model

The published β_2 -adrenoceptor structure was used as a template for generating a partial SUCNR1 structure model (Rasmussen et al., 2011). The SUCNR1 primary sequence was aligned to β_2 -adrenoceptor (PDB code 3P0G) using the SYBYL 8.0 software. The binding mode of succinate, composed of R99^{3.29}, R281^{7.39}, R252^{6.55} and H101^{3.33}, onto SUCNR1 was explored by docking analysis using the GOLD 5.2 program.

V.3.1.2. Docking of the ZINC database

A pharmacophore model generated by Unity[®] ([CSL STYLE ERROR: reference with no printed form.]) was used to screen and locate compounds in ZINC database. Compounds that have the best theoretical score to fit to the pharmacophore, superior or equal to succinate, were next explored by docking analysis using the GOLD 5.2 program.

V.3.1.3. Pharmacophore model

The pharmacophore model was built using the program phase 3.3. of the Schrödinger Suite package and based on the results generated during primary SAR study performed by Pierre Geubelle. Structural conformers were generated with the thorough sampling option. Hypotheses matching the AH (hydrogen bond acceptor) and N (Negative charge) were kept. The top hypothesis matching the elements two AH and two N was selected after scoring actives and inactives. Excluded volumes were added according the superimposition of inactive ligands. Ligprep of the Schrödinger Suite package was used for generating 3D structures.

V.3.2. SUCNR1 mutants

V.3.2.1. Site-Directed Mutagenesis

SUCNR1 mutants were generated from psG5.FLAG.SUCNR1 by introducing a simple mutation (replacement of the selected AA by an alanine) using the following primers (*Table V-1*), synthetic oligonucleotides and the Site-Directed Mutagenesis kit (#E0554S; Cell signaling). 25 cycles were achieved among the optimized conditions: 15 s at 98°C, 30 s at Tannealing (*Table V-1*) and ended for 3 min at 72°C.

<i>Mutation</i>	<i>Primers forward (F) /Reverse (R)</i>	<i>T_{annealing}</i>
R99A	F: cataagcaacgcatatgtgcttcatgccaac R: cagagcacgtctccatatac	60.5°C
H103A	F: cgaagctgccaacctc R: acatatcggttgcttatgcag	63.5°C
R252A	F: tcacgtcatggccaatgtgaggatcgcttcac R: tagggtgtaaaaagcacag	61.4°C
R281A	F: cattgtgacagccccttggcctttctgaacag R: taaaaggagttgatgacgac	57.8°C

Table V-1 : PCR conditions for the different mutants.

V.3.2.2. Transient transfection of mutants

Mutants were transfected in HEK293.pGlo cells plated at 50% confluence in a 60 cm² dish using calcium phosphate transfection method. They were evaluated with our cAMP assay according to the protocol described above (See V.1.4.1.). 10.10⁶ cells contained in a dish were distributed into one column of 96-well plate.

V.3.3. *In vivo* experiments

All experiments were performed under protocols approved by the Institutional Animal Care and Use Committee. Animals were housed in a light- and temperature-controlled room with ad libitum access to water and food. Blood pressure (BP) was measured in twelve awake male Wistar rats (about 300 g) by the tail-cuff method using CODA system (Kent Scientific Corporation; NIBP-CODA8-PACK).

Compounds (succinate, cis-CPDC and trans-CPDC) to test were dissolved in physiological solution, cis-CPDC and trans-CPDC solutions were adjusted to pH 7.

After acclimation of the animals to the holder and cuffs, compounds to test were injected via the tail vein. Immediately after injection, systolic, diastolic and mean BP were recorded 15 times (CODA software).

Results are expressed as mean \pm SEM. Statistical significance was evaluated by Student's t-test or two-way analysis of variance.

VI. BIBLIOGRAPHY

- Adams, J.W., Wang, J., Davis, J.R., Liaw, C., Gaidarov, I., Gatlin, J., et al. (2008). Myocardial expression, signaling, and function of GPR22: a protective role for an orphan G protein-coupled receptor. *Am. J. Physiol. Heart Circ. Physiol.* *295*: H509–H521.
- Adams, S.R., Harootunian, A.T., Buechler, Y.J., Taylor, S.S., and Tsien, R.Y. (1991). Fluorescence ratio imaging of cyclic AMP in single cells. *Nature* *349*: 694–7.
- Aguiar, C.J., Andrade, V.L., Gomes, E.R.M., Alves, M.N.M., Ladeira, M.S., Pinheiro, A.C.N., et al. (2010). Succinate modulates Ca²⁺ transient and cardiomyocyte viability through PKA-dependent pathway. *Cell Calcium* *47*: 37–46.
- Aguiar, C.J., Rocha-Franco, J. a, Sousa, P. a, Santos, A.K., Ladeira, M., Rocha-Resende, C., et al. (2014). Succinate causes pathological cardiomyocyte hypertrophy through GPR91 activation. *Cell Commun. Signal.* *12*: 1–17.
- Ahmad, R., Wojciech, S., and Jockers, R. (2015). Hunting for the function of orphan GPCRs - beyond the search for the endogenous ligand. *Br. J. Pharmacol.* *172*: 3212–3228.
- Ahn, S., Shenoy, S.K., Wei, H., and Lefkowitz, R.J. (2004). Differential kinetic and spatial patterns of β -arrestin and G protein-mediated ERK activation by the angiotensin II receptor. *J. Biol. Chem.* *279*: 35518–35525.
- Alexander, S., Davenport, A., Kelly, E., Marrion, N., Peters, J., Benson, H., et al. (2015). The Concise Guide to PHARMACOLOGY 2015/16: G protein-coupled receptors. *Br J Pharmacol.* *172*: 5744–5869.
- Allen, M., Hall, D., Collins, B., and Moore, K. (2002). A homogeneous high throughput nonradioactive method for measurement of functional activity of Gs-coupled receptors in membranes. *J. Biomol. Screen.* *7*: 35–44.
- Al-Sabah, S., Al-Fulajj, M., Shaaban, G., Ahmed, H.A., Mann, R.J., Donnelly, D., et al. (2014). The GIP receptor displays higher basal activity than the GLP-1 receptor but does not recruit GRK2 or arrestin3 effectively. *PLoS One* *9*: e106890.
- Amisten, S., Braun, O.O., Bengtsson, A., and Erlinge, D. (2008). Gene expression profiling for the identification of G-protein coupled receptors in human platelets. *Thromb. Res.* *122*: 47–57.

Ariza, A.C., Deen, P.M.T., and Robben, J.H. (2012). The succinate receptor as a novel therapeutic target for oxidative and metabolic stress-related conditions. *Front. Endocrinol. (Lausanne)*. *3*: 1–8.

Atwood, B.K., Lopez, J., Wager-Miller, J., Mackie, K., and Straiker, a (2011). Expression of G protein-coupled receptors and related proteins in HEK293, AtT20, BV2, and N18 cell lines as revealed by microarray analysis. *BMC Genomics* *12*: 14.

Audet, M., and Bouvier, M. (2012). Restructuring G-Protein- Coupled Receptor Activation. *Cell* *151*: 14–23.

Azzi, M., Charest, P.G., Angers, S., Rousseau, G., Kohout, T., Bouvier, M., et al. (2003). Beta-arrestin-mediated activation of MAPK by inverse agonists reveals distinct active conformations for G protein-coupled receptors. *Proc. Natl. Acad. Sci. U. S. A.* *100*: 11406–11.

Baker, J.G., Hall, I.P., and Hill, S.J. (2003). Agonist and inverse agonist actions of beta-blockers at the human beta 2-adrenoceptor provide evidence for agonist-directed signaling. *Mol. Pharmacol.* *64*: 1357–69.

Baker, J.G., Hall, I.P., and Hill, S.J. (2004). Temporal characteristics of cAMP response element-mediated gene transcription: requirement for sustained cAMP production. *Mol. Pharmacol.* *65*: 986–98.

Ballesteros, J., & Weinstein, H. (1995). Integrated methods for the construction of three-dimensional models and computational probing of structure-function relations in G protein-coupled receptors. *Methods Neurosci.* *25*: 366–428.

Baubet, V., Mouellic, H. Le, Campbell, a K., Lucas-Meunier, E., Fossier, P., and Brúlet, P. (2000). Chimeric green fluorescent protein-aequorin as bioluminescent Ca²⁺ reporters at the single-cell level. *Proc. Natl. Acad. Sci. U. S. A.* *97*: 7260–7265.

Begley, C.G. (2013). Six red flags for suspect work. *Nature* *497*: 433–4.

Benovic, J.L., Kühn, H., Weyand, I., Codina, J., Caron, M.G., and Lefkowitz, R.J. (1987). Functional desensitization of the isolated beta-adrenergic receptor by the beta-adrenergic receptor kinase: potential role of an analog of the retinal protein arrestin (48-kDa protein). *Proc. Natl. Acad. Sci. U. S. A.* *84*: 8879–8882.

Bhat, S., Bajwa, B.S., Dornauer, H., and Souza, N.J. de (1977). Structure and stereochemistry of new lardanes diterpenoids from *coleus forskohlii*. *Tetrahedron Lett* 1669–1672.

- Bhuniya, D., Umrani, D., Dave, B., Salunke, D., Kukreja, G., Gundu, J., et al. (2011). Discovery of a potent and selective small molecule hGPR91 antagonist. *Bioorganic Med. Chem. Lett.* *21*: 3596–3602.
- Binkowski, B., Fan, F., and Wood, K. (2009). Engineered luciferases for molecular sensing in living cells. *Curr. Opin. Biotechnol.* *20*: 14–18.
- Binkowski, B.F., Butler, B.L., Stecha, P.F., Eggers, C.T., Otto, P., Zimmerman, K., et al. (2011). A luminescent biosensor with increased dynamic range for intracellular cAMP. *ACS Chem. Biol.* *6*: 1193–7.
- Bohn, L.M., Lefkowitz, R.J., Gainetdinov, R.R., Peppel, K., Caron, M.G., and Lin, F.T. (1999). Enhanced morphine analgesia in mice lacking beta-arrestin 2. *Science* *286*: 2495–8.
- Boute, N., Jockers, R., and Issad, T. (2002). The use of resonance energy transfer in high-throughput screening: BRET versus FRET. *Trends Pharmacol. Sci.* *23*: 351–4.
- Bouvier, M., Hausdorff, W.P., Blasi, A. De, O'Dowd, B.F., Kobilka, B.K., Caron, M.G., et al. (1988). Removal of phosphorylation sites from the beta 2-adrenergic receptor delays onset of agonist-promoted desensitization. *Nature* *333*: 370–3.
- Bremnes, T., Paasche, J.D., Mehlum, A., Sandberg, C., Bremnes, B., and Attramadal, H. (2000). Regulation and intracellular trafficking pathways of the endothelin receptors. *J. Biol. Chem.* *275*: 17596–604.
- Brideau, C. (2003). Improved Statistical Methods for Hit Selection in High-Throughput Screening. *J. Biomol. Screen.* *8*: 634–647.
- Brivanlou, A.H., and Darnell, J.E. (2002). Signal transduction and the control of gene expression. *Science* *295*: 813–818.
- Buccioni, M., Marucci, G., Dal Ben, D., Giacobbe, D., Lambertucci, C., Soverchia, L., et al. (2011). Innovative functional cAMP assay for studying G protein-coupled receptors: application to the pharmacological characterization of GPR17. *Purinergic Signal.* *7*: 463–8.
- Callander, G.E., Thomas, W.G., and Bathgate, R.A.D. (2009). Prolonged RXFP1 and RXFP2 signaling can be explained by poor internalization and a lack of beta-arrestin recruitment. *Am. J. Physiol. Cell Physiol.* *296*: C1058–66.

Cao, W., Luttrell, L.M., Medvedev, A. V, Pierce, K.L., Daniel, K.W., Dixon, T.M., et al. (2000). Direct binding of activated c-Src to the beta 3-adrenergic receptor is required for MAP kinase activation. *J. Biol. Chem.* *275*: 38131–4.

Cavasotto, C.N., and Palomba, D. (2015). Expanding the horizons of G protein-coupled receptor structure-based ligand discovery and optimization using homology models. *Chem. Commun.* *57*: 13576–94.

Chen, C.Z., Southall, N., Xiao, J., Marugan, J.J., Ferrer, M., Hu, X., et al. (2013). Identification of small-molecule agonists of human relaxin family receptor 1 (RXFP1) by using a homogenous cell-based cAMP assay. *J. Biomol. Screen.* *18*: 670–7.

Chen, L., Jin, L., and Zhou, N. (2012). An update of novel screening methods for GPCR in drug discovery. *Expert Opin. Drug Discov.* *7*: 791–806.

Chen, Z., Gaudreau, R., Gouill, C. Le, Rola-Pleszczynski, M., and Stanková, J. (2004). Agonist-induced internalization of leukotriene B(4) receptor 1 requires G-protein-coupled receptor kinase 2 but not arrestins. *Mol. Pharmacol.* *66*: 377–386.

Cheng, Y., and Prusoff, W.H. (1973). Relationship between the inhibition constant (K_1) and the concentration of inhibitor which causes 50 per cent inhibition (I_{50}) of an enzymatic reaction. *Biochem. Pharmacol.* *22*: 3099–108.

Chouchani, E.T., Pell, V.R., Gaude, E., Aksentijevic, D., Sundier, S.Y., Robb, E.L., et al. (2014). Ischaemic accumulation of succinate controls reperfusion injury through mitochondrial ROS. *Nature* *515*: 431–449.

Civelli, O., Reinscheid, R.K., Zhang, Y., Wang, Z., Fredriksson, R., and Schiöth, H.B. (2013). G Protein-Coupled Receptor Deorphanizations. *Annu. Rev. Pharmacol. Toxicol.* *53*: 127–46.

Cobbold, P.H., and Rink, T.J. (1987). Fluorescence and bioluminescence measurement of cytoplasmic free calcium. *Biochem. J.* *248*: 313–28.

Congreve, M., Langmead, C.J., Mason, J.S., and Marshall, F.H. (2011). Progress in Structure Based Drug Design for G Protein-Coupled Receptors. *J. Med. Chem.* *54*: 4283–4311.

Conner, D.A., Mathier, M.A., Mortensen, R.M., Christe, M., Vatner, S.F., Seidman, C.E., et al. (1997). beta-Arrestin1 knockout mice appear normal but demonstrate altered cardiac responses to beta-adrenergic stimulation. *Circ. Res.* *81*: 1021–6.

- Conti, E., Franks, N.P., and Brick, P. (1996). Crystal structure of firefly luciferase throws light on a superfamily of adenylate-forming enzymes. *Structure* *4*: 287–98.
- Costa, T., and Herz, A. (1989). Antagonists with negative intrinsic activity at delta opioid receptors coupled to GTP-binding proteins. *Proc. Natl. Acad. Sci. U. S. A.* *86*: 7321–5.
- Couturier, C., and Deprez, B. (2012). Setting Up a Bioluminescence Resonance Energy Transfer High throughput Screening Assay to Search for Protein/Protein Interaction Inhibitors in Mammalian Cells. *Front. Endocrinol. (Lausanne)*. *3*: 100.
- Cubitt, A.B., Heim, R., Adams, S.R., Boyd, A.E., Gross, L.A., and Tsien, R.Y. (1995). Understanding, improving and using green fluorescent proteins. *Trends Biochem. Sci.* *20*: 448–55.
- Daugherty, A., Rateri, D., Hong, L., and Balakrishnan, A. (2009). Measuring blood pressure in mice using volume pressure recording, a tail-cuff method. *J. Vis. Exp.*
- Davenport, A.P., Alexander, S.P.H., Sharman, J.L., Pawson, A.J., Benson, H.E., Monaghan, A.E., et al. (2013). International Union of Basic and Clinical Pharmacology. LXXXVIII. G protein-coupled receptor list: recommendations for new pairings with cognate ligands. *Pharmacol. Rev.* *65*: 967–86.
- Davenport, A.P., and Harmar, A.J. (2013). Evolving pharmacology of orphan GPCRs: IUPHAR Commentary. *Br. J. Pharmacol.* *170*: 693–695.
- Deen, P.M.T., and Robben, J.H. (2011). Succinate receptors in the kidney. *J. Am. Soc. Nephrol.* *22*: 1416–1422.
- Degorce, F., Card, A., Soh, S., Trinquet, E., Knapik, G.P., and Xie, B. (2009). HTRF: A technology tailored for drug discovery - a review of theoretical aspects and recent applications. *Curr. Chem. Genomics* *3*: 22–32.
- DiRaddo, J.O., Miller, E.J., Hathaway, H.A., Grajkowska, E., Wroblewska, B., Wolfe, B.B., et al. (2014). A real-time method for measuring cAMP production modulated by Gai/o-coupled metabotropic glutamate receptors. *J. Pharmacol. Exp. Ther.* *349*: 373–82.
- Donaldson, J., Hill, S.J., and Brown, A.M. (1988). Kinetic studies on the mechanism by which histamine H1 receptors potentiate cyclic AMP accumulation in guinea pig cerebral cortical slices. *Mol. Pharmacol.* *33*: 626–33.

- Drake, E.J., and Gulick, A.M. (2011). Structural characterization and high throughput screening of inhibitors of PvdQ, an NTN hydrolase involved in pyoverdine synthesis. *ACS Chem Biol.* *6*: 1277–1286.
- Dunlop, J., and Eglén, R.M. (2004). Identifying orphan G protein coupled receptors in drug discovery. *Drug Discov. Today Technol.* *1*: 61–68.
- Eglén, R.M., and Reisine, T. (2008). Photoproteins: important new tools in drug discovery. *Assay Drug Dev. Technol.* *6*: 659–71.
- Eglén, R.M., Reisine, T., Roby, P., Rouleau, N., Illy, C., Bossé, R., et al. (2008). The use of AlphaScreen technology in HTS: current status. *Curr. Chem. Genomics* *1*: 2–10.
- Emkey, R., and Rankl, N.B. (2009). Screening G protein-coupled receptors: measurement of intracellular calcium using the fluorometric imaging plate reader. *Methods Mol. Biol.* *565*: 145–58.
- Fan, F., Binkowski, B.F., Butler, B.L., Stecha, P.F., Lewis, M.K., and Wood, K. V. (2008). Novel genetically encoded biosensors using firefly luciferase. *ACS Chem. Biol.* *3*: 346–351.
- Fedotcheva, N.I., Sokolov, A.P., and Kondrashova, M.N. (2006). Nonezymatic formation of succinate in mitochondria under oxidative stress. *Free Radic. Biol. Med.* *41*: 56–64.
- Feldkamp, T., Kribben, A., Roeser, N.F., Senter, R. a, Kemner, S., Venkatachalam, M. a, et al. (2004). Preservation of complex I function during hypoxia-reoxygenation-induced mitochondrial injury in proximal tubules. *Am. J. Physiol. Renal Physiol.* *286*: F749–F759.
- Ferguson, S.S. (2001). Evolving concepts in G protein-coupled receptor endocytosis: the role in receptor desensitization and signaling. *Pharmacol. Rev.* *53*: 1–24.
- Ferré, S., Baler, R., Bouvier, M., Caron, M.G., Devi, L. a, Durroux, T., et al. (2010). Building a new conceptual framework for receptor heteromers. *Nat Chem Biol* *5*: 131–134.
- Fields, T.A., and Casey, P.J. (1997). G-proteins. *571*: 561–571.
- Foord, S.M., Bonner, T.O.M.I., Neubig, R.R., Rosser, E.M., Pin, J., Davenport, A.P., et al. (2005). International Union of Pharmacology . XLVI . G Protein-Coupled Receptor List. *Pharmacol. Rev.* *57*: 279–288.
- Frearson, J. a., and Collie, I.T. (2009). HTS and hit finding in academia - from chemical genomics to drug discovery. *Drug Discov. Today* *14*: 1150–1158.

- Fredriksson, R., Lagerström, M.C., Lundin, L.-G., and Schiöth, H.B. (2003). The G-protein-coupled receptors in the human genome form five main families. Phylogenetic analysis, paralogon groups, and fingerprints. *Mol. Pharmacol.* *63*: 1256–1272.
- Gabriel, D., Vernier, M., Pfeifer, M.J., Dasen, B., Tenaillon, L., and Bouhelal, R. (2003). High throughput screening technologies for direct cyclic AMP measurement. *Assay Drug Dev. Technol.* *1*: 291–303.
- Galandrin, S., Oligny-Longpré, G., and Bouvier, M. (2007). The evasive nature of drug efficacy: implications for drug discovery. *Trends Pharmacol. Sci.* *28*: 423–30.
- Galloway, W.R., and Spring, D.R. (2009). Is synthesis the main hurdle for the generation of diversity in compound libraries for screening? *Expert Opin. Drug Discov.* *4*: 467–72.
- Galloway, W.R.J.D., Isidro-Llobet, A., and Spring, D.R. (2010). Diversity-oriented synthesis as a tool for the discovery of novel biologically active small molecules. *Nat. Commun.* *1*: 80.
- Galloway, W.R.J.D., and Spring, D.R. (2011). A question of library design Better leads come from diversity. *Nat. Commun.* *470*: 43.
- Ge, L., Ly, Y., Hollenberg, M., and DeFea, K. (2003). A beta-arrestin-dependent scaffold is associated with prolonged MAPK activation in pseudopodia during protease-activated receptor-2-induced chemotaxis. *J. Biol. Chem.* *278*: 34418–26.
- Gilissen, J., Jouret, F., Pirotte, B., and Hanson, J. (2016). Insight into SUCNR1 (GPR91) structure and function. *Pharmacol. Ther.*
- Gnana-Prakasam, J.P., Ananth, S., Prasad, P.D., Zhang, M., Atherton, S.S., Martin, P.M., et al. (2011). Expression and iron-dependent regulation of succinate receptor GPR91 in retinal pigment epithelium. *Investig. Ophthalmol. Vis. Sci.* *52*: 3751–3758.
- Goetz, A.S., Andrews, J.L., Littleton, T.R., and Ignar, D.M. (2000). Development of a facile method for high throughput screening with reporter gene assays. *J. Biomol. Screen.* *5*: 377–84.
- Goldsmith, Z.G., and Dhanasekaran, D.N. (2007). G protein regulation of MAPK networks. *Oncogene* *26*: 3122–42.
- Golla, R., and Seethala, R. (2002). A homogeneous enzyme fragment complementation cyclic AMP screen for GPCR agonists. *J. Biomol. Screen.* *7*: 515–25.

Gonzalez, N.S., Communi, D., Hannedouche, S., and Boeynaems, J.M. (2004). The fate of P2Y-related orphan receptors: GPR80/99 and GPR91 are receptors of dicarboxylic acids. *Purinergic Signal.* *7*: 17–20.

Gordon, E.J. (2007). Small-molecule screening: it takes a village... *ACS Chem. Biol.* *2*: 9–16.

Grady, E.F., Garland, A.M., Gamp, P.D., Lovett, M., Payan, D.G., and Bunnett, N.W. (1995). Delineation of the endocytic pathway of substance P and its seven-transmembrane domain NK1 receptor. *Mol. Biol. Cell* *6*: 509–24.

Granzin, J., Wilden, U., Choe, H.W., Labahn, J., Krafft, B., and Büldt, G. (1998). X-ray crystal structure of arrestin from bovine rod outer segments. *Nature* *397*: 918–21.

Gray, J.A., Bhatnagar, A., Gurevich, V. V, and Roth, B.L. (2003). The interaction of a constitutively active arrestin with the arrestin-insensitive 5-HT(2A) receptor induces agonist-independent internalization. *Mol. Pharmacol.* *63*: 961–72.

Gray, J.A., Sheffler, D.J., Bhatnagar, A., Woods, J.A., Hufeisen, S.J., Benovic, J.L., et al. (2001). Cell-type specific effects of endocytosis inhibitors on 5-hydroxytryptamine(2A) receptor desensitization and resensitization reveal an arrestin-, GRK2-, and GRK5-independent mode of regulation in human embryonic kidney 293 cells. *Mol. Pharmacol.* *60*: 1020–30.

Grynkiewicz, G., Poenie, M., and Tsien, R.Y. (1985). A new generation of Ca²⁺ indicators with greatly improved fluorescence properties. *J. Biol. Chem.* *260*: 3440–50.

Gurevich, V. V, and Gurevich, E. V (2003). The new face of active receptor bound arrestin attracts new partners. *Structure* *11*: 1037–42.

Gurevich, V. V, and Gurevich, E. V (2006). The structural basis of arrestin-mediated regulation of G-protein-coupled receptors. *Pharmacol. Ther.* *110*: 465–502.

Gutkind, J.S. (2000). Regulation of Mitogen-Activated Protein Kinase Signaling Networks by G Protein-Coupled Receptors.

Hajduk, P.J. (2011). A question of library design Small molecules, great potential. *Nat. Commun.* *470*: 42.

Hakak, Y., Lehmann-Bruinsma, K., Phillips, S., Le, T., Liaw, C., Connolly, D.T., et al. (2009). The role of the GPR91 ligand succinate in hematopoiesis. *J. Leukoc. Biol.* *85*: 837–843.

- Hamel, D., Sanchez, M., Duhamel, F., Roy, O., Honoré, J.C., Noueihed, B., et al. (2014). G-protein-coupled receptor 91 and succinate are key contributors in neonatal postcerebral hypoxia-ischemia recovery. *Arterioscler. Thromb. Vasc. Biol.* *34*: 285–293.
- Han, M., Gurevich, V. V., Vishnivetskiy, S.A., Sigler, P.B., and Schubert, C. (2001). Crystal structure of beta-arrestin at 1.9 Å: possible mechanism of receptor binding and membrane Translocation. *Structure* *9*: 869–880.
- Hanson, J., Ferreirós, N., Pirotte, B., Geisslinger, G., and Offermanns, S. (2013). Heterologously expressed formyl peptide receptor 2 (FPR2/ALX) does not respond to lipoxin A4. *Biochem. Pharmacol.* *85*: 1795–1802.
- Hase, M., Yokomizo, T., Shimizu, T., and Nakamura, M. (2008). Characterization of an orphan G protein-coupled receptor, GPR20, that constitutively activates Gi proteins. *J. Biol. Chem.* *283*: 12747–12755.
- Hattori, Tanaka, Takakura, Aoki, Miura, Anzai, et al. (2013). Analysis of temporal patterns of GPCR-β-arrestin interactions using split luciferase-fragment complementation. *Mol. Biosyst.* *9*: 957–964.
- Hausdorff, W.P., Bouvier, M., O’Dowd, B.F., Irons, G.P., Caron, M.G., and Lefkowitz, R.J. (1989). Phosphorylation sites on two domains of the beta 2-adrenergic receptor are involved in distinct pathways of receptor desensitization. *J. Biol. Chem.* *264*: 12657–65.
- He, W., Miao, F.J.-P., Lin, D.C.-H., Schwandner, R.T., Wang, Z., Gao, J., et al. (2004). Citric acid cycle intermediates as ligands for orphan G-protein-coupled receptors. *Nature* *429*: 188–193.
- Hebert, S.C. (2004). Physiology: orphan detectors of metabolism. *Nature* *429*: 143–5.
- Hems, D.A., and Brosnan, J.T. (1970). Effects of ischaemia on content of metabolites in rat liver and kidney in vivo. *Biochem. J.* *120*: 105–11.
- Hermans, E., Vanisberg, M.A., Geurts, M., and Maloteaux, J.M. (1997). Down-regulation of neurotensin receptors after ligand-induced internalization in rat primary cultured neurons. *Neurochem. Int.* *31*: 291–9.
- Heydorn, A., Ward, R.J., Jorgensen, R., Rosenkilde, M.M., Frimurer, T.M., Milligan, G., et al. (2004). Identification of a novel site within G protein alpha subunits important for specificity of receptor-G protein interaction. *Mol. Pharmacol.* *66*: 250–259.

Hill, S.J., Baker, J.G., and Rees, S. (2001). Reporter-gene systems for the study of G-protein-coupled receptors. *Curr. Opin. Pharmacol.* *1*: 526–32.

Hill, S.J., Williams, C., and May, L.T. (2010). Insights into GPCR pharmacology from the measurement of changes in intracellular cyclic AMP; advantages and pitfalls of differing methodologies. *Br. J. Pharmacol.* *161*: 1266–75.

Högberg, C., Gidlöf, O., Tan, C., Svensson, S., Nilsson-öhrman, J., Erlinge, D., et al. (2011). Succinate independently stimulates full platelet activation via cAMP and phosphoinositide 3-kinase- β signaling. *J. Thromb. Haemost.* *9*: 361–372.

Houslay, M.D., and Milligan, G. (1997). Tailoring cAMP-signalling responses through isoform multiplicity. *Trends Biochem. Sci.* *22*: 217–224.

Hu, J., Li, T., Du, S., Chen, Y., Wang, S., Xiong, F., et al. (2015). The MAPK signaling pathway mediates the GPR91-dependent release of VEGF from RGC-5 cells. *Int. J. Mol. Med.* 130–138.

Hu, J., Wu, Q., Li, T., Chen, Y., and Wang, S. (2013). Inhibition of high glucose-induced VEGF release in retinal ganglion cells by RNA interference targeting G protein-coupled receptor 91. *Exp. Eye Res.* *109*: 31–39.

Inouye, S., and Tsuji, F.I. (1994). Aequorea green fluorescent protein. Expression of the gene and fluorescence characteristics of the recombinant protein. *FEBS Lett.* *341*: 277–80.

Irannejad, R., Tomshine, J.C., Tomshine, J.R., Chevalier, M., Mahoney, J.P., Steyaert, J., et al. (2013). Conformational biosensors reveal GPCR signalling from endosomes. *Nature* *495*: 534–538.

Irwin, J.J., and Shoichet, B.K. (2005). ZINC--a free database of commercially available compounds for virtual screening. *J. Chem. Inf. Model.* *45*: 177–82.

Isberg, V., Andersen, K.B., Bisig, C., Dietz, G.P.H., Bräuner-Osborne, H., and Gloriam, D.E. (2014). Computer-aided discovery of aromatic l- α -amino acids as agonists of the orphan G protein-coupled receptor GPR139. *J. Chem. Inf. Model.* *54*: 1553–7.

Jacoby, E., Bouhelal, R., Gerspacher, M., and Seuwen, K. (2006). The 7TM G-protein-coupled receptor target family. *ChemMedChem* *1*: 760–782.

- Jiang, L.I., Collins, J., Davis, R., Lin, K.-M., DeCamp, D., Roach, T., et al. (2007). Use of a cAMP BRET sensor to characterize a novel regulation of cAMP by the sphingosine 1-phosphate/G13 pathway. *J. Biol. Chem.* *282*: 10576–84.
- Joost, H.G., Habberfield, A.D., Simpson, I.A., Laurenza, A., and Seamon, K.B. (1988). Activation of adenylate cyclase and inhibition of glucose transport in rat adipocytes by forskolin analogues: structural determinants for distinct sites of action. *Mol. Pharmacol.* *33*: 449–53.
- Joost, P., and Methner, A. (2002). Phylogenetic analysis of 277 human G-protein-coupled receptors as a tool for the prediction of orphan receptor ligands. *Genome Biol.* *3*: RESEARCH0063.
- Kelley, G.G., Kaproth-Joslin, K. a., Reks, S.E., Smrcka, A. V., and Wojcikiewicz, R.J.H. (2006). G-protein-coupled receptor agonists activate endogenous phospholipase Cepsilon and phospholipase Cbeta3 in a temporally distinct manner. *J. Biol. Chem.* *281*: 2639–2648.
- Kenakin, T. (2002). Drug efficacy at G protein-coupled receptors. *Annu. Rev. Pharmacol. Toxicol.* *42*: 349–79.
- Kenakin, T. (2003). Ligand-selective receptor conformations revisited: the promise and the problem. *Trends Pharmacol. Sci.* *24*: 346–54.
- Kenakin, T. (2014). A pharmacology primer.
- Kenakin, T.M., Holliday, N., Hill, S.T., and Al., E. (2010). GPCR molecular pharmacology and drug targeting: shifting paradigms and new directions (USA: John Wiley & Sons).
- Kim, J., Ahn, S., Ren, X.-R., Whalen, E.J., Reiter, E., Wei, H., et al. (2005). Functional antagonism of difKim, J., Ahn, S., Ren, X.-R., Whalen, E. J., Reiter, E., Wei, H., et al. (2005). Functional antagonism of different G protein-coupled receptor kinases for beta-arrestin-mediated angiotensin II receptor signaling. *Proc. Natl. Acad. Sci. U. S. A.* *102*: 1442–7.
- Kim, J.W., Roberts, C.D., Berg, S.A., Caicedo, A., Roper, S.D., and Chaudhari, N. (2008). Imaging cyclic AMP changes in pancreatic islets of transgenic reporter mice. *PLoS One* *3*: e2127.
- Klein, M.T., Dukat, M., Glennon, R.A., and Teitler, M. (2011). Toward selective drug development for the human 5-hydroxytryptamine 1E receptor: a comparison of 5-hydroxytryptamine 1E and 1F receptor structure-affinity relationships. *J. Pharmacol. Exp. Ther.* *337*: 860–7.

- Klenc, J., Lipowska, M., and Taylor, A.T. (2015). Identification of lead compounds for ^{99m}Tc and ^{18}F GPR91 radiotracers. *Bioorg. Med. Chem. Lett.* *25*: 2335–2339.
- Kohout, T. a, and Lefkowitz, R.J. (2003). Regulation of G protein-coupled receptor kinases and arrestins during receptor desensitization. *Mol. Pharmacol.* *63*: 9–18.
- Koo, J., Schmidt, S.P., and Schuster, G.B. (1978). Bioluminescence of the firefly: key steps in the formation of the electronically excited state for model systems. *Proc. Natl. Acad. Sci. U. S. A.* *75*: 30–33.
- Kostenis, E. (2001). Is Galpha16 the optimal tool for fishing ligands of orphan G-protein-coupled receptors? *Trends Pharmacol. Sci.* *22*: 560–4.
- Kostenis, E., Degtyarev, M.Y., Conklin, B.R., and Wess, J. (1997). The N-terminal extension of Galphaq is critical for constraining the selectivity of receptor coupling. *J. Biol. Chem.* *272*: 19107–10.
- Kostenis, E., Martini, L., Ellis, J., Waldhoer, M., Heydorn, a, Rosenkilde, M., et al. (2005). A highly conserved glycine within linker I and the extreme C terminus of G protein alpha subunits interact cooperatively in switching G protein-coupled receptor-to-effector specificity. *J. Pharmacol. Exp. Ther.* *313*: 78–87.
- Kretsinger, R.H., and Nockolds, C.E. (1973). Carp muscle calcium-binding protein. II. Structure determination and general description. *J. Biol. Chem.* *248*: 3313–26.
- Krueger, K.M., Daaka, Y., Pitcher, J.A., and Lefkowitz, R.J. (1997). The role of sequestration in G protein-coupled receptor resensitization. Regulation of beta2-adrenergic receptor dephosphorylation by vesicular acidification. *J. Biol. Chem.* *272*: 5–8.
- Kunapuli, P., Ransom, R., Murphy, K.L., Pettibone, D., Kerby, J., Grimwood, S., et al. (2003). Development of an intact cell reporter gene beta-lactamase assay for G protein-coupled receptors for high-throughput screening. *Anal. Biochem.* *314*: 16–29.
- Kushnir, M.M., Komaromy-hiller, G., Shushan, B., Urry, F.M., and Roberts, W.L. (2002). Analysis of Dicarboxylic Acids by Tandem Mass Spectrometry. High-Throughput Quantitative Measurement of Methylmalonic Acid in Serum , Plasma , and Urine. *Endocrinol. Metab.* *47*: 1993–2002.
- Langley, J.N. (1901). Observations on the physiological action of extracts of the supra-renal bodies. *J. Physiol.* *27*: 237–56.

- Langmead, C.J., and Christopoulos, A. (2006). Allosteric agonists of 7TM receptors: expanding the pharmacological toolbox. *Trends Pharmacol. Sci.* *27*: 475–81.
- Laschet, C. (2014). Mesure temporelle et spatiale de l' activation de la voie des MAP kinases au moyen d' un biosenseur FRET. Mémoire Master En Sci. Biomédicales.
- Lau, W. de, Barker, N., Low, T.Y., Koo, B.-K., Li, V.S.W., Teunissen, H., et al. (2011). Lgr5 homologues associate with Wnt receptors and mediate R-spondin signalling. *Nature* *476*: 293–7.
- Laurenza, A., Sutkowski, E.M., and Seamon, K.B. (1989). Forskolin: a specific stimulator of adenylyl cyclase or a diterpene with multiple sites of action? *Trends Pharmacol. Sci.* *10*: 442–7.
- Lazareno, S., Popham, A., and Birdsall, N.J. (2000). Allosteric interactions of staurosporine and other indolocarbazoles with N-[methyl-(3)H]scopolamine and acetylcholine at muscarinic receptor subtypes: identification of a second allosteric site. *Mol. Pharmacol.* *58*: 194–207.
- Lazo, J.S., Brady, L.S., and Dingledine, R. (2007). Building a pharmacological lexicon: small molecule discovery in academia. *Mol. Pharmacol.* *72*: 1–7.
- Lefkimmiatis, K., and Zaccolo, M. (2014). cAMP signaling in subcellular compartments. *Pharmacol. Ther.* *143*: 295–304.
- Lefkowitz, R.J., Rajagopal, K., and Whalen, E.J. (2006). New roles for beta-arrestins in cell signaling: not just for seven-transmembrane receptors. *Mol. Cell* *24*: 643–52.
- Lefkowitz, R.J., and Shenoy, S.K. (2005). Transduction of Receptor Signals by β -Arrestins. *Science* (80-.). *308*: 512–518.
- Li, T., Hu, J., Du, S., Chen, Y., Wang, S., and Wu, Q. (2014). ERK1 / 2 / COX-2 / PGE 2 signaling pathway mediates GPR91- dependent VEGF release in streptozotocin-induced diabetes. *Mol. Vis.* *20*: 1109–1121.
- Liggett, S.B., Freedman, N.J., Schwinn, D.A., and Lefkowitz, R.J. (1993). Structural basis for receptor subtype-specific regulation revealed by a chimeric beta 3/beta 2-adrenergic receptor. *Proc. Natl. Acad. Sci. U. S. A.* *90*: 3665–9.
- Limbird, L. (1996). Cell surface receptors: a short course on theory and methods (Massachusetts: Kluwer academic publishers).

Lin, F., Sepich, D.S., Chen, S., Topczewski, J., Yin, C., Solnica-Krezel, L., et al. (2005). Essential roles of Galpha12/13 signaling in distinct cell behaviors driving zebrafish convergence and extension gastrulation movements. *J. Cell Biol.* *169*: 777–87.

Lissandron, V., Terrin, A., Collini, M., D'alfonso, L., Chirico, G., Pantano, S., et al. (2005). Improvement of a FRET-based indicator for cAMP by linker design and stabilization of donor-acceptor interaction. *J. Mol. Biol.* *354*: 546–55.

Lohse, M.J., Benovic, J.L., Codina, J., Caron, M.G., and Lefkowitz, R.J. (1990). beta-Arrestin: a protein that regulates beta-adrenergic receptor function. *Science (80-.)*. *248*: 1547–50.

Luttrell, L.M., Ferguson, S.S., Daaka, Y., Miller, W.E., Maudsley, S., Rocca, G.J. Della, et al. (1999). Beta-arrestin-dependent formation of beta2 adrenergic receptor-Src protein kinase complexes. *Science (80-.)*. *283*: 655–661.

Luttrell, L.M., and Lefkowitz, R.J. (2002). The role of beta-arrestins in the termination and transduction of G-protein-coupled receptor signals. *J. Cell Sci.* *115*: 455–65.

Macaulay, I.C., Tijssen, M.R., Thijssen-Timmer, D.C., Gusnanto, A., Steward, M., Burns, P., et al. (2007). Comparative gene expression profiling of in vitro differentiated megakaryocytes and erythroblasts identifies novel activatory and inhibitory platelet membrane proteins. *Blood* *109*: 3260–3269.

Magalhaes, A.C., Dunn, H., and Ferguson, S.S.G. (2012). Regulation of GPCR activity, trafficking and localization by GPCR-interacting proteins. *Br. J. Pharmacol.* *165*: 1717–1736.

Malo, N., Hanley, J.A., Cerquozzi, S., Pelletier, J., and Nadon, R. (2006). Statistical practice in high-throughput screening data analysis. *Nat. Biotechnol.* *24*: 167–75.

Manglik, A., Kim, T.H., Masureel, M., Altenbach, C., Yang, Z., Hilger, D., et al. (2015). Structural Insights into the Dynamic Process of β 2-Adrenergic Receptor Signaling. *Cell* *161*: 1101–11.

Mangmool, S., and Kurose, H. (2011). Gi/o protein-dependent and -independent actions of pertussis toxin (ptx). *Toxins (Basel)*. *3*: 884–899.

McMurray, J.J.V. and, and Pfeffer, M.A. (2005). Heart failure. *Lancet* *365*: 1877–89.

McMurry, J.B., T. (2005). *Chimie organique des processus biologiques*.

- Millar, R.P., and Newton, C.L. (2010). The year in G protein-coupled receptor research. *Mol. Endocrinol.* *24*: 261–274.
- Miyano, K., Sudo, Y., Yokoyama, A., Hisaoka-Nakashima, K., Morioka, N., Takebayashi, M., et al. (2014). History of the G Protein–Coupled Receptor (GPCR) Assays From Traditional to a State-of-the-Art Biosensor Assay. *J. Pharmacol. Sci.* *126*: 302–309.
- Moers, A., Nieswandt, B., Massberg, S., Wettschureck, N., Grüner, S., Konrad, I., et al. (2003). G13 is an essential mediator of platelet activation in hemostasis and thrombosis. *Nat. Med.* *9*: 1418–22.
- Monteith, G.R., and Bird, G.S.J. (2005). Techniques: high-throughput measurement of intracellular Ca(2+) - - back to basics. *Trends Pharmacol. Sci.* *26*: 218–23.
- Morrison, D.K., and Davis, R.J. (2003). Regulation of MAP kinase signaling modules by scaffold proteins in mammals. *Annu. Rev. Cell Dev. Biol.* *19*: 91–118.
- Morton, D., Leach, S., Cordier, C., Warriner, S., and Nelson, A. (2009). Synthesis of natural-product-like molecules with over eighty distinct scaffolds. *Angew. Chem. Int. Ed. Engl.* *48*: 104–9.
- Mukherjee, S., Hanson, A.M., Shadrick, W.R., Ndjomou, J., Sweeney, L., Hernandez, J.J., et al. (2012). Identification and analysis of hepatitis C virus NS3 helicase inhibitors using nucleic acid binding assays. *Nucleic Acid Res.* 1–15.
- Nakata, H., Kameyama, K., Haga, K., and Haga, T. (1994). Location of agonist-dependent-phosphorylation sites in the third intracellular loop of muscarinic acetylcholine receptors (m2 subtype). *Eur. J. Biochem.* *220*: 29–36.
- Nakaya, M., Chikura, S., Watari, K., Mizuno, N., Mochinaga, K., Mangmool, S., et al. (2012). Induction of cardiac fibrosis by β -blocker in G protein-independent and G protein-coupled receptor kinase 5/ β -arrestin2-dependent Signaling pathways. *J. Biol. Chem.* *287*: 35669–77.
- Nikolaev, V.O., Bünemann, M., Hein, L., Hannawacker, A., and Lohse, M.J. (2004). Novel single chain cAMP sensors for receptor-induced signal propagation. *J. Biol. Chem.* *279*: 37215–8.
- Nikolaev, V.O., Bünemann, M., Schmittecker, E., Lohse, M.J., and Engelhardt, S. (2006). Cyclic AMP imaging in adult cardiac myocytes reveals far-reaching beta1-adrenergic but locally confined beta2-adrenergic receptor-mediated signaling. *Circ. Res.* *99*: 1084–91.

Nikolaev, V.O., Moshkov, A., Lyon, A.R., Miragoli, M., Novak, P., Paur, H., et al. (2010). Beta2-adrenergic receptor redistribution in heart failure changes cAMP compartmentation. *Science* 327: 1653–7.

NobelPrize.org (2012). 'The Nobel Prize in Chemistry 2012'.

O'Dowd, B.F., Nguyen, T., Jung, B.P., Marchese, a, Cheng, R., Heng, H.H., et al. (1997). Cloning and chromosomal mapping of four putative novel human G-protein-coupled receptor genes. *Gene* 187: 75–81.

Oakley, R.H., Hudson, C.C., Cruickshank, R.D., Meyers, D.M., Payne, R.E., Rhem, S.M., et al. (2002). The cellular distribution of fluorescently labeled arrestins provides a robust, sensitive, and universal assay for screening G protein-coupled receptors. *Assay Drug Dev. Technol.* 1: 21–30.

Oakley, R.H., Laporte, S. a., Holt, J. a., Caron, M.G., and Barak, L.S. (2000). Differential affinities of visual arrestin, β arrestin1, and β arrestin2 for G protein-coupled receptors delineate two major classes of receptors. *J. Biol. Chem.* 275: 17201–17210.

Offermanns, S. (2003). G-proteins as transducers in transmembrane signalling. *Prog. Biophys. Mol. Biol.* 83: 101–130.

Overington, J.P., Overington, J.P., Al-Lazikani, B., Al-Lazikani, B., Hopkins, A.L., and Hopkins, A.L. (2006). How many drug targets are there? *Nat. Rev. Drug Discov.* 5: 993–6.

Paing, M.M., Stutts, A.B., Kohout, T.A., Lefkowitz, R.J., and Trejo, J. (2002). Arrestins Regulate Protease-activated Receptor-1 Desensitization but Not Internalization or Down-regulation. *J. Biol. Chem.* 277: 1292–1300.

Palczewski, K. (2000). Crystal Structure of Rhodopsin: A G Protein-Coupled Receptor. *Science* (80-.). 289: 739–745.

Pantel, J., Williams, S.Y., Mi, D., Sebag, J., Corbin, J.D., Weaver, C.D., et al. (2011). Development of a high throughput screen for allosteric modulators of melanocortin-4 receptor signaling using a real time cAMP assay. *Eur. J. Pharmacol.* 660: 139–47.

Paramonov, V.M., Mamaeva, V., Sahlgren, C., and Rivero-Müller, A. (2015). Genetically-encoded tools for cAMP probing and modulation in living systems. *Front. Pharmacol.* 6: 196.

- Parnot, C., Miserey-Lenkei, S., Bardin, S., Corvol, P., and Clauser, E. (2002). Lessons from constitutively active mutants of G protein-coupled receptors. *Trends Endocrinol. Metab.* *13*: 336–43.
- Peti-Peterdi, J., Gevorgyan, H., Lam, L., and Riquier-Brison, A. (2012). Metabolic control of renin secretion. *Pflügers Arch. - Eur. J. Physiol.* 53–58.
- Pitcher, J.A., Freedman, N.J., and Lefkowitz, R.J. (1998). G protein-coupled receptor kinases. *Annu. Rev. Biochem.* *67*: 653–92.
- Pluznick, J.L., and Caplan, M.J. (2015). Chemical and Physical Sensors in the Regulation of Renal Function. *Clin. J. Am. Soc. Nephrol.* *10*: 1626–35.
- Poul, E. Le, Hisada, S., Mizuguchi, Y., Dupriez, V.J., Burgeon, E., and Detheux, M. (2002). Adaptation of aequorin functional assay to high throughput screening. *J. Biomol. Screen. Off. J. Soc. Biomol. Screen.* *7*: 57–65.
- Prasher, D., McCann, R.O., and Cormier, M.J. (1985). Cloning and expression of the cDNA coding for aequorin, a bioluminescent calcium-binding protein. *Biochem. Biophys. Res. Commun.* *126*: 1259–68.
- Prasher, D.C., Eckenrode, V.K., Ward, W.W., Prendergast, F.G., and Cormier, M.J. (1992). Primary structure of the *Aequorea victoria* green-fluorescent protein. *Gene* *111*: 229–33.
- Qi, M., and Elion, E.A. (2005). MAP kinase pathways. *J. Cell Sci.* *118*: 3569–72.
- Rajagopal, K., Lefkowitz, R.J., and Rockman, H. a. (2005). When 7 transmembrane receptors are not G protein-coupled receptors. *J. Clin. Invest.* *115*: 2971–2974.
- Rajagopal, S., Kim, J., Ahn, S., Craig, S., Lam, C.M., Gerard, N.P., et al. (2010a). Beta-arrestin- but not G protein-mediated signaling by the 'decoy' receptor CXCR7. *Proc. Natl. Acad. Sci. U. S. A.* *107*: 628–32.
- Rajagopal, S., Rajagopal, K., and Lefkowitz, R.J. (2010b). Teaching old receptors new tricks: biasing seven-transmembrane receptors. *Nat. Rev. Drug Discov.* *9*: 373–86.
- Rasmussen, S.G.F., Choi, H.-J., Fung, J.J., Pardon, E., Casarosa, P., Chae, P.S., et al. (2011). Structure of a nanobody-stabilized active state of the $\beta(2)$ adrenoceptor. *Nature* *469*: 175–180.
- Regard, J.B., Sato, I.T., and Coughlin, S.R. (2008). Anatomical Profiling of G Protein-Coupled Receptor Expression. *Cell* *135*: 561–571.

- Reinscheid, R.K., Kim, J., Zeng, J., and Civelli, O. (2003). High-throughput real-time monitoring of Gs-coupled receptor activation in intact cells using cyclic nucleotide-gated channels. *Eur. J. Pharmacol.* *478*: 27–34.
- Ren, X.D. and Schwartz, M.A. (2000). Determination of GTP loading on Rho. *Methods Enzymol.* *325*: 264–72.
- Robben, J.H., Fenton, R. a, Vargas, S.L., Schweer, H., Peti-Peterdi, J., Deen, P.M.T., et al. (2009). Localization of the succinate receptor in the distal nephron and its signaling in polarized MDCK cells. *Kidney Int.* *76*: 1258–1267.
- Rubic, T., Lametschwandtner, G., Jost, S., Hinteregger, S., Kund, J., Carballido-Perrig, N., et al. (2008). Triggering the succinate receptor GPR91 on dendritic cells enhances immunity. *Nat. Immunol.* *9*: 1261–1269.
- Sadagopan, N., Li, W., Roberds, S.L., Major, T., Preston, G.M., Yu, Y., et al. (2007). Circulating Succinate is Elevated in Rodent Models of Hypertension and Metabolic Disease. *Am. J. Hypertens.* *20*: 1209–1215.
- Sapieha, P., Sirinyan, M., Hamel, D., Zaniolo, K., Joyal, J.-S., Cho, J.-H., et al. (2008). The succinate receptor GPR91 in neurons has a major role in retinal angiogenesis. *Nat. Med.* *14*: 1067–76.
- Sapieha, P., Zaniolo, K., Hamel, D., Joyal, J.-S., and Chemtob, S. (2009). Supply and demand: the influence of energy metabolism on angiogenesis. *Médecine Sci.* *25*: 346–8.
- Schena, M., Shalon, D., Davis, R.W., and Brown, P.O. (1995). Quantitative monitoring of gene expression patterns with a complementary DNA microarray. *Science (80-.)*. *270*: 467–70.
- Schreiber, S.L. (2009). Organic chemistry: Molecular diversity by design. *Nature* *457*: 153–4.
- Scott, M.G.H., Pierotti, V., Storez, H., Lindberg, E., Thuret, A., Muntaner, O., et al. (2006). Cooperative regulation of extracellular signal-regulated kinase activation and cell shape change by filamin A and beta-arrestins. *Mol. Cell. Biol.* *26*: 3432–45.
- Seamon, K.B., Padgett, W., and Daly, J.W. (1981). Forskolin: unique diterpene activator of adenylate cyclase in membranes and in intact cells. *Proc. Natl. Acad. Sci. U. S. A.* *78*: 3363–7.
- Shanahan, M.F., Morris, D.P., and Edwards, B.M. (1987). [³H]forskolin. Direct photoaffinity labeling of the erythrocyte D-glucose transporter. *J. Biol. Chem.* *262*: 5978–84.

Shenoy, S.K., Drake, M.T., Nelson, C.D., Houtz, D.A., Xiao, K., Madabushi, S., et al. (2006). beta-arrestin-dependent, G protein-independent ERK1/2 activation by the beta2 adrenergic receptor. *J. Biol. Chem.* *281*: 1261–73.

Shenoy, S.K., and Lefkowitz, R.J. (2003). Multifaceted roles of beta-arrestins in the regulation of seven-membrane-spanning receptor trafficking and signalling. *Biochem. J.* *375*: 503–515.

Shimomura, Johnson, F.H., and Saiga, Y. (1962). Extraction, purification and properties of aequorin, a bioluminescent protein from the luminous hydromedusa, *Aequorea*. *J. Cell. Comp. Physiol.* *59*: 223–39.

Shimomura, O. and Johnson, F.H. (1978). Peroxidized coelenterazine, the active group in the photoprotein aequorin. *Proc. Natl. Acad. Sci. U. S. A.* *75*: 2611–5.

Shimomura, O., and Johnson, F.H. (1969). Properties of the bioluminescent protein aequorin. *Biochemistry* *8*: 3991–7.

Shinde, R., Perkins, J., and Contag, C.H. (2006). Luciferin derivatives for enhanced in vitro and in vivo bioluminescence assays. *Biochemistry* *45*: 11103–12.

Siehler, S. (2007). G12/13-dependent signaling of G-protein-coupled receptors: disease context and impact on drug discovery. *Expert Opin. Drug Discov.* *2*: 1591–1604.

Smit, M.J., Vischer, H.F., Bakker, R.A., Jongejan, A., Timmerman, H., Pardo, L., et al. (2007). Pharmacogenomic and structural analysis of constitutive G protein-coupled receptor activity. *Annu. Rev. Pharmacol. Toxicol.* *47*: 53–87.

Smyth, E.M., Austin, S.C., Reilly, M.P., and FitzGerald, G.A. (2000). Internalization and Sequestration of the Human Prostacyclin Receptor. *J. Biol. Chem.* *275*: 32037–32045.

Southern, C., Cook, J.M., Neetoo-Isseljee, Z., Taylor, D.L., Kettleborough, C. a., Merritt, a., et al. (2013). Screening -Arrestin Recruitment for the Identification of Natural Ligands for Orphan G-Protein-Coupled Receptors. *J. Biomol. Screen.* *18*: 599–609.

Spath, B., Hansen, A., Bokemeyer, C., and Langer, F. (2012). platelet inhibition by acetylsalicylic acid and P2Y receptor antagonists. *Platelets* *23*: 60–68.

Strader, C.D., Fong, T.M., Graziano, M.P., and Tota, M.R. (1995). The family of G-protein-coupled receptors. *FASEB J* *9*: 745–54.

- Strynadka, N.C., and James, M.N. (1989). Crystal structures of the helix-loop-helix calcium-binding proteins. *Annu. Rev. Biochem.* *58*: 951–98.
- Sundström, L., Greasley, P.J., Engberg, S., Wallander, M., and Ryberg, E. (2013). Succinate receptor GPR91, a G α i coupled receptor that increases intracellular calcium concentrations through PLC β . *FEBS Lett.* *587*: 2399–2404.
- Sweis, R.F. (2015). Target (In)Validation: A Critical, Sometimes Unheralded, Role of Modern Medicinal Chemistry. *ACS Med. Chem. Lett.* *6*: 618–21.
- Takakura, H., Hattori, M., Takeuchi, M., and Ozawa, T. (2012). Visualization and quantitative analysis of G protein-coupled receptor- β -arrestin interaction in single cells and specific organs of living mice using split luciferase complementation. *ACS Chem. Biol.* *7*: 901–910.
- Thomas, P., and Smart, T.G. (2005). HEK293 cell line: A vehicle for the expression of recombinant proteins. *J. Pharmacol. Toxicol. Methods* *51*: 187–200.
- Thomsen, W., Frazer, J., and Unett, D. (2005). Functional assays for screening GPCR targets. *Curr. Opin. Biotechnol.* *16*: 655–65.
- Thorne, N., Inglese, J., and Auld, D.S. (2010). Illuminating Insights into Firefly Luciferase and Other Bioluminescent Reporters Used in Chemical Biology. *Chem. Biol.* *17*: 646–657.
- Titus, S., Neumann, S., Zheng, W., Southall, N., Michael, S., Klumpp, C., et al. (2008). Quantitative high-throughput screening using a live-cell cAMP assay identifies small-molecule agonists of the TSH receptor. *J. Biomol. Screen.* *13*: 120–7.
- Toma, I., Kang, J.J., Sipos, A., Vargas, S., Bansal, E., Hanner, F., et al. (2008). Succinate receptor GPR91 provides a direct link between high glucose levels and rennin release in murine and rabbit kidney. *J. Clin. Invest.* *118*: 2526–2534.
- Topiol, S., and Sabio, M. (2009). X-ray structure breakthroughs in the GPCR transmembrane region. *Biochem. Pharmacol.* *78*: 11–20.
- Toyooka, M., Tujii, T., and Takeda, S. (2009). The N-terminal domain of GPR61, an orphan G-protein-coupled receptor, is essential for its constitutive activity. *J. Neurosci. Res.* *87*: 1329–1333.

Trejo, J., and Coughlin, S.R. (1999). The cytoplasmic tails of protease-activated receptor-1 and substance P receptor specify sorting to lysosomes versus recycling. *J. Biol. Chem.* *274*: 2216–24.

Tsuji, F.I., Inouye, S., Goto, T., and Sakaki, Y. (1986). Site-specific mutagenesis of the calcium-binding photoprotein aequorin. *Proc. Natl. Acad. Sci. U. S. A.* *83*: 8107–11.

Ullman, E.F., Kirakossian, H., Singh, S., Wu, Z.P., Irvin, B.R., Pease, J.S., et al. (1994). Luminescent oxygen channeling immunoassay: measurement of particle binding kinetics by chemiluminescence. *Proc. Natl. Acad. Sci. U. S. A.* *91*: 5426–30.

Ungrin, M.D., Singh, L.M., Stocco, R., Sas, D.E., and Abramovitz, M. (1999). An automated aequorin luminescence-based functional calcium assay for G-protein-coupled receptors. *Anal. Biochem.* *272*: 34–42.

Vargas, S.L., Toma, I., Kang, J.J., Meer, E.J., and Peti-Peterdi, J. (2009). Activation of the succinate receptor GPR91 in macula densa cells causes renin release. *J. Am. Soc. Nephrol.* *20*: 1002–1011.

Visegrády, A., Boros, A., Némethy, Z., Kiss, B., and Keseru, G.M. (2007). Application of the BD ACTOne technology for the high-throughput screening of Gs-coupled receptor antagonists. *J. Biomol. Screen.* *12*: 1068–73.

Vögler, O., Bogatkewitsch, G.S., Wriske, C., Krummenerl, P., Jakobs, K.H., and Koppen, C.J. van (1998). Receptor subtype-specific regulation of muscarinic acetylcholine receptor sequestration by dynamin. Distinct sequestration of m2 receptors. *J. Biol. Chem.* *273*: 12155–60.

Wadzinski, B.E., Shanahan, M.F., and Ruoho, A.E. (1987). Derivatization of the human erythrocyte glucose transporter using a novel forskolin photoaffinity label. *J. Biol. Chem.* *262*: 17683–9.

Walker, J.K., Premont, R.T., Barak, L.S., Caron, M.G., and Shetzline, M.A. (1999). Properties of secretin receptor internalization differ from those of the beta(2)-adrenergic receptor. *J. Biol. Chem.* *274*: 31515–23.

Wang, Y., Kong, Y., Shei, G.J., Kang, L., and Cvijic, M.E. (2011). Development of a cyclic adenosine monophosphate assay for Gi-coupled G protein-coupled receptors by utilizing the endogenous calcitonin activity in Chinese hamster ovary cells. *Assay Drug Dev. Technol.* *9*: 522–31.

Wermuth, C.. (2008). *The practice of medicinal chemistry* (Illkirsh, France.: Academic Press).

- Wermuth, C.G. (2004). Selective optimization of side activities: another way for drug discovery. *J. Med. Chem.* *47*: 1303–14.
- Wettschureck, N., and Offermanns, S. (2005). Mammalian G Proteins and Their Cell Type Specific Functions. *Physiological Rev.* *85*: 1159–1204.
- Wigdal, S.S., Anderson, J.L., Vidugiris, G.J., Shultz, J., Wood, K. V, and Fan, F. (2008). A Novel Bioluminescent Protease Assay Using Engineered Firefly Luciferase. *Curr. Chem. Genomics* *2*: 16–28.
- Williams, C. (2004). cAMP detection methods in HTS: selecting the best from the rest. *Nat. Rev. Drug Discov.* *3*: 125–35.
- Willoughby, D., and Cooper, D.M.F. (2008). Live-cell imaging of cAMP dynamics. *Nat. Methods* *5*: 29–36.
- Wilson, S., Bergsma, D.J., Chambers, J.K., Muir, a I., Fantom, K.G., Ellis, C., et al. (1998). Orphan G-protein-coupled receptors: the next generation of drug targets? *Br. J. Pharmacol.* *125*: 1387–1392.
- Wittenberger, T., Hellebrand, S., Munck, A., Kreienkamp, H.-J., Schaller, H.C., and Hampe, W. (2002). GPR99, a new G protein-coupled receptor with homology to a new subgroup of nucleotide receptors. *BMC Genomics* *3*: 17.
- Wittenberger, T., Schaller, H.C., and Hellebrand, S. (2001). An expressed sequence tag (EST) data mining strategy succeeding in the discovery of new G-protein coupled receptors. *J. Mol. Biol.* *307*: 799–813.
- Wong, Y.H. (1994). Gi assays in transfected cells. *Methods Enzymol.* *238*: 81–94.
- Wu, B., Chien, E.Y.T., Mol, C.D., Fenalti, G., Liu, W., Katritch, V., et al. (2010). Structures of the CXCR4 chemokine GPCR with small-molecule and cyclic peptide antagonists. *Science* *330*: 1066–71.
- Xiao, K., Shenoy, S.K., Nobles, K., and Lefkowitz, R.J. (2004). Activation-dependent conformational changes in {beta}-arrestin 2. *J. Biol. Chem.* *279*: 55744–53.
- Zastrow, M. Von, and Kobilka, B.K. (1994). Antagonist-dependent and -independent steps in the mechanism of adrenergic receptor internalization. *J. Biol. Chem.* *269*: 18448–18452.
- Zhang, D., Gao, Z.-G., Zhang, K., Kiselev, E., Crane, S., Wang, J., et al. (2015a). Two disparate ligand-binding sites in the human P2Y1 receptor. *Nature*.

Zhang, G., Liu, Y., Ruoho, A.E., and Hurley, J.H. (1997). Structure of the adenylyl cyclase catalytic core. *Nature* *386*: 247–53.

Zhang, J., Chung, T.D.Y., and Oldenburg, K.R. (1999). A Simple Statistical Parameter for Use in Evaluation and Validation of High Throughput Screening Assays. *J. Compos. Mater.* *33*: 928–940.

Zhang, J., Ferguson, S.S., Barak, L.S., Bodduluri, S.R., Laporte, S.A., Law, P.Y., et al. (1998). Role for G protein-coupled receptor kinase in agonist-specific regulation of mu-opioid receptor responsiveness. *Proc. Natl. Acad. Sci. U. S. A.* *95*: 7157–62.

Zhang, J., Ferguson, S.S.G., Barak, L.S., Menard, L., and Caron, M.G. (1996). Dynamin and β -Arrestin Reveal Distinct Mechanisms for G Protein-coupled Receptor Internalization. *J. Biol. Chem.* *271*: 18302–18305.

Zhang, J., Zhang, K., Gao, Z.-G., Paoletta, S., Zhang, D., Han, G.W., et al. (2014). Agonist-bound structure of the human P2Y₁₂ receptor. *Nature* *509*: 119–22.

Zhang, M., Liu, X., Zhang, Y., and Zhao, J. (2010). Loss of betaarrestin1 and betaarrestin2 contributes to pulmonary hypoplasia and neonatal lethality in mice. *Dev. Biol.* *339*: 407–17.

Zhang, X., Stevens, R.C., and Xu, F. (2015b). The importance of ligands for G protein-coupled receptor stability. *Trends Biochem. Sci.* *40*: 79–87.

Cheminformatics: data mining. UNITY Locating in database that match a pharmacophore of fit a receptor site. <http://www.tripos.com/tripos_resources/fileroot/pdfs/Unity_111408.pdf>.

VII. APPENDIX

VII.1. Screening results

VII.1.1 Primary screening

Value = 100-(well value / μ_{c-})

Wells	-FSK		+FSK		Wells	-FSK		+FSK	
	pGlo	SUCNR1	pGlo	SUCNR1		pGlo	SUCNR1	pGlo	SUCNR1
P1A02	2,19	-3,07	4,89	-7,76	P1C02	27,22	33,54	2,87	46,88
P1A03	15,46	-4,59	8,74	18,21	P1C03	37,81	21,46	-8,79	39,28
P1A04	6,70	-1,42	4,06	-1,78	P1C04	0,87	6,57	-1,81	4,60
P1A05	11,11	1,84	5,56	8,35	P1C05	-74,85	30,64	5,75	89,01
P1A06	-6,43	-1,60	2,31	-1,08	P1C06	3,91	-4,31	1,44	-6,04
P1A07	7,56	-4,77	7,77	-0,53	P1C07	67,18	94,86	82,17	99,67
P1A08	4,87	0,14	10,01	3,92	P1C08	7,91	-2,02	0,65	8,52
P1A09	8,06	-2,98	13,00	-4,79	P1C09	23,62	57,69	13,38	86,43
P1A10	12,42	-2,29	17,30	-7,19	P1C10	10,85	-0,96	13,88	-0,87
P1A11	20,89	-1,19	26,78	-2,32	P1C11	12,47	-1,05	18,10	1,73
P1B02	64,66	38,08	19,76	47,12	P1D02	-0,86	-5,05	-2,89	14,70
P1B03	13,23	2,49	7,18	32,22	P1D03	1,12	-5,05	-1,21	14,56
P1B04	14,15	5,79	10,61	25,23	P1D04	14,04	4,87	3,63	19,63
P1B05	3,35	-1,51	-3,18	4,02	P1D05	6,09	-8,72	-2,03	-8,98
P1B06	4,42	-7,11	0,47	18,38	P1D06	2,59	-6,20	3,52	-4,69
P1B07	-0,45	75,02	-9,33	94,37	P1D07	0,51	67,93	-1,02	30,60
P1B08	6,39	1,25	5,42	19,25	P1D08	7,81	-4,40	12,28	0,07
P1B09	-546,69	-2,11	-19,75	-2,16	P1D09	12,32	-6,52	16,55	-1,85
P1B10	-76,88	3,08	-5,09	-0,67	P1D10	13,39	-4,45	14,83	-2,32
P1B11	10,80	-0,04	15,85	2,81	P1D11	87,37	79,15	92,05	97,37

P1E02	-0,40	-5,97	-4,12	13,82	P1G08	5,89	-9,82	12,43	-0,50
P1E03	9,18	-4,22	-1,26	15,71	P1G09	18,05	29,03	12,43	65,12
P1E04	1,32	-3,71	-2,21	17,46	P1G10	55,91	4,78	27,30	12,47
P1E05	5,48	-2,02	-2,91	4,77	P1G11	15,46	-7,16	17,68	2,67
P1E06	23,37	54,45	5,68	92,82	P1H02	15,57	-7,48	-5,22	16,82
P1E07	89,41	97,66	95,57	99,33	P1H03	4,21	-11,71	4,10	13,34
P1E08	2,95	-1,46	6,39	2,91	P1H04	42,83	-11,43	30,41	28,37
P1E09	18,30	19,71	12,14	6,56	P1H05	-7,70	-23,83	5,96	21,18
P1E10	13,89	0,56	18,17	1,09	P1H06	84,92	75,55	53,27	92,68
P1E11	15,57	0,01	18,09	7,00	P1H07	0,77	-9,36	10,66	22,33
P1F02	-0,60	-4,36	-2,47	-1,51	P1H08	5,89	-13,64	13,28	15,17
P1F03	1,83	-5,23	2,38	15,68	P1H09	5,28	-7,80	10,98	13,18
P1F04	-2636,78	-119,88	-52,27	-0,20	P1H10	7,61	-7,25	16,48	-0,40
P1F05	-156,75	-19,79	-4,03	17,36	P1H11	3,15	-7,66	12,76	2,74
P1F06	2,08	-6,65	6,67	3,79	P2A02	3,66	1,31	5,25	1,69
P1F07	6,39	-5,09	8,81	0,58	P2A03	-2,47	-1,68	9,75	-2,47
P1F08	7,46	-18,78	17,20	-15,83	P2A04	1,97	-2,13	10,15	-3,07
P1F09	10,70	-4,22	11,63	-1,62	P2A05	-19,41	-6,09	6,93	-7,37
P1F10	61,66	56,25	40,54	83,24	P2A06	-8,35	-3,84	9,31	-3,47
P1F11	12,98	-5,64	19,64	4,80	P2A07	-8,72	-6,38	8,01	-5,77
P1G02	1,93	-15,34	1,71	13,11	P2A08	-10,60	-10,58	-0,94	-12,97
P1G03	-0,70	-5,64	2,41	15,64	P2A09	3,66	1,23	16,54	-1,67
P1G04	15,16	-6,61	1,92	6,29	P2A10	-5,41	-5,07	9,02	-4,47
P1G05	4,06	-10,97	6,60	13,62	P2A11	-6,35	-3,35	10,39	-2,67
P1G06	92,04	90,35	83,84	97,76	P2B02	-6,16	-5,15	2,36	-7,77
P1G07	5,23	-9,32	7,18	16,79	P2B03	-4,16	-2,08	-0,82	-3,17

P2B04	0,47	-1,23	6,42	-0,27	P2D10	1,09	0,78	19,43	-1,67
P2B05	-97,25	-15,90	-54,14	-18,27	P2D11	-1,22	-1,51	16,13	-0,67
P2B06	45,50	53,09	-10,60	75,15	P2E02	-9,10	-4,25	2,47	-5,17
P2B07	-0,97	-4,66	-10,37	1,32	P2E03	-26,29	10,05	-107,29	63,33
P2B08	-0,47	-3,19	5,77	-5,07	P2E04	-234,10	-50,27	-47,55	-33,56
P2B09	54,14	37,47	14,28	49,07	P2E05	7,03	-1,10	2,96	-2,57
P2B10	-4,41	-2,78	18,92	-4,37	P2E06	-12,41	-0,57	-7,72	-1,67
P2B11	20,16	-2,37	20,21	6,52	P2E07	-0,53	-0,20	9,01	-0,27
P2C02	6,35	10,75	4,19	8,31	P2E08	11,78	22,80	5,44	27,04
P2C03	-2,66	-3,88	1,43	-3,47	P2E09	20,98	15,28	16,91	20,86
P2C04	6,47	7,52	4,83	3,68	P2E10	83,31	83,56	85,32	96,65
P2C05	51,00	67,62	66,18	95,43	P2E11	-6,47	-3,23	13,05	-1,77
P2C06	-1,66	0,53	-4,35	4,18	P2F02	-6,41	2,00	5,36	1,84
P2C07	52,28	57,17	-22,02	87,55	P2F03	5,53	-2,70	10,65	-7,77
P2C08	72,30	61,58	-21,96	87,21	P2F04	-12,04	-2,94	6,00	-5,27
P2C09	-0,22	-9,07	9,01	-13,27	P2F05	-7,91	-5,27	2,92	-5,57
P2C10	23,10	6,91	6,78	5,57	P2F06	-16,22	-11,44	-14,35	-11,07
P2C11	15,79	11,36	-18,72	13,17	P2F07	-7,35	-1,19	14,20	-0,47
P2D02	-6,91	2,08	-0,27	5,60	P2F08	-22,85	2,94	-5,81	15,89
P2D03	35,73	33,18	-27,03	40,09	P2F09	-0,91	-13,32	5,77	-16,07
P2D04	0,59	-2,29	4,87	-4,47	P2F10	-6,66	-1,47	19,01	-0,77
P2D05	-31,10	-27,42	24,79	-24,57	P2F11	93,25	90,93	69,55	97,94
P2D06	2,91	-3,39	10,23	-4,87	P2G02	-1,66	2,13	6,66	1,05
P2D07	11,53	33,39	9,27	38,01	P2G03	2,53	-1,59	5,28	-3,17
P2D08	-8,10	-1,39	6,46	-4,87	P2G04	24,23	8,54	18,88	9,48
P2D09	-35,42	-8,66	-14,84	-9,17	P2G05	53,94	31,18	8,93	44,54

P2G06	-12,22	-7,97	-43,60	-11,37	P3B02	40,65	-13,21	30,97	46,28
P2G07	97,35	97,74	97,96	99,25	P3B03	1,32	-2,49	4,50	16,83
P2G08	10,28	8,01	51,95	4,97	P3B04	82,12	75,18	94,04	85,21
P2G09	-7,47	-2,37	3,57	-3,47	P3B05	56,88	14,09	28,48	18,15
P2G10	-7,47	-1,92	9,84	-0,27	P3B06	6,75	1,87	0,86	-36,76
P2G11	38,15	22,19	98,42	39,93	P3B07	6,21	6,08	15,31	9,24
P2H02	-3,59	0,61	9,30	-3,97	P3B08	20,20	-3,06	15,32	5,51
P2H03	-6,91	0,16	-0,98	0,28	P3B09	-102,33	6,80	-18,91	-17,54
P2H04	33,85	22,68	13,83	24,38	P3B10	62,32	85,90	51,27	93,10
P2H05	57,36	47,28	32,46	79,56	P3B11	-214,70	1,94	8,37	2,62
P2H06	-10,91	-2,70	11,01	-2,17	P3C02	26,28	48,58	57,67	57,58
P2H07	-9,72	2,21	14,41	-0,37	P3C03	-6,33	-2,56	-0,77	13,78
P2H08	99,58	99,87	98,90	99,80	P3C04	99,24	99,26	99,85	99,96
P2H09	-6,22	-5,19	-15,45	-4,17	P3C05	-811,14	-46,59	-17,40	-43,30
P2H10	21,98	8,70	10,79	11,41	P3C06	47,66	42,78	77,20	90,38
P2H11	-1,16	-0,49	14,14	-1,07	P3C07	59,10	72,65	58,64	74,67
P3A02	36,45	27,24	9,58	-12,00	P3C08	56,33	54,97	35,51	62,98
P3A03	6,06	-1,35	2,19	3,85	P3C09	5,37	9,01	18,76	42,74
P3A04	11,56	-4,21	15,43	15,24	P3C10	67,84	82,93	97,93	99,72
P3A05	30,80	17,59	14,58	20,96	P3C11	31,89	12,16	40,86	46,32
P3A06	67,45	58,82	74,40	94,66	P3D02	0,10	-1,92	0,56	-6,65
P3A07	35,86	-0,99	16,76	3,89	P3D03	4,30	-1,71	1,29	28,23
P3A08	13,85	-5,14	16,03	14,53	P3D04	9,65	-2,49	0,48	-6,81
P3A09	40,90	8,30	26,10	15,05	P3D05	76,50	24,67	32,61	30,31
P3A10	58,53	89,29	84,62	93,99	P3D06	5,45	0,08	7,92	6,11
P3A11	85,56	60,41	83,91	86,65	P3D07	-3,19	-0,49	3,26	1,41

P3D08	-749,99	-0,92	-32,92	-18,87	P3G04	59,99	49,24	64,37	81,85
P3D09	74,24	60,19	63,82	66,40	P3G05	6,36	-19,43	-6,17	-10,64
P3D10	-7,47	1,15	5,77	27,76	P3G06	78,64	73,71	76,64	99,25
P3D11	12,17	0,58	17,25	0,82	P3G07	48,96	68,00	65,15	86,70
P3E02	10,57	37,68	-7,99	15,91	P3G08	4,38	3,44	-3,65	9,02
P3E03	89,76	87,50	98,52	99,98	P3G09	8,43	-0,28	13,38	25,19
P3E04	-1,59	-3,71	1,00	-3,83	P3G10	19,51	4,51	14,72	20,47
P3E05	-42,33	-7,92	-14,78	-39,55	P3G11	16,76	-3,14	19,56	15,22
P3E06	-340,59	1,65	-17,16	-37,00	P3H02	8,05	-3,28	6,59	0,55
P3E07	53,11	53,07	73,79	89,60	P3H03	-11,75	30,73	-5,84	42,05
P3E08	1,47	46,24	9,18	46,24	P3H04	9,57	1,51	11,90	13,08
P3E09	1,62	-0,06	7,37	18,86	P3H05	14,08	0,72	5,29	-0,49
P3E10	21,80	49,03	34,10	43,35	P3H06	77,39	49,08	81,51	92,76
P3E11	17,52	1,65	23,29	7,74	P3H07	63,07	36,73	86,26	96,34
P3F02	31,64	-0,42	12,48	24,13	P3H08	98,31	81,07	99,78	99,85
P3F03	-19,17	-3,28	-8,03	-0,96	P3H09	8,89	-8,21	13,11	58,64
P3F04	28,39	4,37	4,33	11,71	P3H10	97,08	58,25	86,91	80,24
P3F05	1,47	-1,85	0,71	0,88	P3H11	23,75	2,37	17,89	20,21
P3F06	88,54	99,69	99,83	99,87	P4A02	91,99	91,75	99,90	99,92
P3F07	-86,97	51,78	54,76	72,57	P4A03	12,25	-3,33	29,52	31,29
P3F08	-67,70	5,58	-15,06	-16,80	P4A04	-6,51	-1,85	29,80	10,70
P3F09	61,36	60,55	62,89	86,99	P4A05	-10,91	-3,33	13,48	12,18
P3F10	3,69	6,30	4,21	17,17	P4A06	32,80	39,08	30,64	46,11
P3F11	46,16	18,38	30,38	25,13	P4A07	16,44	9,78	-11,86	36,73
P3G02	-17,03	-2,49	0,55	1,77	P4A08	-8,42	-4,65	-15,75	14,14
P3G03	5,29	3,80	1,21	23,32	P4A09	-9,89	-2,92	36,13	53,70

P4A10	56,17	59,58	59,01	69,86	P4D06	11,44	4,83	-3,80	-1,24
P4A11	-9,44	3,76	-32,29	28,80	P4D07	11,36	19,81	15,19	37,26
P4B02	54,54	62,49	34,24	94,88	P4D08	-6,31	-2,42	8,38	20,78
P4B03	-10,05	-5,89	28,04	0,47	P4D09	-27,19	-13,14	9,44	24,90
P4B04	7,16	12,83	30,06	10,65	P4D10	-7,37	0,88	11,11	23,45
P4B05	-9,85	-0,11	11,17	6,18	P4D11	-4,97	6,24	13,90	9,46
P4B06	64,35	65,00	89,32	85,09	P4E02	-4,11	2,20	10,72	-2,49
P4B07	5,78	4,83	9,12	11,23	P4E03	-1,99	3,35	39,28	12,56
P4B08	-13,23	1,04	5,55	19,50	P4E04	-17,09	-7,12	44,04	3,62
P4B09	-12,25	-5,80	21,90	24,83	P4E05	25,72	33,89	16,92	20,50
P4B10	-6,96	4,17	12,81	23,94	P4E06	-3,99	-5,47	11,40	9,14
P4B11	0,37	21,53	26,17	45,94	P4E07	-18,23	-8,03	9,47	10,12
P4C02	-9,12	25,15	-9,84	12,75	P4E08	-0,81	-1,43	18,56	57,03
P4C03	-1,59	3,52	20,46	-15,54	P4E09	37,85	12,09	0,44	65,22
P4C04	-12,05	-3,00	28,58	3,54	P4E10	-9,65	-4,32	11,40	20,85
P4C05	-15,14	23,25	-4,51	17,04	P4E11	89,12	92,24	99,86	99,83
P4C06	-11,36	4,50	8,31	12,73	P4F02	13,31	16,46	-13,15	6,07
P4C07	-9,36	-1,19	13,36	19,70	P4F03	7,61	2,36	42,11	17,21
P4C08	-9,73	6,57	8,25	16,20	P4F04	-8,55	5,33	43,94	3,10
P4C09	-7,81	-7,12	8,02	17,56	P4F05	-39,32	-11,16	-15,97	-85,13
P4C10	90,72	94,86	99,18	99,06	P4F06	-14,16	-3,58	-1,16	3,78
P4C11	-10,22	1,95	9,60	0,88	P4F07	-23,00	-8,20	8,89	8,21
P4D02	-3,17	-4,32	11,17	10,85	P4F08	-12,58	-6,63	10,91	13,20
P4D03	12,09	55,58	56,47	41,04	P4F09	-18,40	-6,71	8,22	15,26
P4D04	10,38	21,98	42,85	0,07	P4F10	22,18	32,09	67,92	60,78
P4D05	-16,00	-2,09	13,20	8,63	P4F11	19,09	21,95	10,30	15,29

P4G02	-2,36	4,92	41,31	58,69	P5A08	3,89	3,39	10,66	14,78
P4G03	-10,70	6,07	19,91	4,39	P5A09	7,83	2,00	1,01	8,79
P4G04	16,48	28,72	15,03	26,68	P5A10	18,98	10,16	16,04	43,39
P4G05	-12,41	3,93	14,64	0,66	P5A11	4,86	1,91	1,49	7,29
P4G06	-15,95	-6,38	7,54	16,37	P5B02	12,40	7,26	-7,93	-25,88
P4G07	24,01	23,64	20,10	8,17	P5B03	57,55	67,58	82,30	75,57
P4G08	37,61	44,15	1,15	53,18	P5B04	0,77	-5,93	10,16	19,77
P4G09	-7,20	3,10	-0,71	-17,45	P5B05	2,43	-7,32	-1,01	8,45
P4G10	-10,13	-2,09	-33,77	7,25	P5B06	39,33	44,87	52,02	59,93
P4G11	-18,68	-5,47	10,59	5,23	P5B07	-2,35	2,10	4,64	5,12
P4H02	-8,22	5,99	13,61	5,91	P5B08	0,01	-4,18	9,58	5,79
P4H03	18,84	19,54	32,21	26,88	P5B09	-127,82	-71,63	-27,34	-90,94
P4H04	1,55	4,34	27,75	18,41	P5B10	5,55	8,47	-1,82	29,35
P4H05	26,94	32,60	20,42	59,46	P5B11	-4,01	0,80	4,16	10,27
P4H06	-0,08	11,27	36,58	96,88	P5C02	-2,83	8,05	-22,68	-181,52
P4H07	-11,56	-8,36	11,20	6,35	P5C03	0,08	-5,84	10,36	-5,17
P4H08	-9,52	3,02	31,54	35,98	P5C04	1,95	-3,53	0,37	-4,90
P4H09	-12,33	5,74	15,35	52,81	P5C05	0,56	-2,61	6,80	-2,72
P4H10	-18,27	-6,05	13,58	15,69	P5C06	-5,53	4,86	-33,34	-162,10
P4H11	-12,45	8,96	9,73	20,84	P5C07	56,78	65,53	90,23	99,08
P5A02	14,62	11,90	-4,41	-31,29	P5C08	67,00	71,44	83,58	94,12
P5A03	0,91	-0,21	23,39	-0,47	P5C09	-3,45	36,79	6,71	48,12
P5A04	-65,71	-21,99	-35,50	-152,14	P5C10	-6,50	0,71	5,35	27,21
P5A05	-238,13	-215,95	1,91	-112,48	P5C11	4,79	-2,06	8,13	18,43
P5A06	77,77	78,14	8,62	-3,71	P5D02	81,38	84,27	-9,74	23,93
P5A07	-2,21	-0,40	-2,64	13,46	P5D03	-6,15	25,49	5,58	7,38

P5D04	-0,55	-1,04	1,52	-15,64	P5F10	-15,09	3,66	5,56	25,08
P5D05	0,91	-1,96	5,95	-9,25	P5F11	78,95	81,28	92,90	86,06
P5D06	-15,16	-13,68	-10,57	-18,87	P5G02	5,62	-1,78	16,22	-106,77
P5D07	-2,83	-6,21	8,09	-4,77	P5G03	4,30	13,58	1,98	-12,62
P5D08	26,88	22,08	42,28	47,71	P5G04	-7,26	-2,61	19,99	-6,96
P5D09	25,98	27,83	18,15	23,92	P5G05	-8,79	-6,67	-22,66	-163,40
P5D10	-48,67	-15,99	-43,61	-152,14	P5G06	-4,70	-3,63	8,34	4,14
P5D11	-1,79	2,65	-10,13	-31,36	P5G07	8,32	2,47	4,53	-22,09
P5E02	55,05	59,90	10,82	95,68	P5G08	-10,79	-1,96	7,51	4,06
P5E03	0,63	-3,35	23,85	10,91	P5G09	-9,13	-4,18	8,02	-7,87
P5E04	-0,20	-3,53	0,71	-29,89	P5G10	-11,14	-5,93	0,80	4,38
P5E05	4,09	2,00	2,55	-17,03	P5G11	-29,84	-12,58	-33,11	-84,09
P5E06	-17,44	-10,27	-24,29	-66,14	P5H02	5,13	1,73	6,18	-59,49
P5E07	-4,15	-4,55	6,69	3,96	P5H03	25,28	28,67	35,34	-43,06
P5E08	66,75	72,68	92,90	98,95	P5H04	-57,53	-35,83	40,46	1,90
P5E09	-4,01	-0,03	6,59	8,67	P5H05	-2,90	-7,50	32,47	8,31
P5E10	19,54	30,44	21,97	13,49	P5H06	-4,15	-2,61	18,34	8,23
P5E11	17,46	34,84	24,03	43,79	P5H07	52,23	-3,90	17,62	92,84
P5F02	2,36	3,94	4,92	-19,40	P5H08	13,23	21,01	29,20	39,86
P5F03	-9,48	-4,18	-5,58	7,17	P5H09	-12,46	-8,24	10,20	6,98
P5F04	80,74	85,90	96,72	99,57	P5H10	-0,20	4,86	28,52	51,56
P5F05	-2,07	-2,52	8,13	-6,05	P5H11	-0,68	2,37	11,01	12,51
P5F06	-6,02	-5,56	3,52	-3,09	P6A02	63,43	70,35	55,69	20,77
P5F07	4,23	2,00	8,96	0,73	P6A03	2,18	-1,46	-6,06	1,87
P5F08	-1,51	-3,16	6,27	3,11	P6A04	18,96	33,62	-3,09	0,46
P5F09	11,23	14,06	15,42	0,78	P6A05	6,48	3,76	-1,52	7,40

P6A06	0,78	10,12	8,98	-1,60	P6D02	-1,96	-0,67	-7,73	-11,00
P6A07	32,89	36,97	15,18	39,47	P6D03	37,34	56,55	-15,49	-18,80
P6A08	2,39	8,64	18,95	14,54	P6D04	1,30	-1,72	-7,39	-7,84
P6A09	1,97	35,63	7,36	31,63	P6D05	47,03	47,86	-29,72	-19,05
P6A10	43,87	34,78	51,76	48,37	P6D06	20,62	19,76	21,98	14,08
P6A11	29,63	22,80	14,27	13,78	P6D07	6,01	3,07	1,04	3,88
P6B02	-0,93	3,33	-16,51	-15,03	P6D08	47,49	54,24	53,32	50,80
P6B03	59,72	44,24	63,00	59,17	P6D09	-1,08	-6,07	4,79	-1,80
P6B04	14,30	11,51	39,66	57,99	P6D10	16,68	10,38	40,46	39,92
P6B05	2,44	0,72	-5,10	4,43	P6D11	-9,83	-21,12	-33,62	-33,83
P6B06	13,16	3,94	-21,66	-8,74	P6E02	49,85	52,15	33,60	22,18
P6B07	51,08	57,69	31,52	68,94	P6E03	94,52	94,34	93,76	93,29
P6B08	0,89	-1,20	-2,13	-12,76	P6E04	79,37	84,95	91,34	85,84
P6B09	11,45	17,96	-23,49	-30,76	P6E05	-3,10	-3,11	-3,00	0,11
P6B10	3,22	0,37	9,91	16,09	P6E06	6,32	1,33	15,77	2,32
P6B11	8,14	3,07	-16,69	-17,59	P6E07	22,69	59,62	90,07	93,28
P6C02	-0,05	4,46	-10,68	-11,41	P6E08	-1,08	-1,46	24,17	7,65
P6C03	41,48	44,85	27,89	57,27	P6E09	20,15	29,28	23,85	41,23
P6C04	2,18	1,15	-10,21	-5,47	P6E10	5,08	-4,59	6,56	10,36
P6C05	12,49	8,03	-42,75	-70,28	P6E11	48,16	71,80	77,41	94,23
P6C06	8,19	11,25	12,71	3,88	P6F02	24,66	27,39	25,59	27,61
P6C07	41,90	31,02	5,82	1,36	P6F03	-0,46	-1,72	-4,04	-0,45
P6C08	74,44	77,24	95,97	93,71	P6F04	-32,25	-31,30	-10,69	-13,12
P6C09	-2,63	-6,94	7,37	6,09	P6F05	-0,36	-2,76	1,47	6,59
P6C10	4,87	-2,41	7,52	9,01	P6F06	3,11	-1,72	11,96	1,51
P6C11	99,64	32,05	49,90	54,22	P6F07	22,48	21,31	9,75	10,82

P6F08	79,15	81,75	92,41	91,46	P7A04	7,89	7,18	1,92	3,37
P6F09	-3,00	-3,20	3,74	11,47	P7A05	55,41	17,78	-11,31	19,49
P6F10	5,75	-3,02	11,01	7,90	P7A06	49,91	-3,66	70,37	44,98
P6F11	-5,22	-8,16	17,57	34,34	P7A07	50,56	57,85	79,17	79,15
P6G02	-2,27	0,98	1,94	-8,04	P7A08	-3239,61	-33,82	-142,78	1,15
P6G03	-3,36	28,93	7,61	39,12	P7A09	-396,90	-18,19	-79,50	-10,32
P6G04	94,67	95,83	99,58	98,85	P7A10	6,79	-8,96	-11,76	-5,00
P6G05	44,28	39,57	34,92	57,93	P7A11	-35,16	-1,87	-15,27	0,88
P6G06	-5,85	-6,85	-6,03	-10,10	P7B02	-5,05	2,97	-0,82	0,45
P6G07	2,85	4,55	0,16	-2,96	P7B03	-8,26	2,38	-4,74	0,03
P6G08	33,61	40,36	31,58	12,47	P7B04	-4,57	3,75	1,02	1,60
P6G09	-4,91	1,07	7,09	12,02	P7B05	98,78	87,65	98,69	97,57
P6G10	-0,10	2,55	8,69	4,88	P7B06	25,61	31,08	2,19	25,95
P6G11	-130,69	-70,37	-47,53	-116,07	P7B07	7,07	8,09	-4,02	4,66
P6H02	2,75	2,89	6,64	5,39	P7B08	-459,38	19,84	-29,63	14,41
P6H03	-0,36	-0,24	-22,09	-10,80	P7B09	-3156,12	-8,59	-111,95	-7,71
P6H04	18,54	16,64	-33,23	-90,44	P7B10	-1275,53	19,24	66,50	14,95
P6H05	19,32	3,33	-0,02	4,83	P7B11	-1176,30	3,29	-34,04	2,43
P6H06	89,77	94,55	99,70	99,23	P7C02	30,13	2,93	6,79	3,12
P6H07	2,65	2,63	8,95	3,78	P7C03	-3550,98	-1,92	-101,55	-2,91
P6H08	8,65	10,81	26,60	-1,80	P7C04	-816,34	26,46	46,89	33,14
P6H09	15,85	17,69	-34,42	-65,20	P7C05	-566,35	27,10	33,88	32,41
P6H10	-1,29	6,37	27,35	14,54	P7C06	93,01	86,23	95,99	91,07
P6H11	-1,13	3,68	11,16	14,49	P7C07	-34,82	5,35	-4,42	4,07
P7A02	82,66	46,98	83,12	66,63	P7C08	-29,55	20,66	24,92	45,61
P7A03	52,73	98,20	99,96	99,56	P7C09	49,19	88,57	99,36	97,86

P7C10	-18,60	21,85	51,61	47,05	P7F06	-69,65	8,04	-3,43	5,49
P7C11	92,42	96,99	99,73	99,42	P7F07	-7,78	6,58	-10,54	1,98
P7D02	-9,97	12,34	-5,59	6,72	P7F08	-8,81	2,24	-8,88	0,13
P7D03	-13,19	4,98	8,95	5,22	P7F09	-893,67	11,97	-12,97	8,16
P7D04	24,11	23,90	26,81	26,28	P7F10	-138,02	1,69	-7,84	0,01
P7D05	7,20	5,90	0,35	1,93	P7F11	-156,63	0,78	-6,90	1,00
P7D06	-11,41	6,58	0,89	8,36	P7G02	97,00	99,78	99,93	99,80
P7D07	-4,77	2,47	-1,86	1,15	P7G03	92,08	22,58	76,12	27,75
P7D08	38,09	36,47	72,52	41,37	P7G04	0,98	4,25	11,20	3,26
P7D09	36,19	61,34	90,89	85,64	P7G05	-3720,70	-8,09	-109,52	-8,12
P7D10	-36,80	36,47	45,18	36,85	P7G06	-94,56	14,17	-10,09	9,79
P7D11	95,79	79,82	95,72	86,32	P7G07	51,16	18,01	29,20	29,22
P7E02	3,71	5,44	-10,59	1,73	P7G08	58,34	44,47	46,26	43,94
P7E03	-3589,31	0,27	-64,10	-2,72	P7G09	63,89	12,84	4,85	7,29
P7E04	30,61	19,10	32,31	21,79	P7G10	-94,15	3,98	-7,44	2,38
P7E05	-5,05	24,45	-7,26	13,95	P7G11	-28,52	10,05	-6,00	6,96
P7E06	6,59	-49,50	-31,70	-8,31	P7H02	-264,76	65,01	99,11	90,32
P7E07	-40,70	3,52	-3,97	0,41	P7H03	33,41	80,13	97,71	90,47
P7E08	22,40	28,11	66,47	60,25	P7H04	9,26	9,41	-0,78	9,33
P7E09	-381,78	75,81	98,82	95,96	P7H05	44,43	41,18	42,79	52,20
P7E10	-1840,12	1,92	-20,45	0,86	P7H06	51,71	76,72	98,91	95,30
P7E11	78,13	75,95	98,06	91,25	P7H07	-203,64	4,20	3,45	3,46
P7F02	38,18	1,78	2,28	2,14	P7H08	82,17	77,02	92,23	90,00
P7F03	-79,02	6,22	5,93	3,30	P7H09	25,27	47,85	53,60	61,72
P7F04	36,94	17,50	24,65	19,40	P7H10	-2378,70	12,25	-28,86	13,39
P7F05	51,66	19,61	23,75	21,07	P7H11	72,11	49,22	87,76	84,12

P8A02	6,51	1,60	0,21	-1,26	P8C08	20,28	-18,50	13,34	-18,76
P8A03	46,79	-8,87	14,65	4,80	P8C09	-27,33	-3,97	-0,21	-0,05
P8A04	0,81	0,46	-1,71	-4,12	P8C10	-5,70	3,13	4,11	4,37
P8A05	14,56	-0,05	12,53	0,38	P8C11	-12,94	-0,60	5,65	2,46
P8A06	87,59	34,18	64,25	51,01	P8D02	-37,51	0,76	-11,33	-2,82
P8A07	5,83	3,83	-1,41	3,76	P8D03	-28,30	9,91	-2,38	3,68
P8A08	18,07	1,08	7,65	-3,77	P8D04	31,30	4,12	23,02	2,98
P8A09	-0,10	2,51	-26,42	-1,09	P8D05	39,51	4,45	27,67	6,88
P8A10	14,18	-4,88	8,60	-3,77	P8D06	-30,82	-4,22	33,97	-6,03
P8A11	0,37	16,68	40,86	25,93	P8D07	-15,49	-1,48	-0,99	-4,21
P8B02	-2,42	3,87	-4,78	-0,74	P8D08	99,14	95,81	99,84	99,14
P8B03	47,51	3,43	7,21	2,72	P8D09	11,81	11,52	5,90	10,69
P8B04	11,63	-1,26	5,00	9,83	P8D10	30,77	8,81	5,26	6,01
P8B05	80,43	69,97	94,06	88,71	P8D11	10,46	7,20	35,09	13,78
P8B06	91,59	99,73	94,60	99,86	P8E02	52,89	9,80	15,99	12,42
P8B07	0,41	1,38	3,14	4,89	P8E03	-6,40	2,70	2,86	11,64
P8B08	7,47	1,23	4,17	5,84	P8E04	-0,28	1,63	4,06	-5,07
P8B09	-13,48	1,01	5,65	0,21	P8E05	14,64	-1,40	15,04	-1,96
P8B10	-19,79	-5,21	2,30	-0,05	P8E06	74,65	18,99	45,57	31,69
P8B11	-12,24	-3,89	0,71	8,61	P8E07	45,35	8,41	4,81	2,90
P8C02	-4,01	0,83	-8,02	6,62	P8E08	-12,64	2,29	1,16	4,45
P8C03	-23,32	-2,76	3,78	8,61	P8E09	70,11	35,75	-5,79	46,75
P8C04	71,66	66,85	50,62	91,00	P8E10	-5,41	1,56	-0,26	-0,83
P8C05	30,65	28,72	15,46	15,89	P8E11	21,48	3,61	10,72	17,50
P8C06	55,08	2,51	41,06	4,63	P8F02	72,48	70,05	77,54	74,49
P8C07	-1240,96	-2,76	-30,60	-1,26	P8F03	13,89	4,01	4,03	11,56

P8F04	6,37	-0,97	5,84	6,53	P8H10	-6,88	-2,21	-2,24	2,98
P8F05	15,60	-3,24	10,86	-4,29	P8H11	-4410,01	-35,85	-36,60	-5,16
P8F06	89,83	67,54	93,92	85,99	P9A02	46,99	56,07	8,15	63,23
P8F07	16,54	-1,19	-4,17	-0,14	P9A03	-2,70	-2,22	0,03	0,04
P8F08	91,19	84,81	56,64	95,48	P9A04	-2,98	-0,56	23,15	-3,59
P8F09	-2,06	-0,89	1,77	12,08	P9A05	2,95	8,75	22,86	10,66
P8F10	79,35	33,85	94,69	75,62	P9A06	2,89	0,81	21,82	-2,55
P8F11	33,99	9,14	-8,69	12,51	P9A07	3,80	0,38	10,19	0,32
P8G02	-9,47	4,27	-2,72	11,30	P9A08	81,28	4,90	80,94	-0,23
P8G03	1,83	-1,66	5,45	8,96	P9A09	30,52	44,42	45,66	66,67
P8G04	97,52	84,31	99,85	97,32	P9A10	62,49	80,96	27,22	93,24
P8G05	-388,94	-5,29	-17,52	9,65	P9A11	59,97	75,21	27,42	78,83
P8G06	19,33	22,13	38,02	43,69	P9B02	1,09	2,13	23,41	-3,74
P8G07	-13,40	-1,59	-1,46	3,42	P9B03	-1,32	2,19	24,23	1,32
P8G08	-0,62	-1,33	-0,26	8,96	P9B04	-116,00	-84,19	22,08	-31,97
P8G09	-0,04	-0,89	-3,83	6,01	P9B05	3,53	9,69	2,04	8,00
P8G10	96,33	99,15	99,89	99,70	P9B06	14,16	13,45	23,26	18,71
P8G11	65,40	7,56	5,59	19,59	P9B07	-1,21	-1,67	22,99	-2,85
P8H02	-11,36	9,83	3,58	21,58	P9B08	7,57	8,20	33,19	23,55
P8H03	3,60	-2,17	4,53	1,68	P9B09	46,02	72,28	46,12	94,70
P8H04	9,28	35,86	26,25	61,06	P9B10	9,53	19,35	8,21	20,44
P8H05	-2,97	1,85	-9,02	12,34	P9B11	80,16	93,00	32,86	99,08
P8H06	79,79	-29,59	38,02	-2,47	P9C02	34,34	60,59	23,89	69,05
P8H07	-5,53	0,24	2,50	16,21	P9C03	-8,71	-2,22	40,94	12,24
P8H08	-7,60	-2,28	3,55	-2,82	P9C04	-2,56	-0,09	12,55	-4,87
P8H09	-43,55	-4,04	-1,49	9,57	P9C05	-2,40	3,62	15,04	-0,84

P9C06	5,80	1,89	2,05	0,68	P9F02	5,71	19,64	25,25	14,59
P9C07	50,59	52,95	23,71	73,36	P9F03	25,78	57,09	25,47	58,53
P9C08	58,09	87,10	20,41	84,69	P9F04	32,87	66,11	20,66	88,50
P9C09	1,17	-0,38	1,64	19,56	P9F05	2,25	2,04	19,75	-0,20
P9C10	1,84	-2,63	18,19	-5,17	P9F06	75,45	91,81	24,12	98,30
P9C11	-16,85	-12,00	0,48	-10,02	P9F07	-2,81	37,88	25,84	50,08
P9D02	-89,54	-62,47	24,74	-17,19	P9F08	74,14	92,68	25,49	98,59
P9D03	-106,73	-80,28	24,09	-35,42	P9F09	10,12	7,61	26,16	13,73
P9D04	-58,45	-26,54	18,12	-14,96	P9F10	3,17	8,49	25,62	12,64
P9D05	17,26	20,20	21,58	37,98	P9F11	5,13	1,69	24,31	7,24
P9D06	8,15	17,07	24,44	49,81	P9G02	1,70	5,37	0,05	0,32
P9D07	1,67	5,02	23,97	-1,60	P9G03	12,22	21,77	9,27	31,91
P9D08	2,89	0,41	9,62	-3,07	P9G04	6,82	10,56	22,10	5,62
P9D09	4,36	1,98	8,29	1,29	P9G05	2,39	11,64	46,83	4,62
P9D10	0,57	-0,56	14,73	1,60	P9G06	-1,15	-4,64	26,14	-8,49
P9D11	66,17	92,85	2,49	99,36	P9G07	8,29	14,59	19,06	10,56
P9E02	94,86	98,43	26,21	99,59	P9G08	24,15	40,25	15,45	51,82
P9E03	-13,83	-7,04	42,39	-6,39	P9G09	70,02	76,82	23,81	89,22
P9E04	7,85	65,47	18,56	42,76	P9G10	26,37	29,57	24,92	52,86
P9E05	70,85	84,96	24,33	96,83	P9G11	21,52	27,06	23,71	45,36
P9E06	-3,48	-8,79	59,83	-10,69	P9H02	-109,03	-81,56	2,16	-33,99
P9E07	6,21	7,53	24,07	4,89	P9H03	-40,29	-13,55	2,01	-10,39
P9E08	6,38	5,25	17,65	7,51	P9H04	-4,44	-1,08	23,17	-3,71
P9E09	-1,90	1,78	3,67	0,20	P9H05	11,69	20,98	16,39	32,00
P9E10	1,20	-6,25	26,58	-4,56	P9H06	35,89	53,27	3,68	63,68
P9E11	1,17	-4,44	2,74	-3,68	P9H07	-1,68	-0,97	27,04	2,82

P9H08	38,91	54,79	5,83	83,31	P10C04	-0,60	-10,89	-0,74	-15,47
P9H09	52,66	59,75	15,25	68,23	P10C05	22,55	20,79	59,93	-0,29
P9H10	26,64	52,51	26,79	73,92	P10C06	6,15	-2,97	-4,43	-13,28
P9H11	23,54	62,99	10,23	56,33	P10C07	64,31	60,40	35,04	84,64
P10A02	-0,76	4,95	-6,76	-8,54	P10C08	3,32	4,95	-8,19	-10,15
P10A03	40,58	28,71	24,00	44,71	P10C09	79,46	92,08	49,80	98,84
P10A04	3,90	4,95	9,24	-14,89	P10C10	1,94	4,95	-5,48	-6,06
P10A05	64,83	68,32	97,27	93,66	P10C11	7,61	4,95	-3,94	-6,20
P10A06	6,23	4,95	-5,67	-10,58	P10D02	2,07	-2,97	-24,91	5,99
P10A07	75,41	84,16	86,19	99,31	P10D03	78,78	84,16	26,19	95,43
P10A08	84,50	84,16	64,70	92,67	P10D04	17,68	12,87	0,02	-7,52
P10A09	1,11	4,95	4,31	-17,88	P10D05	49,16	52,48	16,96	66,91
P10A10	57,61	60,40	9,66	88,76	P10D06	4,32	4,95	-5,41	-6,64
P10A11	42,83	44,55	50,40	44,71	P10D07	3,19	4,95	-9,59	-3,87
P10B02	74,81	68,32	31,20	76,71	P10D08	8,15	4,95	-10,49	-7,96
P10B03	19,31	12,87	3,29	16,35	P10D09	11,81	4,95	-3,37	12,19
P10B04	10,94	28,71	16,96	16,57	P10D10	8,44	4,95	-6,27	-10,00
P10B05	-73,38	-74,26	-32,37	-26,79	P10D11	29,84	36,63	52,74	55,43
P10B06	99,27	100,00	99,91	99,71	P10E02	22,72	20,79	-14,78	29,30
P10B07	9,23	12,87	11,05	5,99	P10E03	2,28	-2,97	0,20	10,51
P10B08	5,48	4,95	-17,95	-11,39	P10E04	46,45	44,55	35,87	54,38
P10B09	76,74	76,24	88,71	77,41	P10E05	-0,43	4,95	0,81	-3,72
P10B10	52,70	52,48	10,45	65,34	P10E06	-1,01	-18,81	-15,42	-7,66
P10B11	21,22	28,71	25,29	57,59	P10E07	43,79	44,55	45,09	44,52
P10C02	-13,38	-10,89	-23,97	-0,51	P10E08	7,48	12,87	0,32	-1,82
P10C03	17,35	12,87	-32,37	26,35	P10E09	9,11	4,95	-4,05	-5,69

P10E10	4,48	4,95	-4,77	-4,45	P10H06	-0,60	4,95	5,74	14,16
P10E11	7,11	4,95	-2,54	5,77	P10H07	-0,39	-2,97	-3,90	10,51
P10F02	6,48	-2,97	-21,19	9,42	P10H08	1,65	-2,97	-5,75	-4,23
P10F03	8,06	4,95	-8,53	8,91	P10H09	-8,84	4,95	19,60	26,93
P10F04	93,89	92,08	99,73	99,48	P10H10	6,82	4,95	0,02	-4,45
P10F05	92,72	92,08	95,63	99,34	P10H11	9,65	44,55	45,88	56,55
P10F06	3,98	-2,97	-1,41	9,56	P11A02	30,09	39,81	73,42	46,18
P10F07	30,76	20,79	-21,83	18,47	P11A03	-0,37	8,32	0,56	3,75
P10F08	4,98	4,95	-7,74	-4,16	P11A04	-8,05	29,61	-8,47	15,95
P10F09	10,98	4,95	-0,59	0,66	P11A05	35,70	7,92	-7,02	3,49
P10F10	65,25	68,32	55,60	64,56	P11A06	-8,73	-1,54	-11,44	-2,44
P10F11	5,61	4,95	3,97	13,36	P11A07	-0,84	0,65	1,63	-0,90
P10G02	-0,14	-2,97	-19,08	10,00	P11A08	-1,62	7,03	-45,37	6,50
P10G03	64,11	68,32	86,50	89,90	P11A09	-2,64	1,27	-5,76	2,62
P10G04	35,05	28,71	0,81	65,45	P11A10	68,49	75,58	94,27	93,21
P10G05	-3,26	4,95	2,09	11,09	P11A11	-6,53	-2,49	11,68	-1,31
P10G06	2,94	-2,97	5,93	1,68	P11B02	-0,77	2,12	-9,99	-1,96
P10G07	4,28	4,95	-0,10	15,77	P11B03	10,39	25,83	16,23	28,52
P10G08	11,98	4,95	0,62	-6,86	P11B04	0,34	30,85	-9,61	19,43
P10G09	9,27	12,87	6,98	7,01	P11B05	45,99	37,23	82,30	50,32
P10G10	5,36	-2,97	-7,29	12,41	P11B06	-30,69	-4,64	-69,12	5,73
P10G11	77,43	92,08	17,72	99,77	P11B07	2,47	0,90	-7,97	-2,84
P10H02	45,79	60,40	32,14	55,44	P11B08	-0,77	8,55	-13,15	10,79
P10H03	6,23	4,95	-21,83	10,58	P11B09	-2,26	1,17	-8,98	5,99
P10H04	-1,93	4,95	11,05	11,31	P11B10	55,81	68,29	-7,78	84,38
P10H05	-7,76	52,48	7,13	34,24	P11B11	3,69	3,72	-13,66	2,21

P11C02	18,41	24,39	-3,04	27,86	P11E08	99,66	6,19	100,00	17,86
P11C03	-2,03	1,83	-15,61	5,22	P11E09	1,05	99,56	-7,15	99,83
P11C04	-0,74	33,58	-18,58	20,49	P11E10	22,00	25,15	-12,45	35,37
P11C05	0,99	5,11	-12,20	1,44	P11E11	-2,70	1,00	-7,02	2,69
P11C06	35,40	43,04	8,20	60,21	P11F02	-1,86	2,87	-26,48	2,10
P11C07	-2,64	0,68	-7,34	0,27	P11F03	2,64	-1,79	-7,78	-12,81
P11C08	-1,55	6,74	-4,31	10,35	P11F04	0,44	2,03	-14,79	-11,01
P11C09	2,44	-1,56	-3,17	5,62	P11F05	-1,32	2,15	-17,82	-0,68
P11C10	3,15	3,86	-3,10	4,08	P11F06	52,42	49,69	73,79	62,70
P11C11	-3,72	5,00	-8,35	1,55	P11F07	-3,99	0,66	-29,64	1,48
P11D02	-0,74	2,18	-11,32	18,00	P11F08	80,75	6,07	81,19	2,58
P11D03	2,10	1,53	-9,68	7,67	P11F09	-0,03	83,59	-14,10	93,20
P11D04	6,06	3,72	-27,24	7,19	P11F10	-1,04	70,42	-9,61	94,62
P11D05	1,66	-0,05	11,17	-1,60	P11F11	15,87	21,81	-0,89	22,99
P11D06	2,37	4,45	7,64	2,80	P11G02	-4,77	3,88	-19,85	18,99
P11D07	35,84	27,74	81,29	43,54	P11G03	-1,82	0,96	-2,22	17,42
P11D08	4,78	8,63	-117,64	9,25	P11G04	1,97	34,48	-6,01	24,38
P11D09	0,44	5,77	-13,59	15,69	P11G05	1,70	5,73	-33,11	6,21
P11D10	-0,20	6,02	-15,55	6,65	P11G06	-0,71	1,81	-15,68	4,23
P11D11	-51,06	8,10	-44,36	16,79	P11G07	98,50	97,62	100,00	98,25
P11E02	-1,72	3,27	-15,36	-1,01	P11G08	55,06	3,49	54,44	10,53
P11E03	34,18	34,06	27,60	40,54	P11G09	28,56	77,47	-4,37	95,17
P11E04	37,09	52,07	65,28	38,19	P11G10	59,19	71,18	55,57	81,34
P11E05	97,62	98,86	90,42	99,75	P11G11	69,95	77,12	85,20	95,83
P11E06	74,02	70,54	97,05	81,08	P11H02	4,78	10,65	-17,51	8,81
P11E07	-0,77	-3,70	-21,93	-2,51	P11H03	3,56	35,68	-18,14	27,31

P11H04	24,23	17,01	-41,77	16,43	P12B10	36,80	38,74	-7,78	27,82
P11H05	31,95	22,18	51,73	29,65	P12B11	15,33	53,00	-13,66	3,88
P11H06	0,68	32,78	-17,26	33,39	P12C02	11,40	7,66	-3,04	-0,27
P11H07	30,93	2,88	-31,34	11,01	P12C03	-0,09	-7,38	-15,61	-23,02
P11H08	82,90	5,65	95,84	5,22	P12C04	6,25	0,35	-18,58	21,11
P11H09	-0,47	90,80	-5,13	98,56	P12C05	5,43	-4,58	-12,20	6,83
P11H10	43,96	56,90	58,57	75,51	P12C06	7,48	-2,62	8,20	18,72
P11H11	4,57	5,40	5,17	7,60	P12C07	18,90	48,79	-7,34	7,08
P12A02	74,74	76,13	73,42	78,53	P12C08	0,44	-10,95	-4,31	14,99
P12A03	4,60	4,43	0,56	7,19	P12C09	3,02	-14,69	-3,17	5,37
P12A04	4,70	0,86	-8,47	17,03	P12C10	8,20	1,37	-3,10	9,55
P12A05	7,48	7,49	-7,02	6,83	P12C11	0,51	-1,01	-8,35	10,37
P12A06	18,47	99,67	-11,44	9,32	P12D02	15,90	-2,54	-11,32	-1,74
P12A07	-2,13	-5,09	1,63	8,27	P12D03	10,45	2,05	-9,68	-6,74
P12A08	0,44	-8,99	-45,37	2,89	P12D04	1,27	-2,54	-27,24	1,05
P12A09	-1,34	0,18	-5,76	6,58	P12D05	2,89	-8,57	11,17	22,00
P12A10	-0,15	0,01	94,27	72,01	P12D06	94,64	97,02	7,64	27,72
P12A11	2,59	20,88	11,68	22,99	P12D07	5,82	-8,14	81,29	68,41
P12B02	58,20	55,58	-9,99	-1,07	P12D08	1,80	-1,52	-117,64	-22,55
P12B03	84,57	91,10	16,23	20,51	P12D09	2,29	6,30	-13,59	-0,59
P12B04	26,33	75,08	-9,61	20,08	P12D10	30,03	42,07	-15,55	3,71
P12B05	9,19	3,92	82,30	29,96	P12D11	-14,38	-7,55	-44,36	-21,18
P12B06	43,24	65,20	-69,12	-40,10	P12E02	65,16	71,36	-15,36	-6,59
P12B07	4,14	7,06	-7,97	6,27	P12E03	19,46	12,33	27,60	15,88
P12B08	20,91	27,51	-13,15	4,92	P12E04	47,50	64,52	65,28	18,89
P12B09	71,65	83,01	-8,98	-0,67	P12E05	1,43	0,01	90,42	88,58

P12E06	2,92	-3,73	97,05	98,38	P12H02	-2,86	1,37	-17,51	6,24
P12E07	64,87	66,72	-21,93	5,25	P12H03	0,84	-7,30	-18,14	17,45
P12E08	19,23	24,71	100,00	99,68	P12H04	14,01	3,92	-41,77	2,31
P12E09	12,16	3,41	-7,15	-0,32	P12H05	8,07	5,36	51,73	4,05
P12E10	16,06	16,34	-12,45	7,98	P12H06	-3,19	5,45	-17,26	16,16
P12E11	85,57	78,48	-7,02	3,61	P12H07	-2,89	-8,82	-31,34	14,14
P12F02	25,37	9,87	-26,48	-7,68	P12H08	44,23	58,57	95,84	87,95
P12F03	1,07	-20,38	-7,78	-6,14	P12H09	5,92	-1,43	-5,13	6,26
P12F04	0,90	-8,14	-14,79	-4,00	P12H10	-2,43	-10,44	58,57	70,70
P12F05	43,93	64,39	-17,82	-1,22	P12H11	-7,38	-8,82	5,17	10,36
P12F06	97,54	99,29	73,79	86,00	P13A02	21,19	26,29	25,44	27,94
P12F07	-1,74	-5,77	-29,64	-3,92	P13A03	-1,93	2,96	-2,50	-0,05
P12F08	-7,25	-18,93	81,19	97,05	P13A04	72,59	80,58	35,02	92,37
P12F09	-2,56	-16,05	-14,10	-4,00	P13A05	0,62	-0,49	0,24	1,02
P12F10	-3,85	-11,88	-9,61	8,83	P13A06	33,88	53,20	8,07	43,11
P12F11	-8,08	1,54	-0,89	9,40	P13A07	-1,67	2,58	-0,89	-0,35
P12G02	71,24	71,99	-19,85	-7,33	P13A08	0,65	-4,45	0,32	-7,10
P12G03	28,58	26,34	-2,22	-6,29	P13A09	-104,88	-46,61	7,92	-17,21
P12G04	-8,08	-6,11	-6,01	21,98	P13A10	41,90	64,03	27,74	69,32
P12G05	30,69	30,45	-33,11	0,50	P13A11	-21,60	-27,00	27,08	-30,55
P12G06	22,07	23,03	-15,68	-4,57	P13B02	11,83	8,85	-2,94	6,76
P12G07	53,97	58,76	100,00	99,76	P13B03	4,04	4,60	-2,76	4,98
P12G08	26,20	15,68	54,44	48,79	P13B04	32,30	29,97	52,97	31,19
P12G09	99,75	99,60	-4,37	6,73	P13B05	11,42	21,56	17,10	17,82
P12G10	-2,33	-4,24	55,57	33,55	P13B06	3,30	2,66	2,77	4,12
P12G11	-4,74	-1,69	85,20	0,69	P13B07	-52,82	-6,03	-24,26	2,31

P13B08	88,98	91,45	98,99	95,90	P13E04	-1,90	35,80	-0,96	19,78
P13B09	4,95	4,05	32,86	6,30	P13E05	19,95	43,78	26,86	44,34
P13B10	44,89	53,96	34,36	54,79	P13E06	0,35	19,26	10,66	7,31
P13B11	1,59	-5,52	0,90	-3,67	P13E07	14,18	21,50	18,82	19,57
P13C02	0,21	44,02	2,44	34,71	P13E08	22,97	18,53	45,66	30,79
P13C03	-2,50	2,26	-8,72	-6,91	P13E09	0,52	16,92	45,18	2,43
P13C04	72,58	72,84	55,06	87,96	P13E10	10,62	16,53	7,30	16,26
P13C05	6,46	9,05	-7,66	7,12	P13E11	13,81	39,47	19,48	26,28
P13C06	11,16	7,77	15,31	7,40	P13F02	-4,65	3,62	-16,98	7,03
P13C07	-1,03	29,62	4,56	15,58	P13F03	79,31	79,66	91,89	93,36
P13C08	7,03	-0,06	22,29	2,83	P13F04	-2,77	15,87	-4,33	7,71
P13C09	8,50	6,31	35,86	8,14	P13F05	2,26	5,35	2,55	3,29
P13C10	5,35	0,81	2,51	1,02	P13F06	-4,55	0,16	6,93	-0,57
P13C11	-0,16	-1,22	2,69	-2,99	P13F07	22,10	11,26	79,85	6,85
P13D02	0,35	4,56	-4,00	20,37	P13F08	74,33	74,44	98,40	90,99
P13D03	12,30	28,91	2,84	50,31	P13F09	96,17	96,65	99,89	99,38
P13D04	17,67	19,40	13,37	17,39	P13F10	42,74	44,84	65,47	61,01
P13D05	14,48	27,95	9,71	27,26	P13F11	2,19	1,27	-2,46	1,09
P13D06	2,53	40,06	5,54	31,31	P13G02	-0,32	4,87	-1,15	10,25
P13D07	-4,35	18,75	11,40	10,40	P13G03	-1,33	4,52	-8,97	19,88
P13D08	-46,14	-74,91	41,56	-67,88	P13G04	1,39	23,83	9,06	17,30
P13D09	10,79	6,22	60,76	-2,07	P13G05	57,57	80,14	96,45	96,29
P13D10	83,21	89,24	76,58	97,29	P13G06	66,37	67,91	98,31	78,19
P13D11	41,46	51,07	76,58	81,54	P13G07	66,40	64,06	89,46	78,22
P13E02	-12,27	4,63	-1,11	0,53	P13G08	-0,59	18,13	24,01	12,21
P13E03	-10,93	-18,15	-6,38	-21,17	P13G09	32,57	25,55	94,61	19,97

P13G10	6,89	7,46	11,43	9,21	P14B06	-1,14	-9,11	8,70	3,53
P13G11	0,68	0,90	-1,88	-0,23	P14B07	3,94	11,92	12,65	8,28
P13H02	64,86	61,35	69,40	79,44	P14B08	22,51	-8,88	16,20	7,66
P13H03	19,08	12,84	29,24	8,20	P14B09	89,98	-5,47	82,50	58,41
P13H04	38,28	46,77	30,96	24,99	P14B10	6,97	-1,91	21,66	11,84
P13H05	20,32	50,76	52,83	47,65	P14B11	-7,94	-9,32	4,31	3,78
P13H06	0,05	0,53	7,52	0,66	P14C02	0,44	-49,36	33,26	22,75
P13H07	-0,12	19,18	32,53	10,77	P14C03	41,69	40,09	80,79	82,97
P13H08	7,93	12,13	13,37	6,91	P14C04	0,95	-17,37	1,97	-4,74
P13H09	3,34	4,84	27,89	5,22	P14C05	45,83	76,15	39,94	44,99
P13H10	-4,25	0,74	6,28	-2,78	P14C06	88,36	99,74	99,65	99,03
P13H11	35,42	16,12	25,22	23,74	P14C07	5,25	11,35	5,69	7,49
P14A02	-11,60	-96,06	-7,64	-12,68	P14C08	28,44	50,79	21,18	15,57
P14A03	50,88	74,15	96,89	97,98	P14C09	27,12	66,98	50,55	39,32
P14A04	47,65	42,51	72,78	45,20	P14C10	43,95	13,63	94,61	34,42
P14A05	80,33	100,00	98,21	98,68	P14C11	16,42	24,52	-1,71	-32,29
P14A06	2,76	24,17	10,14	7,34	P14D02	55,42	37,86	49,95	45,42
P14A07	71,95	93,38	97,63	97,22	P14D03	-3,26	-30,73	-9,78	-22,55
P14A08	-3,39	-12,33	11,75	10,77	P14D04	-0,84	-31,12	1,53	-1,03
P14A09	62,35	91,95	99,97	99,04	P14D05	28,10	48,13	15,78	22,62
P14A10	-3,63	2,97	15,89	10,47	P14D06	-5,51	-18,92	4,62	7,09
P14A11	-3,56	18,20	20,50	15,33	P14D07	0,04	-7,95	10,37	4,36
P14B02	57,47	65,99	38,96	25,84	P14D08	-3,02	-23,20	12,17	4,96
P14B03	72,85	44,11	99,19	94,15	P14D09	73,60	63,00	92,97	63,25
P14B04	1,01	-5,08	5,03	-3,82	P14D10	89,65	84,38	73,66	59,31
P14B05	55,69	63,99	60,37	53,79	P14D11	1,11	-9,60	11,26	4,23

P14E02	-3,19	1,85	1,22	2,42	P14G08	6,16	-112,55	-0,49	-1,58
P14E03	32,61	24,56	52,10	49,93	P14G09	99,29	100,00	99,99	99,78
P14E04	11,44	73,19	58,53	22,17	P14G10	-0,20	7,46	20,03	6,85
P14E05	3,10	-3,39	4,45	2,89	P14G11	15,62	-97,91	1,54	-5,53
P14E06	-6,86	-58,72	-5,12	-1,07	P14H02	86,50	98,96	78,87	73,52
P14E07	5,79	35,85	16,90	14,31	P14H03	62,52	88,14	94,91	96,01
P14E08	5,35	7,38	14,88	8,58	P14H04	32,57	2,55	66,51	54,73
P14E09	2,26	-6,34	16,36	0,97	P14H05	-0,74	-1,07	6,73	4,44
P14E10	2,02	1,80	30,21	8,09	P14H06	19,32	44,22	-7,76	-27,07
P14E11	-37,41	-542,54	-12,56	-19,06	P14H07	99,73	-21,03	49,89	6,83
P14F02	30,35	92,81	48,40	55,64	P14H08	3,37	18,01	37,54	22,34
P14F03	-1,21	-19,27	-0,55	3,10	P14H09	-4,91	-6,04	8,91	5,51
P14F04	2,97	-12,41	10,37	9,47	P14H10	53,00	61,13	92,11	91,24
P14F05	1,59	-3,18	33,44	5,81	P14H11	-5,61	-135,78	-3,97	-3,63
P14F06	2,63	20,90	10,99	11,26	P15A02	97,48	98,64	98,67	98,95
P14F07	-2,69	-8,40	5,15	1,95	P15A03	2,90	9,61	1,06	-0,34
P14F08	5,12	22,38	17,79	12,24	P15A04	0,05	3,19	1,84	4,85
P14F09	-36,17	-518,93	-5,52	-16,48	P15A05	-1,37	7,95	2,24	-21,64
P14F10	72,61	82,78	94,65	96,07	P15A06	1,69	12,77	4,68	0,82
P14F11	60,33	-41,70	91,96	78,94	P15A07	-23,03	-45,87	-4,75	-13,77
P14G02	-3,46	-13,65	-3,67	-5,29	P15A08	27,94	49,69	41,81	73,03
P14G03	2,22	-6,33	5,00	7,60	P15A09	2,08	-26,91	7,81	-63,91
P14G04	-6,05	-25,84	2,55	2,61	P15A10	3,97	7,64	4,58	-21,87
P14G05	5,59	-4,35	2,51	3,42	P15A11	3,15	2,62	8,81	-25,16
P14G06	89,43	94,96	92,87	91,88	P15B02	61,92	89,68	94,41	98,78
P14G07	0,81	-17,40	6,10	3,32	P15B03	38,91	70,54	50,82	91,45

P15B04	0,80	4,84	1,97	3,36	P15D10	27,69	50,98	39,69	70,81
P15B05	2,12	5,78	2,87	-13,63	P15D11	62,89	77,65	76,38	90,14
P15B06	0,34	8,00	4,53	-15,80	P15E02	90,32	88,81	89,68	91,39
P15B07	-1,23	5,21	2,04	-11,45	P15E03	10,95	23,75	11,08	29,94
P15B08	0,69	5,46	4,79	-18,68	P15E04	39,95	50,05	40,12	60,24
P15B09	-2,62	-0,70	0,03	-26,83	P15E05	81,89	31,31	72,09	57,14
P15B10	1,12	0,28	3,30	-15,30	P15E06	51,38	82,96	80,17	98,45
P15B11	7,11	7,54	8,23	-21,22	P15E07	54,30	74,28	74,08	92,49
P15C02	8,07	6,66	9,06	4,80	P15E08	1,59	5,67	5,49	-23,31
P15C03	3,26	65,70	8,49	79,35	P15E09	80,13	91,42	94,62	99,15
P15C04	7,96	20,90	6,50	21,98	P15E10	-28,87	-19,66	-14,62	-12,01
P15C05	46,46	64,87	67,71	88,86	P15E11	13,34	23,39	45,96	59,17
P15C06	-3,51	2,82	2,47	1,61	P15F02	85,75	90,16	89,92	96,68
P15C07	55,12	84,83	91,03	98,89	P15F03	-4,65	-2,15	-0,45	-2,52
P15C08	78,15	89,86	92,16	98,50	P15F04	7,14	16,76	7,30	42,35
P15C09	4,29	10,44	6,55	-20,62	P15F05	1,59	92,85	4,28	83,48
P15C10	-4,40	-14,27	2,47	-29,79	P15F06	80,23	95,01	94,67	99,50
P15C11	7,07	40,90	8,11	57,59	P15F07	25,63	81,50	75,54	98,07
P15D02	1,51	5,67	7,40	5,12	P15F08	53,66	75,61	82,28	94,49
P15D03	-2,80	-2,87	0,48	-3,90	P15F09	75,15	94,53	94,81	99,59
P15D04	0,30	5,31	2,52	3,18	P15F10	6,29	3,13	25,63	5,49
P15D05	3,62	2,41	3,85	1,88	P15F11	-0,12	4,07	18,80	24,71
P15D06	47,03	78,72	85,28	97,14	P15G02	-0,59	-0,13	5,41	4,94
P15D07	8,46	65,19	7,93	66,84	P15G03	-6,46	-0,65	-0,48	8,41
P15D08	71,73	88,82	95,54	99,32	P15G04	-3,86	-3,19	0,66	-0,62
P15D09	74,84	84,37	93,34	97,91	P15G05	-5,93	-5,41	-0,83	-2,47

P15G06	0,66	-1,01	3,33	1,51	P16B02	0,54	10,88	3,72	2,66
P15G07	25,38	58,37	20,39	81,53	P16B03	7,53	19,77	4,78	11,07
P15G08	-6,32	-3,19	0,58	-0,39	P16B04	4,95	17,99	89,25	19,91
P15G09	-2,15	-2,31	2,70	-0,02	P16B05	14,08	51,04	7,75	32,51
P15G10	-0,55	46,85	6,57	26,28	P16B06	-121,48	21,95	6,10	-24,61
P15G11	14,98	38,05	15,51	65,96	P16B07	13,99	7,92	13,57	3,74
P15H02	34,89	61,75	59,25	89,99	P16B08	80,88	95,61	99,11	98,87
P15H03	15,69	39,13	8,41	11,38	P16B09	73,79	89,64	98,23	95,70
P15H04	89,37	79,83	87,86	76,60	P16B10	7,09	5,10	7,37	5,32
P15H05	-3,40	-3,76	1,61	1,88	P16B11	4,53	-1,22	13,78	-0,53
P15H06	1,44	-2,20	2,39	-1,27	P16C02	67,31	70,13	60,92	72,34
P15H07	-22,67	1,94	-32,41	2,53	P16C03	-13,82	10,18	10,55	-2,11
P15H08	1,98	6,71	6,67	13,00	P16C04	0,83	9,19	0,12	-0,56
P15H09	51,31	75,14	77,85	94,21	P16C05	4,74	12,70	6,84	5,19
P15H10	1,98	-2,62	11,38	6,56	P16C06	92,53	95,44	95,38	94,72
P15H11	-1,87	3,03	5,46	-8,63	P16C07	6,80	12,08	15,53	2,43
P16A02	16,17	38,61	37,98	39,89	P16C08	18,34	26,79	31,74	23,21
P16A03	15,93	36,42	18,44	36,82	P16C09	3,48	-8,41	23,32	-12,83
P16A04	9,38	9,07	70,48	2,92	P16C10	45,22	75,77	89,29	86,16
P16A05	-1,19	2,93	8,70	0,01	P16C11	72,58	91,07	58,16	95,20
P16A06	1,54	13,67	10,45	8,10	P16D02	19,52	24,41	10,76	18,23
P16A07	-6,74	1,17	6,26	-2,08	P16D03	68,39	93,01	83,55	98,77
P16A08	8,88	41,32	16,43	16,25	P16D04	-0,55	8,31	-3,38	-1,39
P16A09	2,54	2,55	13,25	-0,51	P16D05	11,29	21,78	-6,87	15,47
P16A10	26,10	64,55	43,07	71,98	P16D06	-3,48	18,60	5,20	12,30
P16A11	-0,08	-3,70	16,70	-4,61	P16D07	5,71	11,28	12,19	1,79

P16D08	12,08	19,34	21,83	16,20	P16F10	32,47	71,10	61,41	58,34
P16D09	0,80	2,14	24,69	-14,97	P16F11	5,86	-2,32	13,68	6,43
P16D10	-52,92	15,73	10,82	39,89	P16G02	50,27	54,90	70,10	61,62
P16D11	12,79	14,31	1,23	17,59	P16G03	53,24	82,70	72,05	97,38
P16E02	52,30	83,00	34,33	93,33	P16G04	33,73	78,88	40,00	91,04
P16E03	69,10	87,14	64,39	93,86	P16G05	38,31	52,24	15,32	63,65
P16E04	54,94	73,29	87,81	88,50	P16G06	-4,16	33,71	4,09	17,38
P16E05	42,63	55,73	16,32	19,03	P16G07	5,00	12,17	6,74	6,86
P16E06	58,82	89,03	93,74	96,85	P16G08	-2,31	5,26	16,70	3,64
P16E07	5,68	11,49	5,47	3,92	P16G09	-12,00	-7,69	35,92	-9,20
P16E08	0,13	11,08	13,62	6,63	P16G10	3,77	12,48	9,23	13,67
P16E09	5,09	15,37	42,17	22,67	P16G11	-1,81	-4,53	-0,04	-3,73
P16E10	10,12	11,56	5,47	3,33	P16H02	1,71	8,80	7,53	0,39
P16E11	4,01	0,03	5,36	0,21	P16H03	94,76	99,27	99,40	99,85
P16F02	92,92	96,99	97,61	98,45	P16H04	-0,78	5,03	11,98	2,04
P16F03	75,58	94,25	94,15	99,31	P16H05	58,96	75,74	79,93	90,47
P16F04	3,89	15,26	24,85	15,29	P16H06	6,83	23,63	12,94	24,68
P16F05	80,67	97,08	99,35	98,91	P16H07	18,49	57,92	22,41	42,39
P16F06	65,78	82,18	55,31	92,11	P16H08	0,01	1,42	16,06	-0,82
P16F07	0,10	10,81	-9,04	18,28	P16H09	58,02	69,23	71,30	69,09
P16F08	14,11	18,59	33,54	12,12	P16H10	-69,69	-75,74	8,38	-52,43
P16F09	-15,56	-55,88	14,95	-24,23	P16H11	5,42	7,20	17,49	14,83

VII.1.2. Cherry pick for secondary screening

	1	2	3	4	5	6	7	8	9	10	11	12
A	+	P1B03	P2E08	P3G03	P5D03	P8H02	P11B04	P11F09	P12D06	P15F05	-	-
B	+	P1B07	P2F08	P3G09	P5E02	P8H04	P11B10	P11F10	P13A06	P15G03	-	-
C	+	P1C02	P3D03	P3H03	P5G03	P8H07	P11C04	P11G04	P13C02	P15G10	-	-
D	+	P1C03	P3D10	P3H09	P6A09	P10A10	P11C06	P11G09	P13D03	P16B05	-	-
E	-	P1C04	P3E02	P4A07	P6G03	P10B10	P11E09	P11H03	P13D05	P16D10	+	+
F	-	P1C05	P3E08	P4E09	P7B06	P10G04	P11E10	P11H06	P13D06	-	+	+
G	-	P1D07	P3E10	P4G08	P8E09	P10H05	P11B04	P11H09	P13E04	-	+	+
H	-	P1E06	P3F02	P5C09	P8G11	P10H11	P11B10	P12B10	P15C03	-	+	+

VII.2. Publications related to the dissertation